Enzymatic Production Of Chiral Non-Canonical Amino Acids With Decarbamoylating Enzymes

Zur Erlangung des akademischen Grades eines
DOKTORS DER NATURWISSENSCHAFTEN (Dr. rer. nat.)

von der KIT-Fakultät für Chemie- und Biowissenschaften
des Karlsruher Instituts für Technologie (KIT)

genehmigte
DISSERTATION
von
M. Sc. Carolin Sabine Lohmann

aus
Darmstadt

KIT-Dekan: Prof. Dr. Reinhard Fischer
Referent: Prof. Dr. Stefan Bräse
Korreferent: Prof. Dr. Christoph Syldatk
Tag der mündlichen Prüfung: 16.10.2019

Erklärung

Hiermit erkläre ich, dass ich die vorliegende Arbeit selbstständig angefertigt und keine anderen als die darin angegebenen Quellen und Hilfsmittel benutzt, sowie die wörtlich oder inhaltlich übernommenen Stellen als solche kenntlich gemacht und die Satzung des Karlsruher Institut für Technologie (KIT) zur Sicherung guter wissenschaftlicher Praxis in der gültigen Fassung beachtet habe. Zudem versichere ich, dass die elektronische Version dieser Arbeit mit der schriftlichen übereinstimmt.

Ich versichere außerdem, dass ich diese Dissertation nur in diesem und keinem anderen Promotionsverfahren eingereicht habe und dass diesem Promotionsverfahren keine endgültig gescheiterten Promotionsverfahren vorausgegangen sind.

Ort, Datum

Unterschrift

ABSTRACT

Chiral non-canonical amino acids like β-amino acids exist in countless variants. The development of a suiting biotechnological production process for them is mandatory, since they are used as components in many drugs and lend them novel bioactive properties. The chemical synthesis of non-canonical amino acids is often elaborate and has many disadvantages. By using enantioselective enzymes a 100 % yield of an enantiomers can be achieved. The established Hydantoinase process is successfully applied in industry for the production of non-canonical D-α-amino acids. The aim of this work was to identify enzymes for a modified Hydantoinase process to synthesize optically pure β^3-amino acids.

Therefore, several novel enzyme substrates like *N*-carbamoyl-β-homo-serine or *N*-carbamoyl-β-phenylalanine (NCβPhe) were chemically synthesized. Suiting analytical assays and HPLC-methods were established to monitor enzymatic substrate degradation and product formation. To identify one or more new enzymes able to convert *N*-carbamoyl-β-amino acids 200 wild-type strains of the institutes own microorganism strain collection were screened for growth on *N*-carbamoyl-β-phenylalanine as the sole nitrogen source. Some strains showed growth on NCβPhe. By using bioinformatic sequence alignment tools seven genes from three bacterial strains (*Burkholderia phytofirmans, Pseudomonas aeruginosa* and *Pseudomonas oleovorans*) were identified for potential production of chiral β-amino acids. These genes were cloned and recombinantly expressed in *Escherichia coli*. Although none of the enzymes showed degradation of NCβPhe, the enzymatic synthesis of L-β-homo-alanine and L-β-homo-serine as well as other non-canonical α-amino acids was shown for the first time using decarbamoylating enzymes. In addition, the active centres of these seven novel enzymes were predicted using various *in silico* methods. Furthermore, the enzymes were characterized and classified by *in vitro* and *in silico* experiments.

In the course of the work five further decarbamoylating enzymes from four different enzyme classes already known from the literature were examined. For these enzymes, previously unknown cross-class activities could be detected. In addition, catalysis of these enzymes made it possible for the first time to synthesize the β^3-amino acids L- and D-β-homo-alanine, L- and D-β-homo-serine, L-β-homo-methionine, as well as the non-canonical α-amino acids β-2-thienylalanine, L-α-neopentylglycine biocatalytically. By combining results from *in silico* ligand docking and *in vitro* experiments, an affinity of all enzymes to substrates with polar or charged side chains could be predicted.

ZUSAMMENFASSUNG

Chirale nicht-kanonische Aminosäuren, wie β-Aminosäuren, existieren in unzähligen Varianten. Die Entwicklung eines geeigneten Verfahrens zu ihrer biotechnologischen Herstellung ist zwingend erforderlich, da sie als Bausteine von Medikamenten diesen neue biologische Eigenschaften verleihen. Ihre chemische Synthese ist oft aufwändig und bietet viele weitere Nachteile im Vergleich zu biotechnologischen Verfahren. Durch enantioselektive Enzyme kann beispielsweise eine 100 %-ige Ausbeute eines Enantiomers erzielt werden. Der etablierte Hydantoinaseprozess wird industriell erfolgreich zur enzymatischen Synthese nicht-kanonischer D-α-Aminosäuren verwendet. Ziel dieser Arbeit war es, neue Enzyme für einen modifizierten Hydantoinaseprozess zur Herstellung optisch reiner β^3-Aminosäuren zu identifizieren.

Dafür wurden mehrere Enzymsubstrate, wie beispielsweise *N*-carbamoyl-β-homo-serin oder *N*-carbamoyl-β-phenylalanin (NCβPhe) chemisch synthetisiert. Passende analytische Assays und HPLC-Methoden wurden etabliert, um den enzymatischen Substratabbau und Produktaufbau zu verfolgen. Um neue Enzyme zu identifizieren, die *N*-carbamoyl-β-Aminosäuren zur entsprechenden β-Aminosäure katalysieren, wurden 200 Wildtyp-Stämme der institutseigenen Mikroorganismenstammsammlung auf Wachstum auf NCβPhe als einziger Stickstoffquelle untersucht. Für einige Stämme konnte ein geringes Wachstum beobachtet werden. Mit Hilfe von bioinformatischen Sequenzvergleichen konnten sieben Gene aus drei verschiedene Organismen (*Burkholderia phytofirmans, Pseudomonas aeruginosa* und *Pseudomonas oleovorans)* identifiziert werden, für die eine putative Synthese von β-Aminosäure angenommen wurde. Diese Gene wurden kloniert und rekombinant in *Escherichia coli* exprimiert. Zwar zeigte keines der Enzyme einen Umsatz von NCβPhe, allerdings konnte erstmals die enzymatische Synthese von L-β-Homo-alanin und L-β-Homo-serin sowie anderen nicht-kanonischen α-Aminosäuren gezeigt werden. Zusätzlich wurden die Aktivzentren dieser sieben neuen Enzyme mit Hilfe verschiedener *in silico* Methoden prognostiziert. Des Weiteren wurden die Enzyme durch *in vitro* und *in silico* Experimente charakterisiert und klassifiziert.

Im Verlauf der Arbeit wurden fünf weitere bereits aus der Literatur bekannte decarbamoylierende Enzyme aus vier unterschiedlichen Enzymklassen untersucht. Für diese Enzyme konnten bisher nicht bekannte klassenübergreifende Aktivitäten detektiert werden. Außerdem konnten durch Katalyse dieser Enzyme erstmals die β^3-Aminosäuren L- und D-β-

Homo-Alanin, L- und D-β-Homo-Serin, L-β-Homo-Methionin, sowie die nicht-kanonischen α-Aminosäuren β-2-Thienylalanin, L-α-Neopentylglycin biokatalytisch hergestellt werden. Durch Kombination von Ergebnissen aus *in silico* Ligand-Dockings und *in vitro* Experimenten konnte eine Affinität aller Enzyme gegenüber Substraten mit polaren oder geladenen Seitenketten prognostiziert werden.

PUBLICATIONS

Poster Presentations

Lohmann, C., Engel, U, Syldatk, C., *Biocatalytic Production of Chiral Non-Canonical Amino Acids with Decarbamoylizing Enzymes*, Annual Conference 2019 of the Association for General and Applied Microbiology (VAAM) 2019, Biospektrum, BTP594.

Lohmann, C., Engel, U., *Screening, Purification and Characterization of Decarbamyolizing Enzymes for the Production of Chiral β-Amino acids*, 9th International Congress on Biocatalysis - biocat 2018.

Lohmann, C., Engel, U., *Screening, Purification and Characterization of Decarbamyolizing Enzymes for the Production of Chiral β-Amino acids*, Summer School Biotransformation 2017.

TABLE OF CONTENT

ABBREVATIONS

Å	Ångström
*At*βcar	β-Ureidopropionase from *Agrobacterium tumefaciens* C58
Boc	Tert-butyloxycarbonyl protecting group
D/LβhAla	D/L-β-homo-alanine
D/LβhSer	D/L-β-homo-serine
E. coli	*Escherichia coli*
Fmoc	Fluorenylmethoxycarbonyl protecting group
I Δ	Interface delta value
IBLC	*N*-isobutyryl-L-cysteine
mAU	Milli absorption unit
mM	Milli molar
NCαAA	*N*-carbamoyl-α-amino acids
NCβAA	*N*-carbamoyl-β-amino acids
NCβHep	*N*-carbamoyl-3-Aminoheptanoic acid
NCβ(h)AAs	*N*-carbamoyl-β-amino acids and *N*-carbamoyl-β-homo-amino acids
NCβHep	*N*-carbamoyl-3-amino heptanoic acid
NCβPhe	D/L-*N*-carbamoyl-β-phenylalanine
noncAA	Non-canonical amino acid
OD_{600}	Optical density at 600 nm
OPA	O-Phtaldialdehyde
PheDU	Phenyldihydrouracil
PutβUp	β-Ureidopropionase from *Pseudomonas putida*
SklβUp	β-Ureidopropionase from *Lachancea kluyveri*
βcar_{AT}	βUp from *A. tumefaciens* C58
T_m	Primer melting temperature
αAA	α-amino acids
βAA	β-amino acid
βhAA	β-homo-amino acid
β(h)AAs	β-amino acids and β-homo-amino acids
βUBut	β-Ureidoisobutyric aid

1 INTRODUCTION

The aim of this thesis is the enzymatic production of optically pure non-canonical amino acids with focus on β^3-amino acids using decarbamoylating enzymes. In section 1.1 and 1.2 selected examples of the countless number of non-canonical amino acids are highlighted. 1.3 underlines the versatile application of these valuable building blocks. Section 1.4 gives an overview on known biosynthetic, chemical and biotechnological routes to obtain optical pure non-canonical amino acids. The focus of this thesis is on enzymes that are supposed to be used in a modification of the known hydantoinase process for the production of chiral β^3-amino acids. The theoretical background of the process and the involved enzymes are described in section 1.5. Essential methods used in this work are highlighted in section 1.6 and 1.7.

1.1 Non-canonical amino acids as important building blocks

Twenty canonical α-amino acids occur in nature, which are incorporated into proteins during translation of protein biosynthesis in living organisms [1]. Production of most of proteinogenic α-amino acids is well established and builds a billion dollar market.

The term of non-canonical amino acids (noncAAs) includes all amino acids that are not naturally incorporated into proteins. The number and diversity of noncAAs is countless. Depending on the position of their amino-group they are classified as α-, β-, γ-, or δ-amino acids [2]. Many noncAAs exhibit pharmacological activity and thereby they offer a wide range of applications in drug discovery. These extraordinary properties result from their complex structures including several chiral centres or complex *N*-heterocycles. NoncAAs can also be integrated into peptides and proteins, either for adding novel properties to the protein or for protein-function studies. In addition to chemical synthesis protein engineering enhances the number of possibilities to a growing collection of valuable noncAAs [3].

Non-canonical α-amino acids exist in many different structure variants. Some occur in nature and many can be chemically synthesized [4]. Structurally they have their amino group substituted at the α-C-atom, but they can have very diverse chemical constitutions: aliphatic, aromatic, including one or more chiral centres, containing heterocyclic structures or they are the D-enantiomer of their proteinogenic L-α-amino acid counterpart. The constitution of the cyclic peptide antibiotic daptomycin represents the diversity of non-canonical α-amino acids (Figure 1).

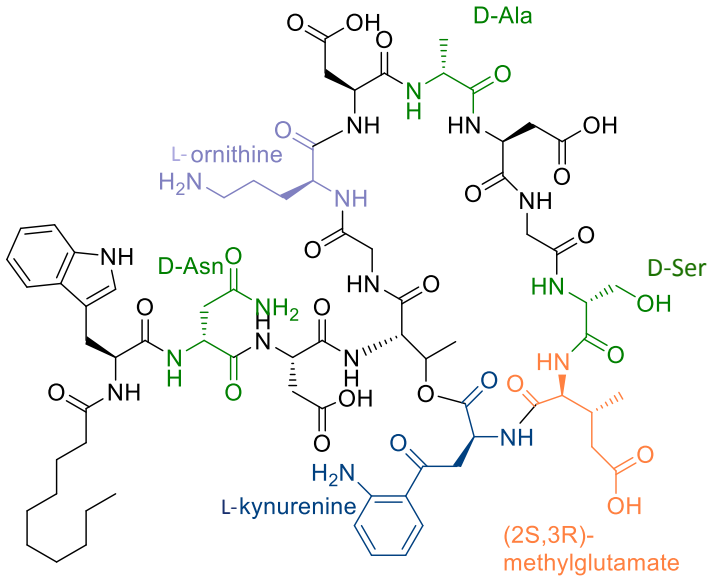

Daptomycin

Figure 1: Daptomycin peptide antibiotic containing diverse non-canonical-α-amino acids.
The cyclic peptide antibiotic daptomycin [5] includes several non-canonical-α-amino acids: D-alanine, D-asparagine, D-Ser (green), ornithine (purple) and (2*S*, 3*R*)-methylglutamate (orange).

Compared to proteinogenic α-amino acids, which play an essential role in the primary metabolism in living matter, β-amino acids (βAAs) are often found in secondary metabolites. Bacteria, cyanobacteria, fungi and plants are able to integrate βAAs into natural products such as peptides, depsipeptides, cyclopeptides, terpenoids or alkaloids [6]. These complex molecules are used as defence mechanism against other organisms [7, 8]. Thereby natural products containing βAA moieties can be utilized as lead structures for the developments of new drugs [9]. Often the βAA unit in those compounds is essential for a potent biological and physiological activity of the molecule [10]. In literature natural products containing βAAs are described for showing anti-tumour [11]–[18], antibiotic [19]–[26] anti-inflammatory [27]–[29] antifungal [30]–[33] as well as enzyme inhibiting [27], [34]–[37] features. Not only as part of natural products but also in free form βAAs show interesting pharmacological effects [38], providing a wide range of applications explained in more detail in the following sections.

βAAs exist in *open chain* or *cyclic* form. In comparison to their α-analoga, the amino group is substituted at the β-C-atom. Seebach and his co-workers established the β^2/β^3-convention [39][40], in the early 2000s. They proposed three general forms of *open-chain* βAAs and two *cyclic* types as shown in Figure 2. In free form a variety of chemically synthesized βAAs exists. Depending on the position of the substituents several categories are distinguished:

$\beta^2/\beta^{2,2}/\beta^{2,3}/\beta^{3,3}/\beta^{2,2,3}/\beta^{2,2,3,3}$/- di/tri or tetra-substituted-β-amino acids. Several additional forms exist, for example α-hydroxy-β-amino acids or β^3-alkyl-β-amino acids. The number of variations and possibilities is countless [3].

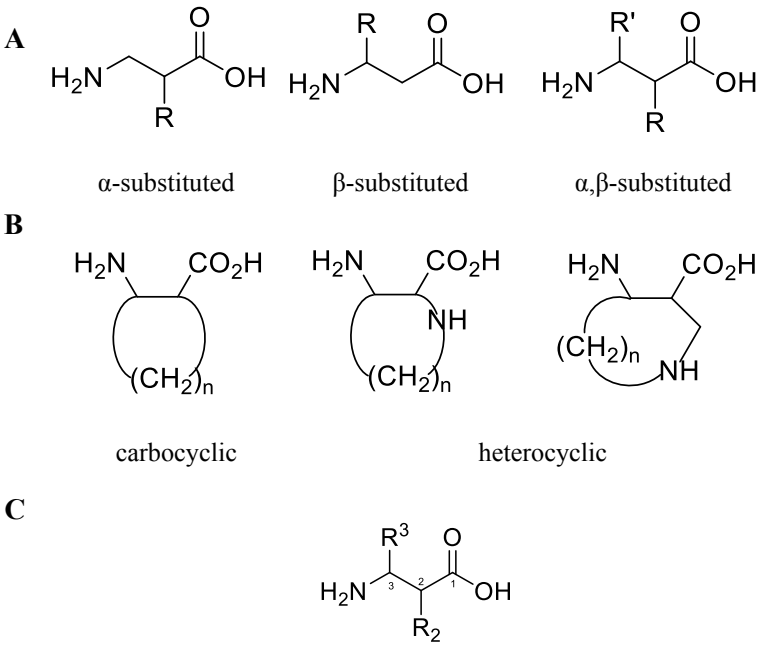

Figure 2: Types of β-amino acids.
A) βAAs can be distinguished between α-, α,β- or β-substituted, depending on the position of their substituent. B) βAAs occur in cyclic forms, if a heteroatom is included they are described as heterocyclic. C) Overview and comparison of the different βAA types.

1.2 Occurrence in nature

NoncAAs have been found in plants, microorganisms and animals [41]. Examples for natural non-canonical-α-amino acids are L-*m*-tyrosine, L-canavanine, β-*N*-oxalyl-L-α,β-diaminopropionic acid (β-ODAP) or L-Theanine (Figure 3A). In nature L-*m*-tyrosine is used as root toxin by the grasses *Festuca arizonica* and *F. rubra* against competitive species [42]. Some non-canonical-α-amino acids are also toxic for humans. E.g. L-canavanine causes muscle palsy and can induce the autoimmune disease systemic lupus erythematosus [43]. Also the β-*N*-oxalyl-L-α,β-diaminopropionic acid (β-ODAP) found in *Lathyrus sativus* is toxic and leads to irreversible paralytic and neurobiotic disorders [44]. On the contrary other noncAAs show beneficial pharmaceutical effects. L-Theanine, present in tea plants, is known for lowering blood pressure, relieving stress and inhibiting tumour growth [45]. L-Citrulline (5) and L-ornithine (6) are intermediates in the urea cycle and are used for treatment of liver cell damage. Additionally L-citrulline is a building block in a novel antibody-drug conjugate

as linker molecule [46]. L-Lanthionine (7) extracted from wool shows antibacterial effects [47].

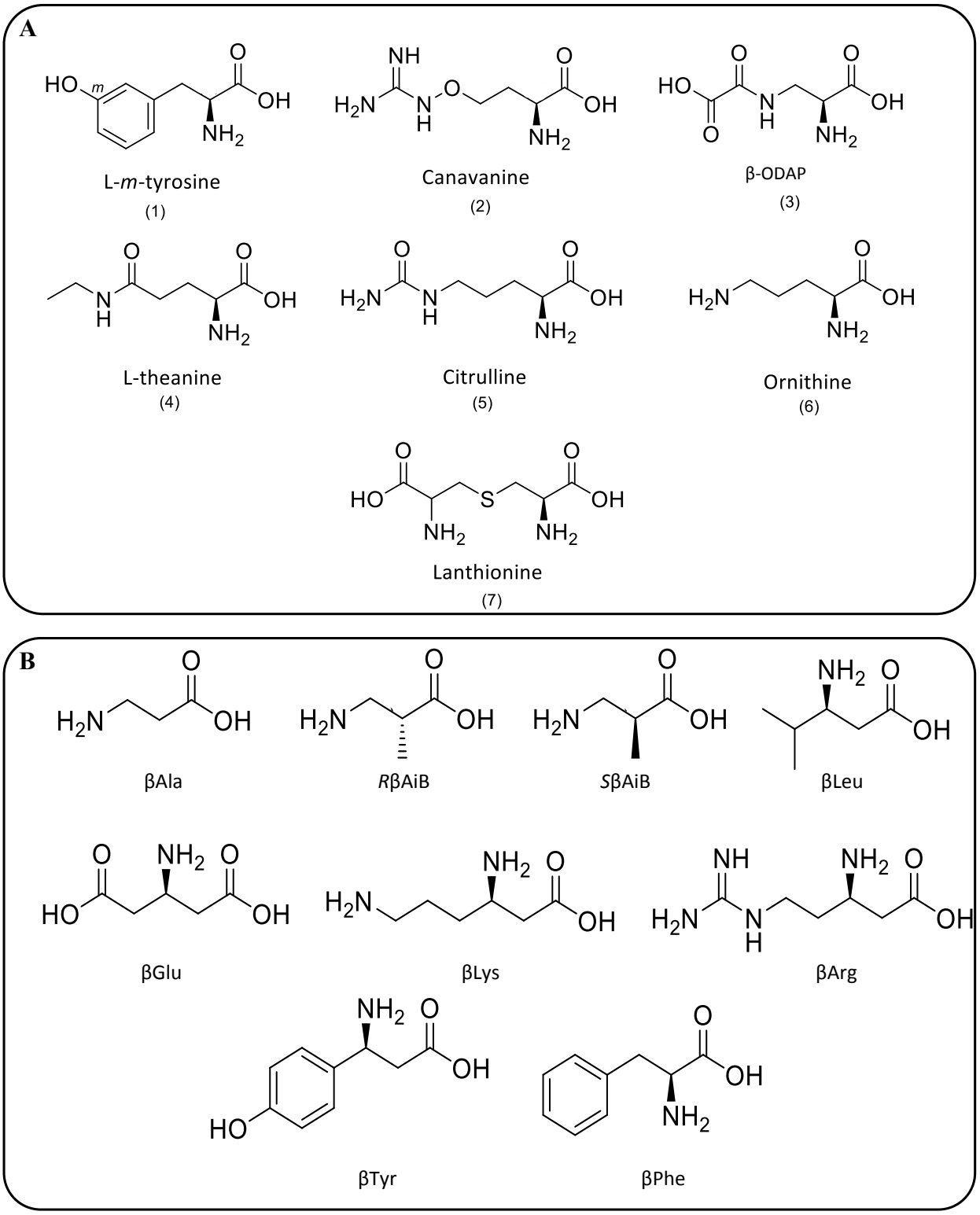

Figure 3: Naturally occurring non-canonical amino acids.
A) Non-canonical α-amino acids found in nature B) Non-canonical β-amino acids found in nature.

In contrast to the fact, that many βAAs are chemically synthesized, only a few occur in nature in free form, especially β^3-amino acids (Figure 3 B) [48]. The non-chiral β-alanine (βAla) was isolated from betain in 1909 [49] and the structurally related *R*-β-aminoisobutyric acid (RβAiB) purified from human urine in 1951 [50], [51]. βAla and RβAiB are present in all five kingdoms of living organisms, since they are metabolites in the pyrimidine catabolism. They are formed *via* the conversion of *N*-carbamoyl-β-alanine or respectively *N*-carbamoyl-β-aminoisobutyric acid. Their conversion is catalysed by a β-Ureidopropionase [52]. Additionally β-alanine is found as moiety in betaine (4) in plants (Figure 4) [53]. *S*-β-aminoisobutyrate is formed in the catabolism of L-valine and β-leucine was found as precursor of L-leucine in mammals [54]. Another βAA found in free form in nature is β-lysine, which is formed by an aminomutase from L-α-lysine as an intermediate in the catabolism of *Clostridium* species [55]. Other βAAs such as β-arginine [56], β-tyrosine [57], β-glutamic acid [58] or β-phenylalanine [59], [60] are found in natural products shown in (Figure 4). They mostly contain α-hydroxy-β-amino acids. The most prominent example is Paclitaxel (Figure 4, (3)) produced from the tree *Taxus brevifolia* and shows a strong anti-tumour activity [61]. It incorporates α-hydroxy-β-phenylalanine and directly receives this βAA from proteinogenic αAAs through a 2,3-aminomutase. The reaction mechanism of aminomutases will be explained in more detail in section 1.4.3 (p. 16). Blasticidin S (Figure 4, (1)) contains β-arginine and was found in *Streptomyces griseochromogenes* and protects rice plants from fungal infections [62]. Edeine A1 (Figure 4, (2)) contains β-tyrosine and was detected in cultures from *Bacillus bevris* Vm4 in 1959 [63]. In plant alkaloids βAAs are produced from cinnamic acid *via* Micheal-type addition reactions [64], Mannich-type condensations or oxidative cyclizations [65]. The greatest diversity of βAAs is found in bacteria, especially cyanobacteria. Beside their ability to produce βAAs from their proteinogenic α-counterpart they are also capable of producing a variety on βAAs with no existing αAA analogue [15].

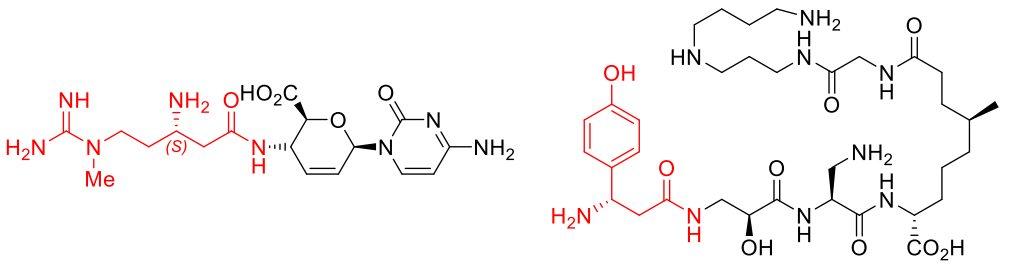

(1)

Blasticidin S

(2)

Edeine A1

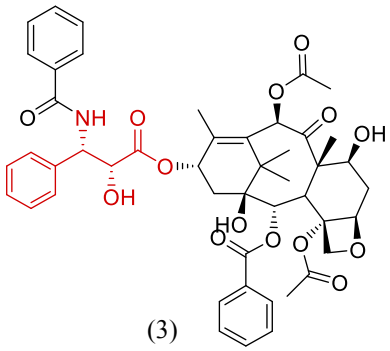

(3)

Paclitaxel

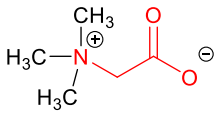

(4)

Betaine

Figure 4: Natural products with βAA moiety.
1) Basticidin S with β-arginine moiety from *Streptomyces griseochromogenes* 2) Edeine A1 with β-tyrosine moiety 3) Paclitaxel incorporates a hydroxylated derivate of β-phenylalanine 4) Bestaine is a derivate of β-alanine.

1.3 Application of non-canonical amino acids

NoncAAs can lend interesting and novel properties to molecules and their application is versatile. The probably biggest application area of noncAAs is their use as buildings blocks in drug development for the medical sector. Beside, they are used for fundamental research of protein functions and are used as substitutes for canonical-αAAs. Other approaches, like incorporation of noncAAs into the murine proteome [66] and *in vivo* incorporation into proteins have been accomplished [67].

The application for noncAAs in medical chemistry is extremely diverse. For drug discovery either natural products or chemically synthesized molecules are used. There are many different molecule classes in which noncAAs occur as moiety, e.g. β-lactam antibiotics, alkaloids, peptides or the innovative class of antibody-drug conjugates (Figure 5). L-α-3-hydroxy-1-adamantyl-glycine is a building block of the diabetes drug saxagliptin (1). The macrocyclic peptide bottromycin (2) is a natural product from *Streptomyces bottropensis*.

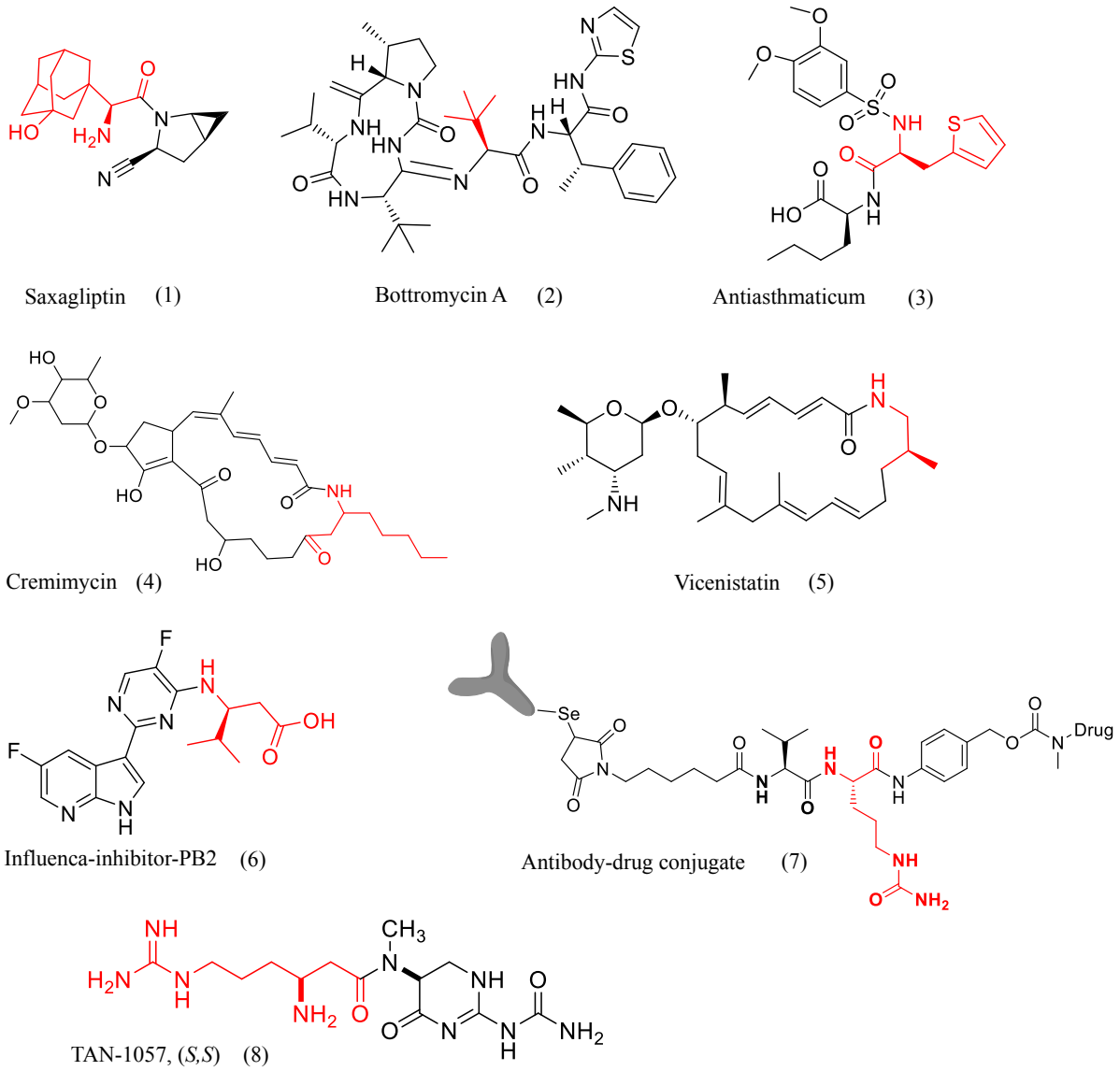

Figure 5: Selected pharmaceutical drugs containing non-canonical amino acids moieties (red).

It was discovered in 1957 and includes the noncAA tertiary-leucine [68]. The molecule inhibits *Staphylococcus aureus* (MRSA) and vancomycin-resistant *Enterococci* (VRE), as well as other Gram-positive bacteria and mycoplasma [69]. *N*-[(3,4-dimethoxyphenyl)sulfonyl]-3-(2-thienyl)-L-alanyl-L-norleucine (3) is applied as an anti-asthmaticum and contains β-2-thienylalanine as building block. The macrocyclic lactam antibiotic cremimycin (4) was isolated from a culture of a *Streptomyces* strain in 1997. It shows broad antibacterial activities against Gram-positives bacteria such as methicillin-resistent-*Staphylococcus aureus* (MRSA). In its structure the βAA 3-amino-heptanoic acid is incorporated [70]. Another antibiotic drug is vicenistatin (5). It is a macrolactam polyketide (β-amino acid starter polyketide) and in its synthesis the starter unit β-aminoisobutyrate is

used. It is condensed with an enolate α-carbon on an ACP-tethered acyl intermediate by a Claisen-type condensation [71]. Furthermore it exhibits anti-tumour and antibiotic activities [72].

The novel class of antibody-drug conjugates (ADCs) is used as strong tool in the treatment of cancer. These consist of a suiting antibody that is connected to a highly effective anti-cancer drug *via* a linker molecule [73], [74]. Through the antibody unit the anti-cancer drug is directed to the cancer cells and set free due to cleavage of the linker. In the shown ADC (7) the noncAA citrulline is used in a valine-citrulline linker. Another application of noncAAs for drugs are artificial peptides. E.g. the dipeptide antibiotic TAN-1057 A,B (8) contains a β-homo-arginine subunit and shows activity against MRSA [75]. Flourine-containing noncAAs exhibit anti-viral and anti-cancer activities. The fast protein biosynthesis of cancer cells is disturbed when fluorophenylalanine is present. Thereby the incorporation of phenylalanine into the proteins in inhibited [76].

1.3.1 *In vivo* incorporation of non-canonical amino acids into proteins

In vivo incorporation of noncAAs into peptides and proteins offers novel and peerless properties over conventional peptide mutagenesis [77]. This method provides many new tools to investigate enzyme structures, functions or dynamics [78] and is an important field especially for the development of new antimicrobial peptides (AMPs) [67], [79]. Protein engineering with noncAAs can be used for enhanced enzyme activity or improvement of drugs [80]. This is reported for *E. coli* [81], mammalian cells [82] plants cells [83] and yeasts [84, 85]. Until 2015 more than 150 noncAAs had been incorporated into proteins. Especially for the modification of the active side in enzymes this technique offers a broad set of molecules rarely or never found in nature.

There are several novel methods for the introduction of noncAAs into proteins. One technique in enzyme engineering is the *site-specific method*. Thereby the genetic code is redesigned. This means that new codons are added to the translation code table and thus novel noncAAs can be integrated into proteins. New codons can be incorporated by using quadruplet codons [86] or with codons made of unnatural bases [87]. By using this method e.g. the noncAAs were integrated into proteins for enhancement of enzyme enantioselectivity [88]. Also regioselectivity has been investigated using noncAAs. Furthermore the enzyme activity could be increased [89]. Several other noncAAs led to enhancement of photo-controllable activity.

Incorporation of noncAAs was used for investigation of biophysical properties, such as protein-protein interactions, protein-ligand interactions or mechanistic studies [90].

Another approach of *in vivo* incorporations of noncAAs into proteins is the *residue-specific method.* Thereby ribosomes integrate noncAAs with their tRNAs into the translated amino acid sequence. Especially proteins containing β^3-amino acids show enormous potential, since they show resistance against proteases [91] and additionally altered immunogenicity to provoke an immune response in the body [92]. Recently an article was published on *in vivo* biosynthesis of a β-amino acid containing protein in *E. coli* [93]. Several wild-type *E. coli* aminoacyl-tRNA synthetases were able to use β^3-amino acids as substrates. E.g. β^3-phenylalanine was integrated into a peptide.

1.3.2 β-peptides

Additionally to the *in vivo* incorporation of noncAAs, peptides can also be generated by *in vitro* incorporation of noncAAs. One example for such artificial peptides are β-peptides. They either consist completely or partly of one or several βAAs covalently bound by an amide-bond. In comparison to their α-analogues they show different properties and are used either for investigation of physical forces during molecular folding or for biomedical applications [94]. They are chemically synthesized whether in solution or due solid phase peptide synthesis manually or automatically [40].

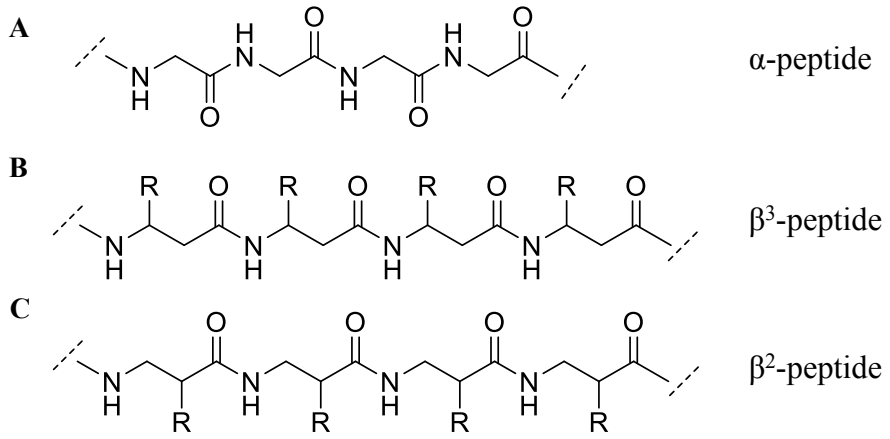

Figure 6: Comparison of α- and β-peptides.
A) Primary structure of a α-peptide compared to a B) β^3-peptide and C) β^2-peptide.

Figure 6 shows the structure of β^3- and β^2-peptides compared with their α-analogue. Due to their molecular structure a higher number of conformations are possible than in α-peptides. Especially β^3-peptides show flexibility in their secondary structure. Already at a peptide length of four amino acid residues β-peptides can form stable secondary structures, such as helices, sheets and turns [48]. In comparison α-peptides require much longer amino acid sequences to form stable secondary structures [91]. Additionally Seebach and his co-workers showed that short-chain β-peptides are soluble in pyridine and methanol solutions making them interesting for industry applications [95].

Since β-peptides are highly stable against proteolytic degradation [91], stable to metabolism and exhibit slow microbial degradation, they are gaining interest for their application in medicinal chemistry. Furthermore they can mimic α-peptides in peptide-protein and protein-protein interactions [96]. β-peptides e.g. are applied in the human body for inhibition of cholesterol and fat uptake due to their amphiphilicity [97] or as antimicrobial molecules. β^3-peptides with at least three trimer-repeats inhibit the growth of *E. coli* at µM concentrations (Figure 7). The reason for this antibiotic effect is the formation of the stable secondary structure with a similar three-residue repeat [98].

Peptides containing β^2-amino acids only rarely occur in nature [96].

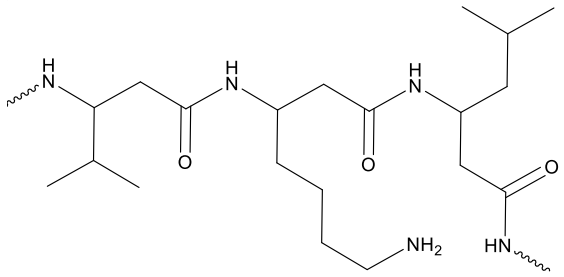

β³HVal β³HLys β³HLeu

Figure 7: Chemical structure of a β^3-peptide.
Chemical structure of the β^3-peptide trimer unit (β^3HVal-β^3HLys-β^3HLeu). Figure was modified after [98].

1.4 Synthesis routes for the production of non-canonical amino acids

The previous sections underline the fact that chiral noncAAs are of high relevance and thus chiral synthesis strategies are needed. This thesis focuses on the enzymatic synthesis of highly optically pure non-canonical α- and β-amino acids using decarbamoylating enzymes. Beside that, other routes to noncAAs are highlighted in the following sections with regard towards their advantages and disadvantages. In general they can are produced naturally by a few known biosynthetic routes, many chemical and other biotechnological routes.

1.4.1 Biosynthesis of non-canonical amino acids

Compared to the well-studied canonical amino acids, only a few biosynthetic pathways for noncAAs are known. Several can be synthesized *via* metabolic pathways. Non-canonical α-amino acids found in the urea cycle are citrulline and ornithine. Thereby citrulline is obtained from ornithine or from arginine by a nitric oxide synthase [99]. Theanine is produced in the metabolism in tea plants from glutamic acid and alanine [45, 100]. Another example is homocysteine, which is an intermediate in the methionine metabolism process [101]. Many of these biosynthetic routes are based on a natural pathway for a α-amino acid and improved due metabolic engineering. An overview of the known biosynthetic pathways for the production of noncAAs is given in Figure 8 [41].

Some βAAs are produced in plants by aminomutases. These enzymes perform a shift of the amino group of α-amino acids to the β-position. An example for this is the natural production of βAAs in the biosynthetic pathway in the plant *Taxus brevifolia* [12]. It is able to produce L-β-phenylalanine through a natural pathway from its α-analogue through a phenylalanine 2,3-aminomutase. *R*-β-phenylalanine is generated in the same way in *Taxus baccata* [102]. Other examples of aminomutases-syntheses are L-β-arginine, which can be found in the antibiotic blasticidin in *Streptomyces griseochromogenes* or the production of L-β-leucine in *Andrographis paniculata* [102]. Furthermore some plant alkaloids contain a βAAs, which can be generated from cinnamic acid through Michael-type addition reactions [64].

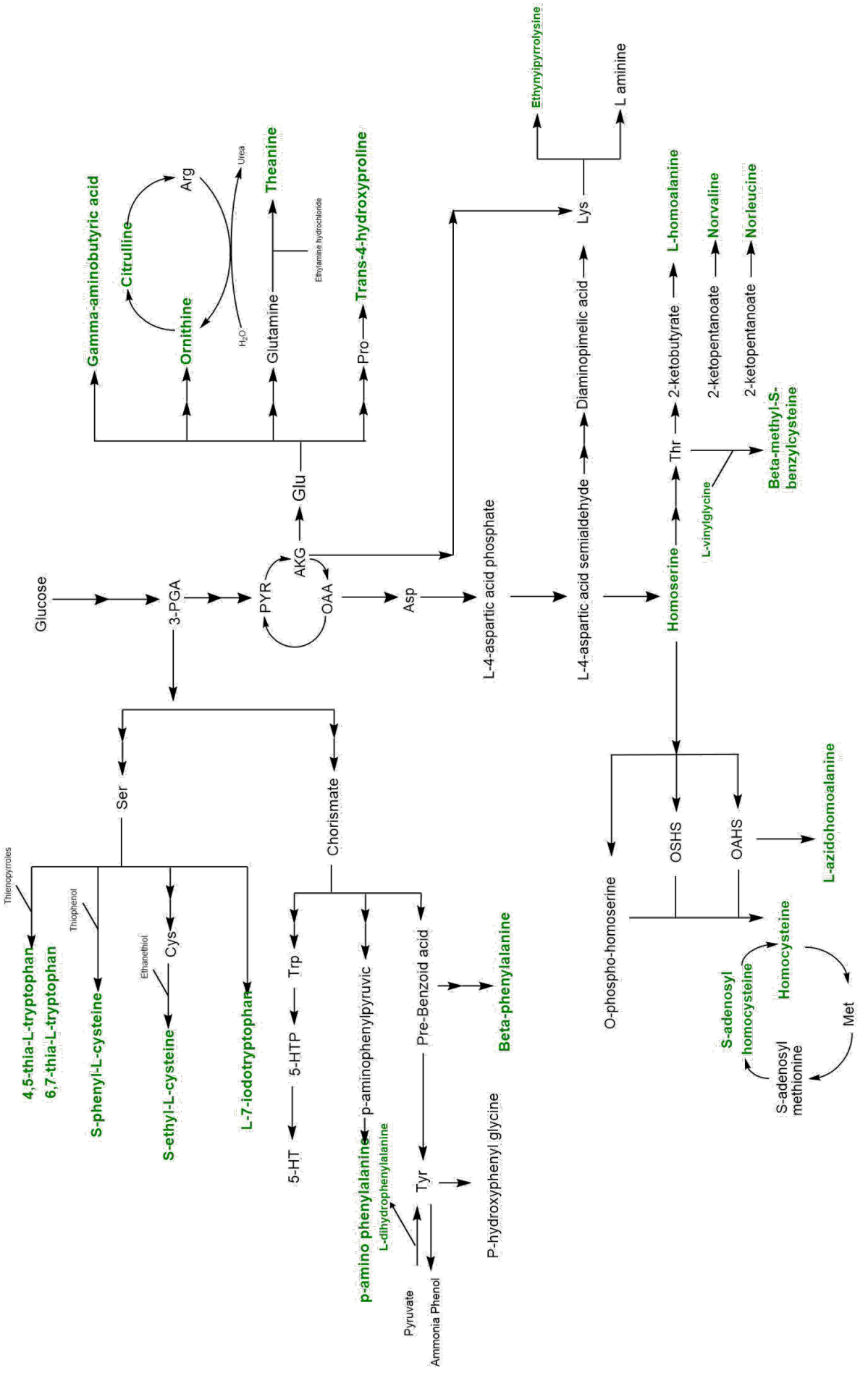
Glucose
3-PGA
PYR
AKG
OAA
Glu
Asp
Gamma-aminobutyric acid
Citrulline
Arg
Ornithine
Urea
H_2O
Glutamine
Theanine
Ethylamine hydrochloride
Pro
Trans-4-hydroxyproline
L-4-aspartic acid phosphate
L-4-aspartic acid semialdehyde
Diaminopimelic acid
Lys
Ethynylpyrrolysine
L aminine
Homoserine
Thr
2-ketobutyrate
L-homoalanine
2-ketopentanoate
Norvaline
2-ketopentanoate
Norleucine
L-vinylglycine
Beta-methyl-S-benzylcysteine
Ser
Chorismate
Thienopyrroles
4,5-thia-L-tryptophan
6,7-thia-L-tryptophan
Thiophenol
S-phenyl-L-cysteine
Ethanethiol
Cys
S-ethyl-L-cysteine
L-7-iodotryptophan
Trp
5-HTP
5-HT
p-aminophenylpyruvic
p-amino phenylalanine
L-dihydrophenylalanine
Pre-Benzoid acid
Beta-phenylalanine
Tyr
Pyruvate
Ammonia Phenol
P-hydroxyphenyl glycine
O-phospho-homoserine
OSHS
OAHS
L-azidohomoalanine
S-adenosyl homocysteine
Homocysteine
S-adenosyl methionine
Met

Figure 8: Known biosynthesis routes of non-canonical amino acids.
NoncAAs are highlighted in green. Figure was modified after [41]. Abbreviations: 3-PGA: 3-phosphoglyceric acid; 5-HTP: 5-hydroxy-L-tryptophan; 5-HT: 5-hydroxytryptamine; PYR: pyruvate; AKG: α-ketoglutaric acid; OAA: oxaloacetic acid; OSHS: O-succinyl-L-homoserine; OAHS: O-acetyl-L-homoserine; Trp: Tryptophan; Tyr: Tyrosine; Ser: Serine; Phe: Phenylalanine; Glu: Glutamic acid; Pro: Proline; Asp: Aspartic acid; Lys: Lysine; Cys: Cysteine; Met: Methionine; Thr: Threonine.

1.4.2 Chemical synthesis of non-canonical amino acids

Many synthesis routes for the chemical production of noncAAs are known. One advantage of chemical synthesis is that often one approach is applied for the production of several noncAAs. But there are also many disadvantages. The synthesis is quite elaborate, used catalysts and solvents are harmful to the environment and racemates have to be further purified [103]. Additionally reactive amino- or carbonyl groups have to be protected by protecting groups such as tert-butyloxycarbonyl (Boc) or fluorenylmethoxycarbonyl (Fmoc). Although many special catalysts have been developed over time, multiple stereocentres, amines, heterocycles and non-protected functional groups as well as C-X and C-C bond formations still represent a challenge to organic chemical synthesis [103][104]. Asymmetric synthesis and metal-catalysed cross coupling reactions developed over the past decades are strong features but the synthetic methodology for the production of noncAAs is still limited [104].

For the preparation of non-canonical α -amino acids many methods are known [107], [108], [109], [110]. One example is the formation of non-proteinogenic D-amino acids from their natural L-enantiomer counterpart due to dynamic resolution. E.g. D-proline is obtained from L-proline through racemization with butyraldehyde. Subsequently the D-isomer is removed as a salt with D-tartaric acid (Figure 9A) [105], [106]. Another synthesis approach used Rhodium complexes of the type $[(COD)Rh(DuPhos)]^{+}X^{-}$ (X-weakly or non coordinating anion; COD = cyclooctadiene). This class of catalysts is generally used for the hydrogenation of enamids. They lead to an enantioselective synthesis under low pressures Figure 9B) [107], [108].

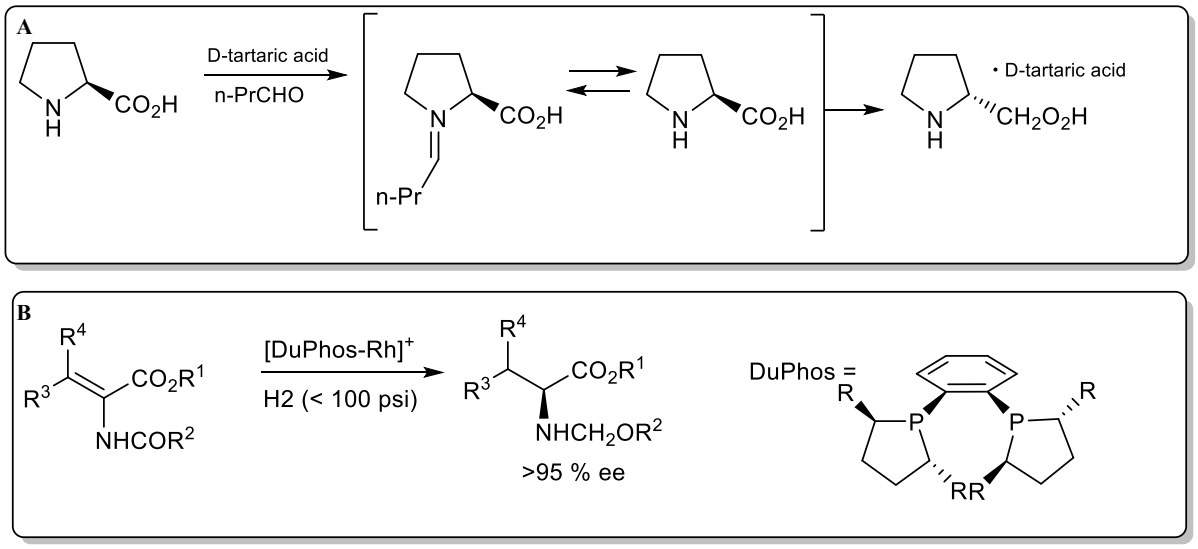

Figure 9: Selected chemical routes for the synthesis of non-canonical α-amino acids
A) Dynamic resolution and B) Metal catalysed hydrogenation of enamids for the production of non-canonical α-amino acids. Figure modified after [105], [106] and [107].

βAAs are chemically generated through asymmetric synthesis, stoichiometric use of chiral auxiliaries of homologation of α-amino acids. Due to the high number of synthesis approaches only a few examples will be described. An example for the use of metal catalysts is the hydrogenation of (*Z*)-enamine esters to the corresponding amino ester by using a ferrocenylphospine ligand. The advantage of this method is the enantiomeric excess (*ee)* of up to 97 % but using trifluoroethanol as solvent is a disadvatantage. Furthermore the amino ester has to be converted to the corresponding amino acid afterwards, a high pressure of ~6 bar of H_2 and a temperature of 50 ° C are needed (Figure 10 A) [109]. Another approach is the use of Mannich-reaction. E.g. βAAs were obtained by Sodeoka and co-workers through Pd-catalyzed addition of β-ketoesters to α-imino esters. During the reaction several protecting groups (p-methoxyphenyl, Boc and tosyl) are needed (Figure 10 B) [110].

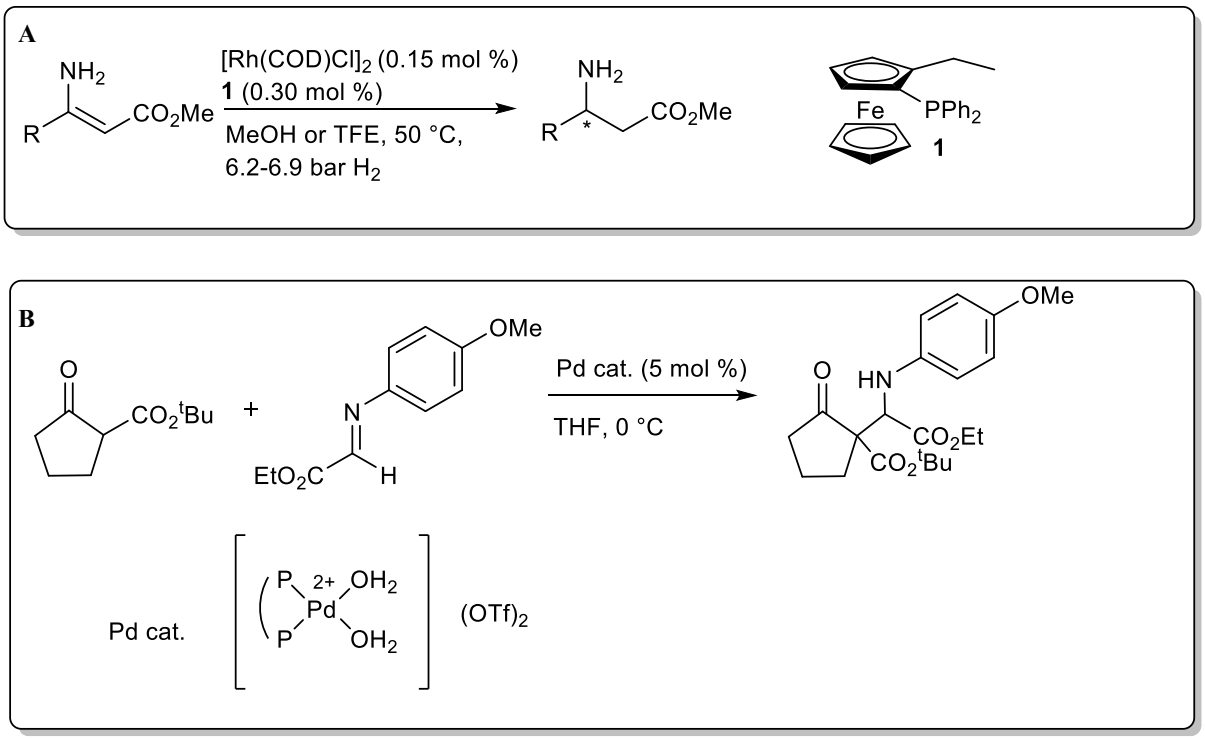

Figure 10: Selected chemical routes for the production of non-canonical-β-amino acid.
A) Hydrogenation of *Z*-enamine esters B) Pd-catalyzed Mannich reaction. Figure modified after [109], [110].

1.4.3 Biotechnological production of non-canonical amino acids

While chemical synthesis of noncAAs is still challenging, enzymes offer an opportunity for a more environmentally friendly synthesis [111]. Benefits are mild and environmentally friendly reaction conditions than in chemical approaches. However the variety of enzymatic biocatalysts is still limited regarding substrate scope and enzyme stability. For special synthesis routes a suitable enzyme has to be discovered first. Drug discovery as well as new trends in biotechnology, such as generation of artificial bio-macromolecules or *in vivo* incorporation of noncAAs into proteins, underline the demand for novel biotechnological synthetic pathways for the production of noncAAs of which selected known enzymatic routes will be highlighted in this section.

NoncAAs are also produced by fermentation or enzymatic production [112]. E.g. L-norvaline, L-norleucine and L-β-methylnorleucine are produced with *E. coli* and directly incorporated into cellular and recombinant proteins [113]. Disadvantage of these processes is the need for a suitable production strain. Engineered strains have to be elaborately developed and many biosynthetic pathways for noncAAs are simply unknown (see section 1.4.1) Furthermore the yields are often quite low [114].

Several non-canonical α-amino acids can be produced using the hydantoinase process, which will be described in more detail in section 1.5. Examples are given in Table 1 p. 24.

Several processes for the production of D/L-α-tertiary leucine are described. In 1987 Hoechst presented a penicillin G acylase (E.C. 3.5.1.4) to hydrolyse *N*-Phac-(*RS*)-tertiary-leucine immobilized on a phenol resin. However, the use of this enzyme requires subsequent separation of (*R*)- and (*S*)-enantiomers. Additionally an enantioselective approach for the production of α-tertiary leucine using Lipozyme™ is described. The conditions of this process were quite harsh since toluene, BuOH and a additional Et_3N catalyst are needed (Figure 11 A) [115]. Degussa presented a synthesis using a D-Hydantoinase to convert tert-butylhydantoin to *N*-carbamoyl-(*R*)-tert-leucine. However the second step to α-tertiary leucine is conducted chemically with HNO_2 at extreme acidic conditions of pH 0 [115] (Figure 11 B).

Different thienylalanine derivates were generated using a whole cell process. Thereby enolcarbonyl acids were transferred to the corresponding L-3-(2-thienylalanine) through catalysis of transaminases [116].

Several enzymatic routes for the production of non-canonical α-amino acids through engineered enzymes have been developed over the past years. Ammonia lyases are described for the asymmetric addition of ammonia to easy available prochirale substrates like fumarate or cinnamic acid analogues. They catalyse the reversible carbon-nitrogen bond cleavage to *trans*-α,β-unsaturated carboxylic acid and ammonia [117]. Depending on their substrate they are distinguished in different classes [117]. One example for the production of non-canonical α-amino acids is the engineered methylaspartate ammonia lyase (MAL) from *Clostridium tetanomorphum* (C*t*MAL). This mutant was able to produce noncAAs with bulky sidechains like *threo*-L-2-hexylaspartate, *threo*-L-2-benzyloxyaspartate and *threo*-L-2-benzylthioaspartate (Figure 11 C) [118]. Another example is the active side remodelling of a tyrosine phenol lyase (TPL) to produce 3-(methylthio)-L-tyrosine. In Figure 11 D the natural catalysis product of TPL is shown, which already represents a noncAA [119].

L-neopentylglycine is obtained through an industrial process developed by Degussa AG in up to 88 g/L scale [120]. Whole cell biocatalysts harvest a leucine dehydrogenase able to catalyse the reductive amination of the corresponding α-keto acid with a conversion efficiency of 95 % and high enantioselectivity (>99 % *ee*) within 25 h. However this process is dependent on the cofactor NADH that is oxidized to NAD^+ during the reaction. Thus an additional enzyme, a formate dehydrogenase has to be present to reduce NAD^+ to NADH again.

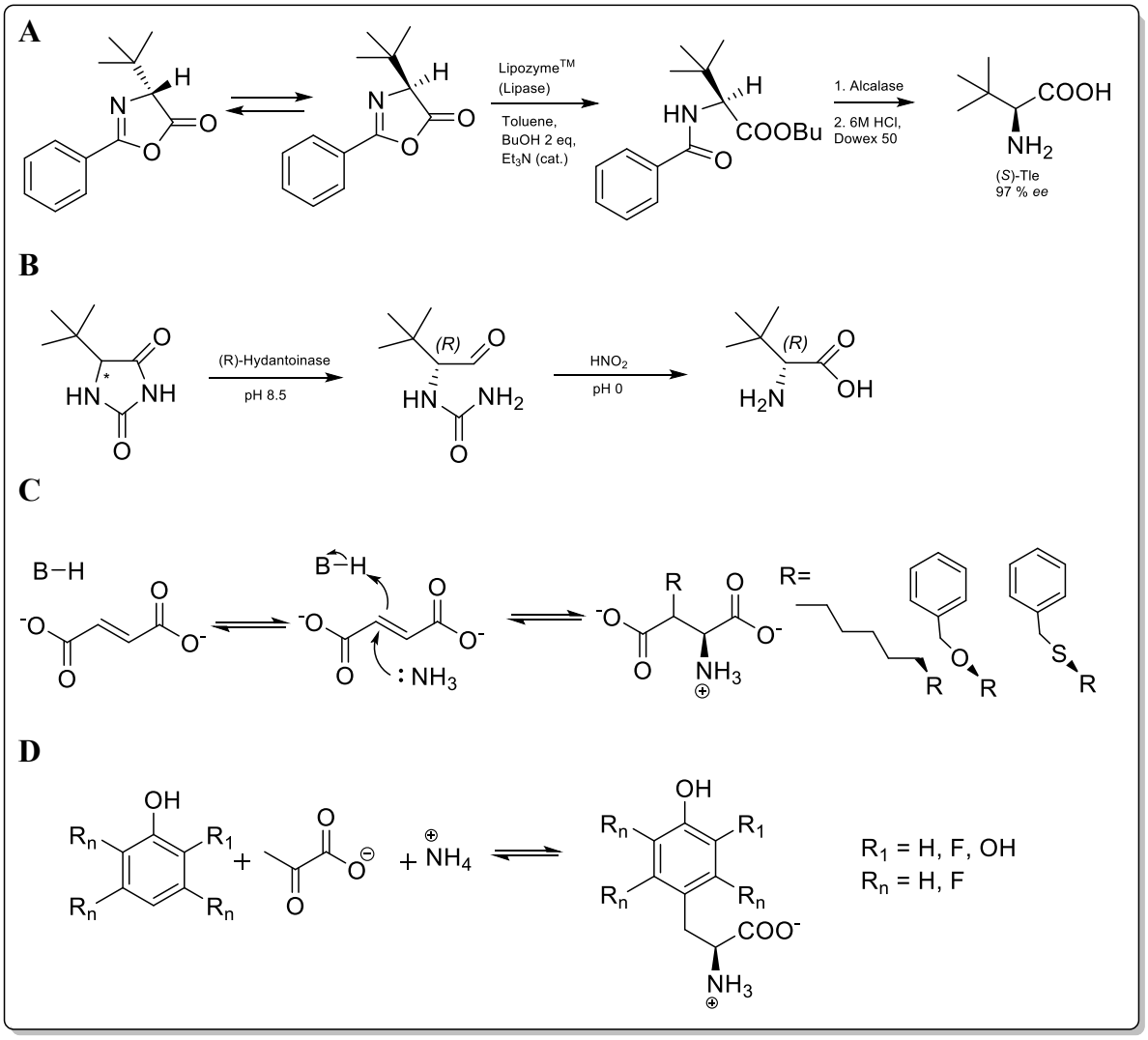

Figure 11: Selected routs for the biotechnological production of non-canonical α-amino acids.
A + B) Industrial processes for the production of α-tertiary leucine. A) Production of (*S*) α-tertiary leucine with Lipozyme B) Semi biocatalytic synthesis of (*R*)-α-tertiary leucine using a hydantoinase. The second step is performed chemically. C) Engineered ammonia lyase from *Clostridium tetanomorphum* for the production of non-canonical α-amino acids. D) Engineered tyrosine phenol lyase for the production of non-canonical α-amino acids. Synthesis routes were modified after [115]–[119]**.**

Several biotechnological routes for the production of chiral aromatic βAAs, especially β-phenylalanine, are known. Often elaborate protein engineering had to be conducted to find one mutant out of hundred thousands which catalyse the reaction [121], [122]. The use of a mutant of a dehydrogenase from *Candidatus Cloacamonas acidaminovorans* leads to βAAs [121]. First a β-keto ester is generated by a nitrilase or lipase and subsequently converted to the corresponding β-amino acid by an engineered β-amino acid dehydrogenase (Figure 12). The chiral βAAs D-β-homo-methionine, D-β-phenylalanine, L-β-aminobutyric acid were produced. One disadvantage is the NAD(P)H dependency of the enzyme, which has so be

regenerated after each cycle. Thus an additional enzyme, an D-glucose dehydrogenase is needed [121].

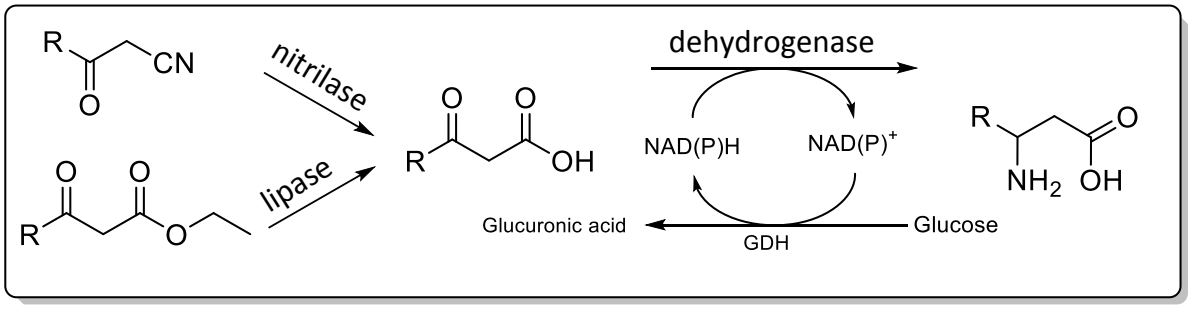

Figure 12: Dehydrogenase mutant from *C. Cloacamonas acidaminovorans* for the production of βAAs. First a β-keto ester has to be generated by a nitrilase or lipase. This β-keto ester is then converted to the corresponding β-amino acid. Figure modified after [121].

A β-amino acid lyase was obtained in 2014 through a high-throughput screening of the aspartase from *Bacillus sp.* YM55-1. Naturally this thermostable enzyme has a limited substrate scope and catalyses the reversible deamination of aspartate to fumarate and ammonia [123]. The mutant BSASP-C6 (Figure 13 A) was found to convert crotonic acid into (*R*)-3-aminobutyrate [122]. Recently in 2018 Li and his co-workers generated several mutants of this enzyme by computational redesign. Four of their designed enzymes were able to catalyse another specific hydroamination reaction (Figure 13 B-E): Design B19 was able to convert 300 g/L crotonic acid to (*R*)-β-aminobutanoic acid (92 % isolated yield), design P1 converted 80 g/L (E)-2-pentenoic acid to (*R*)-β-aminopentanoic acid (84 % isolated yield), design N5 catalyzed the reaction from fumaric acid monoamide (130 g/L) to (*S*)-β-asparagine (88 % isolated yield) and design F29 was able to produce (*S*)-β-phenylalanine (43 % yield out of 15 g/L (E)-cinnamic acid) [124].

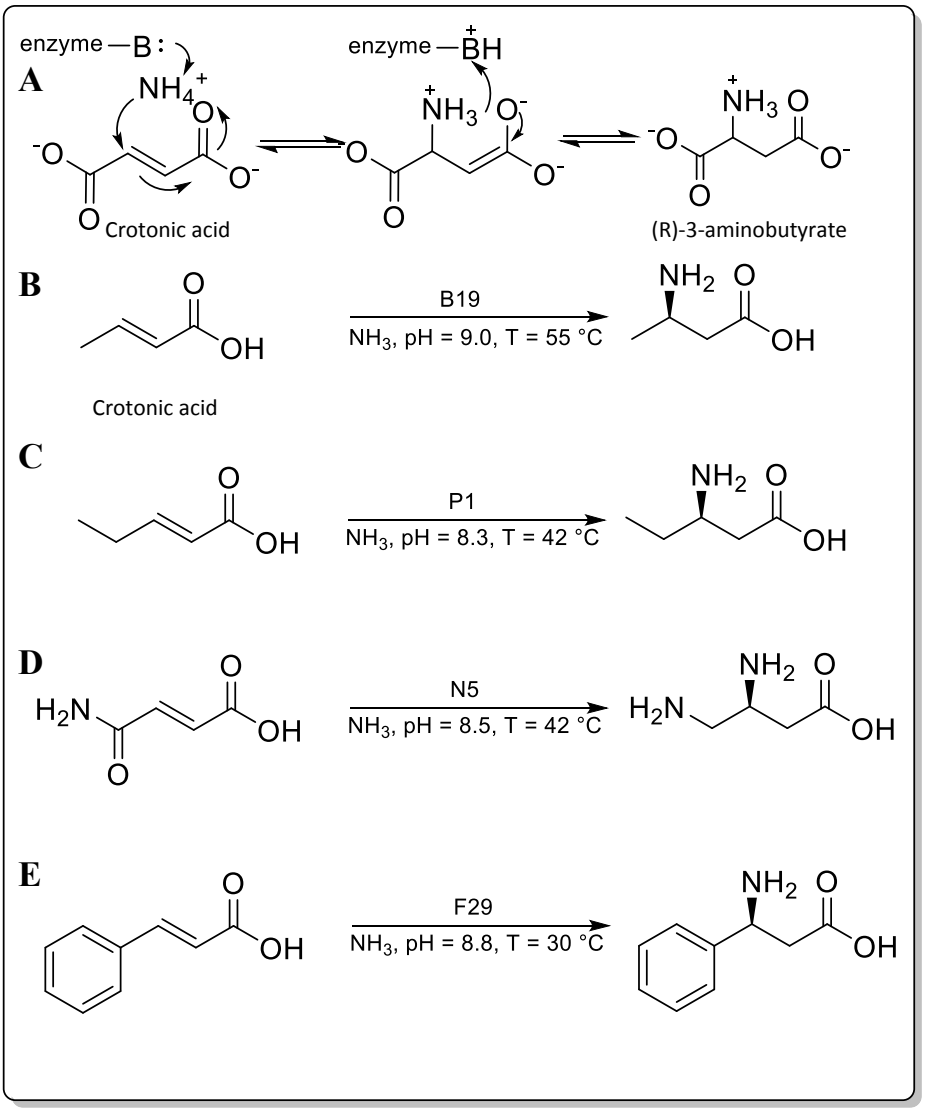

Figure 13: Different β-amino acid lyases for the production of βAAs.
Catalysis of A) Mutant BSASP-C6 B) mutant B19 C) mutant P1 D) mutant N5 and E) mutant F29. Figure modified after [122] and [124].

Aminomutates are strong catalysts, able to shift the amino group of an amino acid from the α- to the β-position. Several approaches have been published for the production of noncAAs using amino mutates as biocatalyst. A phenylalanine aminomutase was used to catalyse the amination of cinnamic acid derivates to chiral β-phenylalanine. As side product also chiral α-phenylalanine was obtained (Figure 14) [125]. Another synthesis of β-phenylalanine was achieved through an engineered metabolic pathway in *E. coli*. The engineered strain expresses a phenylalanine aminomutase from *Pantoea agglomerans*, which converts from 20 mM α-phenylalanine present in minimal medium ~1.4 mg/ml β-phenylalanine. Also other derivates like *m*-bromo-β-phenylalanine was obtained with a 96 % yield in 6 h in 5 ml scale [126].

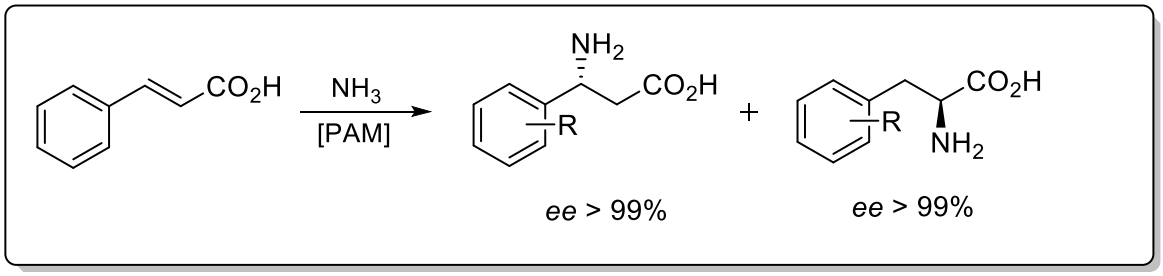

Figure 14: General phenylalanine-aminomutase reaction mechanism.
Figure modified after [125].

Furthermore chiral βAAs are produced using ω-Transaminases (ωTAs). This enzyme class is able to perform the transfer of an amino group from a donor onto an acceptor substrate. The transamination process thereby is dependent on the co-substrate pyridoxal-5'-phosphate (PLP). The formation of chiral (*R*)- and (*S*)-β-phenylalanine was shown by Buß *et al.* in 2018. The screened mutants were able to transfer an amino group onto β-phenylalanine ethyl ester, which is transformed to (*R*)- or (*S*)-β-phenylalanine through isolation or hydrolysation. Amination of β-keto esters is quite challenging since they decompose easily in aqueous solution, which can be circumvented by using an enzyme cascade [127] (Figure 15 A).

Another example for the successful production of a chiral βAA is the amination of β-keto nitriles using nitrilases. In the first step a nitrilase from *Bradyrhizobium japonicum* USDA 110 converts a substituted β-keto-nitrile to the corresponding β-keto ester [128]. Subsequently a ωTA aminates the ester to the chiral βAA. Nitriles are easy to synthesize in a simple and cost-effective way. Several different enantiomerically pure derivates of (*S*)-β-phenylalanine (*ee* 99 %) were obtained using this enzyme cascade (e.g. *p*-fluoro or *o*-methyl-(*S*)-β-phenylalanine) (Figure 15 B) [128]. In 2014 Mathew and co-workers presented the ωTA from *Burkholderia graminis* for the production of chiral βAAs *via* kinetic resolution. (*R*)-β-phenylalanine was obtained out of a solution of *rac*-β-phenylalanine with an enantiomeric excess > 99 % and 50 % conversion (Figure 15 C) [129].

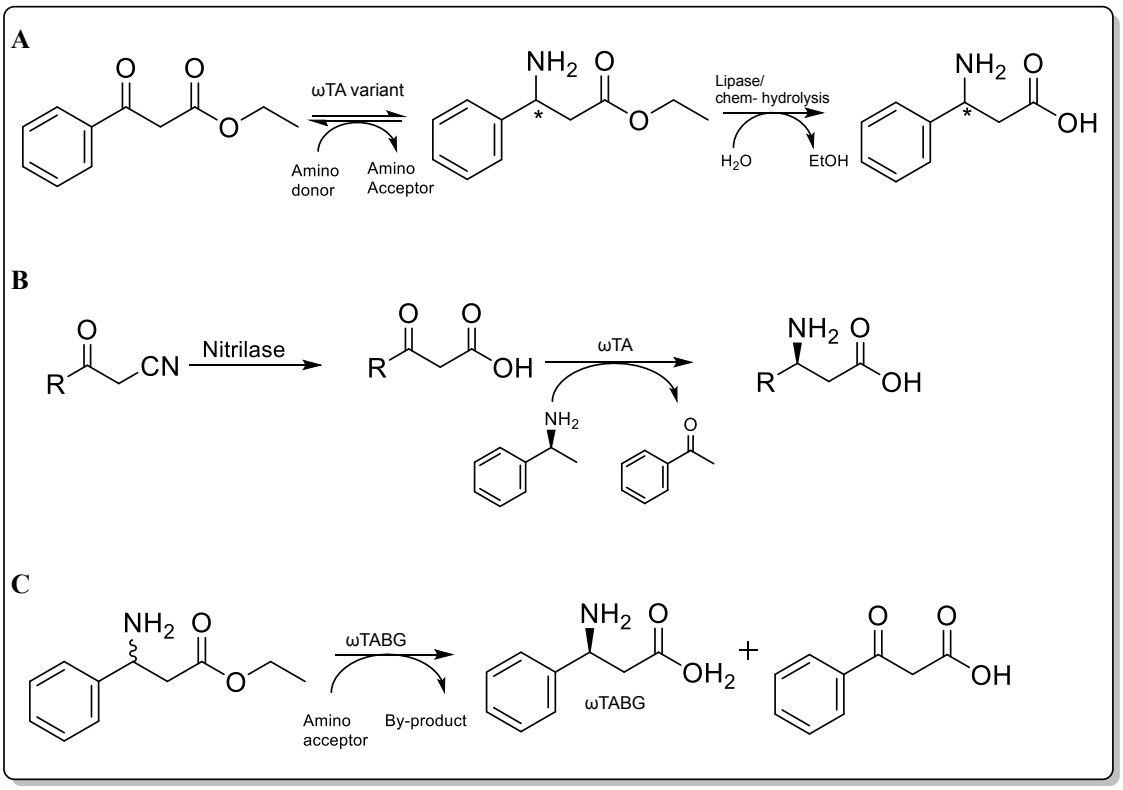

Figure 15: Selected ω-transaminases for the production of β-phenylalanine.
Figure modified after [127] (A), [128] (B) and [129] (C).

Aminoacylases [EC 3.5.1.14] are already applied in industry for the production of α-amino acids and convert an *N*-acyl-L-amino acid to a carboxylate and a L-amino acid. When Gröger and co-workers tried to apply this process to the formation of β-amino acids in 2004 they found that the porcine kidney acylase of type I (PKA I) has a high activity towards cleaving *N*-chloroacetyl-β-amino acid. Several aromatic β-amino acids, such as β-phenylalanine, 4-fluoro-β-phenylalanine, 4-methoxy-β-phenylalanine and 2-thienyl-β-phenylalanine were generated with high enantiomeric excess (*ee* 95-99 %) within 24-48 h [130] (Figure 16).

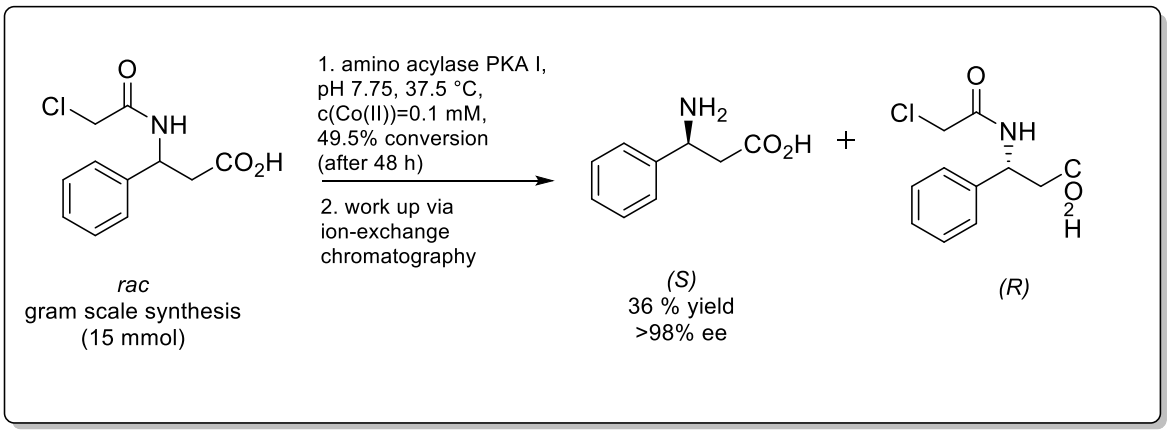

Figure 16: Amino acylase for the production of β-phenylalanine and derivates.
Figure modified after [130].

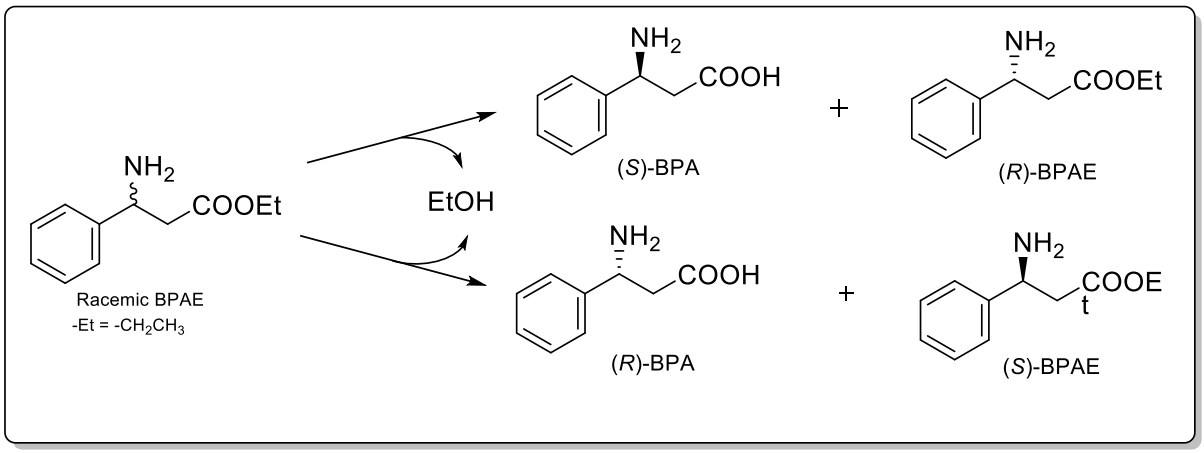

Figure 17: Whole-cell biocatalysts for the production of (*R*)- or (*S*)- β-phenylalanine.
Figure modified after [131].

Additionally whole cell biocatalysts are described for the production of chiral β-phenylalanine. *Sphingobacterium sp. 238C5* and *Arthrobacter sp. 219D2* were found to be able to produce (*R*)- or (*S*)-β-phenylalanine ethyl esters respectively within 48 h and enantiomeric purity of 99 % [131] (Figure 17).

In this work another synthesis strategy for the production of chiral non-canonical α- and β-amino acids was investigated: the hydantoinase-process, which will be explained in more detail in the following section.

There are general advantages for the application of biocatalysts and thus production of noncAAs [111], [132][133]. First there are ecological benefits. Biocatalysts are biodegradable and thus more environmentally friendly. The environmental balance is improved through lower generation of waste and by products. Furthermore the process conditions are safe also due to moderate reaction conditions. For instance the solvent for most enzyme reactions is water. There are also economical advantages such as lower costs, less power requirements and raw material input as well as water consumption. Third there are several functional benefits. E.g. new catalytic reactions can be applied, which are conductible using chemical catalysts. A big advantage is the synthesis without any protective groups since those are often toxic. Biocatalysts can also perform enantioselective reactions with an additional higher specificity. Furthermore usually less purification steps are needed. Thus a higher space-time yield is achieved also due to less synthesis steps. [111], [132][133]

1.5 Hydantoinase process

The hydantoinase process has been established in industry and is applied for the production of non-canonical D-αAAs [134]–[138]. In total the hydantoinase process consists of a cascade of three enzymes [139]. A substituted hydantoin- or pyrimidine-ring is cleaved by a hydantoinase. The enzyme hydrolyses the amid bond as marked in Figure 18 A, resulting in the formation of a corresponding *N*-carbamoyl-α-amino acid. In a second step a carbamoylase leads to the release of CO_2 and NH_3 by cleaving off the carbamoyl-residue. Due to specificity of the enzymes an enantiopure product is generated. In addition a hydantoin-racemase [E.C. 5.1.99.5] is used for the racemisation of the remaining 5-monosubstitued hydantoin [140]. Thus a 100 % yield of the desired enantiomer is achieved. D-α-amino acids are involved in the synthesis of antibiotics, pesticides, sweeteners and other biologically active peptides [135]. E.g. D-phenylglycines are intermediates in semi-synthetic penicillins and cephalosporins and D-homo-citrulline is a building block of the potent LH-RH antagonist [141]. In general the chirality of the compounds plays an essential role in these products. During industrial application of the hydantoinase process whole cells are used in free or immobilized form [142].

Canonical and non-canonical amino acids produced with the hydantoinase process are given in Table 1. Additionally the production of L-β-2-thienylylanine can be performed with the hydantoinase process using cells from *Arthrobacter sp*. and *Flavobacterium sp*. [140].

Table 1: Amino acid produced with the hydantoinase process.
Data obtained from Pietzsch and Syldatk (2002) [140].

5-Substituted Hydantoins	Corresponding amino Acid
p-Hydroxyphenylhydantoin	*p*-Hydroxy-phenylglycine
Phenylhydantoin	Phenylglycine
Hydroxymethylhydantoin	Serine
Phenylethylhydantoin	Homo-phenylalanine
Benzylhydantoin	Phenylalanine
Methylthioethylhydantoin	Methionine
Neopentylhydantoin	γ -Methyleucine
1-Hydroxyethylhydantoin	Alothreonine
Trimethylsilylmethylhydantoin	1-3-Trimethylsilyl-alanine
3´-Ureidopropylhydantoin	Citruline
1´-Methylethylhydantoin	Aloisoleucine
Imidazolylmethylhydantoin	Histidine
Isobutylhydantoin	Leucine
Methylhydantoin	Alanine
Ethylhydantoin	2-Aminobutyric acid
Isopropylhydantoin	Valine

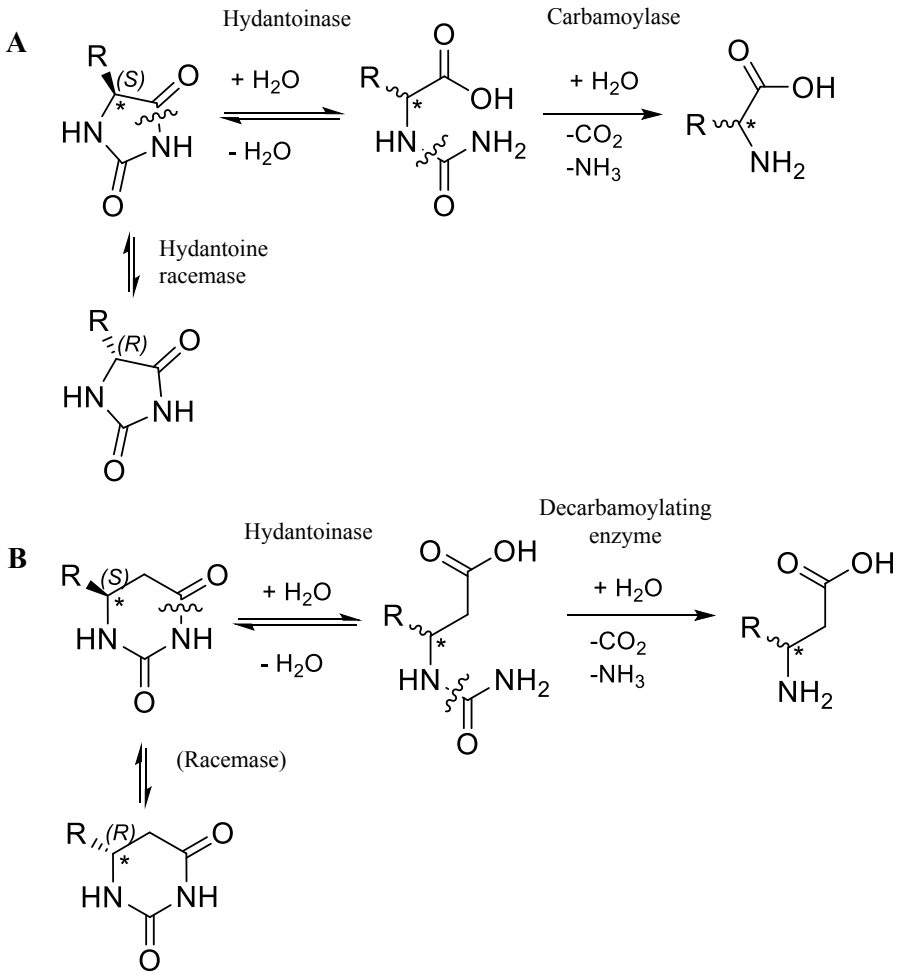

Figure 18: Hydantoinase process and dihydropyrimidinase process.
A) Hydantoinase process for the production of chiral α-amino acids. A hydantoinase cleaves the substituted hydantoin, which leads to the formation of an *N*-carbamoyl-α-amino acid that is further cleaved by a carbamoylases to the corresponding D- or L-α-amino acid. The process is applied in industry for the production of D-α-amino acids. B) Theoretical modified hydantoinase process for the production of chiral β-amino acids. Starting molecule is a substituted dihydropyrimidine instead of a hydantoin. By cleavage of the amide bond a N-carbamoyl-β-amino acid is formed and a second decarbamoylating enzyme would lead to the corresponding chiral β-amino acid. This process is only theoretical and not established yet. R= amino acid residue.

The starting molecules of the process - hydantoins - were already discovered in 1861 by Baeyer [143]. Since the 1930s 5,5'-disubstituted hydantoin derivates have been of pharmacological interest. Hydantoins can be easily synthesized from cheap chemicals as shown in Figure 19 [140], [144]. This circumstance makes the hydantoinase process economically useful since highly valuable optically pure α-amino acids are produced from cheap bulk chemicals.

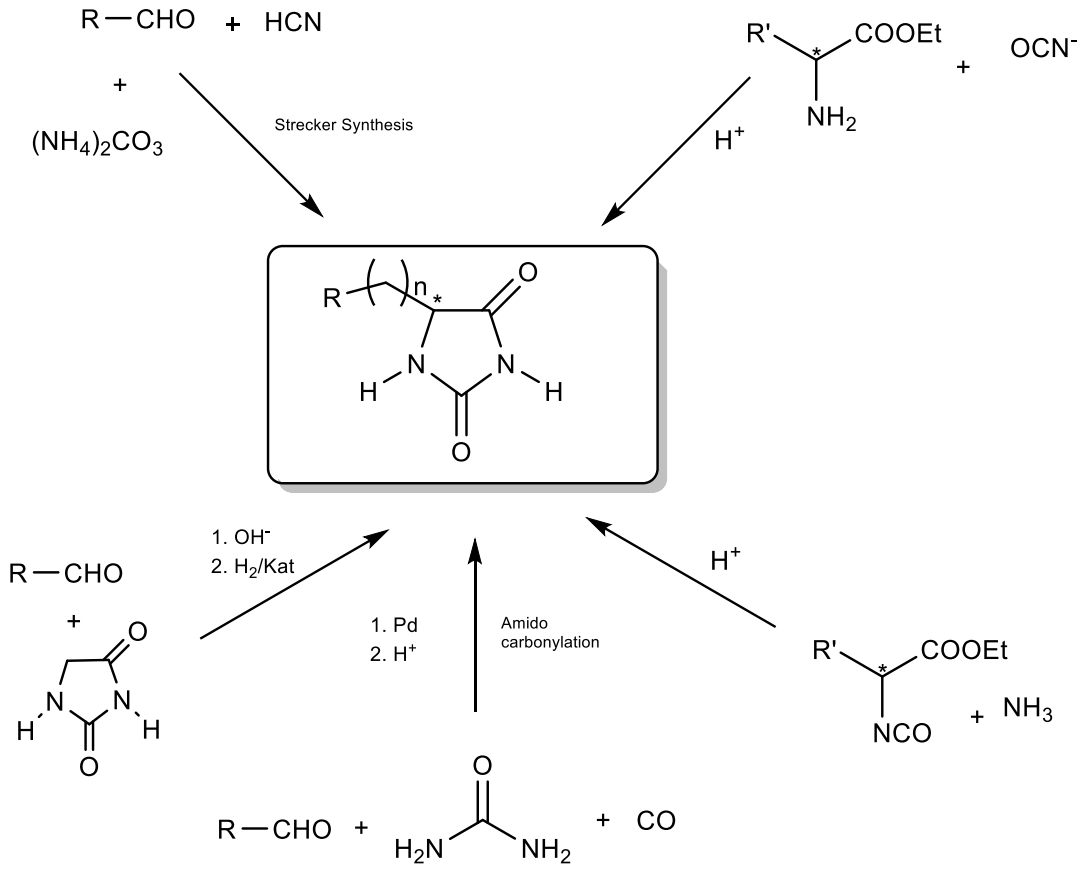

Figure 19: Chemical routes for the synthesis of substituted hydantoines.
Figure was modified after [140].

Aim of this thesis is the enzymatic production of chiral β^3-amino acids. By using a dihydropyrimidine as educt instead of a hydantoin chiral β^3AAs could be formed as demonstrated in Figure 18 B [145]. In this theoretical modified hydantoinase process a substituted dihydropyrimidine is cleaved to a *N*-carbamoyl-β^3-amino acid by a cyclic amidase (hydantoinase). A suitable decarbamoylating enzyme with affinity towards this substrate would lead to the formation of the corresponding chiral β^3AA. For example the conversion of phenyldihydrouracil (PheDU) to *N*-carbamoyl-β^3-phenylalanine has already been reported

[146]. However until today no decarbamoylating enzyme for the conversion of *N*-carbamoyl-β^3-phenylalanine to β^3-phenylalanine is known. The only aliphatic β^3AA which has been generated by a decarbamoylating enzyme (except the natural βAla) is β-homo-L-alanine with the β-ureidopropionase from *Agrobacterium tumefaciens* C58 [147]. In contrast to that the formation of several β^2-amino acids has been reported e.g. α-phenyl-β-alanine [147][148].

1.5.1 Hydantoinases

Hydantoinases, also called dihydropyrimidinases [E.C. 3.5.2.2] belong to the family of amidohydrolases and catalyse the first step of the hydantoinase process, the hydrolysis of hydantoins (imidazolidine-2,4-dione) [149]. The biological function of hydantoinases still remains unclear, although some D-hydantoinases exhibit dihydropyrimidinase activity [150]. Dihydropyrimidinases are involved in the reductive catabolism of pyrimidines [151] and hydrolyse dihydrouracil to β-ureidopropionate (*N*-carbamoyl-β-alanine) [1]. Hydantoinase activity can be induced in wild-type strains with 5-substituted hydantoins, such as indolymethylhydantoin [152].

As already mentioned hydantoinases are of great importance for the production of α-amino acids by using the hydantoinase process [135]. Since there is a big interest in new non natural amino acid derivates there have been many investigations on hydantoinases and the chemical synthesis of hydantoin derivates [140]. The most important application for hydantoinases is the production of D-(4-hydroxyphenyl)glycine, used for the semi synthetic production of the antibiotics amoxicillin and cephadroxyl [138], [153]. The appropiate D-hydantoinases and hydantoin racemases for this process can be found in *Agrobacterium sp*., *Pseudomonas sp*., *Arthrobacter crystallopoites*, and *Sinorhizobium morelense* [154]–[157]. One example of a well-known enzyme of this class is the hydantoinase from *Arthrobacter aurescens* DSM 3745, which shows a broad substrate scope [158].

During the past decades the focus for hydantoinases was mostly on the production of natural L- and unnatural α-D-amino acids. However the industrial production of canonical L-α-amino acids is mostly conducted by fermentation processes [159]. Only a few hydantoinases are known for the production of chiral βAAs. Engel *et al.* presented several bacterial strains which were able to convert PheDU enantioselectively to D- or L-NCβPhe [146]. Furthermore the hydantoinase from *Arthrobacter crystallopoietes* DM20117 converts 6-(4-

nitrophenyl)dihydropyrimidine-2,4(1H,3H)-dione (pNO2PheDU) leading to the corresponding *para*-nitro-β-phenylalanine [160].

Hydantoinases show significant sequence similarities, even if their function is diverse. A few 3D-tertiary crystal structures of hydantoinases are available giving some insight into the L- or D-enantioselectivity. Examples are the L-hydantoinase from *Arthrobacter aurescens* (PDB 1GKR) [161] and the D-hydantoinase from *Geobacillus stearothermophilus* (PDB 1K1D) [162]. They show a classic TIM barrel fold and build a tetramer, whereby the tetramer (Figure 20). The active site of D-hydantoinase of *G. stearothermophilus* consists of Met-63, Leu-65, Phe-152, Phe-159 and Tyr-155 [162].

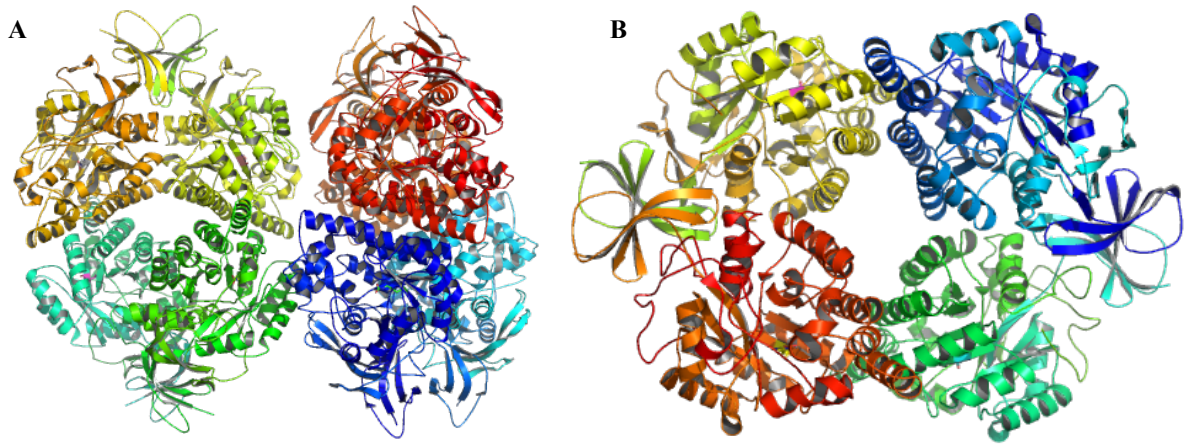

Figure 20: Tertiary structures of hydantoinases.
A) D-hydantoinase from *G. stearothermophilus* B) L-hydantoinase from *A. aurescens*. Structures were edited in PyMol.

1.5.2 Decarbamoylating enzymes

In this thesis the term “decarbamoylating enzyme” will be used to summarize all enzyme classes known to cleave off the carbamoyl-residue of a *N*-carbamoyl-amino acid and leads to the release of a CO_2 and NH_3 molecule. This definition applies to four enzyme classes: β-Ureidopropionases, L-carbamoylases, D-carbamoylases and Allantoate amidohydrolases [163]. An overview of the four enzyme classes and their catalytic reactions is given in Figure 21.

β-ureidopropionases (βUps), L-carbamoylases and allantoate amidohydrolases share a high sequence and structure similarity. Compared to this D-carbamoylases have a quite different tertiary structure (Figure 22).

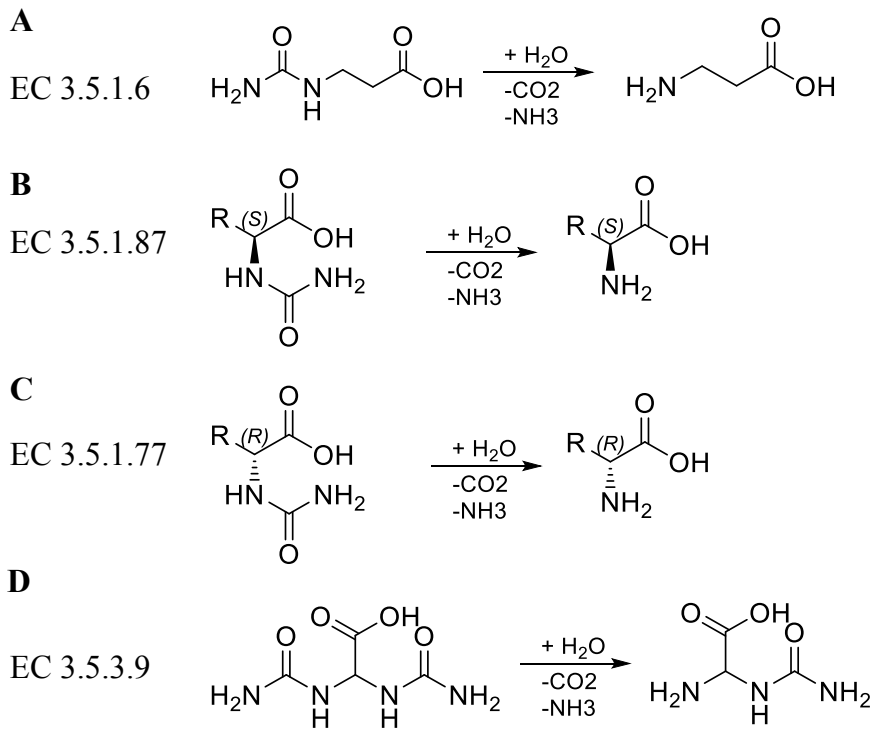

Figure 21: Classes of decarbamoylating enzymes.
A) βUps convert *N*-carbamoyl-β-alanine to β-alanine B) L-Carbs convert *N*-carbamoyl-L-α-amino acids to L-α-amino acids C) D-Carbs convert *N*-carbamoyl-D-α-amino acids to D-α-amino acids D) AaHyds convert allantoic acid to ureidoglycine.

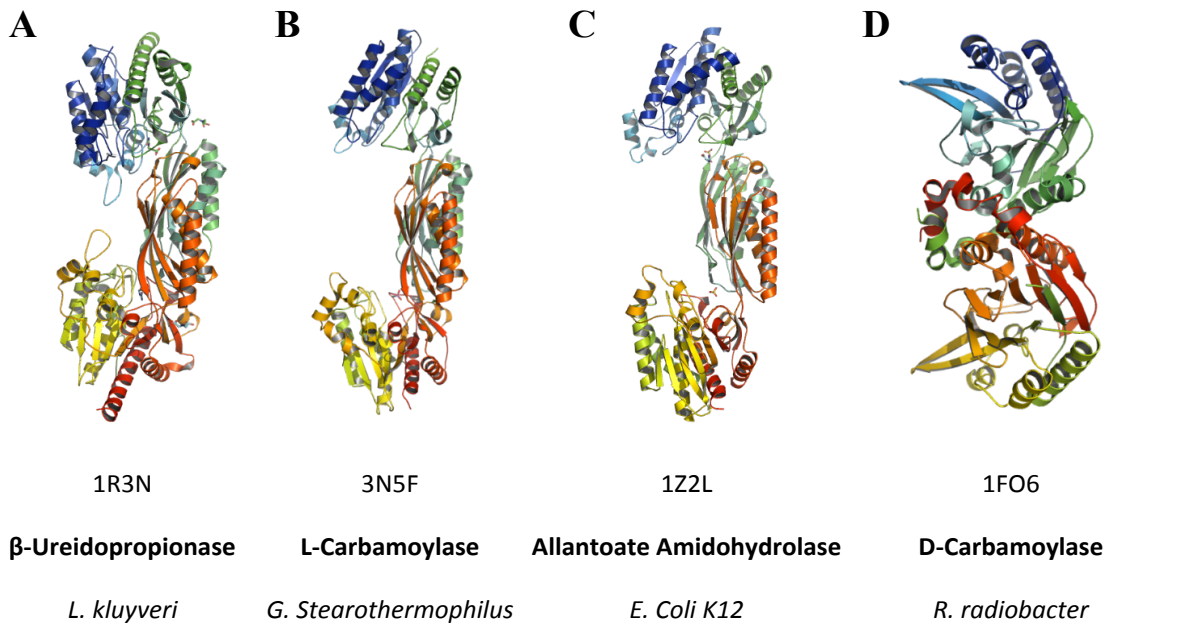

Figure 22: Comparison of representative homodimer crystal structures of each class of decarbamoylating enzyme.
A) βUp from *Lachancea kluyveri* (PDB 1R3N) in open conformation without bound substrate B) L-Carb from *Geobacillus stearothermophilus* (PDB 3N5F) without bound substrate C) Allantoate amidohydrolases from *Escherichia coli* K12 with bound substrate allantoic acid (PDB 1Z2L) D) D-Carb from *Rhizobium radiobacter* (PDB 1FO6) without bound substrate.

β-ureidopropionases (also known as β-alanine synthase or *N*-carbamoyl-β-alanine amidohydrolase) [E.C. 3.5.1.6] are part of the pyrimidine catabolism. They hydrolyze their natural substrate 3-ureido-propionic acid (NCβAla) or β-ureidoisobutyric (βUBut) acid to the βAA 3-amino-propionic acid (β-alanine (βAla)) or 3-aminoisobutyric acid (Figure 21 A, p. 29) [164]. In the humans e.g. a βUp deficiency leads to neurological disorder [165]. Several βUps were isolated e.g. from human [166], rats [167], plants [168] or bacteria [169] [52]. Still the knowledge of βUps is quite limited. Furthermore only a few of these enzymes have been recombinantly expressed in *E. coli* and characterized towards their substrate scope beside NCβAla or βUBut.

The best-known bacterial enzymes of this class are the βUps from *Agrobacterium tumefaciens* C58 ATCC 33970 *(A. tumefaciens)* [148], *Lachancea kluyveri (L. kluyveri)* [170]–[173] and *Pseudomonas putida* (*P. putida*) [52]. For all of them a degradation of NCβAla was proven. The βUp from *A. tumefaciens (At*βcar) shows broad substrate promiscuity [148]. It is able to degrade aliphatic substrates such as *N*-carbamoyl-α-L-glycine (NCαGly), *N*-carbamoyl-α-L-methionine and or aromatic *N*-carbamoyl-α-L-phenylalanine. The hydrolysis of *N*-carbamoyl-α-amino acids is strictly L-enantiomer specific. A degradation of corresponding D-enantiomers was not observed for this enzyme. For some *N*-carbamoyl-β-amino acids (NCβAAs) an

activity was observed, but only α-substituted (= β^2-amino acids) and not β-substituted βAAs were detected (e.g. α-phenyl-β-alanine). The only β^3-amino acid that was obtained was β-homo-alanine. A degradation of other NCβAAs such as *N*-carbamoyl-β-L-homo-methionine, *N*-carbamoyl-β-L-phenylalanine or *N*-carbamoyl-β-L-leucine was not observed. It is worth mentioning that the affinity towards *N*-acetyl-β-alanine was over a hundred times lower than towards NCβAla. This observation demonstrates the high substrate specificity of this enzyme class. Additionally Atβcar was able to cleave a couple of *N*-carbamoyl-γ- and δ-amino acids [147]. Furthermore some protein engineering studies were performed. It was shown that the mutation of alanine at position 359 to glycine caused a higher affinity towards NCβAla and NCαGly. Thereby the K_m-values compared to the wild-type enzyme were lowered from 5.41 to 5.02 mM for NCβAla and from 2.61 to 1.99 mM for NCαGly respectively [147]. The influence of this mutation towards the enantioselectivity of the mutant was not investigated in this study.

The βUp enzyme from *P. putida* (PutβUp) is described as a βUp even though the K_m-values for NCβAla (3.74 mM) are higher than for aliphatic NCαAAs (0.68 mM) with small substituents [52]. The PutβUp is not degrading other α-substrates with more bulky substituents like *N*-carbamoyl-α-leucine, *N*-carbamoyl-α-phenylalanine or *N*-carbamoyl-α-tryptophan. For this enzyme also L-enantiomer specificity is described, *N*-carbamoyl-α-D-amino acids were not converted.

In comparison to Atβcar and PutβUp the βUp from *L. kluyveri* (SklβUp) is way less characterized regarding to the substrate scope. Only the degradation of NCβAla (K_m ~ 60 mM), βUBut and 2-methyl-3-ureidopropionic acid is described. However until today SklβUp is the sole βUp for which a 3D-x-ray crystal structure is available (1R3N). Regarding to its structure SklβUp was identified as a member of the aminoacylase-1/metallopeptidase 20 family. Lundgren *et al.* proposed a reaction mechanism on basis of the enzyme structure with co-crystallized natural substrate NCβAla (2V8H) and its degradation product βAla (2V8G) [170]. Site directed mutagenesis experiments of SklβUp revealed the residues Q159 and R322 as crucial for the catalysis. Residues H262 and H397 are described as important but not essential for the functionality (see Figure 23 C). One monomer consists of two domains: a catalytic domain, harbouring a di-zinc centre and a smaller dimerization domain. Through substrate-binding the enzyme undergoes a conformation change from an open to a closed conformation, comparable to a snapping trap (Figure 23 A and B).

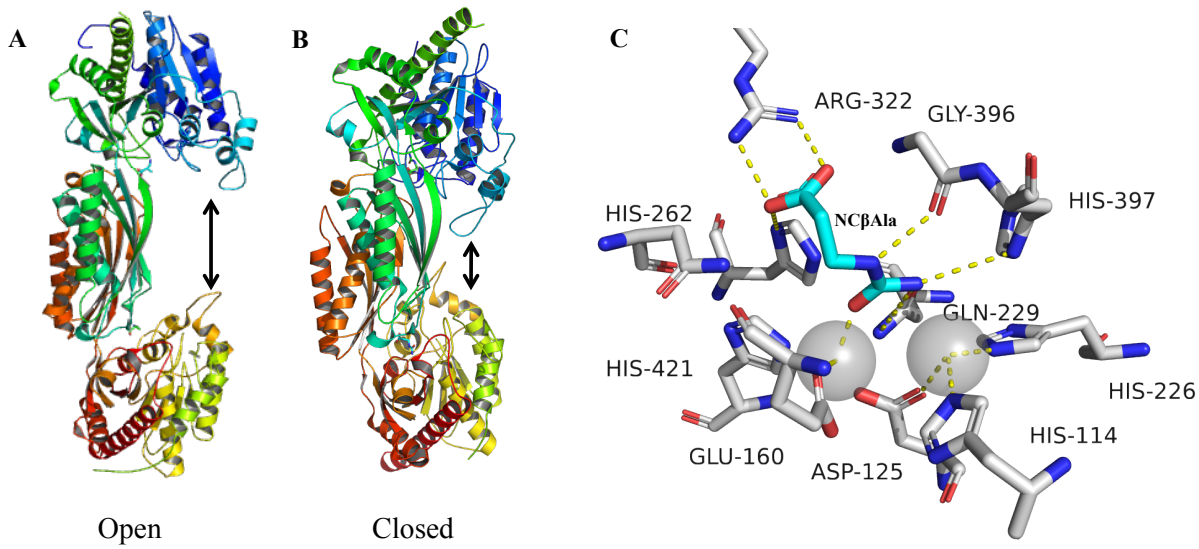

Figure 23: Overview of SklβUps conformation and active site.
A) Open conformation and B) closed conformation of SklβUp. C) Active site of SklβUp with incorporated substrate NCβAla. Figures modified after [173] and [170] using PyMol.

Their quaternary structure is usually built of two homodimers whereby one monomer has a molecular mass of approximately 50 kDa [163].

The reaction mechanism proposed by Lundgren *et al.* is shown in Figure 24 (p. 34). In the first step of catalysis NCβAla binds to the carboxylate-anchoring residues R322, N309 and H262. At the same time the substrate interacts with the metal-ion centre due to domain movements (step 2). Thereby a metal-bound water molecule is activated by Q159. Subsequently in step 3 the OH^- of the activated water molecule nucleophilicly attacks the carbonyl group of NCβAla and a tetrahedral intermediate is formed. This is coordinated by metal-ions, residues H397 and Q229. Then the product βAla is formed by the cleavage of the carbamoyl-residue. This spontaneously decays to CO_2 and NH_3, which are released by the opening of the active site in step 5. Finally the generated βAla is released from the active site and a new bridging water molecule is added.

βUps are usually active in a broad pH- and temperature range. Furthermore for other *N*-carbamoyl-substrates than NCβAla their activity can be enhanced by the addition of divalent metal-ions, such as Mn^{2+}, Ni^{2+} and Co^{2+}.

L-carbamoylases [E.C. 3.5.1.87] convert *N*-carbamoyl-L-α-amino acids to L-α-amino acids (Figure 21, p. 29). Many L-carbamoylases (L-Carbs) are known, since they have been studied intensively for usage in the hydantoinase process. The natural function of these enzymes is still unknown. Like βUps also several L-Carbs are described to degrade more bulky substituted *N*-carbamoyl-α-amino acids, such as *N*-carbamoyl-α-leucine or aromatic *N*-

carbamoyl-α-tyrosine [174], [175]. From all L-carbamoylases known in literature only three were investigated on conversion of NCβAla whereby no degradation was detected. For other L-Carbs the degradation of NCβAla was never tested. L-Carbs are strictly L-specific and are known to be unstable, which makes enzyme purification difficult. Additionally ver L-Carbs require divalent cations for enzymatic activity [175].

While most decarbamoylating enzymes have an optimal temperature in the area of 30-40 °C the L-Carb of *Geobacillus stearothermophilus* CECT43 (GstCarb) has its optimal activity at 60°C [176]. This makes this enzyme quite attractive for the industrial application. Also the formation of L-amino acids was better, when *N*-carbamoyl- instead of *N*-formyl-substrates were used [176]. GstCarb possesses a homodimeric native structure [177], which can be divided in a catalytic and a dimerization domain (Figure 25 A, p. 35). The crystal structure for this enzyme is available (PDB 3N5F) and revealed that the enzyme is member of the peptidase M20/M25/M40 family and possesses a bimetallic centre. By mutational analysis it was proven that Arg286, His225 and Asn273 are involved in substrate binding (His-Asn-Arg triad) (Figure 25 B, p. 35) [178].

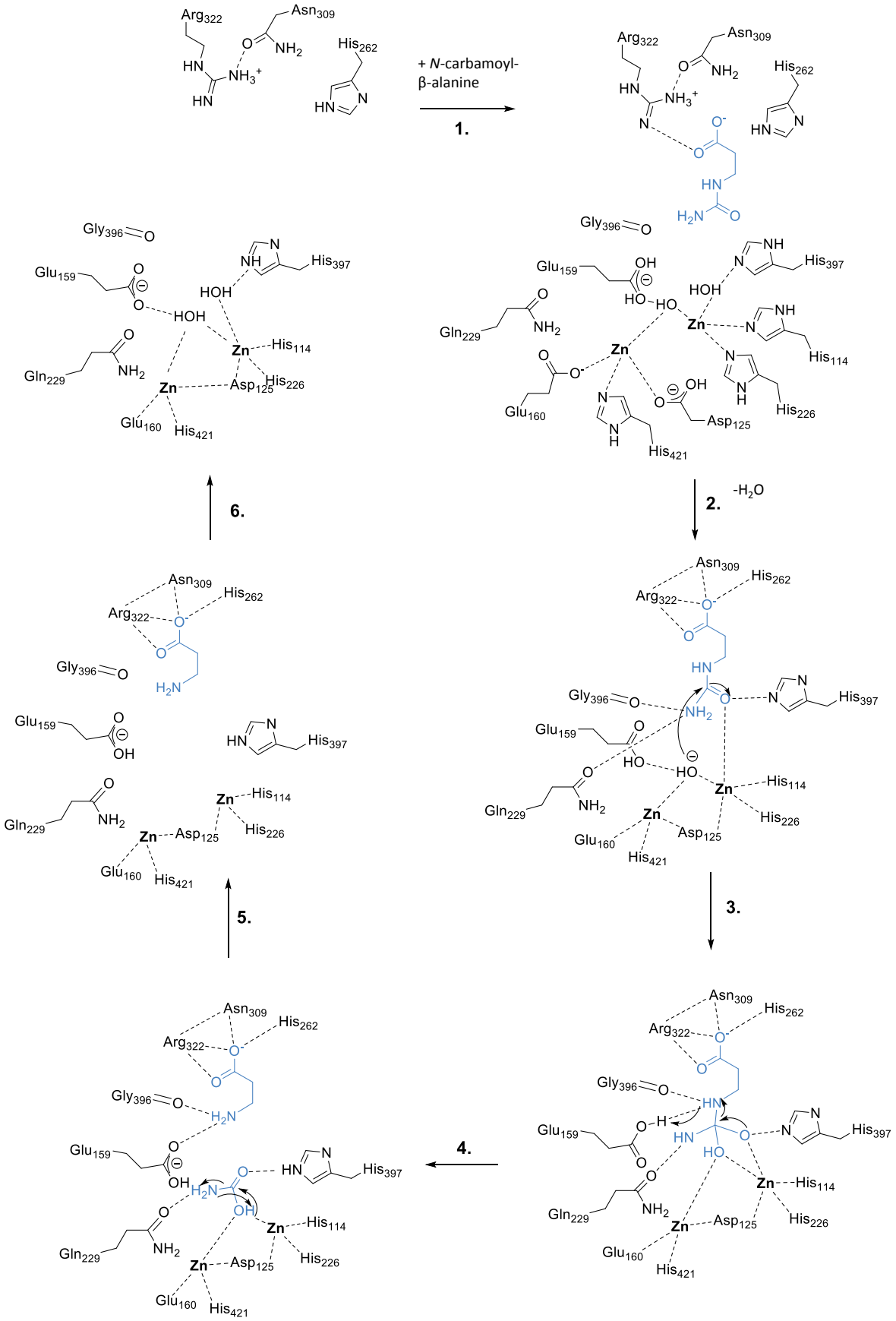

Figure 24: Proposed catalytic mechanism in the active site of SklβUp [173]**.**
Steps 1-6 show the coordination and cleavage of NCβAla (blue) in the catalytic centre. Figure modified after [173]**.**

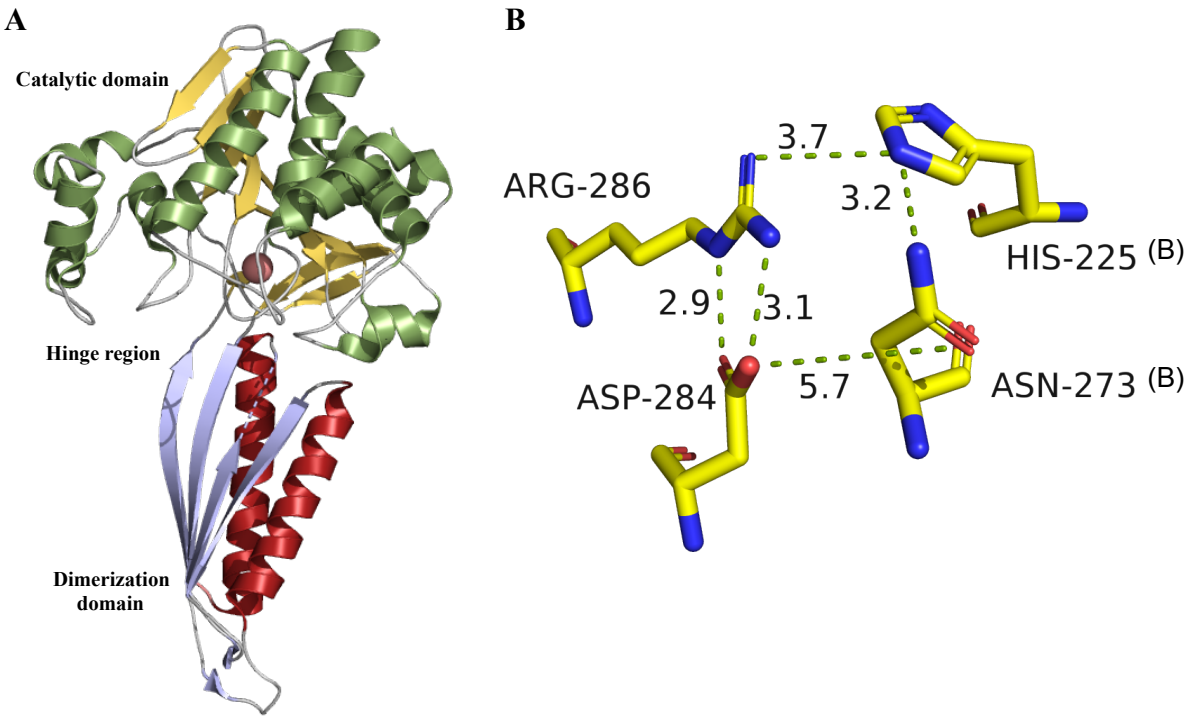

Figure 25: L-Carb from *G. stearothermophilus* (3N5F).
A) The Monomer of the enzyme is divided into a catalytic domain (green and orange) and a dimerization domain (red). B) Highly conserved catalytic triade including Arg286, His225 and Asn273 in the active site of the enzyme. Figures modified after [178] using PyMol.

D-carbamoylases [E.C. 3.5.1.77] show D-enantiomer specificity and convert *N*-carbamoyl-D-α-amino acids (NCDαAA) to D-α-amino acids (Figure 21, p. 29). Like L-Carbs, D-carbamoylases (D-Carbs) are applied in the hydantoinase process for the production of αAAs. Many D-Carbs are well studied in literature but like for L-Carbs their natural function is unknown. D-Carbs are able to hydrolyse NCDαAAs with small residues, but often they also cleave NCDαA with aromatic or bulky amino acid residues [179], [180]. 3D-tertiary crystal structures of D-Carbs are available (PDB 1FO6, 1UF5), whereby 1UF5 is co-crystallized with its substrate *N*-carbamoyl-D-methionine. Hsu et al. first solved the crystal structure of the D-Carb from *Rhizobium radiobacter* in 1998 at a resolution of 2.8 Å [181] and later Wang et al. obtained a structure at 1.95 Å [181]. According to Hsu the natural substrate of this enzyme is *N*-carbamoyl-D-hydroxy-phenyl glycine (K_m: 19 mM and v_{max}: 12 units mg^{-1}). It was revealed that the enzyme exists as a homotetramer. Each subunit consists of one active site and the two sites in the AB dimer are close pairwise across the dyad axis. Each monomer exhibits a four-layer α/β-fold with two six-stranded β-sheets packed on either side by two α-helices (Figure 26 A).

It is suggested that the highly conserved amino acids of the catalytic cleft constitute of Glu47, Lys127, Glu146, Cys172 and Arg176. Probably Cys172 nucleophilicly attacks the C-atom of the carbonyl group, the adjacent Glu47 accepts the proton of the -SH group. Lys127 possibly stabilizes the intermediate. Glu47 then donates a proton to the C-N bond, leading to its instability and cleavage. Subsequently Glu47 activates a water molecule and the resulting OH^- group attacks the carbonyl C-atom of the acyl group, attached to Cys172. After this deacylation Glu47 donates a proton to Cys172 and the acid component is released. Metal-ions are not involved in the catalysis. Site-directed mutagenesis studies of this enzyme revealed that residues His129, His144 are needed to maintain a stable conformation of the putative cleft. Also His215 plays an important role for keeping the tight dimer conformation, which is essential for the enzymatic activity (Figure 26 B) [181].

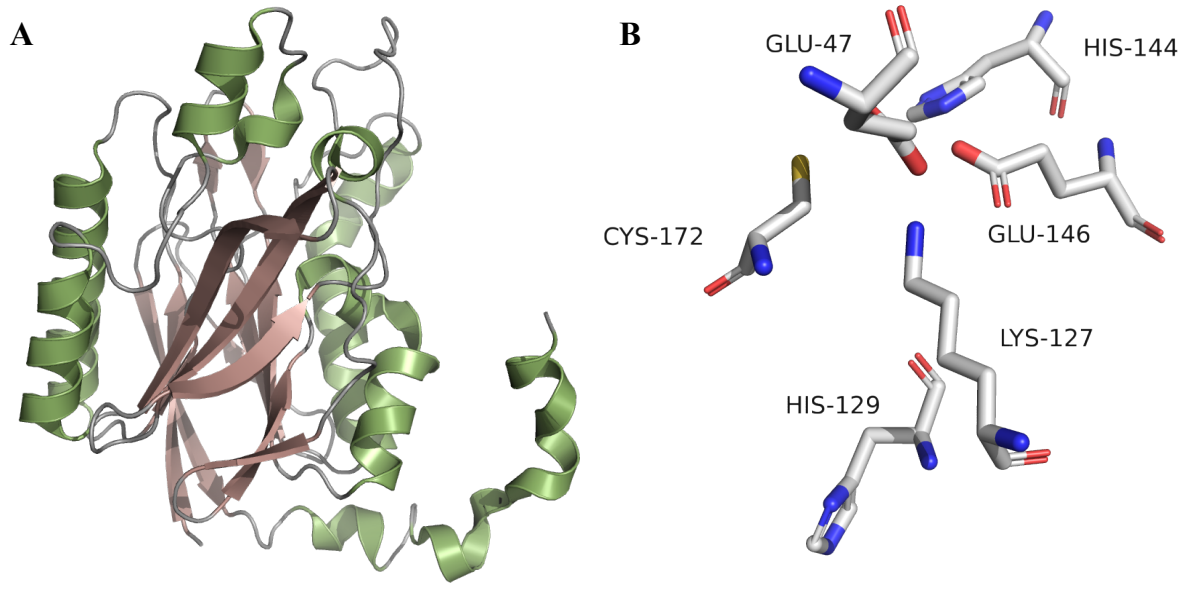

Figure 26: Monomer and active site of D-carbamoylase 1FO6.
A) Monomer with four-layer α/β-fold with two six-stranded β-sheets packed on either side by two α-helices. Figure modified after [181] B) Amino acid residues involed in the catalytic reaction. Figures were made using PyMol.

Allantoate amidohydrolases [E.C. 3.5.3.9] are part of the purine catabolism and naturally convert allantoic acid to ureidoglycine that subsequently decays into (*S*)-ureidoglycolate and ammonia (Figure 21, p. 29). Due to their presence in the purine metabolism they can be found in all five kingdoms. In contrast to that only one recombinantly overexpressed allantoate amidohydrolases (AaHyds) from *E. coli* K12 is described [182].

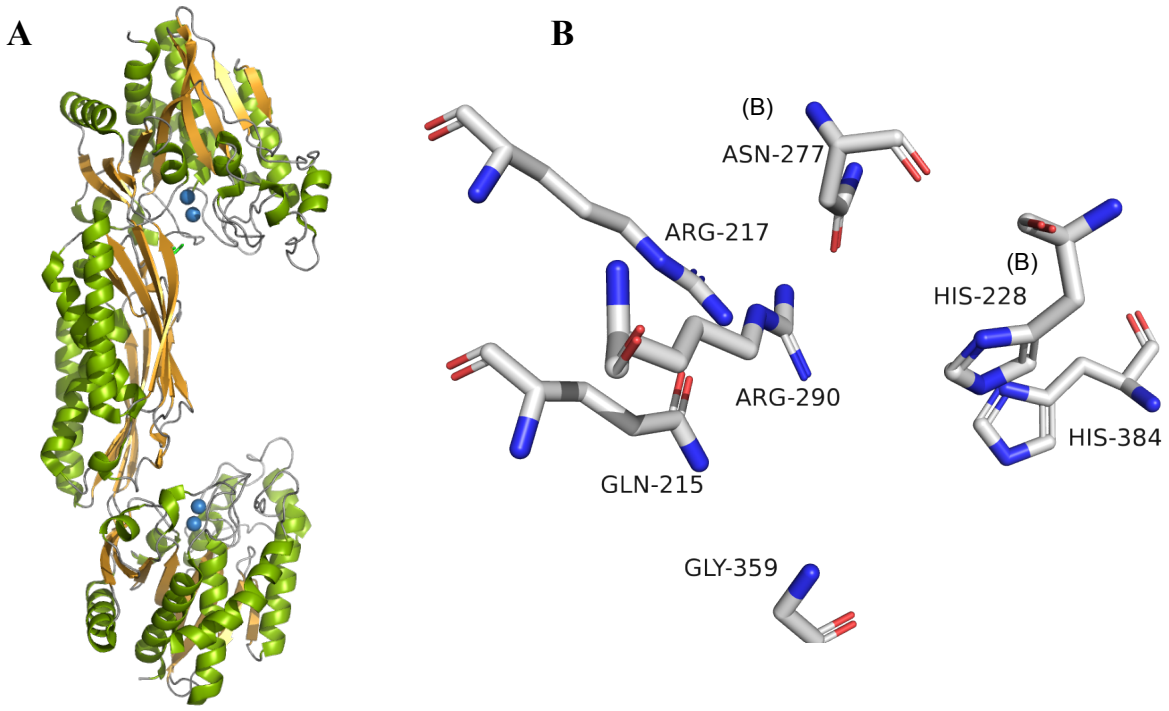

Figure 27: Insights into the AaHyd of *E. coli* K12.
A) Proposed conformation of 1Z2L B) Highly conserved amino acid residues His228, Asn277, Arg290 and His384 of the catalytic centre in complex with allantoic acid (purple). Figures modified after [182].

Also a 3D-tertiary crystal structure is available co-crystallized with bound substrate allantoic acid (PDB 1Z2L). However beside the degradation of allantoic acid to (*S*)-ureidoglycolate no further studies on their substrate scope or enzyme characterization were conducted. By analysis of the crystal structure the residues binding the substrate were identified: His228, Asn277, Arg290 and His384 (Figure 27 A). Like for βUp of *L. kluyveri* an open and closed conformations was proposed by Agarwal and co-workers (Figure 27 B) [182].

Even if structural data of several decarbamoylating enzymes is available, in contrast to other enzyme classes the number of crystal structures is low. The amount of enzymes co-crystallized with their natural substrate is even lower. With a few exceptions it has never been investigated whether these enzymes also accept other naturally occurring *N*-carbamoyl amino acids beside their physiological substrates. Of almost all enzymes able to perform a decarbamoylation-reaction no information about their conversion of *N*-carbamoyl-β-amino acids to the corresponding β-amino acid is known. The sole exception is the conversion of *N*-carbamoyl-β-alanine to β-alanine [172][52], [147]. The βUp *Agrobacterium tumefaciens* C58 is the sole enzyme that has been tested towards its conversion *N*-carbamoyl-β-phenylalanine but no activity was detected: [147, 148]. *N*-carbamoyl-β-amino acids with smaller, less bulky substituents have never been intensively investigated.

1.6 Protein-Ligand Docking

Over the past years the development of experimental techniques like high-throughput protein purification and protein crystallography built the foundation for computational approaches to investigate structural details of proteins and protein-ligand complexes [183]. In contrast to high-throughput screening virtual screening offers the opportunity for a more direct and thus more efficient screening approach with lower costs. Computational methods are a strong tool to predict model ligand interactions when experimental data is not available. Especially when a homologous structure at a sufficient resolution is known [184]. There are several docking programs available, e.g. on ROSIE [185] (Rosetta Online Server that Includes Everyone). Every docking program relies on two components: a method for exploration of the conformational space of the ligand and protein plus a scoring function, evaluating the proposed binding modes [186].

The ligand-docking function available on ROSIE is based on Rosetta and is used for docking of small-molecule ligands into comparative models. Rosetta software includes experimentally validated algorithms for computational modelling and analysis of protein structures and mostly has its advances in computational biology for *de novo* protein design, enzyme design, ligand docking and structure prediction of biological macromolecule and macromolecular complexes [187]–[193]. The Rosetta online server gives non-bioinformaticians the opportunity to conduct docking-simulations in a simplified way [185].

1.7 Protein Engineering

Natural enzymes with a high sequence homology often show a great variability with regard to their substrate scope, activity and stability [194]. The exchange of one single amino acid may drastically influences these properties. Since the beginning of protein engineering in the 1990s nowadays engineering a wild-type enzyme may only take a few months instead of years [195]. Thus protein engineering and the use of single enzymes is now considered more economic and practical nowadays [111]. There exist different strategies for protein engineering: rational design, directed evolution and semi-rational design, a combination of previous two.

For directed evolution the availability of a 3D-strucuture is not necessary. Due to error-prone PCR the full gene is randomly mutated and thus may also lead to unexpected beneficial mutations [196]. An easy high-throughput 96-well plate screening method is essential for

screening of hundred thousands of mutants of the big random mutant-libraries [197]. Rational enzyme design is applied, if the structure and mechanism of an enzyme is already known. Through analysis of the protein structure in combination with bioinformatic tools focused libraries are built [198]. Often big steric residues in the active site are mutated to smaller amino acids, like alanine. Thereby the binding of bulky substrate may be improved.

Semi-rational enzyme design offers the opportunity to identify hot-spot residues without the knowledge of the protein structure. The information on protein sequence, structure and function is combined with computational predictive algorithms to limit the amino acid diversity for protein engineering. This method focuses on specific amino acid residues and thereby reduces the number of mutants which leads to high-quality libraries [199].

2 RESEARCH PROPOSAL

The aim of this thesis is the enzymatic production of chiral non-canonical amino acids, with focus on chiral β^3-amino acids, since they play an important role as building blocks of pharmaceutical drugs or fine chemicals [3]. Until today only a few biotechnological routes for the synthesis of chiral β-amino acids or other non-canonical α-amino acids are known.

A modification of the established hydantoinase process is to be evolved as strategy for this. In this work the focus lies on the second step of this enzyme cascade in which an enzyme may be employed to convert a chiral *N*-carbamoyl-α/β-amino acid to the corresponding non-canonical D- or L-α/β-amino acid. The goal is first and foremost to identify new enzymes and to investigate enzymes known from literature that are able to catalyse this reaction. By using this strategy no enzyme is known to be able to convert chiral *N*-carbamoyl-β-phenylalanine to β-phenylalanine. A hydroxylated derivate of β-phenylalanine is moiety of the cancer drug paclitaxel. Also the production of other aliphatic β^3-amino acids with smaller, less bulky substituents has never been intensively investigated.

Therefor several chiral *N*-carbamoyl-β-amino acid model substrates are to be synthesized. Additionally suiting analytical methods for the detection of these enzyme substrates (*N*-carbamoyl-α/β -amino acids) and their corresponding products (chiral α/β-amino acids) are to be developed. To identify novel enzymes screening of wild-type microorganisms of the institutes own strain collection is to be performed using *N*-carbamoyl-β-alanine and chiral *N*-carbamoyl-β-phenylalanine as model substrate. Therefore an appropriate screening method has to be established. Responsible genes coding for decarbamoylating enzymes from wild-type strains with activity towards selected model substrates are to be identified. These genes are to be cloned and their corresponding enzymes are supposed to be recombinantly expressed in *E. coli*. For the production of chiral non-canonical amino acids expression and purification methods are to be adapted to investigate these enzymes towards their activity. Additionally the substrate scope of these enzymes is to be investigated. Furthermore *in silico* observation of the enzymes are to be examined and possibilities for protein engineering are to be considered.

3 MATERIAL AND METHODS

3.1 Material

3.1.1 Microorganisms

3.1.1.1 Bacterial strains for genetic work

Table 2: *E. coli* strains used for cloning and recombinant protein expression

Organism	Genotype	Supplier
Escherichia coli BL21 DE3	*E. coli* B / r, $^{-}$ *ompT hsdSB* ($r_B^- m_B^-$) *gal dcm rne131* (DE3)	Insitute strain collection
Escherichia coli XL1blue	*ec*A1, *end*A1, *gyr*A96, *thi-1*, *hsd*R17(r_K^- ,m_K^+), *sup*E44, *rel*A1,l^-, [F' *pro*AB, *lac*I^q Z Δ*M15*, Tn10(Tet^r)]	Stratagene

3.1.1.2 Bacterial and fungal strains used in the screening

Strains used in screening experiments were received from the institutes own strain collection of the Institute of Technical Biology (KIT). The strain collection includes verified DSMZ-strains and isolates from soil.

Table 3: List of all bacteria, yeast and fungi used in screening experiments.
I = Soil isolate; IASC = Isolate of antarctic seal cadaver.

Internal Code	Organism	DSM	Cultivation Temp. (°C)	Type	Source
81	*1*		25	Yeast	I
AA1	*Arthrobacer* sp.		20	Bacterial	IASC
1	*Arthrobacter agilis*	20550	22	Bacterial	
2	*Arthrobacter atrocyaneus*	20127	30	Bacterial	
4	*Arthrobacter aurescens*	20116	30	Bacterial	
3	*Arthrobacter aurescens*	3745	30	Bacterial	
5	*Arthrobacter chlorophenolicus*	12829	28	Bacterial	
6	*Arthrobacter citreus*	20133	30	Bacterial	
AA26	*Arthrobacter cryotolerans*		20	Bacterial	IASC
7	*Arthrobacter crystallopoietes*	20117	30	Bacterial	
8	*Arthrobacter globiformis*	20124	30	Bacterial	
9	*Arthrobacter histidinolovorans*	20115	30	Bacterial	
10	*Arthrobacter ilicis*	20138	30	Bacterial	
11	*Arthrobacter methylotrophus*	14008	25	Bacterial	
12	*Arthrobacter nasiphocae*	13988	30	Bacterial	
13	*Arthrobacter nicotianae*	20123	30	Bacterial	
14	*Arthrobacter nicotinovorans*	420	30	Bacterial	

Internal Code	Organism	DSM	Cultivation Temp. (°C)	Type	Source
AA27	*Arthrobacter nitroguajacolicus*		20	Bacterial	IASC
15	*Arthrobacter oxydans*	20119	30	Bacterial	
16	*Arthrobacter pascens*	20545	30	Bacterial	
17	*Arthrobacter polychromogenes*	20136	30	Bacterial	
18	*Arthrobacter polychromogenes*	342	30	Bacterial	
19	*Arthrobacter protophormiae*	20644	30	Bacterial	
AA7	*Arthrobacter psychrochitinophilus*		20	Bacterial	IASC
20	*Arthrobacter psychrolactophilus*	15612	28	Bacterial	
AA2	*Arthrobacter psychrolactophilus*		20	Bacterial	IASC
AA3	*Arthrobacter psychrolactophilus*		20	Bacterial	IASC
AA4	*Arthrobacter psychrolactophilus*		20	Bacterial	IASC
AA5	*Arthrobacter psychrolactophilus*		20	Bacterial	IASC
AA9	*Arthrobacter psychrolactophilus*		20	Bacterial	IASC
AA12	*Arthrobacter psychrolactophilus*		20	Bacterial	IASC
AA14	*Arthrobacter psychrolactophilus*		20	Bacterial	IASC
AA15	*Arthrobacter psychrolactophilus*		20	Bacterial	IASC
AA16	*Arthrobacter psychrolactophilus*		20	Bacterial	IASC
AA17	*Arthrobacter psychrolactophilus*		20	Bacterial	IASC
AA19	*Arthrobacter psychrolactophilus*		20	Bacterial	IASC
AA20	*Arthrobacter psychrolactophilus*		20	Bacterial	IASC
AA21	*Arthrobacter psychrolactophilus*		20	Bacterial	IASC
AA23	*Arthrobacter psychrolactophilus*		20	Bacterial	IASC
AA25	*Arthrobacter psychrolactophilus*		20	Bacterial	IASC
21	*Arthrobacter roseus*	14508	22	Bacterial	IASC
AA10	*Arthrobacter* sp.		20	Bacterial	IASC
AA11	*Arthrobacter* sp.		20	Bacterial	IASC
AA13	*Arthrobacter* sp.		20	Bacterial	IASC
26	*Arthrobacter* sp. E7		30	Bacterial	I
27	*Arthrobacter* sp. F7		30	Bacterial	I
28	*Arthrobacter* sp. K20		30	Bacterial	I
29	*Arthrobacter* sp. L20		30	Bacterial	I
AA8	*Arthrobacter stackebrandtii*		20	Bacterial	IASC
22	*Arthrobacter sulfonivorans*	14002	28	Bacterial	
23	*Arthrobacter sulfureus*	20167	30	Bacterial	
AA6	*Arthrobacter sulfureus*		20	Bacterial	IASC
AA18	*Arthrobacter sulfureus*		20	Bacterial	IASC
AA22	*Arthrobacter sulfureus*		20	Bacterial	IASC
AA24	*Arthrobacter sulfureus*		20	Bacterial	IASC
24	*Arthrobacter uratoxydans*	20647	30	Bacterial	
25	*Arthrobacter ureafaciens*	20126	30	Bacterial	
P2	*Aspergillus nidulans SAS 12*		28	Fungi	
P1	*Aspergillus nidulans GR5*		28	Fungi	
P5	*Aspergillus niger*	11414	28	Fungi	
P4	*Aspergillus niger IFGB*	1822	28	Fungi	
	Aspergillus niger	NRRL	28	Fungi	
P3		3			
P6	*Aspergillus oryzae*	1861	28	Fungi	

Internal Code	Organism	DSM	Cultivation Temp. (°C)	Type	Source
P7	*Aspergillus oryzae*	1863	28	Fungi	
B1	*Bacillus* sp. A16		30	Bacterial	
B2	*Bacillus* sp. A16	25052	30	Bacterial	
B3	*Bacillus* sp. F16	18825	30	Bacterial	
B4	*Bacillus* sp. F18		30	Bacterial	
B5	*Bacillus* sp. G18		30	Bacterial	
B6	*Bacillus* sp. H20		30	Bacterial	
B7	*Bacillus subtilis*	21332	30	Bacterial	
B8	*Bacillus subtilis*	10^T	30	Bacterial	
B9	*Bacillus subtilis*	28227	30	Bacterial	
B10	*Bacillus subtilis*	3258	30	Bacterial	
B11	*Bacillus subtilis* LM43a50°C		30	Bacterial	
B12	*Bacillus subtilis subsp. subtilis*	1090	30	Bacterial	
B13	*Bacillus subtilis subsp. subtilis*	3256	30	Bacterial	
B14	*Bacillus subtilis subsp. subtilis*	3257	30	Bacterial	
B15	*Bacillus subtilis subsp. subtilis*	5214	30	Bacterial	
B16	*Bacillus subtilis subsp. subtilis*	6198	30	Bacterial	
B17	*Bacillus subtilis subsp. subtilis*	6223	30	Bacterial	
30	*Burkholderia glumae*	9512	30	Bacterial	
31	*Burkholderia glumae* PG1		30	Bacterial	
37	*Burkholderia phytofirmans PsJN*	17436 ^{T}	30	Bacterial	
32	*Burkholderia plantarii*	6535	30	Bacterial	
33	*Burkholderia plantarii*	9509	30	Bacterial	
34	*Burkholderia plantarii* mutant	9509	30	Bacterial	
35	*Burkholderia plantarii* mutant 3.2 LO4	9509	30	Bacterial	
38	*Burkholderia* sp. M3		30	Bacterial	
36	*Burkholderia thailandensis*	13276	30	Bacterial	
72	*Candida bombicola*	22214	25	Yeast	
Ax1	*Carnobacterium mobile*		20	Bacterial	IASCI
90	*Cryptococcus curvatus*	3112	25	Yeast	
73	*Cryptococcus curvatus*	20508	25	Yeast	
74	*Cryptococcus curvatus*	20509	25	Yeast	
O10	*Cytophaga marinoflava* Hel 21		20	Marine bacterial	
M2	*Delftia* sp. E24		30	Bacterial	
M1	*Delftia* sp. I24	18833	30	Bacterial	
E1	*Escherichia coli* K12	498	37	Bacterial	
M3	*Flavobacterium* sp. F8		30	Bacterial	
M4	*Gordonia namibiensis NAM-BN063A*		30	Bacterial	
M5	*Gordonia namibiensis NAM-BN063B*		30	Bacterial	
O1	*Halomonas variabilis* Hel 04		20	Marine bacterial	
O2	*Janibacter limosus* Hel 01		20	Marine bacterial	
O3	*Jannaschia helgolandensis* Hel 10		20	Marine bacterial	

Internal Code	Organism	DSM	Cultivation Temp. (°C)	Type	Source
			20	Marine	
O4	*Jannaschia helgolandensis* Hel 26			bacterial	
76	*Klyveromyces lactis CBS*	2359	25	Yeast	
75	*Klyveromyces marxianus CBS*	6556	25	Yeast	
M6	*Lactob. delbrueckii subsp.delbrueckii*	20074	30	Bacterial	
M7	*Lactococcus lactis subsp. Lactis*	20481	30	Bacterial	
M8	*Leifsonia* sp. K3	27212	30	Bacterial	
		20408	20	Marine	
O14	*Marinicoccus halophilus*			bacterial	
Ax6	*Massilia aurea*		20	Bacterial	IASC
M9	*Microbacterium* sp. 40A	27211	30	Bacterial	
			20	Marine	
O5	*Mikrobakterium* sp. Hel 12			bacterial	
M10	*Mircrobacteriacae* sp. K3		30	Bacterial	
M11	*Nocadia butanica*	21197	30	Bacterial	
M12	*Nocadia EH1-B*		30	Bacterial	
M13	*Nocadia H8*		30	Bacterial	
M14	*Nocadia TB1*		30	Bacterial	
			20	Marine	
O6	*Oceanibulbus indoliflex* Hel 45			bacterial	
M15	*Ochrobactrum* sp.C15		30	Bacterial	
M16	*Ochrobactrum* sp.D24		30	Bacterial	
M17	*Ochrobactrum* sp.F21	25042	30	Bacterial	
M18	*Ochrobactrum* sp.F21		30	Bacterial	
M19	*Ochrobactrum* sp.G21	18825	30	Bacterial	
M20	*Ochrobactrum* sp.I21		30	Bacterial	
M21	*Ochrobactrum* sp.J24		30	Bacterial	
82	*OHA1*		25	Yeast	I
84	*OHA12*		25	Yeast	I
83	*OHA4*		25	Yeast	I
M22	*Paenibacillus* sp. 32A	27214	30	Bacterial	
G	*Parageobacillus thermoglucosidasius*	6285	55	Bacterial	
			20	Marine	
O7	Planctomyces maris Hel 23			bacterial	
Ax5	*Planococcus psychrotolerans*		20	Bacterial	IASC
			20	Marine	
O13	Prochlorococus Med4			bacterial	
68	*Pseud. Km-1*		30	Bacterial	
69	*Pseud. KM-3s*		30	Bacterial	
70	*Pseud. PN I*		30	Bacterial	
AP2	*Pseudomonas antarctica*		20	Bacterial	IASC
AP4	*Pseudomonas antarctica*		20	Bacterial	IASC
AP5	*Pseudomonas antarctica*		20	Bacterial	IASC
AP7	*Pseudomonas antarctica*		20	Bacterial	IASC
53	*Pseudomonas chibensis*	329	30	Bacterial	
55	*Pseudomonas chlororaphis*	50083	30	Bacterial	
56	*Pseudomonas chlororaphis*	30761	30	Bacterial	

Internal Code	Organism	DSM	Cultivation Temp. (°C)	Type	Source
54	*Pseudomonas cruciviae*	10833	30	Bacterial	
AP6	*Pseudomonas extremaustralis*		20	Bacterial	IASC
AP10	*Pseudomonas flourescens*		20	Bacterial	IASC
52	*Pseudomonas fluorescens*	50090 T	30	Bacterial	IASC
AP1	*Pseudomonas gessardii*		20	Bacterial	IASC
AP3	*Pseudomonas lini*		20	Bacterial	IASC
AP8	*Pseudomonas mandelii*		20	Bacterial	IASC
AP11	*Pseudomonas mandelii*		20	Bacterial	IASC
71	*Pseudomonas oleovorans*	1045	30	Bacterial	
57	*Pseudomonas plantarii*	9509	30	Bacterial	
58	*Pseudomonas putida*	5235	28	Bacterial	
59	*Pseudomonas putida*	12735	28	Bacterial	
60	*Pseudomonas putida*	KT2440	28	Bacterial	
61	*Pseudomonas* sp. G6		30	Bacterial	
62	*Pseudomonas* sp. G7		30	Bacterial	
63	*Pseudomonas* sp. L9		30	Bacterial	
64	*Pseudomonas* sp. M18		30	Bacterial	
65	*Pseudomonas* sp. N7		30	Bacterial	
66	*Pseudomonas* sp. N8		30	Bacterial	
67	*Pseudomonas* sp. P8		30	Bacterial	
AP12	*Pseudomonas syringae*		20	Bacterial	IASC
APsy8	*Psychrobacter aguimaris*		20	Bacterial	IASC
APsy3	*Psychrobacter cibarius/urativorans*		20	Bacterial	IASC
AP9	*Psychrobacter cryhalolentis*		20	Bacterial	IASC
APsy9	*Psychrobacter cryhalolentis*		20	Bacterial	IASC
APsy5	*Psychrobacter cryohalolentis*		20	Bacterial	IASC
APsy6	*Psychrobacter cryohalolentis*		20	Bacterial	IASC
APsy2	*Psychrobacter maritimus*		20	Bacterial	IASC
APsy7	*Psychrobacter maritimus*		20	Bacterial	IASC
APsy1	*Psychrobacter* sp.		20	Bacterial	IASC
APsy4	*Psychrobacter urativorans*		20	Bacterial	IASC
M23	*Rhodococccus ruber USA-AN012*			Bacterial	
M24	*Rhodococcus erythropolis 122-AN065*			Bacterial	
M25	*Rhodococcus erythropolis 67-BN001*			Bacterial	
M26	*Rhodococcus erythropolis 870-AN019*			Bacterial	
M27	*Rhodococcus erythropolis 871-AN042*			Bacterial	
M28	*Rhodococcus erythropolis 871-AN053*			Bacterial	
M29	*Rhodococcus erythropolis ANT-AN007*			Bacterial	

M30	*Rhodococcus erythropolis ANT-AN037*			Bacterial	
M31	*Rhodococcus erythropolis ARG-AN024*			Bacterial	
M32	*Rhodococcus erythropolis ARG-AN025*			Bacterial	
M33	*Rhodococcus erythropolis ENG-AN033*			Bacterial	
M34	*Rhodococcus erythropolis IND-AN014*			Bacterial	
M35	*Rhodococcus opacus 871-AN040*			Bacterial	
M36	*Rhodococcus opacus ANT-AN002*			Bacterial	
O8	*Roseobacter* sp. Hel 78		20	Marine bacterial	
S3	*S. flavovirens*	40062		Bacterial	
77	*Saccharomyces cerevisiae DSM*	11285	25	Yeast	
80	*Saccharomyces kluyveri*	70517	25	Yeast	
O11	*SB* 177		20	Marine bacterial	
O9	*SB* 89		20	Marine bacterial	
85	*ST2*		25	Yeast	I
86	*ST6*		25	Yeast	I
87	*ST6a*		25	Yeast	I
89	*ST6b*		25	Yeast	I
S1	*Staphylococcus capitis*	20326		Bacterial	
S2	*Staphylococcus sp. H7*			Bacterial	
S4	*Stenotrophomonas sp. N1*			Bacterial	
S5	*Streptomyces globisporus*	40991		Bacterial	
S6	*Streptomyces griseus*	40236		Bacterial	
91	*SW A*		25	Yeast	I
92	*SW B*		25	Yeast	I
93	*SW D*		25	Yeast	I
94	*SW E*		25	Yeast	I
95	*SW F*		25	Yeast	I
96	*SW G*		25	Yeast	I
O12	Synechococcus WH 8102		20	Marine bacterial	
T1	*Tetragenocccus koreensis*	16501		Bacterial	
Ax2	*Thelebolus globosus*		20	Bacterial	IASC
Ax7	*Thelebolus sp.*		20	Bacterial	IASC
78	*Trigonopsis variabilis*	70714	25	Yeast	
M41	*Tsukamurella pseudospumae*	44117	28	Bacterial	
M42	*Tsukamurella pseudospumae*	44118	28	Bacterial	
M37	*Tsukamurella spumae*	44113	28	Bacterial	
M38	*Tsukamurella spumae*	44114	28	Bacterial	
M39	*Tsukamurella spumae*	44115	28	Bacterial	
M40	*Tsukamurella spumae*	44116	28	Bacterial	
Ax3	*Variovorax paradoxus*		20	Bacterial	IASC
Ax4	*Variovorax paradoxus*		20	Bacterial	IASC

M43	*Variovorax paradoxus SCS-3-L20-3*		30	Bacterial
M44	*Variovorax paradoxus SCS-3-L20-4*		30	Bacterial
79	*Yarrowia lipolytica*	1345	25	Yeast

3.1.2 Genes and proteins

Table 4: Used genes and proteins.

Name	Annotation (NCBI)	Accession number		Organism	DSMZ strain	PDB code
		Gene	Protein (Uniprot)			
P. oleo	Hydantoin utilization protein C	NIUB01000001.1:76233-77522	OWK49263.1	*Pseudomonas oleovorans*	1045	-
P.aeru	*N*-carbamoyl- β-alanin-synthase	NC_002516.2: 498420-499703	AAG03833.1	*Pseudomonas aeruginosa PAO1*	22644	-
Burk 1	Zn-depented hydrolase	NC_010681.1: 3041700-3042980, Chromosome 1	WP_012433677.1	*Paraburkholderia phytofirmans PsJN*	17436	-
Burk 2	Zn-depented hydrolase / β-alanin-synthase	NC_010676.1: 2861449-2862729, Chromosome 2	WP_012428372.1	*Paraburkholderia phytofirmans PsJN*	17436	-
Burk 3	β-alanin-synthase, amidohydrolase	NC_010676.1: 304405-305643, Chromosome 2	WP_012426153.1	*Paraburkholderia phytofirmans PsJN*	17436	-
Burk 4	Allantoate Amidohydrolase	NC_010681.1: 55474-56766, Chromosome 1	WP_012431152.1	*Paraburkholderia phytofirmans PsJN*	17436	-
Burk 5	Allantoate amidoydrolase, β-alanin-synthase	NC_010676.1: 169451-170692	WP_012426027.1	*Paraburkholderia phytofirmans PsJN*	17436	-
PYD3	β-alanin-synthase	AF333185.1:1207-2574	Q96W94	*Lachancea kluyveri*	70517	1R3N, 1R43, 2V8D, 2V8H, 2V8V, 2VL1
amaB	*N*-carbamoyl-L-amino acid hydrolase	-	Q53389.1	*Geobacillus stearothermophilus CECT43*^{T}	22	3N5F
BCep1808_5509	Amidase,hydantoinase / carbamoylase	CP020395.1:511541-512821	A4JQA0	*Burkholderia vietnamiensis G4*	11737	5I4M
allC	Allantoate Amidohydrolase	-	P77425	*Escherichia coli K12*	498	1Z2L
nca	*N*-carbamoyl-D-amino acid hydrolase	-	Q44185	*Rhizobium radiobacter*		1FO6 2GGK 2GGL

3.1.3 Commercial enzymes

Table 5: Commercial enzymes

Enzyme	Description	Supplier
DNAse	DNAse I grade II from bovine pancreas	Sigma Aldrich
Lysozyme	From henn egg white	Fluka
Anza Restriction enzymes	BamHI, Hind III	Invitrogen by Thermo Fisher Scientific
DNA Polymerases	Q5® High-Fidelity DNA	Carl Roth GmbH & Co. KG
	Taq DNA Polymerase	Thermo Fisher Scientific Inc.

3.1.4 Cloned Plasmids

All genes used for cloning were previously codon optimized for expression in *E. coli* using Thermo Fisher Scientific Gene Art codon optimization or optimized by Proteogenix company.

Table 6: Cloned plasmids.
pMA-T vector was obtained from Thermo Fisher Scientific Gene Art, pUC18 and pET19 were obtained from ProteoGenix and pLJSRSF7 vector was bought from Addgene [200].

Name of plasmid	Gene name	Vectors		Gene synthesis Supplier
		Cloning vector	Expression vector	
Burk_bUp1	*Burk 1*	pMA-T	pLJSRSF7	Thermo Fisher Scientific Gene Art
Burk_bUp2	*Burk 2*	pMA-T	pLJSRSF7	Thermo Fisher Scientific Gene Art
Burk_bUp3	*Burk 3*	pMA-T	pLJSRSF7	Thermo Fisher Scientific Gene Art
Burk_bUP4	*Burk 4*	pMA-T	pLJSRSF7	Thermo Fisher Scientific Gene Art
Burk_bUp5	*Burk 5*	pMA-T	pLJSRSF7	Thermo Fisher Scientific Gene Art
P. oleov_bUp6	*P. oleov*	pMA-T	pLJSRSF7	Thermo Fisher Scientific Gene Art
P.aeru_bUp7	*P.aeru*	pMA-T	pLJSRSF7	Thermo Fisher Scientific Gene Art
S.kl_bUp	*PYD3*	pMA-T	pLJSRSF7	Thermo Fisher Scientific Gene Art
	PYD3		pET21b(+)	Thermo Fisher Scientific Gene Art
3N5F	*amaB*	pUC18	pET19	ProteoGenix
1FO6	*nca*	pUC18	pET19	ProteoGenix
5I4M	*BCep1808_5509*	pUC18	pET19	ProteoGenix
1Z2L	*allC*	pUC18	pET19	ProteoGenix

3.1.5 Chemicals

Table 7: List of all used chemicals

Chemical	Chemical Formula	Supplier
1,4-Dithiothreit (DTT)	$C_4H_{10}O_2S_2$	Carl Roth GmbH & Co. KG
2-(4-(2-Hydroxyethyl)-1-piperazinyl)-ethansulfonsäure (HEPES)	$C_8H_{18}N_2O_4S$	Carl Roth GmbH & Co. KG
3-Mercaptopropionsäure	$C_3H_6O_2S$	Sigma-Aldrich
4-(Dimethylamino-)benzaldehyd	$C_9H_{11}NO$	Merck KGAA
Acetic acid	$C_2H_4O_2$	Carl Roth GmbH & Co. KG
Acrylamide	C_3H_5NO	Carl Roth GmbH & Co. KG
Agar	-	Sigma-Aldrich
Agarose Ultra Quality	$C_{12}H_{18}O_9$	Carl Roth GmbH & Co. KG
Ammonium peroxide sulfate (APS)	$(NH_4)_2S_2O_8$	Carl Roth GmbH & Co. KG
Ammonium sulfate (enzyme quality)	$(NH_4)_2SO_4$	Carl Roth GmbH & Co. KG
Ampicillin sodium salt	$C_{16}H_{18}N_3NaO_4S$	Carl Roth GmbH & Co. KG
Boric acid	H_3BO_3	Carl Roth GmbH & Co. KG
Bromphenol blue	$C_{19}H_{10}Br_4O_5S$	Sigma-Aldrich
Calcium chloride	$CaCl_2 \cdot 2\ H_2O$	Sigma-Aldrich
Cobalt (II) chloride Hexahydrate	$CoCl_2 \cdot 6\ H_2O$	Honeywell Specialty Chemicals Seelze GmbH
Coomassie Brilliant Blue R250	$C_{45}H_{44}N_3NaO_7S_2$	Carl Roth GmbH & Co. KG
Dipotassium phosphate	K_2HPO_4	Sigma-Aldrich
Disodium phosphate	$Na_2HPO_4 \cdot 2\ H_2O$	Carl Roth GmbH & Co. KG
DNA Ladder (1 kb, Quick-Load®)	-	New England Biolabs
Fmoc		
Gel Loading Dye, Purple (6X)	-	New England Biolabs
Glycerine	$C_3H_8O_3$	Carl Roth GmbH & Co. KG
Hydrochloric acid 32 %	HCl	Carl Roth GmbH & Co. KG
Isopropanol	C_3H8O	Carl Roth GmbH & Co. KG
Isopropyl-β-D-thiogalactopyranosid (IPTG)	$C_9H_{18}O_5S$	Carl Roth GmbH & Co. KG
Kanamycin sulfate	$C_{18}H_{36}N_4O_{11} \cdot H_2SO_4$	Carl Roth GmbH & Co. KG

Magnesium chloride	$MgCl_2 \cdot 7\ H_2O$	Carl Roth GmbH & Co. KG
Magnetic Dynabeads™	-	Thermo Fisher Scientific Inc.
Maltose	$C_{12}H_{22}O_{11}$	Sigma-Aldrich
Manganese (II) chloride tetrahydrate	$MnCl_2 \cdot 4\ H_2O$	Sigma-Aldrich
Methanol	MeOH	Carl Roth GmbH & Co. KG
Monopotassium phosphate	KH_2PO_4	Carl Roth GmbH & Co. KG
Monosodium phosphate	$NaH_2PO_4 \cdot 2\ H_2O$	Carl Roth GmbH & Co. KG
N-isobutyryl-L-Cystein (IBLC)	$C_7H_{13}NO_3S$	Sigma-Aldrich
Nickel (II) chlorid Hexahydrat	$NiCl_2 \cdot 6\ H_2O$	Sigma-Aldrich
Nickel (II) chloride hexahydrate	$NiCl_2 \cdot 6\ H_2O$	Sigma-Aldrich
Nickel beads	-	Sigma-Aldrich
Nicotinamide adenine dinucleotide (NAD)	$C_{21}H_{27}N_7O_{14}P_2$	AppliChem GmbH
Nicotinamide adenine dinucleotide (NADH)	$C_{21}H_{29}N_7O_{14}P_2$	AppliChem GmbH
Nucleoside triphosphate mix (dNTP)		Carl Roth GmbH & Co. KG
Nuklease free water	H_2O	Thermo Fisher Scientific Inc.
Ortho-Phthaldialdehyde (OPA)	$C_8H_6O_2$	Sigma-Aldrich
Prestained Protein Ladder (10-180 kDa)	-	Thermo Fisher Scientific Inc.
Prestained Protein Ladder (11 - 245 kDa)	-	New England Biolabs
Roti®-GelStain	-	Carl Roth GmbH & Co. KG
Sodium chloride	NaCl	Carl Roth GmbH & Co. KG
Sodium dodecyl sulfate (SDS)	$NaC_{12}H_{25}SO_4$	Carl Roth GmbH & Co. KG
Sodium hydroxide	NaOH	Carl Roth GmbH & Co. KG
Taq DNA Polymerase PCR Buffer (10X)	-	Thermo Fisher Scientific Inc.
Tetramethylethylendiamin (TEMED)	$C_6H_{16}N_2$	Carl Roth GmbH & Co. KG
TRIS Pufferan®	$C_4H_{11}NO_3$	Carl Roth GmbH & Co. KG
Tryptone	-	Carl Roth GmbH & Co. KG
Yeast base medium without amino acids		Carl Roth GmbH & Co. KG
Yeast extract	-	Carl Roth GmbH & Co. KG
Zinc chloride	$ZnCl_2$	Fluka

3.1.6 Amino Acids

Table 8: Used amino acids.

Amino acid	Chemical formula	Supplier
Canonical α-amino acids		
α-D/L-Aminobutyric acid	$C_4H_9NO_2$	Carl Roth GmbH & Co. KG
α-D/L-Lysine	$C_6H_{14}N_2O_2$	Carl Roth GmbH & Co. KG
α-D/L-Phenylalanine	$C_9H_{11}NO_2$	Carl Roth GmbH & Co. KG
α-D/L-Tyrosine	$C_9H_{11}NO_3$	Carl Roth GmbH & Co. KG
α-D-Phenylalanine	$C_9H_{11}NO_2$	Carl Roth GmbH & Co. KG
α-D-Serine	$C_3H_7NO_3$	Sigma-Aldrich
α-D-Tryptophan	$C_{11}H_{12}N_2O_2$	Sigma-Aldrich
α-Glycine	$C_2H_5NO_2$	Carl Roth GmbH & Co. KG
α-L-Cysteine	$C_3H_7NO_2S$	Carl Roth GmbH & Co. KG
α-L-Isoleucine	$C_6H_{13}NO_2$	Sigma-Aldrich
α-L-Leucine	$C_6H_{13}NO_2$	Sigma-Aldrich
α-L-Lysine	$C_6H_{14}N_2O_2$	Sigma-Aldrich
α-L-Methionine	$C_5H_{11}NO_2S$	Carl Roth GmbH & Co. KG
α-L-Phenylalanine	$C_9H_{11}NO_2$	Sigma-Aldrich
α-L-Serine	$C_3H_7NO_3$	Sigma-Aldrich
α-L-Tryptophan	$C_{11}H_{12}N_2O_2$	Sigma-Aldrich
α-L-Valine		
Non-canonical α-amino acids		
α-D/L-Neopentylglycine	$C_7H_{15}NO_2$	Evonik Degussa GmbH
α-D-Phenylglycine	$C_8H_9NO_2$	Evonik Degussa GmbH
α-L-Neopentylglycine	$C_7H_{15}NO_2$	Evonik Degussa GmbH
α-L-para-Hydroxy-Phenylglycine	$C_8H_9NO_3$	Sigma-Aldrich
α-L-Phenylglycine	$C_8H_9NO_2$	Carl Roth GmbH & Co. KG
D/L-β-2-Thienylalanine	$C_7H_9NO_2S$	Sigma-Aldrich
L-Tertiary-α-leucine	$C_6H_{13}NO_2$	Evonik Degussa GmbH
α-L-Naphtylalanine	$C_{13}H_{13}NO_2$	Evonik Degussa GmbH
β-(Homo)-amino acids		
L-3-Amino-heptanoic acid	$C_7H_{15}NO_2$	Sigma-Aldrich
β-Alanine	$C_3H_7NO_2$	Carl Roth GmbH & Co. KG
β-D/L-Leucine	$C_6H_{13}NO_2$	Sigma-Aldrich
β-D/L-Phenylalanine	$C_9H_{11}NO_2$	Sigma-Aldrich
β-D/L-Tyrosine	$C_9H_{11}NO_3$	Sigma-Aldrich
β-D-Homoalanine hydrochloride	$C_4H_9NO_2 \cdot HCl$	PepTech Corporation
β-D-Homoserine	$C_4H_9NO_3$	PepTech Corporation
β-L-Homoalanine hydrochloride	$C_4H_9NO_2 \cdot HCl$	PepTech Corporation
β-L-Homomethionine	$C_6H_{13}NO_2S \cdot HCl$	PepTech Corporation
β-L-Homoserine	$C_4H_9NO_3$	PepTech Corporation

3.1.7 *N*-carbamoyl-Amino Acid Derivates

Table 9: Used *N*-carbamoyl-amino acids.
All named *N*-carbamoyl-amino acids in this list were used either for investigations on their turnover by wild-type strains or recombinantly expressed decarbamoylating enzymes.

N-carbamoyl-amino acid	Chemical formula	Synthesis / Origin
Canonical α-amino acids		
N-carbamoyl-L-tertiary leucine	$C_7H_{14}N_2O_3$	TeBi amino acids collection
N-carbamoyl-α-D/L-aminobutyric acid		TeBi amino acids collection
N-carbamoyl-α-D-Aminobutyric acid	$C_5H_{10}N_2O_3$	TeBi amino acids collection
N-carbamoyl-α-L-Aminobutyric acid	$C_5H_{10}N_2O_3$	TeBi amino acids collection
N-carbamoyl-α-D/L-Phenylalanine	$C_{10}H_{12}N_2O_3$	TeBi amino acids collection
N-carbamoyl-α-L-Phenylalanine	$C_{10}H_{12}N_2O_3$	TeBi amino acids collection
N-carbamoyl-α-D-Phenylalanine	$C_{10}H_{12}N_2O_3$	TeBi amino acids collection
N-carbamoyl-α-D-Serine	$C_4H_8N_2O_4$	This work
N-carbamoyl-α-D-Tryptophan	$C_{12}H_{13}N_3O_3$	TeBi amino acids collection
N-carbamoyl-α-Glycine	$C_3H_6N_2O_3$	TeBi amino acids collection
N-carbamoyl-α-L-Cysteine	$C_4H_8N_2O_3S$	This work
N-carbamoyl-α-L-Isoleucine	$C_7H_{14}N_2O_3$	This work
N-carbamoyl-α-L-Leucine	$C_7H_{14}N_2O_3$	This work
N-carbamoyl-α-L-Lysine		TeBi amino acids collection
N-carbamoyl-α-L-Methionine	$C_6H_{12}N_2O_3S$	This work
N-carbamoyl-α-L-Phenylalanine	$C_{10}H_{12}N_2O_3$	TeBi amino acids collection
N-carbamoyl-α-L-Serine	$C_4H_8N_2O_4$	This work
N-carbamoyl-α-L-Tryptophan	$C_{12}H_{13}N_3O_3$	TeBi amino acids collection
N-carbamoyl-α-D-Tryptophan	$C_{12}H_{13}N_3O_3$	TeBi amino acids collection
N-carbamoyl-α-L-Valine	$C_6H_{12}N_2O_3$	This work
Non-canonical α-amino acids		
N-carbamoyl-α-D/L-Neopentylglycine	$C_8H_{16}N_2O_3$	TeBi amino acids collection
N-carbamoyl-α-D-Phenylglycine	$C_9H_{10}N_2O_3$	TeBi amino acids collection
N-carbamoyl-α-L-Neopentylglycine	$C_8H_{16}N_2O_3$	Evonik Degussa GmbH

N-carbamoyl-amino acid	Chemical formula	Synthesis / Origin
N-carbamoyl-α-L-para-Hydroxy-Phenylglycine	$C_9H_{10}N_2O_4$	Sigma-Aldrich
N-carbamoyl-α-L-Phenylglycine	$C_9H_{10}N_2O_3$	Coth GmbH & Co. KG
N-carbamoyl-β-2-L-Thienylalanine		TeBi amino acids collection
N-carbamoyl-α-L-Naphtylalanine	$C_{14}H_{14}N_2O_3$	TeBi amino acids collection
β-(Homo)-amino acids		
N-carbamoyl-L-3-Amino-heptanoic acid	$C_8H_{16}N_2O_3$	This work
N-carbamoyl-β-Alanine	$C_4H_8N_2O_3$	This work
N-carbamoyl-β-D/L-Leucine	$C_7H_{14}N_2O_3$	This work
N-carbamoyl-β-D/L-Phenylalanine	$C_{10}H_{12}N_2O_3$	This work
N-carbamoyl-β-D/L-Tyrosine	$C_9H_{11}NO_3$	Synthesis by Fei Peng
N-carbamoyl-β-D-Homoalanine hydrochloride	$C_5H_{10}N_2O_3$	This work
N-carbamoyl-β-D-Homoserine	$C_5H_{10}N_2O_4$	This work
N-carbamoyl-β-L-Homoalanine hydrochloride	$C_5H_{10}N_2O_3$	This work
N -carbamoyl-β-D-Homoserine hydrochloride	$C_5H_{10}N_2O_4$	This work
N-carbamoyl-β-L-Homomethionine	$C_7H_{14}N_2O_3S$	This work

3.1.8 Media

3.1.8.1 Complex media

Table 10: Complex media.

Medium	Constitution
LB (lysogeny broth)	1 % (w/v) Bacto Tryptone, 0.5 % (w/v) yeast extract, 0.7 % (w/v) NaCl, pH 7, dissolved in ddH_2O, sterilized through autoclaving
LB-Agar	1 % (w/v) Bacto Tryptone, 0.5 % (w/v) yeast extract, 0.7 % (w/v) NaCl, pH 7, 1.5 % agar (w/v), dissolved in ddH_2O, sterilized through autoclaving
TB (terrific broth)	1.2 % (w/v) Bacto Tryptone, 2.4 % (w/v) yeast extract, 0.4 % glycerine (v/v) dissolved in ddH_2O and autoclaved separately. After autoclaving 10 % (v/v) of sterile KPP buffer were added (0.17 M KH_2PO_4, 0.72 M K_2HPO_4), pH 7
YPD (yeast extract-peptone-dextrose)	1 % (w/v) yeast extract, 2 % (w/v) peptone, 2 % (w/v) glucose pH 6.5, dissolved in ddH_2O, sterilized through autoclaving
SOC (Super optimal broth)	2 % (w/v) Bacto Tryptone, 0.5 % (w/v) yeast extract, 0.05 % (w/v) NaCl, 0.25 % (v/v) 1M KCl pH7, 0.2 % (w/v) $MgCl_2 \cdot 6\ H_2O$, 0.25 % (w/v) $MgSO_4$, 2 % (v/v) 1 M Glucose, sterilized through sterile filtration

3.1.8.2 Minimal media

In screening experiments solid minimal media was made with pure agarose. For cultivation of yeasts a 10 x YM3 stock solution of the yeast-base-medium by Roth was used and prepared as described by the manufacturer and sterilized by sterile filtration. Either yeast-base medium with ammonium sulfate or without any amino acids was used. For bacterial minimal medium (BM3) 25 x BM3 stock solution was prepared as follows:

Table 11: 25 x bacterial minimal medium (BM3) stock solution

Component	Concentration (mM)
Na_2HPO_4	778.75
KH_2PO_4	625
NaCl	428.75
Sodium citrate	42.5

All components where dissolved in ddH_2O and autoclaved.

Table 12: Glucose stock solution

Component	Concentration
Glucose monohydrate	400 g/L

All components where dissolved in ddH_2O and autoclaved.

Table 13: Yeast base minimal media

Yeast base medium	Name	$(NH_4)SO_4$ included	Supplier
„YB1“	Yeast nitrogen base medium without amino acids	5 g/L	Carl Roth GmbH & Co. KG
„YB2“	Yeast base medium without amino acids without ammonium sulphate	-	Carl Roth GmbH & Co. KG

Medium was solved as 10 x stock solution as described by the supplier, sterile filtrated and stored at 4 °C

Minimal media for bacteria

Table 14: Minimal medium "BM3-U/T/A"
For bacteria with uracil/thymine/ammonium sulphate as nitrogen source.

Mix	Component	Final concentration	Comment	Sterilisation method
X	Uracil or thymine or $(NH_4)SO_4$	30 mM		Autoclaved together
	25 x BM3 stock solution	1 x		
	pH	bacteria 6.8-7 (*Arthrobacter* 7.2)		
	All components were dissolved in ddH$_2$O ($V_x = V_{total} - V_Y$)			
	(Agarose)	1.5 % (w/v)	Added after everything dissolved	
	Agar was cooled down until it was still dissolved and warm, before it became solid the following solutions were added:			
Y	Glucose stock solution (400 g/L)	8 g/L	Added after autoclaving	Autoclaved seperately
	Trace elements (SL4 solution stock)	1 % (v/v)	Added after autoclaving	Sterile filtration
	$MgSO_4 \cdot 7\ H_2O$ (1M stock)	0.34 mM	Added after autoclaving	Sterile filtration
	$CaCl_2 \cdot 2\ H_2O$ (1M stock)	0.34 mM	Added after autoclaving	Sterile filtration

Table 15: Minimal medium "BM3" for bacteria with *N*CβAla/*N*CβPhe as nitrogen source

Mix	Component	Final concentration	Comment	Sterilisation method
X	25 x BM3	1 x		Autoclaved together
	pH	bacteria 6.8-7 (*Arthrobacter* 7.2)		
	All components were dissolved in ddH$_2$O ($V_x = V_{total} - V_Y$)			
	(Agarose)	1.5 % (w/v)	Added after everything dissolved	
	Agar was cooled down until it was still dissolved and warm, before it became solid the following solutions were added			
Y	20 mM *N*CβAla/*N*CβPhe	10 mM		Sterile filtration
	Glucose stock solution (400 g/L)	100 mM (8 g/L)	Added after autoclaving	Autoclaved separately
	Trace elements (SL-4 solution stock)	1 % (v/v)	Added after autoclaving	Sterile filtration
	$MgSO_4 \cdot 7\ H_2O$ (1M stock)	0.34 mM	Added after autoclaving	Sterile filtration
	$CaCl_2 \cdot 2\ H_2O$ (1M stock)	0.34 mM	Added after autoclaving	Sterile filtration

Bacterial control medium without any nitrogen:

For bacterial minimal medium without any nitrogen source the same mixture was made without any nitrogen source (uracil, thymine, $(NH_4)SO_4$, *N*CβAla or *N*CβPhe).

Minimal media for yeast

Table 16: Minimal media for yeast "YM3" with different nitrogen sources.
Depending on the wanted nitrogen source commercial yeast base medium with or without ammonium sulphate was used. If uracil or thymine were used as nitrogen source they were previously autoclaved together with agarose suspension. Since the commercially available yeast minimal medium included trace elements no additionally trace elements had to be added.

Mix	Component				Final conc.
A	Agarose	Pure agarose was added to ddH_2O ($V_A = V_{Total} - V_B$) and autoclaved separately			
B	Nitrogen source	Uracil or thymine or *N*CβAla or *N*CβPhe	$(NH_4)SO_4$	- (control medium)	30 / 30 / 30 / - 10 / 10 mM
	10 x Yeast base medium (YBM)	10 x "YBM 2"	10 x "YBM 1"	10 x "YBM 2"	1 x
	Carbon source		400 g/L Glucose		8 g/L

Table 17: Trace element solution SL-4

Compound	Concentration per Litre
EDTA	0.50 g
$FeSO_4 \cdot 7\ H_2O$	0.20 g
Trace element solution SL-6	100 ml
ddH_2O	Fill up to 1000 ml

Table 18: Trace element solution SL-6

Compound	Concentration per Litre
$ZnSO_4 \cdot 7\ H_2O$	0.10 g
$MnCl_2 \cdot 4\ H_2O$	0.03 g
H_3BO_3	0.30 g
$CoCl_2 \cdot 6\ H_2O$	0.20 g
$CuCl_2 \cdot 2\ H_2O$	0.01 g
$NiCl_2 \cdot 6\ H_2O$	0.02 g
$Na_2MoO_4 \cdot 2\ H_2O$	0.03 g
ddH_2O	Fill up to 1000.00 ml

3.1.9 HPLC buffers and solutions

Table 19:HPLC buffers

Name	Compounds	Concentration
NaPP buffer	Na_2HPO_4 NaH_2PO_4 pH 6,5	40 mM
KPP buffer	KH_2PO_4 pH 3	20 mM
Acetate buffer	0.003 % (v/v) glacial acetic acid and 0.001 % (v/v) triethylamine , pH 4.2	
NaB buffer	Boric acid, titrated to pH 10.4 with NaOH	133 mM
Borate buffer	0.2 M boric acid in ddH_2O, pH 7.7	
Mobile Phase A	Acetonitrile: MeOH : acetate buffer	10:40:50
Mobile Phase B	Acetonitrile: acetate buffer	1:1

Table 20: Derivatization solutions for HPLC and assays.

Solution	Composition
OPA	100 mM in MeOH
IBLC	133 mM in NaB buffer
OPA/IBLC	1:1 mixture of OPA and IBLC solution
Fmoc	15 mM in acetone
Ehrlich	0.7 M 4-(dimethylamino-)benzaldehyde in 37 % HCl and ddH_2O 1:1 (v/v)
3-MPA	11 µl of 3-mercaptopropionic acid mixed with 989 µl 133 mM NaB buffer pH 10.4.
OPA/3-MPA	1:1 mixture of OPA and 3-MPA solutions
Acetic acid	3 % acetic acid in ddH_2O

Table 21: Enzyme and cell buffers

Buffer	Composition
1 x PBS	0.137 M NaCl, 0.0027 M; 0.01 M Na_2HPO_4; 0.0018 M KH_2PO_4, pH 7
HEPES	50 / 100 mM HEPES; 500 mM NaCl; pH depending on enzyme
Purification via His-Tag	
Buffer A	50 mM HEPES, 0.5 M NaCl, 5-10 mM Imidazole, pH 6.8 - 8
Buffer B	50 mM HEPES, 0.5 M NaCl, 500 mM Imidazole, pH 6.8 - 8
Purification via MBP-Tag	
Buffer A	50 mM HEPES, 0.5 M NaCl, pH 6.8 - 8
Buffer B	50 mM HEPES, 0.5 M NaCl, 10 mM Maltose, pH 6.8 - 8

Table 22: Buffers and solutions for agarose- and SDS-gels

Buffer	Composition
5 x SDS sample buffer	225 mM Tris/HCl pH 6.8; 50 % glycerine, 5 % SDS; 0.05 % bromphenol blue; 250 mM DTT; in ddH_2O
TAE agarose gel buffer (10 x)	0.4 M Tris/HCl, pH 8; 0.2 M acetic acid; 10 mM EDTA; pH 8.0
TGS SDS-Gel buffer (10 x)	0.05 M Tris/HCl, 1.92 M Glycine, 1 % SDS
Agarose gel (0.8 %)	1 x TAE buffer; 0.8 % (w/v) agarose
SDS gel (12.5 %, 5 %)	12.5 % separation gel: 2.4 ml 1.88 M Tris/HCl pH 8.8, 120 µl 10 % SDS, 4.48 ml ddH_2O, 5 ml 30 % acrylamide, 60 µl 10 % APS, 10 µl TEMED. 5 % stacking gel: 800 µl 0.625 M Tris/HCl pH 6.8, 40 µl 10 % SDS, 2.5 ml ddH_2O, 660 µl 30 % acrylamide solution, 20 µl 10 % APS, 4 µl TEMED.
Commassie blue staining solution of SDS-gels	1.5 g Coomassie blue G250 in 455 ml EtOH (96 %), 75 ml acetic acid, filled up to 1 L with ddH_2O.
Destaining solution for SDS-gels	20 % EtOH, 10 % acetic acid

Table 23: Solutions for media and buffers

Name	Composition	Final concentration
Ampicillin	100 mg/ml Ampicillin sodium salt in MilliQ	100 µg/ml
Kanamycin	50 mg/ml Kanamycin sulphate	50 µg/ml
NaCl stock solution	NaCl in ddH_2O	500 mM
IPTG stock solution (x1000)	1 M IPTG in ddH_2O	0.1 mM-1 mM

Table 24: Thin-layer-chromatography solvents.

Solvent for amino acid	Constitution
β-Phenylalanine	AcOH: BuOH: H_2O : acetic acid 4.5 / 2.5 / 2 / 1 (v/v)
Aliphatic β-(Homo)-amino acids	BuOH: AcOH: H_2O 4/1/2 (v/v)
Allantoin, allantoic acid	AcOH:EtOH:BuOH 2 / 2 / 7 (v/v)
Staining solutions	
Ninhydrin	0.3 g Ninhydrin in Ethanol
Ehrlich	1 g 4-(Dimethylamino-)benzaldehyde in 3 ml 37 % HCl filled up to 15 ml with BuOH
Iod-staining	Iodid mixed with sepharose particles

3.1.10 Primers

Table 25: Primers used for plasmid sequencing

Primer	Sequence (5'→ 3')
pET-24a (rev T7)	GGGTTATGCTAGTTATTGCTCAG
pET-RP	CTAGTTATTGCTCAGCGG
pMalE	TCAGACTGTCGATGAAGC
T7 Promotor	TAATACGACTCACTATAGGGG
T7 Terminator	CCCAAGGGGTTATGCTAG

Table 26: Primers used for amplification of 16S rRNA coding DNA and 16S rRNA sequencing

Primer	Sequence (5'→ 3')	Annealing Temperature*
BaC27 f	AGA GTT TGG ATC MTG GCT CAG	60 °C
Univ1492	CGG TTA CCT TGT TAC GAC TT	

* Annealing Tm calculated with ThermoFisher calculator

Table 27: Primers used in Protein Engineering experiments.
The number in the primer name gives the amino acid position, which was mutated. Primers were constructed with approximately 12 bp overlap sequence. The mutation is only present in the reverse Primer (fw= forward, rv = reverse).

Mutated enzyme	Position	Mutation	Direction	Sequence (5'→ 3')	Annealing T_m (°C)
5I4M	288	N → A	fw	GTT ATT CCG GGT CGT GTG TTT TTT ACC	67.3
	288		rv	ACC CGG AAT AAC CGC ACG G	
	228	W → A	fw	TAT GAA ATT ACC TTT ACC GGT CAA	61.2
	228		rv	GGT AAT TTC ATA CGC ACG CTG	
	150	M → A	fw	GTT GCA AGT GGT GTT TTT GCG G	66.6
	150		rv	ACC ACT TGC AAC CGC TGC C	
	150	M.2 → A	fw	GTT GCA AGC GGT GTT TTT GCGG	72
	150		rw	CGC TTG CAA CCG CTG CC	
2V8H	249	Y → A	fw	AAT TGG CAG AAA GTT ACC GTT CAT	64.4
	249		rv	TTT CTG CCA ATT CGC TGC CTG	
	167	S → A	fw	TGT ACC GGT AGC AGT GTT TGG AGC	69.5
	167		rv	GCT ACC GGT ACA CGC ACG TGC AAA	

3.1.11 Supplies

Table 28: List of used supplies.

Supply	Model	Supplier
Sterile Filter	Rotilabo®-Spritzenfilter, steril	Carl Roth GmbH & Co. KG
Ultra filtration unit	Vivaspin® Turbo 15 (10 / 50 kDa MWCO)	Sartorius AG
Glass beads	0.1 mm	Thermo Fisher Scientific Inc
Silica TLC-plates	Alugram® SIL G	Macherey-Nagel

3.1.12 Software and algorithms

Table 29: List of used software and web services

Software/ web service
BLAST [201]
Genome Compiler [202]
MestReNova [203]
PDB [204]
Phyre^2 [205]
ExPASy [206]
PyMol [207]
Reverse complement [208]
SeeMS [209]
SinalP [210]
SnapeGene® Viewer [211]
TCoffee [212]
Uniprot [213]
The Rosetta Online Server that includes everyone (ROSIE) [185]
The ConSurf Server [214]–[219]
ESPript 3.0 [220]

3.1.13 Devices

Table 30: Devices.

Device	Type	Supplier
Autoclave	V-150	Systec, Wettenberg, DE
	HX-430	Thermo Fisher Scientific, Waltham, US
Balances	BP 3100 S	Sartorius AG
	BP 211 D	
	Entris®	
	PR2003 DeltaRange	Mettler Toledo
Centrifuge	5415D Rotor: F45-24-11	Eppendorf Wesseling-Berzdorf, DE
Centrifuges	Heraeus™ Pico™ 17	Thermo Fisher Scientific Inc.
	Heraeus Multifuge X3 FR	Beckman Coulter, Inc.

Device	Type	Supplier
	Avanti J-30I	
Clean bench	Maxisafe 2020	Thermo Fisher Scientific Inc.
Electrophoresis	Biometra P25T	Analytik Jena AG
	1000/500	Bio-Rad Laboratories GmbH
Fast protein liquid chromatrography (FPLC)	Äkta™ Start	GE Healthcare Life Sciences
FPLC colums	MBPTrap™ HP (5ml)	GE Healthcare Life Sciences
	HisTrap™ High Performance	
Flat shaker	Polymax 1040	Heidolph Instruments GmbH & CO. KG
Gel documentation system	GP-05LED	NIPPON Genetics Europe
Gel elektrophoresis	Biometra P25T	Analytik Jena AG
	1000/500	Bio-Rad Laboratories GmbH
High pressure liquid chromatography (HPLC)	1100 Series	Agilent Technologies Deutschland GmbH & Co. KG
	1200 Series	
	1290 Infinity II LC Systems	
HPLC columns	HyperClone™ 5 µm ODS (C18) 120 Å, LC Column 150 x 4,6 mm.	Phenomenex
	Synergi™ 4 µm Fusion-RP 80 Å, LC Column 150 x 4,6 mm	
HPLC pre-columns	SecurityGuard™ cartridges for C18 HPLC columns with 3.2 to 8.0mm internal diameters (ID), 10/Pk	Phenomenex
	SecurityGuard™ cartridges for Fusion-RP HPLC columns with 3.2 to 8.0mm internal diameters (ID), 10/Pk	
Incubator	Multitron	Infors HT, Bottmingen, CH
Photometer for microtiterplates	Infinite® 200 PRO	Tecan Trading AG
Photometer for cuvettes	Amersham Biosciences Europe GmbH	Novaspec II
Spectro photometer	Epoch	BioTek Instruments, Inc.
Micro-Volume-Plate	Take 3	BioTek Instruments, Inc.
Liquid Handling Station	-	BRAND GMBH & CO. KG
Lyophille		Christ Gefriertrocknungsanlagen GmbH
Magnetic stirrer	RCT basic	IKA®-Werke GmbH & Co. KG

Device	Type	Supplier
MilliQ water Ultrapure Lab Water System	Purelab flex	ELGA LabWater
Thermocylcer for PCR	MJ Research PTC-200 Gradient Thermal Cycler	Marshall Scientific LLC
pH-Meter	inoLab pH Level 1	Xylem Inc.
Pipettes	Research plus 10 µl - 10 ml	Eppendorf AG
Vortex	Vortex Genie 2	VWR
	Vortex Mixer	NeoLab Migge GmbH
Microwave	-	Siemens
Rotors	75003424	Thermo Fisher Scientific Inc.
	TX-750	
	Fiberlite™ F15-8 x 50cy	
	Festwinkelrotor	Beckman Coulter, Inc.
	JA-10 Fixed-Angle Aluminum Rotor	
Roto-Shaker	Roto-Shake Genie	Scientific Industries, Inc.
Pump	Watson Marlow 101U/R	Gemini bv.
Thermo shaker	Thermomixer compact	Eppendorf AG
	Thermomixer comfort	
	BioShake iQ	Quantifoil Instruments GmbH
Ultrasonic bath	Sonorex Super RK 100	Bandelin electronic GmbH & Co. KG
Ultrasonic probe	Sonopuls UW3100	Bandelin electronic GmbH & Co. KG
High pressure homogenisator	Avestin, Inc	EmulsiFlex-C3
Agarose gel supply	-	Bio-Rad Laboratories, Inc.
SDS gel supply	Bio-Rad Laboratories, Inc.	Mini-PROTEAN Tetra Cell

3.2 Methods

3.2.1 Molecular biological methods

3.2.1.1 Transformation

Cloned plasmids were transformed into competent *E. coli* cells by heat shock method. Therefor chemical competent *E. coli XL1 blue* or *E. coli BL21 DE3* cells were used and incubated with 1 µl of plasmid DNA for 5 min on ice. Subsequently the cell-DNA-mixture was heat shocked for exactly 90 sec at 42 °C. Cells were chilled on ice immediately for 2 min. Next cells were mixed with 37 °C prewarmed SOC medium and incubated for 30 min at 37 °C and 800 rpm. Cells were plated on a LB-Agar plate with required antibiotic and incubated at 37 °C over night.

3.2.1.2 Restriction & Ligation

For Restriction and Ligation Anza™ Enzymes (Thermo Fisher) and buffers were used. Experiments were performed corresponding to enzyme manuals [221], [222]. In every restriction batch two restriction enzymes were used (BamHI, HindIII). For ligation the corresponding Anza™ T4-Ligase was used. DNA concentration was measured at 260 nm with Epoch photometer. Used pmol of DNA ends were calculated with the following formula:

$$\mu g\ DNA\ x \frac{pmol}{660\ pg}\ x \frac{10^6}{1\ \mu g} x \frac{1}{N} = pmol\ DNA$$

N: number of nucleotides

$\frac{pmol}{660\ pg}$: Average weight of a nucleotide pair

3.2.1.3 Isolation of Plasmid DNA

DNA isolation was performed with the NEB Monarch® Plasmid Miniprep Kit as described in the manual. DNA was eluted with 30 µl nuclease-free water. DNA concentration was determined at 260 nm with Epoch photometer according to Beer Lambert law:

$$\boldsymbol{c = \frac{A_{260} * \varepsilon_{260}}{b}}$$

c: Nucleic acid concentration (ng/µl)
A_{260}: Extinction (absorption) at 260 nm
ε_{260}: Wavelength extinction coefficient [L * $mMol^{-1}$ * cm^{-1}]
b: patch length [cm]

3.2.1.4 Isolation of genomic DNA and 16S rRNA sequencing

For isolation of genomic DNA glass beads for cell disruption were combined with Zymo Research Genomic DNA Extraction Kit. For every strain of which genomic DNA was to be isolated a preculture in required full medium was grown over night at strain-specific optimal growth temperature. 5-10 ml of culture were harvested and centrifuged at 13.000 rpm for 10 min. Supernatant was discarded and cells were resuspended in buffers corresponding to the Kit's manual. For mechanical disruption cells were mixed with 10 mg of 0.1 mm glass beads using Vortex Genie (Scientific Industries) for 10 min at full speed. Afterwards the genomic DNA was isolated with Zymo Genome Extraction Kit whereby the protocol of the kit was followed. Genomic DNA was eluted with nuclease-free water. For amplification of 16S rRNA coding DNA a Touch-Down PCR (Table 33) was performed. Therefore primers Bac27f and Univ1492R (Table 26) were used.

3.2.1.5 Plasmid sequencing

Plasmid sequencing was conducted by GATC (Thermo Fisher Scientific) sequencing service. Results were analysed with Genome Compiler, SnapGeneViewer and sequence alignment web services (TCoffee, NCBI MSA).

3.2.1.6 PCR

3.2.1.6.1 Colony PCR

For 5-10 colonies per ligation batch colony-PCR was performed to examine if the correct gene size had been ligated into the vector. Therefore following mixture was used per PCR-reaction:

Table 31: Colony-PCR batch

PCR component	Volume [µl]
2 x PCR-Master Mix	6,25
T7 Promotor Primer (10 pmol)	1
T7 Terminator Primer (10 pmol)	1
Template DNA	Cell material of one single colony
Taq Polymerase	1
Nuclease-free H_2O	4,25
	∑ 12,5 µl

A tiny amount of cell material was picked with a sterile pipette tip and tapped a few times carefully at the bottom of the PCR tube. Colony PCR was run with the protocol shown in Table 32. 10 µl of PCR product were mixed with 2 µl 6 x DNA Gel Loading Dye Purple (NEB) and size of amplified DNA was analysed with an agarose gel (3.2.1.7). If needed DNA band was cut out of the gel and purified with NEB gel extraction Kit.

Table 32: Colony-PCR protocol

Step	Temperature [°C]	Duration [s]
Pre-heating	95	
Initial denaturation	95	180
Denaturation	95	20
Annealing	48	30
Elongation	72	60
Final Elongation	72	300
Pause	4	∞

3.2.1.6.2 Touch-Down PCR

Reactions for Touch-Down PCR were prepared as described in Q5-Polymerase manual. Touch-Down PCR was performed with a modified nature protocol [223] as follows.

Table 33: Touch-Down PCR protocol.

Step	Temperature [°C]	Duration
Phase 1		
Denaturation	95	3 min
Denaturation	95	30 s
Annealing	T_m + 10 °C	45 s
Elongation	72	60 s or more
Phase 2		
Denaturation	95	30 s
Annealing	T_m or (T_m - 5°C)	45 s
Elongation	72	60 s or more
Completion		
Elongation	72	5 min
Pause	4	∞

Depending on used primers annealing temperature was customized. According to the size of the gene of interest elongation time was modified as described in the Q5 Polymerase manual (60 s / 1 kb).

3.2.1.7 Agarose Gels

For all agarose gels a 0.8 % (w/v) agarose solution was prepared with 1 x TAE-buffer (Table 22). Suspension was heated in the microwave until agarose had been solubilized. The solution was cooled down to around 60°C. 2 µl Roti®- Gel stain were added per 50 ml agarose solution and mixed well. The agarose gel was run at 100 V for approximately 50 min to separate DNA mixture. DNA was detected with a gel documentation system from NIPPON Genetics. If required gel bands were cut out. For every agarose gel 1 kb ladder by NEB was used.

3.2.2 Microbiological methods

3.2.2.1 Production of chemical competent *E. coli* cells

E. coli XL1 blue or *E. coli* BL21 DE3 cells were used to inoculate a preculture with LB medium and incubated at 37 °C and 120 rpm. On the next day a main culture of 100 ml LB medium was inoculated with 1 ml of the preculture and cells were shaken at 37 °C until an OD_{600} of 0.5 was reached. Then cells were chilled on ice for 10 min and centrifuged for 5 min at 4 °C and 3488 x g. The supernatant was discarded and the pellet was resuspended in 10 ml sterile 0.1 M $CaCl_2$ solution and once again chilled on ice for 20 min. Cells were gently centrifuged at 4 °C for 3 min at 78 x g and resuspended in 5 ml of a mixture of sterile 17 ml 0.1 $CaCl_2$ and 3 ml glycerine. Then competent cells were aliquoted in 200 µl cryo vials and frozen with liquid nitrogen. Cells were stored at -80 °C until use.

3.2.2.2 Preparation of glycerol stocks

Preculture of wild type strains were grown over night in LB medium or recommended medium by DSMZ at the corresponding growth temperature given in Table 3. In case of yeasts precultures were grown for two days. For *E. coli* cells containing a cloned plasmid precultures were grown at 37 °C over night. In case of minimal medium-glycerol stocks containing NCβAla as only nitrogen source (*N*CβAla stocks) a corresponding minimal medium depending on the wild type strain was used (Table 15 and Table 16). All strains were incubated in shaking flasks at 120 or 130 rpm. In each case main cultures were inoculated with 0.1 OD_{600} and grown until OD_{600} of 0.8-1 was reached. 850 µl of cells were then transferred to a sterile cryovial and gently mixed with 150 µl of sterile glycerol. Cryovials were frozen with liquid nitrogen immediately.

3.2.2.3 Cultivation of wild type-strains on minimal medium-agarose plates

A cryo culture of each strain was plated on an agarose plate with a recommended complex medium to verify if the cells of the glycerol stock were still alive. In addition cells were directly plated on plates with minimal medium containing uracil, thymine and ammonium sulphate as sole nitrogen source. As a control cells were also plated on a minimal medium without any nitrogen source. For all bacterial strains the minimal media for bacteria (BM3) were used (Table 14) and for all fungi including yeasts the corresponding yeast media (YM3) were used (Table 16).

If a significant growth on uracil or thymine, compared to the negative control, was observed cells were transferred to a minimal medium with a different nitrogen source. Therefor cells

grown on uracil or thymine were picked with an inoculating loop and diluted through distribution in a 20 µl drop of sterile PBS. Subsequently cells were plated on corresponding minimal medium agarose-plate containing 10 mM *N*CβAla as only nitrogen source. For each transfer step the same procedure was conducted to plate cells on a corresponding minimal medium without any nitrogen source as a control. If significant growth on *N*CβAla was observed, compared to the negative control, cells from the *N*CβAla-plate could be transferred to another plate containing 10 mM *N*CβPhe as sole nitrogen source. Transfer was performed as described above. Taking photos documented growth of each strain on various nitrogen sources every one to two days. For all strains with significant growth on *N*CβAla glycerol stocks were prepared (*N*CβAla stocks) (3.2.2.2).

3.2.2.4 Cultivation of wild type strains in liquid minimal medium

A selection of wild type strains showing a significant growth on *N*CβAla-agarose plates as sole nitrogen source was cultivated in liquid culture. Therefor *N*CβAla glycerol stocks were used as explained in section 3.2.2.2. For each strain overnight precultures with BM3 or YM3 containing 10 mM *N*CβAla were grown. In case of yeasts the precultures were incubated for two days. Medium was prepared as described in Table 15 and Table 16 without pure agarose. Cultivation temperature was dependent on the strain (see 3.1.1.2). All flasks were incubated at 130 rpm. Main cultures were inoculated with 0.1 OD_{600}. Each main culture was conducted in triplets consisting of 200 ml medium each in 1 L shaking flasks. Additionally a negative control was carried containing BM3/YM3 medium without any nitrogen source. Measuring OD_{600} monitored strain growth. When a strain reached the end of exponential phase cells were harvested, centrifuged at 30.000 rpm for 30-60 min. The medium was discarded and the pellets were washed 3 x in PBS solution. After final centrifugation cells were first frozen with liquid nitrogen and subsequently freeze dried in a lyophylle. Cells were stored at -20 °C until use for biotransformation experiments.

3.2.3 Biochemical methods

3.2.3.1 Cell disruption

3.2.3.1.1 Gram-negative bacteria

Gram-negative bacteria were lysed either by sonification at 40 % impulse (3 x 10 sec, with 30 sec break in between). For lyse of higher cell amounts homogenisation at 16.000 psi was

contributed using a high-pressure homogenisator. For both methods cells were dissolved in HEPES buffer or PBS (5 ml/ g wet biomass). After cell disruption cell debris were removed by centrifugation. Depending on the lysate volume different centrifuges and rotors were used. Low volumes (< 50 ml) were centrifuges at 14.500 rpm for 10-20 min at 4°C. Volumes higher than 50 ml were centrifuged using rotor JA-10 at 10.000 rpm in a Beckmann centrifuge. In case of subsequent FLPC lysate was centrifuged at 30.000 rpm for 1 h using rotor JA-25.50. Supernatant was transferred in a fresh reaction tube and kept on ice until use.

3.2.3.1.2 Gram-positive bacteria

Gram-positive bacteria were lysed either by sonification or homogenisation. Choice of method was dependent on the experiment. If active enzymes was for further experiments cells were lysed by homogenisation. Therefor cells were resuspended with buffer and homogenized at 21.000 psi for at least 3 min in loop (5 ml/ g wet biomass). Afterwards lysate was chilled on ice immediately. If the enzymes no longer had to be active after disruption sonification was chosen. Cells were pre incubated with HEPES buffer containing 1 % SDS and 2.4 % Triton-X 100 for pre-damaging the cell walls. Additionally 40 mg/ml Lysozyme were incubated with the cells under rotation at room temperature for 30 min. Sonification was performed for 10 min at 60 % amplitude with an interval of 10 sec. Cell debris were removed by centrifugation.

3.2.3.2 Recombinant protein expression in *E.coli*

Proteins were expressed by induction of expression with IPTG in TB medium. Therefore a preculture was inoculated with *E. coli* cells containing the desired plasmid. For pLJSRSF7 vectors kanamycin (50 µg/ml) and for pET vectors ampicillin (100 µg/ml) was used as selection marker. The preculture was incubated at 37 °C over night at 120 rpm in a shaking flask. In order to ensure a good oxygen input, the shake flasks were filled to a maximum of only 20 % of their original volume. The desired amount of main cultures were inoculated with 0.1 OD_{600} and further incubated at 37 °C. Immediately after an OD_{600} of 0.6-0.8 was reached protein expression was induced by adding 0.5 - 1 mM of IPTG final concentration. Then the temperature was decreased to the expression temperature and incubated for the duration given in Table 34. Protein expression conditions for all expressed plasmids are given in Table 34. After protein expression cells were harvested by centrifugation at 10.000 rpm for 20-30 min

at 4 °C. Cells were either chilled on ice and lysed right away or frozen with liquid nitrogen and stored at -20 °C until use.

Table 34: Expression of cloned plasmids

Name of plasmid	Expression vector	Expression		
		IPTG (mM)	T (°C)	Duration (h)
Burk_bUp1	pLJSRSF7	0.5	20	16
Burk_bUp2	pLJSRSF7	0.5	20	16
Burk_bUp3	pLJSRSF7	0.5	20	16
Burk_bUP4	pLJSRSF7	0.5	20	16
Burk_bUp5	pLJSRSF7	0.5	20	16
P. oleov_bUp6	pLJSRSF7	0.5	20	16
P.aeru_bUp7	pLJSRSF7	0.5	20	16
S.kl_bUp	pLJSRSF7	0.5	20	16
	pET21b(+)	1	20	16
3N5F	pET19	1	30	16
1FO6	pET19	1	30	16
5I4M	pET19	1	30	16
1Z2L	pET19	1	30	16

3.2.3.3 Fast Liquid Protein Chromatography (FLPC)

In this work a Äkta-Start system by GE Healthcare was used for purification of fusion proteins *via* His- or MBP-Tag. All used buffers for the different purification methods are given in Table 21. After recombinant protein expression in *E. coli* (3.2.3.2) cells were resuspended in buffer A and if necessary incubated with a spatula tip of lysozyme and DNAse at room temperature for 30 min under rotation using a tube rotator at 100 rpm. Afterwards cells were lysed by homogenisation or sonification as described in 3.2.3.1.1. After equilibration of the column the prepared lysate was loaded on a 5 ml MBP- or 1 ml His-trap column. The choice of column was dependent on the plasmid affinity tag of the expressed enzyme. In the second step the column was rinsed with buffer A to flush all unbound proteins from the column. The washing step continued until the measured UV absorption at 280 nm was close to zero. In the final step a gradient with buffer B (500 mM imidazole or 10 mM maltose) was applied. The steepness and length of the gradient was depended on the protein and had to be determined in previous tests. A high excess of imidazole or maltose in buffer B led to the elution of the protein of interest from the column. The peak containing the enzyme was fractionated in 15 ml reaction tubes, pooled and concentrated by filtration with a Vivaspin concentrator vial (10 kDa cut off value). During concentration the protein was rebuffered to buffer A. Protein concentration was measured as described in 3.2.3.4. Table 6

gives an overview of all cloned plasmids in this work. All enzymes cloned into pLJSRSF7 vector were purified through an MPB-tag affinity column. All pET-vector systems with His-Tag were purified with a Ni/NTA column.

3.2.3.4 Determination of protein concentration

To measure the protein concentration, an UV/Vis spectrophotometer (Epoch) was used at a wavelength of 280 nm. Using Lambert-Beer's law, the instrument calculates the protein concentration (mg/ml) according to:

$$\boldsymbol{A_{280} = c * \varepsilon_{280} * b}$$

c: Protein concentration in mg/µl
A_{280}: Extinction (Absorption) at 280 nm
ε_{280}: Extinction coefficient [L * $mMol^{-1}$ * cm^{-1}]
b: Path length [cm]

3.2.3.5 SDS-PAGE

SDS polyacrylamide gel electrophoresis (SDS-PAGE) was used to separate protein mixtures according to their size in an electric field. The relative molecular weight of a protein was determined using marker proteins. For lysate samples 20 µl were taken and mixed with 5 µl of 5 x SDS sample buffer. For samples of the pellet a little amount of pellet debris was picked a pipette tip and resuspended in 20 µl 2 x SDS-sample buffer. For complete denaturation, the protein-dye mixtures were heated at 95 °C for 5 min before application to the gel. For all SDS-PAGEs a 12.5 % separation gel and a 5 % stacking gel was used. The *Prestained Protein Marker* by NEB or Thermo Fisher was used. All SDS-Gels were run in 1 x TGS buffer at 200 V over 50 min. After electrophoresis, the gel was carefully rinsed with dH_2O and dyed with Coomassie blue staining solution for 30 min under shaking. Then the gel was decoloured with destaining solution for a few minutes or in dH_2O over night.

3.2.3.6 Biotransformations

Biotransformations were conducted with either lysate (3.2.3.1.1) or purified enzyme (3.2.3.3). In general 5 or 10 mM of substrate dissolved in HEPES buffer were incubated with lysate or purified enzyme at a specified temperature during shaking at 1000 rpm. Lysate was obtained resuspending 1 g wet biomass of expressed cells with 5 ml HEPES buffer. Cells were disrupted using sonification (see 3.2.3.1).

The incubation temperature was dependent on the expressed protein. Table 35 gives an

overview of the used reaction conditions for each enzyme. If needed a high concentrated metal cofactor solution was added to the reaction. In case of long-term experiments reactions were stopped by denaturation for 5 min at 95 °C. If reactions had to be stopped after a certain time 10 % (v/v) of a 2 M HCl solution was added to the mixture. After 5 min incubation at room temperature, 10 % (v/v) of 2 M NaOH was added to neutralize the reaction for HPLC measurement. Reactions were directly prepared for analysis or stored at -20 °C. After samples had thawed at room temperature analysis was conducted (assays or HPLC). Before analysis samples were always centrifuged for at least 10 min at 13.000 rpm. After samples had been thawed once, they had never been frozen again to prevent amino acid decay.

Table 35: Reaction conditions of all decarbamoylating enzymes.
For novel uncharacterized enzymes an initial reaction temperature of 30 °C in HEPES buffer pH 7 was used. For 3N5F, 1FO6 and 1Z2L optimal reaction conditions were used as found in literature [176], [182], [224]. *N.d.* = not determined.

Enzyme	Initial T (°C)	Initial pH	T_{opt} (°C)	pH_{opt}
Burk1	30	7	40	6.8
Burk2	30	7	*n.d*	*n.d*
Burk3	30	7	*n.d*	*n.d*
Burk4	30	7	*n.d*	*n.d*
Burk5	30	7	*n.d*	*n.d*
P.oleo	30	7	*n.d*	*n.d*
P.aeru	30	7	40	6.8
2V8H	30	7	30	8
5I4M	30 °C	7	*n.d*	*n.d*
3N5F	-	-	65	7.5
1FO6	-	-	37	7
1Z2L	-	-	30	7

3.2.3.7 Determination of kinetic parameters

Data for kinetic studies were generated with FPLC purified enzymes. Therefor enzyme solutions of different concentrations were incubated with the desired substrate. For each substrate additional substrate and product controls without enzymes were carried. In those buffer was added to the substrate solution instead of enzyme. Prior to reaction start, substrate solutions were heated to the desired temperature. At certain time points enzyme reactions were stopped by adding 2 M HCl (10 % (v/v)). Then samples were incubated at room temperature for at least 5 min and neutralized by adding the same volume of 2 M NaOH. Samples were then analysed as described earlier.

K_M and k_{cat} values were calculated with the following formula.

Lineweaver-Burk:

$$\frac{1}{A_{spez}} = \frac{K_M}{A_{max}} * \frac{1}{c_s} + \frac{1}{A_{max}}$$

Michaelis-Menten:

$$A_{spez} = \frac{A_{max} * c_s}{K_M + c_s}$$

Catalytic efficiency:

$$\frac{k_{cat}}{k_M} = \frac{k_2}{k_M}$$

$$k_2 = \frac{v_{max}}{[E]_0} = \frac{(d[P]dt)_{max}}{[E]_0} = k_{cat}\ (s^{-1})$$

with

A_{spez}: specific activity U/mg (µmol/(min*mg)

K_M: Michaelis-Menten constant (mM)

A_{max}: maximum specific activity

c_s: substrate concentration (mM)

k_{cat}: turnover number (s^{-1})

k_2: constant for product formation

v_{max}: maximum speed (mol * L^{-1} * s^{-1})

$[E]_0$: constant enzyme concentration

[P]: product concentration (mM)

3.2.4 Chemical methods

3.2.4.1 Synthesis of *N*-carbamoyl-amino acid derivates

Since *N*-carbamoyl-substrates were not commercially available they were synthesized. This was conducted through stirring the corresponding amino acid with potassium cyanate (KNCO). The general reaction scheme is shown in Figure 28.

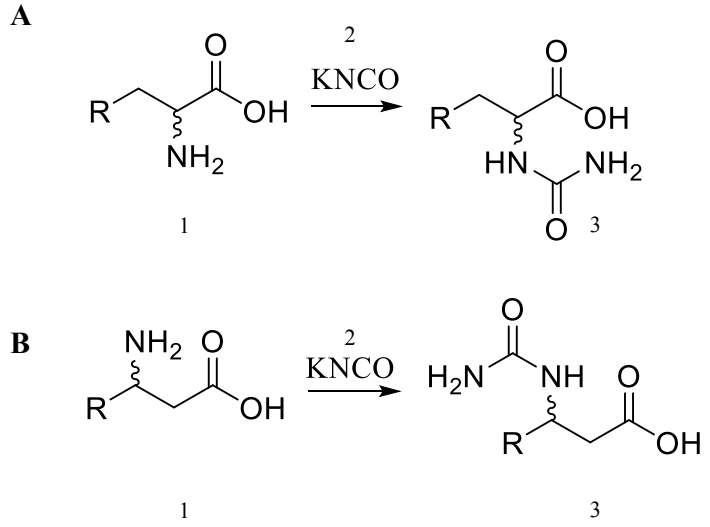

Figure 28: Synthesis of *N*-carbamoyl-amino acids.
A) Chemical synthesis of *N*-carbamoyl-α-amino acid: A α-amino acid (1) reacts with KNCO (2) to a *N*-carbamoyl-α-amino acid (3). B) Chemical synthesis of *N*-carbamoyl-β-amino acid. A β-amino acid (1) reacts with KNCO (2) to a *N*-carbamoyl-β-amino acid (3).

The exact conditions for all reactions are given in Table 36 and Table 37. For the synthesis a stirred glycerine bath was heated to the required temperature. A two-necked flask was connected to a reflux condenser. For stirring a magnetic stirrer was put inside the flask. The required amount of amino acid and KNCO was weighed in and dissolved separately in ddH_2O. The volume of ddH_2O required was dependent on the quantities used. After preheating the dissolved amino acid in the two-neck flask the reaction was started by adding KNCO solution. Reaction time differed between synthesized *N*-carbamoyl-amino acids. In case of *N*Cβ-homo-amino acids the reaction equilibrium was maintained on the product side by pH titration to 7 with 2 M HCl. Reaction was stopped by lowering the pH to 3 with 6 M HCl. Reaction was cooled down in ice. Due to the low water solubility of most of the reaction products they precipitated by crystallization through scratching on the inside of the flask with a glass tube. Afterwards crystals were sucked off with a vacuum tank filter. Because of the high water solubility of *N*Cβ-homo-amino acids the product crystallization was conducted by

freeze-drying. For all reaction products analysis *via* ^{1}H-NMR and/or ^{13}C-NMR and mass spectrometry was performed.

3.2.4.1.1 Chemical synthesis of *N*-carbamoyl-α-amino acids

The synthesis of *N*-carbamoyl-α-amino (NCαAAs) acids was conducted at 80 °C for 1 h. After cooling on ice during titration to pH 3 NCαAAs crystalized immediately. An overview of the NCαAAs synthesized in this work is given in Table 36.

Table 36: Molecular ratios for synthesis of *N*-carbamoyl-α-amino acids.
Reactions were performed in 200 mg scale in 10 ml ddH_2O.

Reaction product	Educt		KNCO	Molecular ratio Amino acid: KNCO
		mmol	mmol	
N-carbamoyl-α-L-leucine	α-L-leucine	1.53	1.87	
N-carbamoyl-α-L-cysteine	α-L-cysteine	1.65	2.02	1:1.233
N-carbamoyl-α-L-lysine	α-L-lysine	1.23	1.50	

3.2.4.1.2 Chemical synthesis of *N*-carbamoyl-β-(homo)-amino acids

NCβAla and NCβPhe were synthesized in one hour at 80 °C and crystallized by scratching. NCβHAAs were synthesized at 50 °C and crystallized by freeze-drying and stored in an excicator due to their hygroscopic properties. *N*-carbamoyl-L-3-amino heptanoic acid was crystallized by storage for three to four days at 4 °C An overview of all synthesized NCβ-(homo)-amino acids is given in Table 37.

Table 37: Molecular ratios for synthesis of *N*-carbamoyl-β-(homo)-amino acids.
Reactions were performed in 100 mg scale in 10 ml ddH_2O.

Reaction product	Educt		KNCO	Molecular ratio Amino acid: KNCO	T (°C)	Time (h)
		mmol	mmol			
N-carbamoyl-β-alanine	β-alanine	2.245	2.746	1:1.2	80	1
N-carbamoyl-β-phenylalanine	β-phenylalanine	1.21	1.48	1:1.2	80	1
N-carbamoyl-β-L-homo-methionine	β-L-homo-methionine	0.61	1.84	1:3	50	144
N-carbamoyl-β-L-homo-alanine	β-L-homo-alanine	0.97	2.91	1:3	50	48
N-carbamoyl-β-D-homo-alanine	β-D-homo-alanine	0.97	2.91	1:3	50	72
N-carbamoyl-β-L-homo-serine	β-L-homo-serine	0.84	1.68	1:2	50	24
N-carbamoyl-β-D-homo-serine	β-D-homo-serine	0.84	1.68	1:2	50	24
N-carbamoyl-β-D/L-leucine	β-D/L-leucine	3.8	4.6	1: 1.21	80	2
N-carbamoyl-L-3-amino heptanoic acid	L-3-amino heptanoic acid	1.37	1.66	1:1.21	80	2

3.2.4.1.3 Synthesis of allantoic acid

Allantoic acid was synthesized due to alkaline hydrolysis of allantoin. Therefor 100 mg of allantoin were dissolved in 10 ml ddH_2O and the pH was titrated so 10-12 with 10 M NaOH. To keep the reaction equilibrium on the product side the pH was regularly increased to 10-12 if the pH was lower than 10. Reaction completion was analysed with TLC.

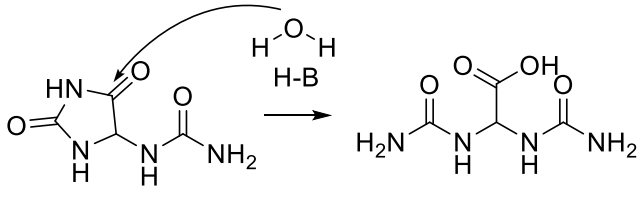

(1) (2)

Figure 29: Synthesis of allantoic acid.
Continuous addition of NaOH to allantoin (1) leads to cleavage of the ring and results in allantoic acid (2).

3.2.4.2 Nuclear Magnetic Resonance and Mass Spectroscopy

Synthesis products were verified by analysis with ^{1}H and ^{13}C nuclear magnetic resonance (NMR) spectroscopy. Therefor 10 mg of compound were dissolved in a deuterized solvent (D_2O or DMSO). Measurements were performed at the institute of organic chemistry (KIT) with a NMR-spectrometer at 300 MHz. Results were visualized using MestReNova [203]. A report of all compounds of with NMR was performed is given in Table 40 (p. 86).

Additional verification of synthesis products was conducted by mass spectrometry (MS) analysis. The institute of organic chemistry at KIT carried out MS measurements. Results were visualized using the program SeeMS.

3.2.5 Analytical methods

3.2.5.1 Photometric Ehrlich-Assay

The Ehrlich-Assay was used for detection of aliphatic *N*-carbamoyl-amino acids. The free amino group of the carbamoyl-residue acts as a nucleophile and attacks the partially positive charge of the carbonyl C-atom of the 4-(Dimethylamino)benzaldehyde as shown in Figure 30.

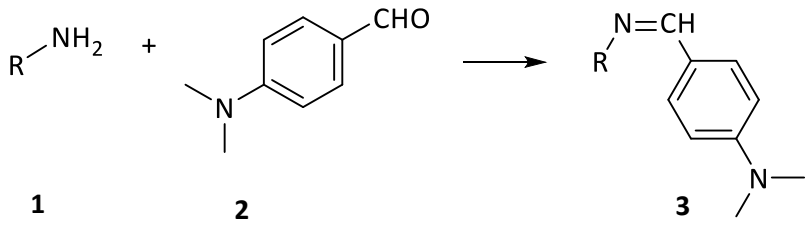

Figure 30: Derivatization of *N*-carbamoyl-amino acids with Ehrlich reagent.
The free amino group of a *N*-carbamoyl-amino acid (2) undergoes a nucleophilic reaction with 4-(Dimethylamino)benzaldehyde (2) which results in a Schiff base (3), detectable at 430 nm.

Often a liquid handling station (BRAND) was used for pipetting the assay. The assay was carried out due mixing 50 µl of sample with 30 µl of Ehrlich reagent (Table 20) in a 96-well microtiter plate. The plate was shaken for 2 min at 800 rpm in a microtiter plate shaker and analysed at 430 nm immediately with Epoch photometer. For all *N*-carbamoyl-amino acid derivates a linear five- to seven-point calibration curve was generated over the concentration range of 0.1 to 10 mM. The correlation coefficient was always 0.99 or better.

3.2.5.2 Thin-Layer-Chromatography (TLC)

Thin-layer-chromatography was mostly used for monitoring substrate synthesis. Therefor silica TLC-plates were used. The choice of solvent was dependent on the amino acid, which was analysed. All used solvents are given in Table 24. A TLC chamber was filled 0.5 cm with required solvents. TLC run was stopped when the running height of the solvent reached the top of the TLC plate. TLC's were dyed using staining solutions given in Table 24 and blow-dried. For staining with Iodid- or Ehrlich-staining solution TLC was air-dried.

3.2.5.3 High Performance Liquid Chromatography (HPLC)

Product analysis for almost all amino acids was performed with HPLC. All aromatic amino acids and corresponding *N*-carbamoyl derivate were detected through their delocalised electron-π-system at a certain UV wavelength. Due the absence of an aromatic-π-electron system, aliphatic amino acids were covalently coupled to an derivatization reagent before for detection via UV. For all amino acids a linear five- to seven-point calibration curve was generated over the concentration range of 0.1 to 10 mM. The correlation coefficient was always 0.99 or better.

3.2.5.3.1 Detection of aliphatic amino acids

All aliphatic amino acids (except L-3-aminoheptanoic acid and D/L-β-leucine) could be detected through precolumn derivatization with o-phtaldialdehyde and *N*-isobutyryl-L-cysteine. The method was based on Brucher [225]. Depending on the amino acid, the method was slightly modified (see Table 38). During the reaction the primary amine of the amino acids nucleophilicly attacks the carbonyl C-atom of OPA. After some rearrangements an amino-acid-OPA complex forms, which can be detected at 338 nm (Figure 31).

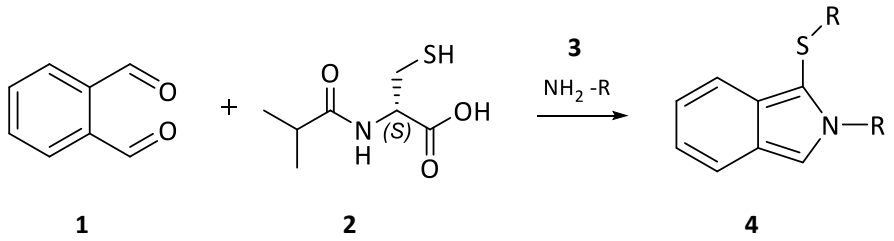

Figure 31: Derivatization of primary amines with OPA/IBLC.
OPA (1) is nucleophilicly attacked by IBLC (2) an amine (3) and an aromatic complex (4) is generated

Due to the chirality of IBLC, both enantiomers of a racemate are separated by HPLC analysis. During automatically precolumn derivatization with an Agilent 1100 series automatic liquid sampler the following solutions were used in the reaction: 2 µl sodium borate buffer (NaB) were mixed with 3 µl of OPA/IBLC solution and a varying volume of the sample (see section 4.2.2, p. 91). After 1 min the reaction was terminated by addition of 3 µl of 3 % acetic acid solution. Immediately afterwards the total volume was injected into the column. The complex was detected at 338 nm with an UV detector. All described solutions are listed in Table 20. As a solvent NaPP buffer was mixed with MeOH by the HPLC in different ratios. All measurements were run with isocratic elution at a flow rate of 0.8 ml/min on a 4.6 x 150 Hyperclone 5 µm ODS C18 120 Å column (Phenomenex). A pre-column-guard containing a security guard catridge C18 with 3 mm internal diameter was attached in front of it. OPA/IBLC mixture was always freshly prepared and never used for a longer period than two days. Measurement of amino acid standards was performed in the beginning and additionally at the end of every measurement to determine the stability of the OPA/IBLC mixture. An overview of the amino acids detected with this method, is listed in Table 38.

Table 38: Aliphatic amino acids detected *via* OPA/IBLC derivatization.

Amino acid	NaPP (%, v/v)	MeOH (%, v/v)	Approximate retention time (min)	Sample volume (µl)
D/L-α-amino-n-butyric acid	60	40	4.0 / 5.1	0.5
L-α-cysteine	60	40	3.1	0.5
L-α-isoleucine	60	40	9-10	0.5
L-α-leucine	45	55	3.1	0.5
L-α-methionine	60	40	5.8	0.5
L-α-serine	60	40	2.2	0.5
L-α-valine	60	40	5.3	0.5
α-glycine	60	40	2.6	0.5
β-alanine	60	40	3	0.5
β-D-homoalanine hydrochloride	60	40	7.8	2.5
β-D-homoserine	60	40	3.4	2.5
β-L-homoalanine hydrochloride	60	40	5.8	2.5
β-L-homomethionine	60	40	14.2	5
β-L-homoserine	60	40	3.3	2.5

3.2.5.3.2 Detection of aromatic amino acids

Aromatic amino acids and their corresponding *N*-carbamoyl-derivates were analysed using a Synergi 4 µ Fusion RP C18 80 Å, 150 mm, 4.6 mm column attached to a pre-column-guard containing a C18 RP pre-column with 3 mm internal diameter. An isocratic elution at a flow rate 0f 0.8 ml/min with a mixture of 20 mM KH_2PO_4 pH 3 and MeOH (70:30 (v/v) ratio) was used. Detection was conducted at 210 nm with an UV-detector. The amino acids and their corresponding *N*-carbamoyl-derivates are listed in Table 39.

Table 39: Aromatic amino acids detected at 210 nm.

	Approximate retention time of	
Amino acid	*N*-carbamoyl-derivate (min)	Amino acid (min)
2-amino-thienylalanine	9.08	3.15
α-D-tryptophan	5.28	2.2
α-L-phenylalanine	13.56	4.05
α-L-tryptophan	18.15	5.65
α-para-hydroxy-phenylglycine	3.05	2.22
α-phenylglycine	6.19	2.69
β-D/L-phenylalanine	8.83	3.28
β-D/L-tyrosine	3.57	2.44

3.2.5.3.3 Derivatisation with Fmoc

Derivatization with Fmoc was tested as an alternative method for aliphatic amino acids, which were not detectable by derivatization with OPA/IBLC. A modified method of Clapp *et al.* and Taillades *et al.* was used [226], [227]. An amino acid dissolved in ddH_2O was mixed with Fmoc solution in a ratio of 1:1 for 40 sec. Afterwards the mixture was washed for three times with the double volume of hexane. Thereby unreacted Fmoc was extracted. The upper organic phase was discarded and the lower watery phase was injected to the column. For measurement an elution program was run at a flow rate of 1.3 ml/min. It started with an isocratic elution with 100 % mobile phase A for 3 min. Then a linear gradient from 100 % A to 100 % mobile phase B was run in 9 min. Subsequently an isocratic elution was performed with 100 % mobile phase B for 11 min and detected at 245 nm with an UV detector. Between to measurements the column had to be equilibrated with 100 % mobile phase A again. All used buffers and solutions are given in Table 19 and Table 20.

3.2.5.4 Fluorescence assay for detection of β-(homo)-amino acids

As HPLC detection with OPA/IBLC derivatization was not successful for L-3-aminoheptanoic acid and D/L-β-leucine another derivatization reagent composition of OPA and 3-MPA (Table 20) was used.

In a black 96-well fluorescence microtiter plate 32 µl of borate buffer (Table 20) were mixed with 4 µl of sample. After addition of 32 µl of OPA/3-MPA solution the microtiterplate was covered with aluminium foil and incubated at room temperature for 7.5 min under light shaking in a microtiter plate shaker. Samples were extincted at 345 nm und their emission was detected at 450 nm with a fluorescence detector (Tecan). Due to the sensitivity of this method all samples with concentrations above 1 mM had to be diluted in HEPES buffer. For all detected amino acids a five-point to seven-point calibration curve in a range from 0.1 - 1 mM was generated. The correlation coefficient was always 0.99 or better.

3.2.6 Bioinformatic methods

3.2.6.1 Generation of enzyme models

For all novel enzymes (Burk1-5, P. oleo and P.aeru) no official crystal structure was available. Because structure is better-conserved evolutionarily than sequence, models were generated with the protein sequences of these enzymes (see Table 4, p. 48) using Phyre^2 tool

[205, 184]. This algorithm performs a profile-profile alignment of the submitted protein sequence against its fold library. As a result distantly related structures that are compatible with the target sequence are identified. The algorithm uses known structures of the PDB-database. Output file is a PDB-file that can be visualized e.g. using PyMol. The Phyre^2 server also proposes residues putatively involved in the catalytic mechanism of the enzyme. Generated models always had a confidence of 100 % and a sequence homology >30 % and thus were assumed as good models since a confidence <90 % is not recommended [205].

3.2.6.2 Substrate docking with ROSIE-ligand

Computational methods like molecular docking are used to predict a ligand-receptor complex structure [183]. ROSIE (Rosetta Online Server that Includes Everyone) [185] is an online tool, which can be used for several modulations. E.g. it can be used for docking a ligand into a proteins tertiary structure at certain coordinates (Ligand_docking). Therefore, enzymes crystal structures were obtained from PDB website in PDB-format. To submit a ligand-docking task the desired PDB-file was uploaded to the ROSIE-ligand docking tool web page as well a previously generated 3D-molecule file. The 3D-file of the substrate was generated with Chem Draw 3D and saved as SDF-file. Ligand conformers were generated automatically and the maximum number of conformers was set to 200. Starting coordinates were set (see section 3.2.6.3) and 200 to 500 structures were generated with the following standard settings: maximum searching radius 5 Å; number of Monte Carlo sampling steps set to 500; randomized initial position of the ligand was given with a radius of 3 Å; low-resolution grid was set to 15 Å; low-resolution translation Monte Carlo step was set to 0.1 Å and the total cycles of highres docking was set to 6; every third cycles of highres dockings was repacked. An overview of the input is shown in Figure 32, p.84.

3.2.6.3 Generation of starting-coordinates

All protein crystal structures are embedded in a 3D-coordinate system (x, y, z). The ligand coordinates of each structure had to be determined to be able to use Ligand-Docking of Rosie-Server. It is important to use the same starting coordinates when comparing different ligands for one enzyme. In case of protein structures of 2V8H, 1Z2L and 5I4M a ligand was co-crystallized and included in the file of the protein structure available at PDB-database. For those enzymes the coordinates were obtained from the read off the PDB-file viewed in the program Notepad. In case of 3N5F and 1FO6 the starting coordinates were obtained by

alignment with highly homologous enzyme structures, co-crystallized with a ligand. 3N5F ligand starting-coordinates were generated with aligning to 2V8H (co-crystallized with *N*-carbamoyl-β-alanine). An alignment of 1FO6 with 1UF5 generated starting coordinates for 1FO6. IUF5 is also a D-Carb co-crystallized with *N*-carbamoyl-α-D-methionine.

3.2.6.4 Evaluation of docking experiments

To differentiate and estimate correct poses from incorrect poses of ligands docked into an active site energy scores are generated [183]. Each docking experiment performed with ROSIE gives out energy scores of the generated models: total score and interface delta (IΔ). The IΔ value represents a measure of binding energy between the ligand and enzyme molecule. It is defined as the contribution to the total score for which the presence of the ligand is responsible [184]. The IΔ is the crucial factor in the docking experiment. The lower those score values are the better the theoretical fit of the ligand into the enzyme model. However, the model with the lowest energy scores does not have to be the most realistic one. To get an idea whether a model is realistic or not it has to be manually evaluated using protein-visualizing software like PyMol.

Dockings of different ligands (*in vitro* tested enzyme substrates) were performed with the same starting-coordinates for each enzyme. Of 500 generated docking-models the top 10 models with the lowest total energies were analysed (Figure 32, p. 84). All of top 10 models were aligned with a model of the corresponding enzymes containing a natural *N*-carbamoyl-substrate (*N*-carbamoyl-β-alanine for βUps and L-Carbs, allantoic acid for AaHyds, and *N*-carbamoyl-α-D-methionine for D-Carb). Out of those 10 models one or two models were picked, which were orientated as similar as possible to the natural co-crystallized substrate. Of all top 10 models a median and standard deviation of the scoring results (total score and interface delta (IΔ) was calculated, which were coordinated in the same way as the natural substrate. An exemplary table with scoring results is shown in Figure 32 C, p 85. Docking experiments were used for proposal of the active centres of novel decarbamoylating enzymes. Additionally they were used to evaluate whether they reflect the results of *in vitro* experiments and to obtain an idea towards the catalysis mechanism in the active centre.

A

Ligand Docking Job 1Z2L_NCbLPhe_500 「№71910」 Details

Inputs

[protein.pdb]

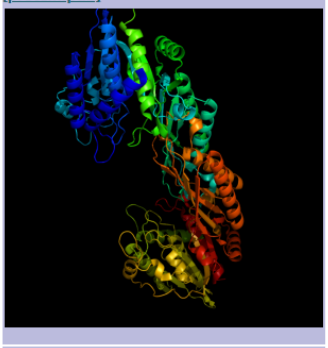

[ligand.sdf]

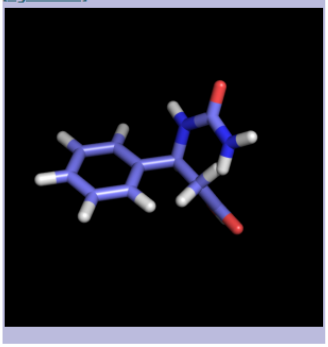

Status

Job ID	71910
Job Name	1Z2L_NCbLPhe_500
Visibility	**PUBLIC** (you can share this job)
Protocol	Ligand Docking
CPU hours used	6.4
user	PredictCaro
Status	**Finished**
Daemon	GrayLab.Rosetta-1
Description	
angle_step	5.0
chain	X
gen_conformers	True
grid_width	15.0
highres_cycles	6
highres_repack_cycles	3
initial_perturb	3.0
move_step	0.1
n_ligand_conformers	200
nstruct	500
pocket_width	5.0
transform_cycles	500
use_input_position	False
x_start	61.468
y_start	32.453
z_start	22.665
Submitted time	2019-06-13 12:37
Start time	2019-06-13 12:56
End time	2019-06-13 13:03
Daemon	GrayLab.Rosetta-1

B

Results

Ten lowest-interface_delta-energy structures created in the ligand-docking run:

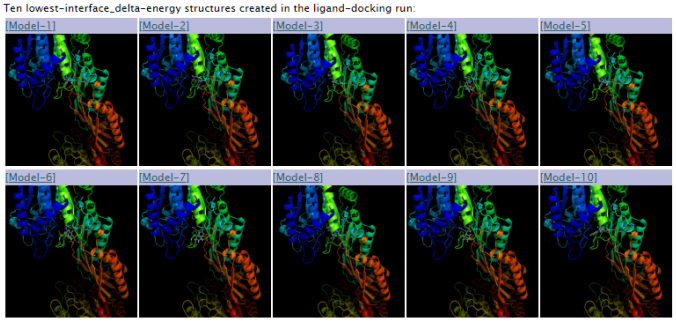

Interface Score/Total Score

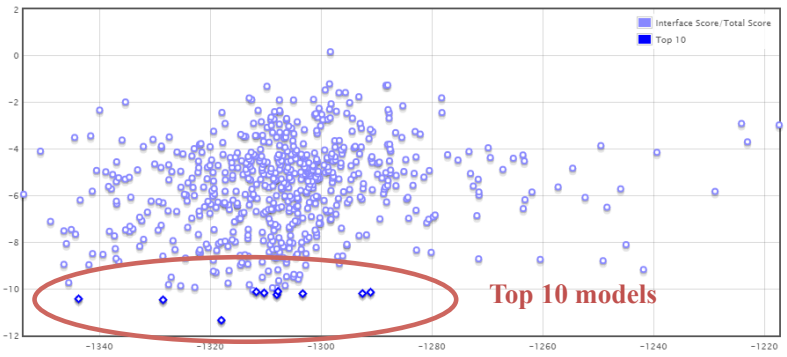

Hover over the graph points to see exact score and download particular result file.

C

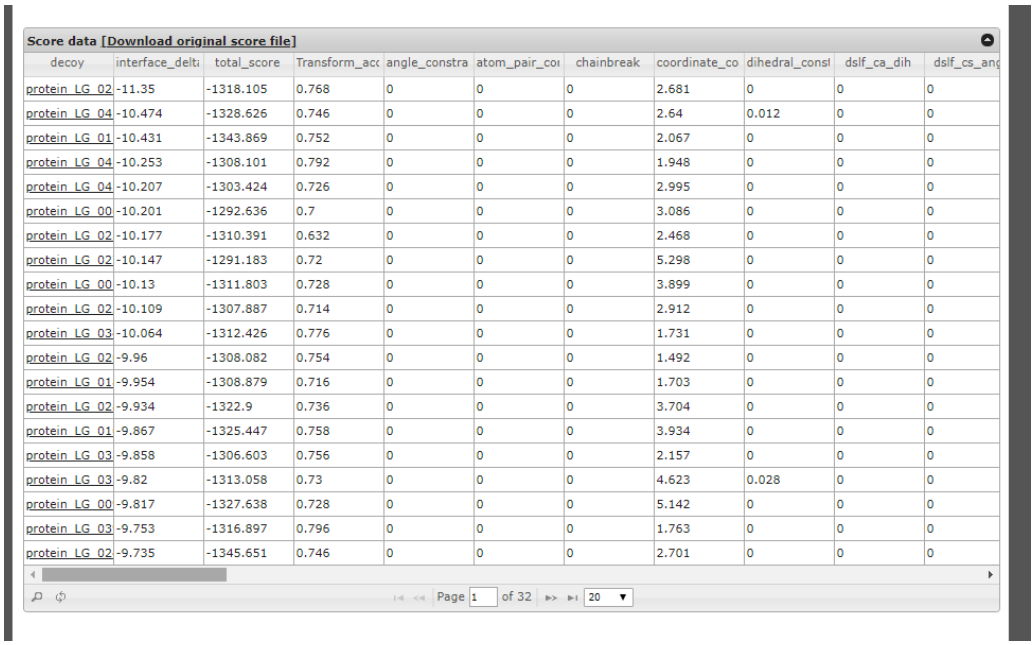

Score data [Download original score file]

decoy	interface_delti	total_score	Transform_acc	angle_constra	atom_pair_cor	chainbreak	coordinate_co	dihedral_consl	dslf_ca_dih	dslf_cs_ang
protein_LG_02	-11.35	-1318.105	0.768	0	0	0	2.681	0	0	0
protein_LG_04	-10.474	-1328.626	0.746	0	0	0	2.64	0.012	0	0
protein_LG_01	-10.431	-1343.869	0.752	0	0	0	2.067	0	0	0
protein_LG_04	-10.253	-1308.101	0.792	0	0	0	1.948	0	0	0
protein_LG_04	-10.207	-1303.424	0.726	0	0	0	2.995	0	0	0
protein_LG_00	-10.201	-1292.636	0.7	0	0	0	3.086	0	0	0
protein_LG_02	-10.177	-1310.391	0.632	0	0	0	2.468	0	0	0
protein_LG_02	-10.147	-1291.183	0.72	0	0	0	5.298	0	0	0
protein_LG_00	-10.13	-1311.803	0.728	0	0	0	3.899	0	0	0
protein_LG_02	-10.109	-1307.887	0.714	0	0	0	2.912	0	0	0
protein_LG_03	-10.064	-1312.426	0.776	0	0	0	1.731	0	0	0
protein_LG_02	-9.96	-1308.082	0.754	0	0	0	1.492	0	0	0
protein_LG_01	-9.954	-1308.879	0.716	0	0	0	1.703	0	0	0
protein_LG_02	-9.934	-1322.9	0.736	0	0	0	3.704	0	0	0
protein_LG_01	-9.867	-1325.447	0.758	0	0	0	3.934	0	0	0
protein_LG_03	-9.858	-1306.603	0.756	0	0	0	2.157	0	0	0
protein_LG_03	-9.82	-1313.058	0.73	0	0	0	4.623	0.028	0	0
protein_LG_00	-9.817	-1327.638	0.728	0	0	0	5.142	0	0	0
protein_LG_03	-9.753	-1316.897	0.796	0	0	0	1.763	0	0	0
protein_LG_02	-9.735	-1345.651	0.746	0	0	0	2.701	0	0	0

Page 1 of 32 20

Figure 32: Example of result output of the ROSIE server ligand-docking tool.
A) Input of docked substrate and PDB protein structure B) Overview of the top 10 models and energy diagram of all 500 generated models with the top 10 models circled in red. C) Energy score table sorted by lowest energy scores.

3.2.6.5 Identification of highly conserved amino acids

For directed protein engineering experiments highly conserved amino acids in each crystal structure were determined using ConSurf-algorithm. The amino acid sequence of the enzyme of interest was compared to 150 related sequences in the PDB-database with a multiple-sequence alignment (MSA) also conducted with ConSurf algorithm. An amino acid was assumed as highly conserved when it was the sole possible amino acid at this position of at least 85 % of the aligned sequences.

3.2.7 Protein Engineering

Protein engineering was performed with enzymes 3D tertiary structure available at PDB-database [228]. Primers for point mutations are given in

Table 27. Primers were designed with an overlap sequence of 10 base pairs with a T_m lower than 40 °C. Only the corresponding reverse primer included the mutation. Mutation-PCR was performed using Touch-Down-PCR protocol (3.2.1.6.2) with fitted elongation time according to the size of the template plasmid DNA. After PCR the methylated-template DNA was digested using DpnI enzyme and amplified DNA was transformed into recombinant *E. coli* BL21 DE3 cells. The resulting mutants of the enzyme of interest were expressed under the same conditions as given in Table 34 (p. 70). Recombinantly expressed proteins were purified through FLPC (3.2.3.3) and tested for substrate conversions.

4 Results

4.1 Synthesis of *N*-carbamoyl-amino acids

Since *N*-carbamoyl-amino acids are not commercially available (except NCβAla) they were chemically synthesized. An overview of the *N*-carbamoyl-amino acids used in this work is given in Table 9 (p. 53). NCαAAs and NCβAAs and allantoic acid were successfully chemically synthesized and analysed by NMR and/or MS.

4.1.1 Synthesis of aliphatic *N*-carbamoyl-α-amino acids

NCαAAs were synthesized as described in section 3.2.4.1. Their structure was verified by ^{1}H-NMR (section 3.2.4.2). Remaining educt was not detected in HPLC analysis. An overview of ^{1}H-NMR analysis of NCαAA synthesized in this work is given in Table 40. ^{1}H-NMR and mass spectrometry chromatograms are given in section 8.7 and 8.8.

Table 40: NMR data of synthesized *N*-carbamoyl-derivates.
"-" = No additional MS-analysis was performed; DMSO = dimethylsulfoxide; D_2O = Deuterium oxide.

Compound	NMR-Data	Mass spectrometry
N-carbamoyl-α-L-cysteine	^{1}H NMR (300 MHz, DMSO-d_6) δ 2.20 (t, *J* = 8.3 Hz, 1H), 2.80 (dd, *J* = 5.0, 7.9 Hz, 2H), 4.34 (dt, *J* = 4.9, 7.9 Hz, 1H), 5.75 (s, 2H), 6.35 (d, *J* = 8.0 Hz, 1H), 12.86 (s, 1H).	-
N-carbamoyl-α-L-isoleucine	^{1}H NMR (300 MHz, DMSO-d_6) δ 0.85 (t, *J* = 6.9 Hz, 7H), 1.00 – 1.45 (m, 2H, 5), 1.71 (ddt, *J* = 4.8, 6.7, 9.2 Hz, 1H, 4), 4.04 (dd, *J* = 5.2, 9.0 Hz, 1H), 5.61 (s, 2H), 6.18 (d, *J* = 9.0 Hz, 1H), 12.52 (s, 1H).	-
N-carbamoyl-α-L-leucine	^{1}H NMR (300 MHz, DMSO-d_6) δ 0.87 (dd, *J* = 6.5, 8.5 Hz, 6H, 6, 7), 1.29 – 1.53 (m, 2H, 5), 1.63 (dq, *J* = 6.7, 13.3 Hz, 1H, 4), 4.06 (td, *J* = 5.8, 8.7 Hz, 1H, 3), 5.57 (s, 2H, 12), 6.19 (d, *J* = 8.4 Hz, 1H, 2), 12.45 (s, 1H, 9).	-
N-carbamoyl-α-L-naphtylalanine	^{1}H NMR (300 MHz, DMSO-d_6) δ 3.05 – 3.63 (m, 2H), 4.09 – 4.65 (m, 1H), 5.59 (s, 2H), 6.35 (d, *J* = 8.3 Hz, 1H), 7.04 – 8.54 (m, 7H), 12.69 (s, 1H).	$[M + H^+]$
N-carbamoyl-α-L-neopentylglycine	^{1}H NMR (300 MHz, DMSO-d_6) δ 1.00 (s, 9H), 1.35 – 1.81 (m, 2H), 4.21 (td, *J* = 3.3, 9.0 Hz, 1H), 5.63 (s, 2H), 6.24 (d, *J* = 8.8 Hz, 1H), 12.48 (s, 1H).	$[M + H^+]$
N-carbamoyl-α-L-para-hydroxy-phenylglycine	^{1}H NMR (300 MHz, DMSO-d_6) δ 3.37 (s, 2H), 5.65 (s, 2H), 6.67 – 7.30 (m, 4H), 9.47 (s, 1H), 12.60 (s, 1H).	$[M + H^+]$
N-carbamoyl-α-L-tertiary-leucine	^{1}H NMR (300 MHz, DMSO-d_6) δ 4.10 (p, *J* = 1.8 Hz, 3H), 4.94 (s, 1H), 5.49 (d, *J* = 9.4 Hz, 1H), 7.20 (s, 2H), 7.80 (d, *J* = 9.4 Hz, 1H), 14.02 (s, 1H).	$[M + H^+]$
N-carbamoyl-α-L-thienyl alanine	^{1}H NMR (300 MHz, DMSO-d_6) δ 3.17 (qd, *J* = 5.9, 14.8 Hz, 2H), 4.34 (ddd, *J* = 4.9, 6.8, 8.2 Hz, 1H), 5.71 (d, *J* = 39.3 Hz, 2H), 6.21 (d, *J* = 8.1 Hz, 1H), 6.29 (s, 1H), 6.85 (dd, *J* = 1.3, 3.4 Hz, 1H), 6.95 (dd, *J* = 3.4, 5.1 Hz, 1H), 7.34 (dd, *J* = 1.3, 5.1 Hz, 1H), 12.78 (s, 1H).	$[M + H^+]$

Compound	NMR-Data	Mass spectrometry
N-carbamoyl-α-L-valine	^{1}H NMR (300 MHz, DMSO-d_6) δ 0.83 (dd, *J* = 6.8, 12.1 Hz, 6H, 5, 6), 1.98 (pd, *J* = 5.0, 6.9 Hz, 1H, 4), 3.98 (dd, *J* = 4.9, 9.0 Hz, 1H, 3), 5.62 (s, 2H, 11), 6.17 (d, *J* = 9.0 Hz, 1H, 2), 12.56 (s, 1H, 8).	-
α-L-neopentylglycine	^{1}H NMR (300 MHz, D_2O) δ 0.97 (s, 7H), 1.49 – 2.03 (m, 2H), 3.69 (dd, *J* = 4.9, 7.2 Hz, 1H).	$[M + H^+]$
α-L-tertiary-leucine	^{1}H NMR (300 MHz, D_2O) δ 1.04 (s, 9H, 9), 3.42 (s, 1H).	$[M + H^+]$

4.1.2 Synthesis of *N*-carbamoyl-β-(homo)-amino acids

In this work the synthesis of several novel *N*-carbamoyl-β-amino acids and *N*-carbamoyl-β-homo-amino acids (NCβ(h)AAs) was established. For the synthesis of these compounds no literature was available. Figure 33 shows an overview of the aliphatic NCβ(h)AAs synthesized in this work.

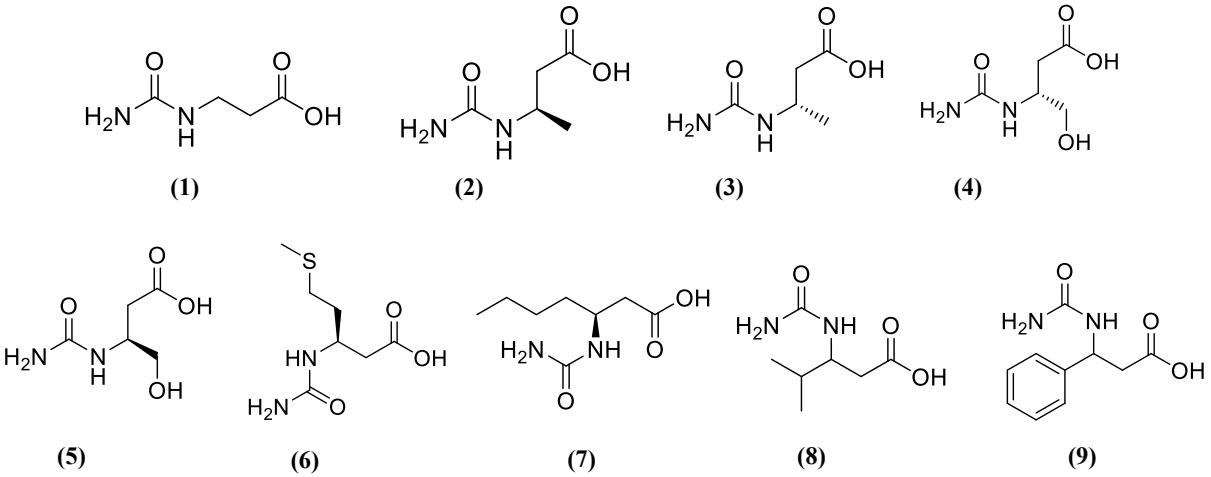

Figure 33: Synthesized *N*-carbamoyl-β-amino acids and *N*-carbamoyl-β-(homo)-amino acids.
(1) *N*-carbamoyl-β-alanine (NCβAla); (2) and (3) *N*-carbamoyl-D/L-β-homo-alanine (NCD/LβhAla); (4) and (5) *N*-carbamoyl-D/L-β-homo-serine (NCD/LβhSer); (6) *N*-carbamoyl-D/L-β-homo-methionine (NCD/LβhMet); (7) *N*-carbamoyl-L-3-amino-heptanoic acid (NCβHep); (8) *N*-carbamoyl-*rac*-β-leucine (NCβLeu); (9) N-carbamoyl-*rac*-β-phenylalanine (NCβPhe).

NCβAla (1), NCβPhe (9), *N*-carbamoyl-*rac*-β-leucine (NCβLeu) (8) and *N*-carbamyol-3-amino-heptanoic acid (NCβHep) (7) were obtained after 1-2 h reaction with KNCO at 80 °C without pH titration (see 4.1.2). Due to their poor water solubility they could easily crystallize after cooling to 1-4 °C. The reaction product was verified by ^{1}H-NMR (Table 41, p. 89). The spectra showed signals for all H-atoms of the corresponding molecule. In HPLC analysis no remains of reaction educt were detected, thereby no additionally MS-analysis was conducted for these synthesis products. Molar yields were ~80 % (mol/mol).

β-homo-amino acids (βhAAs) showed different chemical properties than βAAs. Due to low melting points especially of the educt L-β-homo-methionine (LβhMet), the reaction temperatures for the synthesis of D- and L-*N*-carbamoyl-β-homo-alanine (NCDβhAla and NCLβhAla) ((2) and (3) Figure 33), D- and *N*-carbamoyl-L-β-homo-serine (NCD/LβhSer) ((4) and (5) Figure 33) and NCLβhMet ((6) Figure 33) were set to 50 °C. This led to low activation energy and long reaction times that varied for each amino acid (see Table 37, p. 75). In comparison to the synthesis of NCαAA, the molecular ratio of amino acid to KNCO was two or three times higher. Due to fast pH-shifts during the reaction the pH had to be readjusted to approximately 7 to keep the reaction equilibrium on the product side. The requried amount of KNCO to convert all of the educt was evaluated through TLC analysis (see also Table 37, p. 75). Figure 34 shows an overview of syntheses of different NCβhAAs.

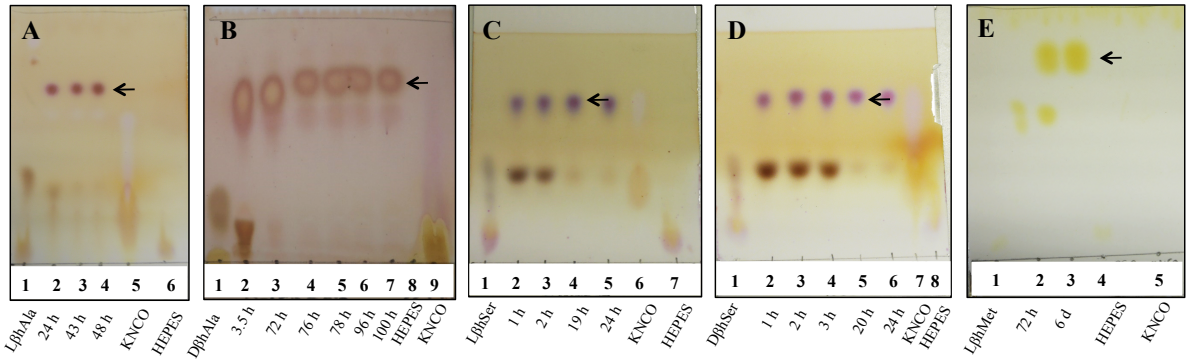

Figure 34: TLC of synthesized aliphatic NCβhAAs.
A) 1: Educt LβhAla in HEPES buffer; 2-4: NCLβhAla was synthesized without remaining educt after at least 48 h and 2.91 mmol KNCO. 5: 40 mM KNCO in ddH_2O 6: 50 mM HEPES buffer B) 1: Educt DβhAla in HEPES buffer; 2-7: NCDβhAla was fully converted with 2.91 mmol KNCO after at least 72 h. 8: 50 mM HEPES buffer; 9: 40 mM KNCO C) 1: LβhSer in HEPES buffer; 2-5: Educt NCLβhSer was fully reacted after 24 h with 1.68 mmol KNCO; 6: 40 mM KNCO; 7: 50 mM HEPES buffer D) 1: Educt DβhSer in HEPES buffer; 2-6: NCDβhSer was synthesized after 24 h and 1.68 mmol KNCO; 7: 40 mM KNCO; 8: 50 mM HEPES buffer E) 1: LβhMet in HEPES buffer; 2-3: Educt NCLβhMet was synthesized after six days and 1.84 mmol KNCO; 4: 50 mM HEPES buffer; 5: 40 mM KNCO. All TLCs except for βhMet stained with ninhydrin staining solution. TLC for βhMet was stained with Ehrlich staining solution. Reaction products are marked with an arrow.

NCβAAs like NCβPhe or NCβAla had a poor water solubility of maximum 20 mM when heated to 80 °C. In contrast to that a higher solubility in water was observed for NCβhAAs with up to 100 mM at room temperature. Hence crystallisation of NCβhAAs was not achieved by to lowering the pH to 3 and cooling to 1-4 °C. To obtain a solid reaction product speed-vacuum-drying and freeze-drying were tested. It was observed, that speed-vacuum-drying was not an appropriate option, since NCβhAAs showed hygroscopic properties. Thus the reaction product was obtained as viscose mass. Prior freezing at -20 °C and subsequent freeze-drying yielded a powdery solid precipitate. In ^{1}H NMR data of NCβhAAs no signal for the H-atom

of the carboxyl- and amino-group was detected. This was due to deuterization of these positions by D_2O. The same phenomenon was observed in ^{1}H-spectra of their corresponding βhAA. To verify the reaction products an additional mass spectrometry measurement was performed for synthesized NCβhAAs. All ^{1}H-spectra are shown in section 8.8. NMR-data are given in Table 41, mass spectrometry data is given in Table 42.

Table 41: NMR date of all synthesized *N*-carbamoyl-β-amino acids.
DMSO = dimethylsulfoxide; D_2O = Deuterium oxide.

Reaction product	NMR-data
N-carbamoyl-L-3-amino-heptanoic acid	^{1}H NMR (300 MHz, DMSO-d_6) δ 0.79 – 0.90 (m, 3H), 1.25 (tddd, *J* = 4.3, 6.7, 10.0, 13.5 Hz, 4H), 1.37 (dq, *J* = 3.9, 4.5, 11.9 Hz, 1H), 2.17 – 2.40 (m, 2H, 7, 8, 12), 3.69 – 3.87 (m, 1H), 5.39 (s, 2H), 5.86 (d, *J* = 8.9 Hz, 1H), 12.04 (s, 1H).
N-carbamoyl-β-alanine	^{1}H NMR (300 MHz, DMSO-d_6) δ 2.33 (t, *J* = 6.5 Hz, 2H), 3.15 (q, *J* = 6.3 Hz, 2H, 3), 5.54 (s, 2H, 8), 6.02 (t, *J* = 5.9 Hz, 1H, 2), 12.28 (s, 1H).
N-carbamoyl-β-*rac*-leucine	^{1}H NMR (300 MHz, DMSO-d_6) δ 0.80 (d, *J* = 6.8 Hz, 6H, 5, 6), 1.71 (dq, *J* = 6.7, 13.1 Hz, 1H, 4), 2.14 – 2.39 (m, 2H, 3), 3.73 (td, *J* = 4.0, 8.1 Hz, 1H), 5.40 (s, 2H, 12), 5.65 – 6.10 (m, 1H, 9), 12.15 (s, 1H).
N-carbamoyl-β-homo-D-serine	^{1}H NMR (300 MHz, D_2O) δ 2.27 – 2.60 (m, 10H), 2.92 (dd, *J* = 8.2, 18.2 Hz, 1H), 3.33 – 3.63 (m, 10H), 3.94 (d, *J* = 7.9 Hz, 5H), 4.20 (dd, *J* = 3.3, 9.7 Hz, 1H), 4.76 (s, 1H), 13.05 (s, 1H).
N-carbamoyl-β-homo-L-serine	^{1}H NMR (300 MHz, D_2O) δ 2.24 – 2.57 (m, 9H), 3.36 – 3.56 (m, 9H), 3.93 (t, *J* = 6.9 Hz, 4H), 4.51 (dd, *J* = 6.4, 9.8 Hz, 0H), 4.58 – 4.65 (m, 1H).
N-carbamoyl-β-homo-L-methionine	^{1}H NMR (300 MHz, D_2O) δ 1.84 – 1.95 (m, 2H), 2.00 (s, 3H), 2.53 (t, *J* = 7.4 Hz, 2H), 2.57 – 2.89 (m, 2H), 3.69 (dt, *J* = 3.6, 7.5 Hz, 1H).
N-carbamoyl-β-L-homo-alanine	^{1}H NMR (300 MHz, D_2O) δ 1.24 (d, *J* = 6.7 Hz, 3H), 2.53 – 2.74 (m, 2H), 3.63 (q, *J* = 6.7 Hz, 1H).
N-carbamoyl-β-*rac*-phenylalanine	^{1}H NMR (300 MHz, DMSO-d_6) δ 2.65 (d, *J* = 2.5 Hz, 1H, 2), 4.99 (q, *J* = 7.5 Hz, 1H, 3), 5.54 (s, 2H, 14), 7.16 – 7.28 (m, 1H, 7), 7.30 (s, 3H, 5, 9, 15), 7.31 (d, *J* = 2.2 Hz, 2H, 6, 8), 12.21 (s, 1H, 11).

Table 42: Mass spectrometry of *N*-carbamoyl-β-homo-amino acids.
"-" = No additional MS-analysis was performed.

Reaction product	Mass (g/mol)	Mass spectrometry
N-carbamoyl-β-homo-L-alanine	147.08	$[M + H^+]$
N-carbamoyl-β-homo-D-serine	163.07	-
N-carbamoyl-β-homo-L-serine	163.07	$[M + H^+]$
N-carbamoyl-β-homo-L-methionine	206.07	$[M - NH_3^+]$
N-carbamoyl-β-D-homo-alanine	147.08	-

4.1.3 Synthesis of allantoic acid

Allantoic acid was synthesized by alkaline hydrolysis of allantoin as described in section 3.2.4.1.3, (p. 76). The reaction was monitored by TLC for several days (Figure 35). After a reaction time of at least 24 h most of allantoin was reacted and an additional spot appeared. The product was verified *via* mass spectrometry analysis. Remaining was not detected with mass spectrometry (see 8.8 Figure 92, p. 237).

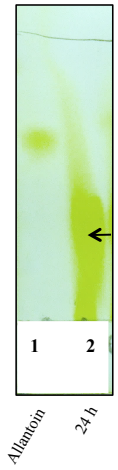

Figure 35: TLC allantoic acid synthesis.
1: Educt Allantoin; 2: Allantoic acid formed after 24 h. TLC was stained with Ehrlich staining solution.

4.2 Establishment of analytics for non-canonical amino acids

4.2.1 Aromatic non-canonical-amino acids

Aromatic amino acids, independent on the position of their amino group, easily can be detected through their delocated electron π-system. To find an analytical method for aromatic non-canonical amino acids without derivatization a new method was established in which no enantiomeric separation was performed. For this several columns, mobile phases and other conditions were tested. Since using HyperClone™ 5 µm ODS (C18) 120 Å, LC Column 150 x 4,6 mm (see Table 30) was not suitable and led to strong peak-tailing and shifting at different concentrations (data not shown). Synergi™ 4 µm Fusion-RP 80 Å, LC Column 150 x 4,6 mm by Phenomenex gave symmetrical peaks of aromatic noncAAs. A mobile phase of 20 mM KH_2PO_4 at pH 3 (adjusted with HCl) was optimal. The method was applied to detect several aromatic non-canonical amino acids and their *N*-carbamoyl-derivate: α-phenylalanine, α-tyrosine, α-hydroxy-phenylglycine, α-hydroxphenylglycine β-2-thienylalanine, β-phenylalanine and β-tyrosine.

4.2.2 Aliphatic non-canonical-amino acids

A detection method for analysis of aliphatic β-(homo)-amino acids was to be established. As aliphatic amino acids are not detectable in UV light, derivatization prior to HPLC analysis was required. Several derivatization reagents were tested, but not suitable for every amino acid and reaction system. Examples are o-phtaldialdehyde (OPA) or flourenylmethoxycarbonyl (Fmoc). One of the most common derivatization reagents for analysing aliphatic α-amino acids is derivatization with OPA in combination with *N*-isobutyryl-L-cysteine (IBLC).

For detection of βAla a method modified after Brucher et al. [225] using HyperClone™ 5 µm ODS (C18) 120 Å, LC Column 150 x 4,6 mm (see Table 30) was used. βAla was analysed with a mobile phase consisting of 60 % 40 mM NaPP pH 6.5 buffer and 40 % MeOH using 0.5 µl of sample volume during the pre-column derivatization (see 3.2.5.3). The signal intensity was very strong, thus concentrations as low as 0.1 mM were still detectable. Peak heights varied depending on the freshness of the UV-sensitive OPA/IBLC mixture.

It was tested whether other aliphatic β(h)AAs were able to build a covalent complex with OPA/IBLC through microtiter plate reactions. Therefor 24 µl borate buffer were mixed with

36 µl OPA/IBLC and 6 µl of each sample (10 mM in HEPES buffer) was incubated for 10 min at room temperature. A spectrum from 250 nm to 400 nm was measured with Tecan photometer. Figure 36 shows that all βAA-OPA/IBLC complexes absorb at the expected 338 nm. The highest absorption of 0.4-0.7 was detected for LβHep, LβHMet. *Rac* βLeu. D/LβhAla, D/LβhSer showed a lower absorption of ~0.1.

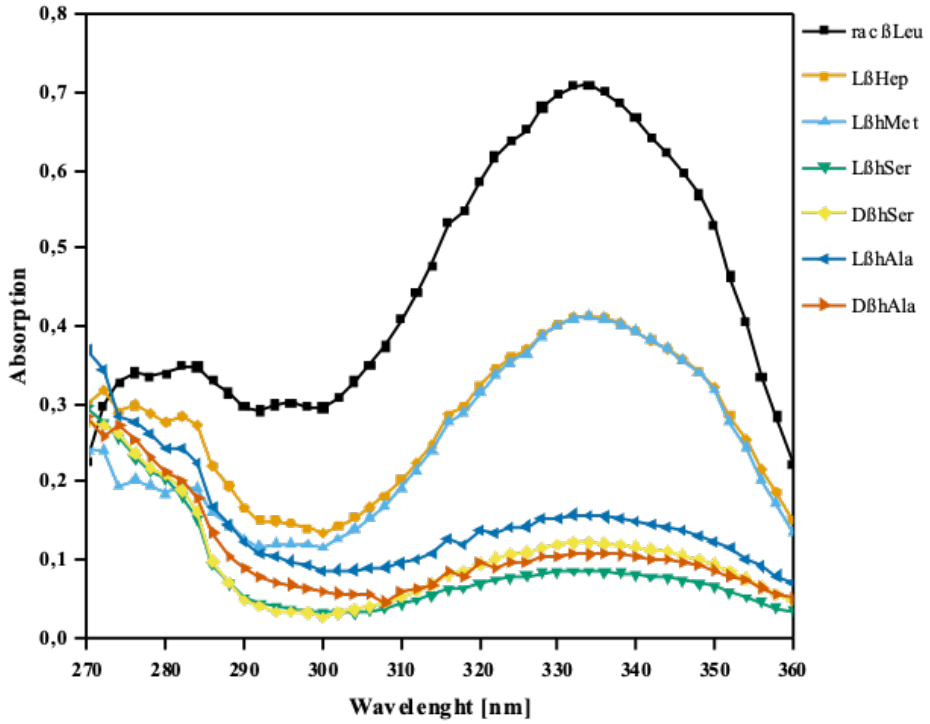

Figure 36: Spectrum of β-(homo)-amino acid-OPA/IBLC complexes.
Data shown with already subtracted base line of OPA/IBLC mixture.

In the next step a detection of βhAAs was tested in the HPLC. It was found that the amino acids with the highest absorptions detected in the spectrum showed the smallest signals in HPLC analysis using the same method as for βAla (0.5 µl of sample mixed with 3 µl OPA/IBLC). For the detection of 10 mM D/LβhAla a signal intensity of ~36 mAU was measured. For 10 mM LβhMet a signal of 16 mAU height was obtained. Accordingly the peak area was small too. Solely for LβhSer a peak height of ~90 mAU at 10 mM was observed. For LβHep and *rac* βLeu signals were even lower. To improve the signal sensitivity for these βhAAs the ratio of amino acid to derivatization reagents was altered. When mixing 2.5 µl of 10 mM βhAA with 3 µl of OPA/IBLC solution the signal intensity was increased to 63 mAU (D/LβhAla) and 187 mAU (LβhSer). The peak height for LβhMet was increased to 25 mAU. By mixing 5 µl of 10 mM LβhMet with 3 µl OPA/IBLC a 40 mAU signal was detected. For D/LβLeu and LβHep the signal intensity was increased through different ratios

of derivatization reagents to βAA. Since Figure 36 shows absorption of a putative *rac* βLeu- or LβHep-OPA/IBLC complex respectively; it was assumed that the derivatization reaction had taken place. A reason for the low detection signal in HPLC analysis may be the non-suiting properties of the HPLC-method. Thus only LβhMet, D/L βhSer and D/L βhAla was detected *via* HPLC in further course of the work.

By analysing aliphatic non-canonical amino acid-OPA/3-MPA-complexes with fluorescence in a microtiter plate (3.2.5.4) all βhAAs and several non-canonical α-amino acids were detected with a high sensitivity. All βhAAs showed a linear relationship from 0-1 mM. Therefore this fluorescence method was used to detect D/LβhLeu, βHep as well as non-canonical α-amino acids L-α-tert-leucin (L-α-tertLeu) and L-α-neopentylglycine (L-α-NeoGly).

Additionally Fmoc was tested for derivatization of βAAs (see 3.2.5.3.3). Derivatization with Fmoc works in a watery reaction system according to literature [229]. Since all analytical samples were dissolved in HEPES buffer a high amount Fmoc reacted with the buffer substance. Thus pre column derivatization with Fmoc was found to be a non-suitable derivatization method for the conditions used in this work. For all *N*-carbamoyl-derivates was observed that they reacted with Ehrlich derivatization reagent and thus was analysed with Ehrlich-assay (see section 3.2.5.1) and showed a linear correlation from 0.1 to 10 mM with an R^2 of 0.99 or better.

4.3 Screening of wild-type strains

The institutes own strain collection was screened for NCβPhe-degrading strains. It was hypothesized that the usage of metabolites of the reductive pyrimidine degradation pathway as sole nitrogen source may induce the expression of decarbamoylating genes. The aim was to find wild-type strains able to convert model substrate NCβPhe to the non-canonical βAA βPhe. In total over 200 wild-type strains were screened with different defined solid media. For selected strains with slight growth on NCβPhe as sole nitrogen source additional lysate biotransformation studies were performed. Thereby also bivalent metal cofactors were tested since metal-dependency has been reported for many decarbamoylating enzymes.

4.3.1 Screening for *N*-carbamoyl-β-phenylalanine degrading strains

In contrast to L-Carbs and D-Carbs for which their natural function is unknown of βUps naturally occur in the pyrimidine metabolism. By addition different metabolites of the

pyrimidine metabolism as sole nitrogen source it is possible that decarbamoylating enzyme activity, e.g. of βUps, from different wild-type strains could be induced or enhanced. The procedure is explained in section 3.2.2.3. Only a significant visible difference in growth towards the negative control (medium without any nitrogen source) was defined as "positive growth" regarding every nitrogen source.

Over 200 wild-type strains, including bacteria, yeasts and fungi (see Table 3 for internal codes of each strain), were cultivated on agarose-plates with a minimal medium (BM3-U/T for bacteria or YM3 for yeast and fungi (see Table 14-Table 16) containing uracil or thymine. Almost all strains showed significant growth on uracil or thymine as sole nitrogen source (data not shown). Only strains with growth on their positive control medium (full medium agar plate) were considered for further transfer, whereby non-living strains could be excluded. After incubation of three to ten days, cells from uracil/thymine-positive strains were transferred to a minimal medium agarose-plate (BM3 for bacteria and YM3 for yeasts) containing NCβAla as sole nitrogen source. After 10 days of incubation at the corresponding optimal growth temperature of 64 strains showed significant growth on NCβAla.

NCβAla-positive strains were subsequently cultivated in a liquid culture in BM3 or corresponding YM3 containing NCβAla as sole source of nitrogen (see 3.2.2.4). To ensure a good viability of the cells for further experiments each strain was cultivated until cells reached the exponential phase. Cells of these cultures in NCβAla-medium were used to make glycerol stocks (section 3.2.2.2). To exclude microorganism able to fix atmospheric nitrogen a negative control for each strain was carried without any nitrogen.

Next NCβAla-glycerol stocks of each NCβAla-positive strain were used to freshly inoculate BM3/YM3-medium agarose plates containing NCβPhe as sole source of nitrogen. For each strain a negative control was carried. After incubation over five days a significant growth in contrast to the negative control was observed for several strains. The regarding agarose-plates are shown in Figure 37.

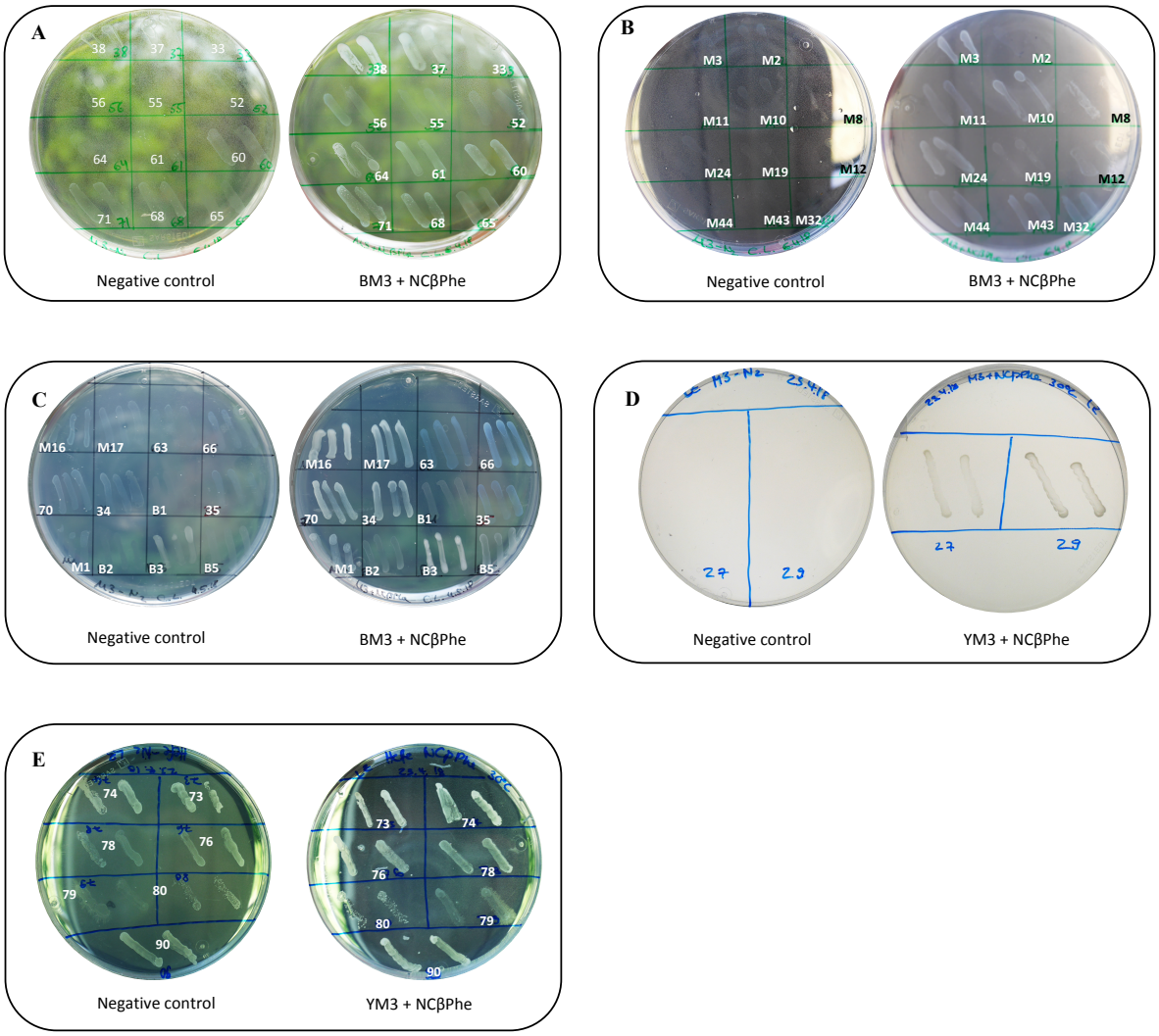

Figure 37: Strains screened for growth on NCβPhe as sole nitrogen source.
A) Growth of strains 38, 37, 33, 56, 55, 52, 64, 61, 60, 71, 68, 65 on BM3 medium containing NCβPhe as sole nitrogen source (right) in contrast to their negative control (left). **B**) Growth of strains M3, M2, M11, M10, M8, M24, M19, M12, M44, M43, M32 on BM3 medium containing NCβPhe as sole nitrogen source (right) in contrast to their negative control (left). **C**) Growth of strains M16, M17, 63, 66, 70, 34, B1, 35, M1, B2, B3, B5 on BM3 medium containing NCβPhe as sole nitrogen source (right) in contrast to their negative control (left). **D**) Growth of strains 27 and 29 on YM3 medium containing NCβPhe as sole nitrogen source (right) in contrast to their negative control (left). **E**) Growth of strains 73, 74, 76, 78, 80, 79, 90 on YM3 medium containing NCβPhe as sole nitrogen source (right) in contrast to their negative control (left).

For strains 38, 37, 64, 61, 60, 71, 86 and 65 slight growth on NCβPhe as nitrogen source was visible (Figure 37 A). Especially for stain 38 and 37 a significant difference to the negative control was observed. Furthermore significant growth was visible for strain M3 (Figure 37 B), strain M16, M17, 70, 34 M1, B3 (Figure 37 C) and strain 27 and 29 (Figure 37 D). Figure 37 E shows several yeast strains. Strain 73, 74, 76, 78, 80, 79 and 90 show no significant difference compared to their negative control. Strain 80, wild type strain of *L. kluyveri* was chosen to estimate growth compared to enzyme activity. Within the thesis the known βUp of

L. kluyveri was recombinantly expressed and in biotransformation assays a high activity towards NCβAla was observed. However no activity towards degradation of NCβPhe was detected.

Several strains, which showed growth on BM3/YM3-medium agar plates containing NCβPhe, were selected for further studies listed in Figure 38. Only screening-positive-strains available at DSMZ strain collection were chosen for further studies (strain M8, M19, 71, 34, 37, B3 and 29). Exception was strain 29 showing good growth on BM3-NCβPhe medium (Figure 37 D). This strain was identified *via* 16S rRNA sequencing (see 4.3.4.). For selected strains the degradation of NCβPhe was verified through biotransformation studies with lysate (see section 4.3.3).

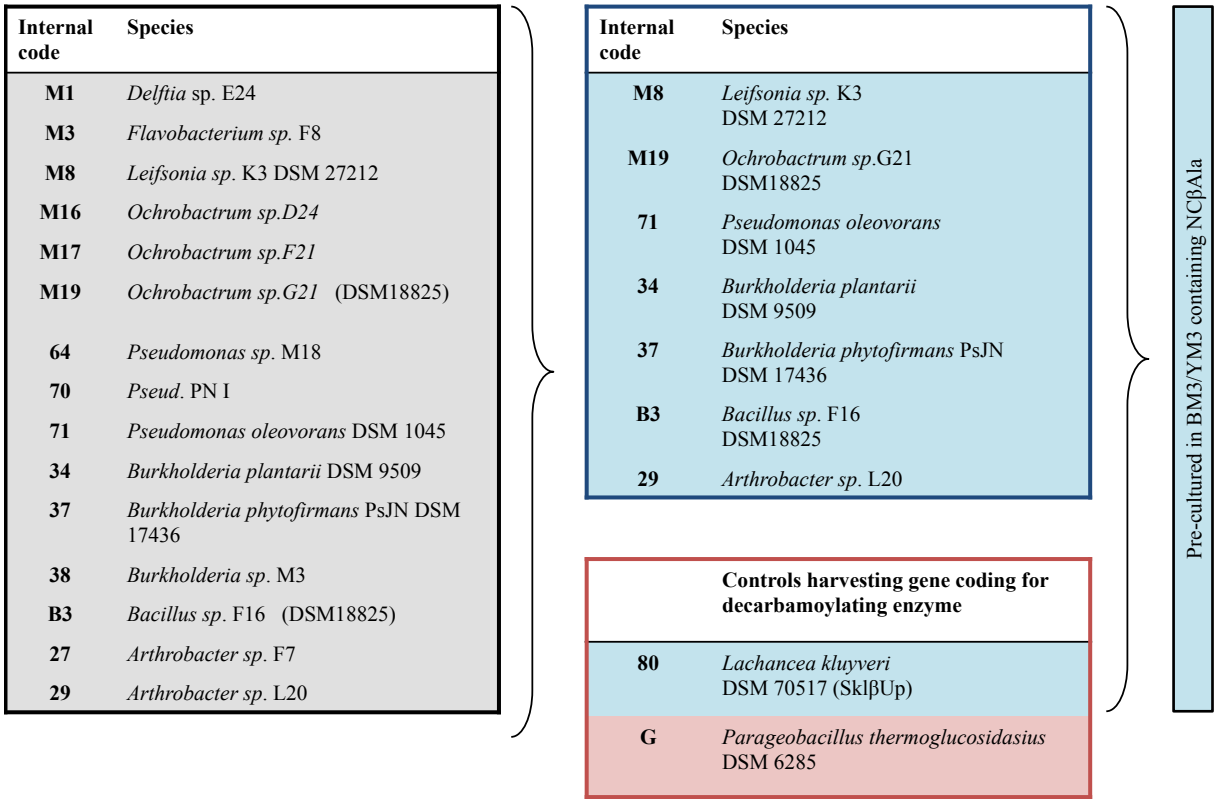

Figure 38: Hit strains observed from screening.
Grey box: all strains showing significant growth on NCβPhe as sole nitrogen source; blue box: strains selected for lysate experiments; red box: carried control strains. *L. kluyveri* possesses a βUp, which is not able to degrade NCβPhe but NCβAla, *Parageobacillus thermoglucosidasius* was not previously cultivated in BM3/YM3 containing NCβAla but its genome codes for a decarbamoylating enzyme.

4.3.2 Monitoring of growth in liquid culture

Direct cultivation in BM3/YM3 containing NCβPhe as sole nitrogen source, inoculated from the corresponding NCβAla glycerol stock of each strain, led to low cell growth (data not shown). Thus the required cell mass for biotransformation studies was obtained through cultivation of all strains (given in the blue and red box in Figure 38) in liquid medium containing NCβAla. Precultures were freshly inoculated with the corresponding NCβAla glycerol stock of each strain and grown over night. Main cultures with 200 ml BM3/YM3-NCβAla liquid medium were inoculated with an OD of 0.1 in triplicate. A positive control with according medium containing ammonium sulphate as nitrogen source and a negative control medium without any nitrogen source were also inoculated with the same amount of cells. The positive control was also conducted in triplicate. Growth of each strain was monitored as shown in Figure 39.

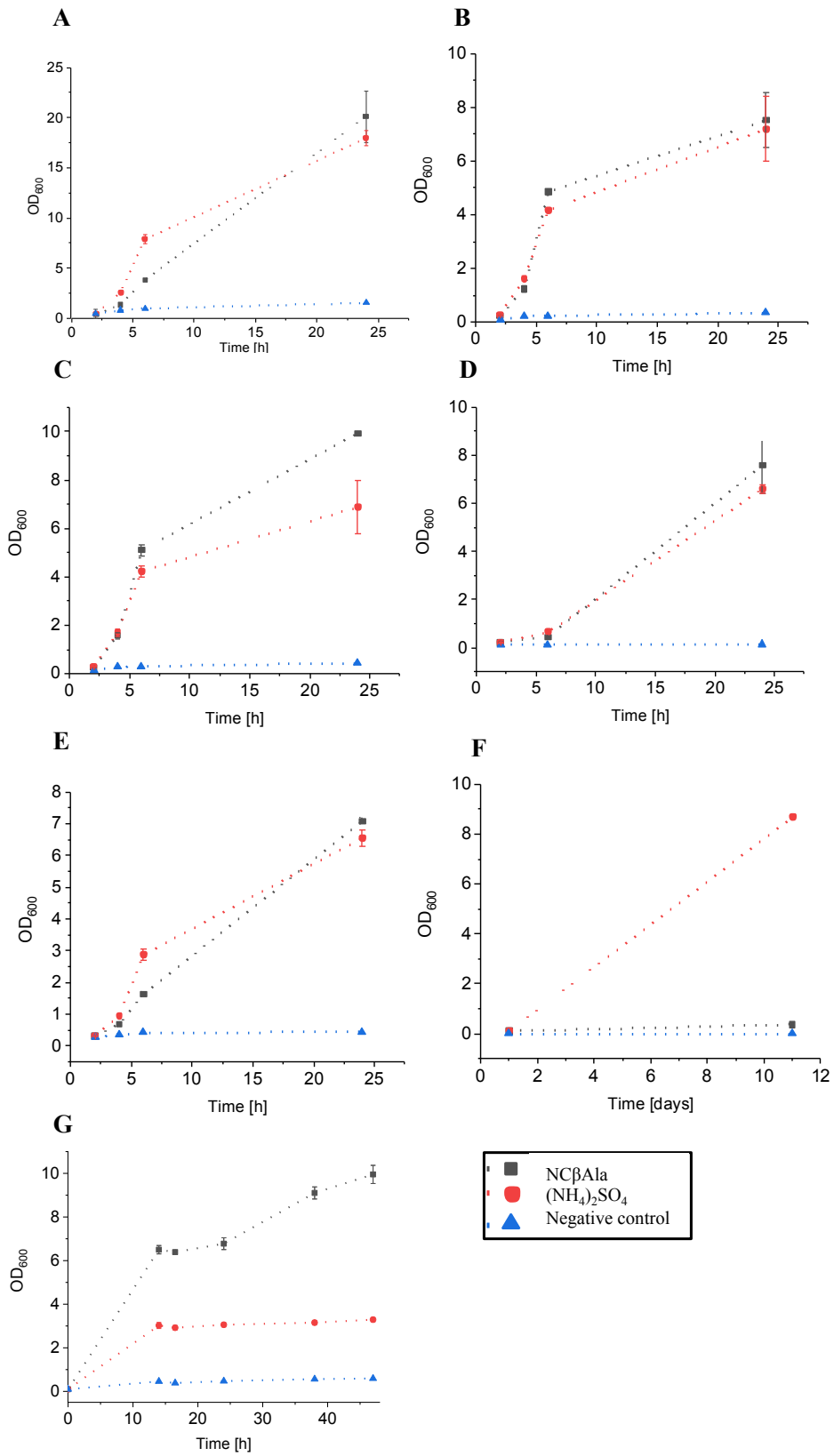

Figure 39: Growth of selected strains in BM3/YM3 liquid medium.
All strains were grown in BM3 or YM3 liquid medium containing NCβAla (grey), $(NH_4)_2SO_4$ (red) and without nitrogen source (blue). A) Strain 29; B) Strain 71; C) Strain M8; D) Strain 37; E) Strain B3; F) Strain M19; G) Control strain 80.

Figure 39 shows that all selected strains except M19 grew to a high OD in BM3 or YM3-NCβAla medium within 24-48 h. Strain M19 only grew in BM3 containing $(NH_4)_2SO_4$ after 12 days. For strains 29, 37, 71, B3 and M8 an exponential growth phase was observed both in medium with NCβAla and in medium with $(NH_4)_2SO_4$ as sole nitrogen source. Final OD_{600} values were from 7 to 19 for NCβAla and 6-16 in $(NH_4)_2SO_4$ after 24 h. Strain 29 showed the strongest growth in both NCβAla and $(NH_4)_2SO_4$ medium with a final OD_{600} of ~18 ($(NH_4)_2SO_4$) and OD_{600} of 20 (NCβAla). Yeast *L. kluyveri* (strain 80) grew to an OD_{600} of ~3 in $(NH_4)_2SO_4$- and ~10 in NCβAla-medium (Figure 39 G). All negative control cultures of the strains grew to a maximum OD_{600} of 0.5. All cells cultivated in NCβAla and $(NH_4)_2SO_4$ were harvested in their late exponential phase after 24 or 48 h respectively, centrifuged, washed with cold PBS and freeze dried in a lyophylle. Cells from strain G (*P. thermoglucosidasius*) pre-cultured in LB-M medium were harvested and freeze dried as well.

4.3.3 Biotransformations with screening-hit strains

For lysate experiments 1 g of freeze-dried cells of each strain cultured in medium with NCβAla and $(NH_4)_2SO_4$ was resuspended in 15 ml cold HEPES buffer (50 mM, pH 7). Resuspended cells were lysed using maximum pressure of a homogenisator. After centrifugation at 30.000 rpm for 30-60 min the supernatant was used for activity studies.

With lysate from each strain and culture medium activity towards NCβAla and NCβPhe was tested. Therefor 400 µl lysate and 100 µl of each substrate (10 mM) were mixed. Thus a theoretical initial amount of 8 mM substrate was present. Also four different metal cofactors were tested ($ZnCl_2$, $MnCl_2$, $CoCl_2$ and $NiCl_2$ with a final concentration of 1,2 mM). Several controls were carried: a substrate control using100 µl buffer instead of lysate were added to the substrate and a product control, in which βAla or βPhe respectively were incubated with lysate of each strain (8 mM initial product concentration). Additionally a pure lysate-control (500 µl) was carried to determine remaining concentrations of NCβAla in the lysate from the previous cultivation. All reactions were carried out in triplicate and incubated at 30 °C (strain 29, 37, 71, B3, M8 and 80) or 55 °C (strain G). After 24 h reactions were stopped by denaturation at 95 °C for 5 min. Samples were centrifuged with 13.000 rpm for 10 min and the supernatant was analysed. NCβAla concentration was analysed by performing Ehrlich-assay (3.2.5.1). Analysis of βAla, NCβPhe and βPhe was conducted *via* HPLC (see 3.2.5.3.1 and 3.2.5.3.2).

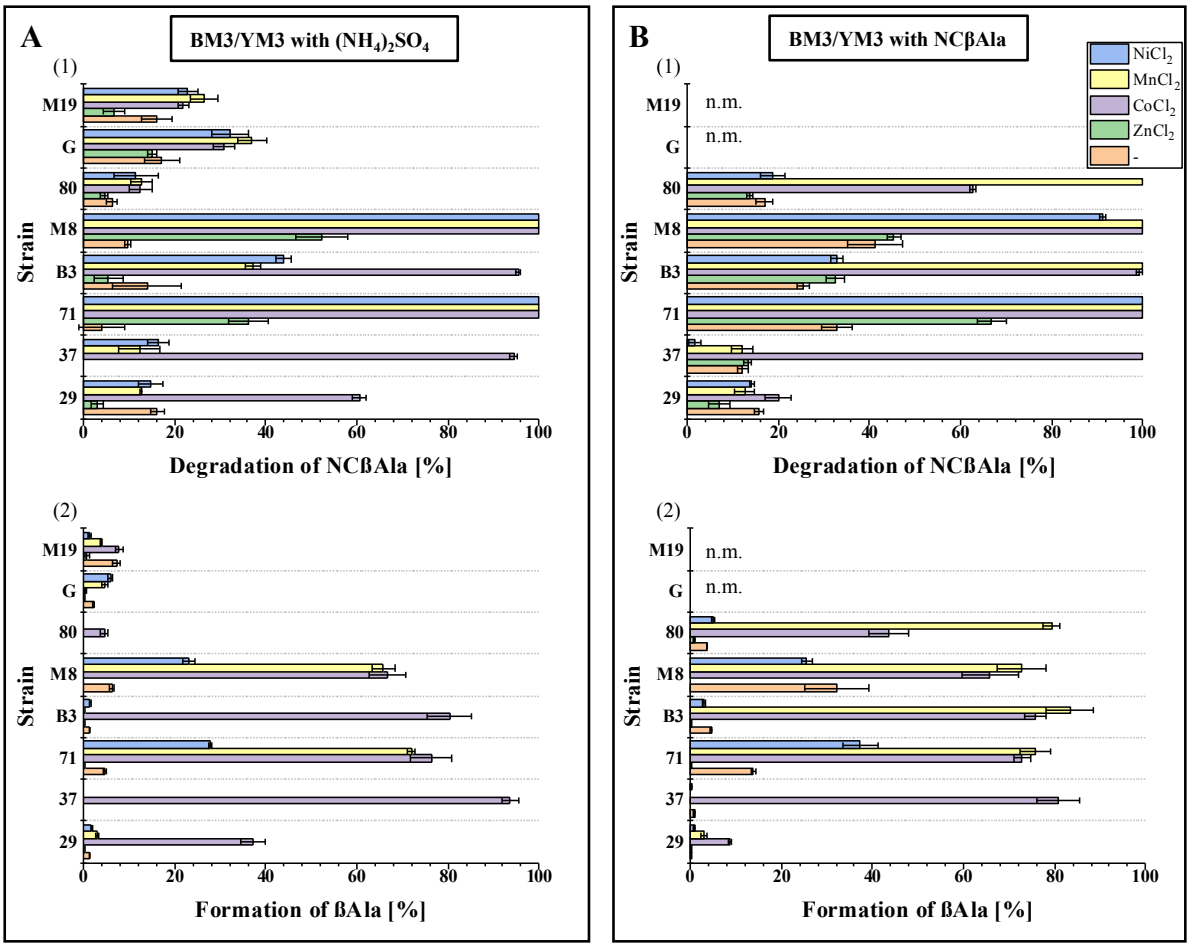

Figure 40: Conversion of NCβAla to βAla of strains obtained from screening.
A-1) Degradation of NCβAla of strains previously cultivated in BM3 or YM3 with $(NH_4)_2SO_4$ or B-1) NCβAla. A-2) Formation of βAla of strains previously cultivated in BM3/YM3 with $(NH_4)_2SO_4$ or B-2) NCβAla. Reactions were conducted with cell lysate and stopped after 20 h.

Figure 40 gives an overview about degradation of NCβAla and the formation of βAla, each with cells from previous cultivation in BM3/YM3 with $(NH_4)_2SO_4$ or NCβAla respectively. Product controls showed degradation of βAla (data not shown). The theoretical βAla-starting concentration of 8 mM was not detected for any strain. Instead approximately 4-6 mM βAla were detected after incubation for 20 h. Percentage product formation was calculated with regard to the amount of NCβAla detected in the substrate control conducted for each strain. In substrates controls without lysate no formation of βAla was observed. Furthermore in pure lysate samples no βAla was detected. Figure 40 A-1 shows the percentage degradation of NCβAla for strains cultivated in medium with $(NH_4)_2SO_4$ relative to the NCβAla concentration detected in substrate controls. Control strain 80 (*L. kluyveri*) converted 6 % without additional cofactor of the initial substrate amount. In comparison to this with present cofactors 12 % of substrate was converted (except for $ZnCl_2$). Other strains showed higher

substrate degradation without cofactor from 4-17 %. The highest NCβAla degradation without cofactor was observed for strain G (*P. thermoglucosidasius*) with 17 %. In general a higher amount of substrate was converted when bivalent metal cofactors were present. Strain M8 (*Leifsonia sp.*) and 71 (*P. oleovorans*) converted 100 % of substrate when $NiCl_2$, $MnCl_2$ or $CoCl_2$ were available. Strain B3 (*Bacillus sp.)* and strain 37 (*Burkholderia phytofirmans*) were able to convert 94-95 % of NCβAla when $CoCl_2$ was added. However, when $NiCl_2$ and $MnCl_2$ were used as cofactors strains 37 and B3 showed only substrate conversion of 12-16 % (37) and 37-43 % (B3) of NCβAla. With $ZnCl_2$ present in the reaction lower conversions were observed compared to other cofactors. Strain 37 showed no degradation without cofactor or when $ZnCl_2$ was present.

Figure 40 A-2 illustrates the amount of βAla formed. The percentage amount of βAla was calculated in relation to the initially present substrate concentrations. For all strains βAla formation was detected. However product amounts lower than initial substrate concentrations were detected, since product degradation of 3-4 mM was observed for all strains. For strains showing a high substrate conversion also high product formation was observed especially with $MnCl_2$ and $CoCl_2$ present. The highest product concentrations were obtained with strains M8, B3, 71 and 37 with 66 %, 80 %, 76 % and 93 % and presence of $CoCl_2$. Without cofactor or with $NiCl_2$ and $ZnCl_2$ in the reaction lower product concentrations of up to 7% were detected, in consideration of low standard deviations.

Comparing to cells grown in BM3 or YM3 medium containing $(NH_4)_2SO_4$ cells previously grown in BM3 or YM3 medium containing NCβAla as sole nitrogen source were able to convert higher substrate amounts (Figure 40 B-1). As strain M19 (*Ochrobactrum sp*.) showed no growth in BM3-NCβAla medium (Figure 38, p.96) and strain G was solely cultivated as a control in LB medium, no data concerning biotransformations of cells grown in BM3-NCβAla medium are available.

In general an increase on NCβAla degradation without additional cofactor was measured for all strains grown in NCβAla-medium. Especially noteworthy is strain 37 showing no NCβAla degradation without cofactors with cells cultivated in $(NH_4)_2SO_4$. For strain 80 in combination with $MnCl_2$ and increase from 12 % to 100 % substrate degradation was observed. Also for strain B3 with $MnCl_2$ present in the reactions an increase from 37 % to 100 % was detected. Additionally the amount of converted NCβAla increased in reactions containing $ZnCl_2$, e.g. for strain 80 from 5 % to 14 %, strain 71 from 36 % to 67 % and strain 37 from 0% to 13 %.

All strains previously cultivated in NCβAla-medium except strain 29 showed a higher formation of βAla, especially without additional cofactor (Figure 40 B-2) compared to cultivation with $(NH_4)_2SO_4$. For strain 80 an increase of βAla formation with cofactors $MnCl_2$ and $CoCl_2$ present from 0% to 72 % or 43 % respectively was measured. Also strain B3 showed an increase for reaction containing $MnCl_2$ from 0 % to 83,3 % βAla. For strain 71 only slight increases for reactions containing $NiCl_2$ (27 % to 37 %) and $MnCl_2$ (72 % to 76 %) could be observed. Strain 37 and 29 showed a decrease from 93 to 80 % and 37 to 9 % respectively for reactions containing $CoCl_2$.

All strains previously cultivated in medium with $(NH_4)_2SO_4$ and NCβAla were tested towards their conversion of NCβPhe in biotransformation experiments since a slight growth on agarose-plates containing NCβPhe had been observed. In contrast to NCβAla degradation only slight degradations of NCβPhe were detected with partly high standard deviations. Results are given in Figure 41.

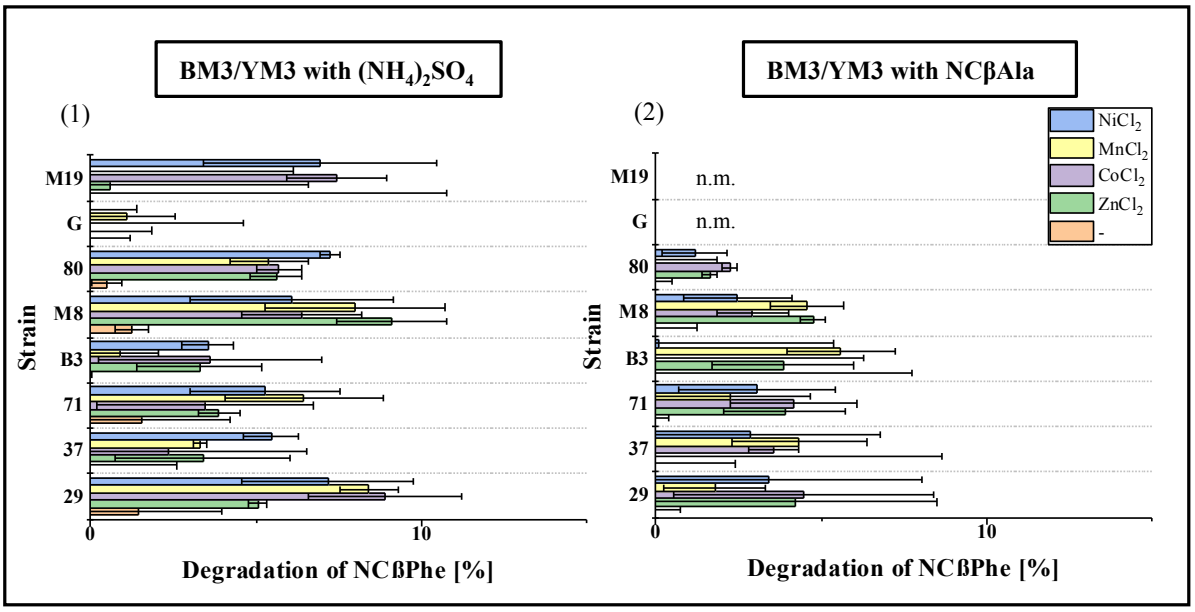

Figure 41: Degradation of NCβPhe of strains obtained from screening.
1) Degradation of NCβPhe previously cultivated in BM3/YM3 with $(NH_4)_2SO_4$ or 2) NCβAla after 20 h. Reactions were performed with cell lysate.

All percentage conversions were calculated relative to the NCβPhe concentration present in substrate controls after incubation. In general formation of βPhe was neither detected in the reactions nor in substrate controls. In the product controls only 4-6 mM βPhe of the theoretically initial 8 mM could be detected. Figure 41 A shows the NCβPhe decrease of strains previously cultivated in BM3/YM3 containing $(NH_4)_2SO_4$. Control strain 80 that

expresses a βUp (highly active towards NCβAla), which is not able to convert NCβPhe to βPhe showed a decrease of NCβPhe of up to 7 % with $NiCl_2$ present in the reaction (corresponds to 0.5 mM of the initial 8 mM substrate concentration). A similar decrease of NCβPhe was measured for strain M19 (7 % with $CoCl_2$), strain M8 (9 % with $ZnCl_2$), strain 71 (6 % with $MnCl_2$) and strain 29 (8 % with $MnCl_2$ and 9 % with $CoCl_2$). Compared to NCβAla degradation standard deviations were relatively high compared to the amount of converted substrate.

However for all strains which had been previously cultivated in BM3 or YM3 medium containing NCβAla lower NCβPhe conversion was observed (Figure 41 B). However, results were not significant since standard deviations were almost at the same level.

4.3.4 Strain identification by 16S rRNA analysis

Strains showing a strong conversion of NCβAla and potential activity towards NCβPhe, were identified. Since all strains selected for lysate biotransformation experiments were strains officially obtained from DSMZ (German Collection of Microorganisms and Cell Cultures) only strain 29 had to be identified *via* 16S rRNA sequencing. Therefore genomic DNA was isolated from cultivated cells of the strain according to section 3.2.1.4. Subsequently the genomic DNA was used as template in a PCR together with 16S rRNA primers (see 3.1.10). Strain 29 was found to be 99.74 % similar to type strain of *Paenarthrobacter nitroguajacolicus* strain G2-1 (T) (NCBI accession AJ512504).

4.4 Identification of novel decarbamoylating enzymes

Only for two strains from all selected screening-positive strains (see Figure 38) whole genome sequences were available on NCBI database: strain 71 *P. oleovorans* DSM 1045 [230] and strain 37 *B. phytofirmans PsJN* DSM 17436 [231]. From a previous screening approach (data not shown) another gene from *Pseudomonas aeruginosa* PAO1 was identified of which a genome sequence was also available on NCBI database [232].

Genes coding for decarbamoylating enzymes were identified through BLASTp search [201]. The alignments were conducted using amino acids sequences of other βUps known from literature (*A. tumefaciens* (NCBI: NP_355337.2)*; L. kluyveri* (GenBank: AAG03833.1)). For *B. phytofirmans PsJN* five genes were identified, located on its two chromosomes, with high sequence homology to other decarbamoylating enzymes. Burk1, Burk2 and Burk3 were

annotated as β-alanine synthases/amidohydrolases, Burk 4 and 5 were annotated coding for allantoate amidohydrolases. In the same way one gene annotated as hydantoin utilization protein C (*P.oleovorans*) and one gene annotated as *N*-carbamoyl-β-alanine amidohydrolases (*P.aeruginosa*) were identified.

All seven corresponding protein sequences see (Table 4, p. 48) to these genes were compared to determine their sequence homology to each other by conducting a multiple sequence alignment using BLASTp. In BLASTp search parameters a threshold of 10 and a word size of 3 was set. Additionally the scoring matrix BLOSUM62 was chosen to generate an overall alignment of the related sequences since its one of the best substitution matrices to find weak protein homologies. All gene accession numbers and corresponding protein sequences are given in section 3.1.2. Burk1 was set as reference protein to which the other proteins were compared (Figure 42, p. 105).

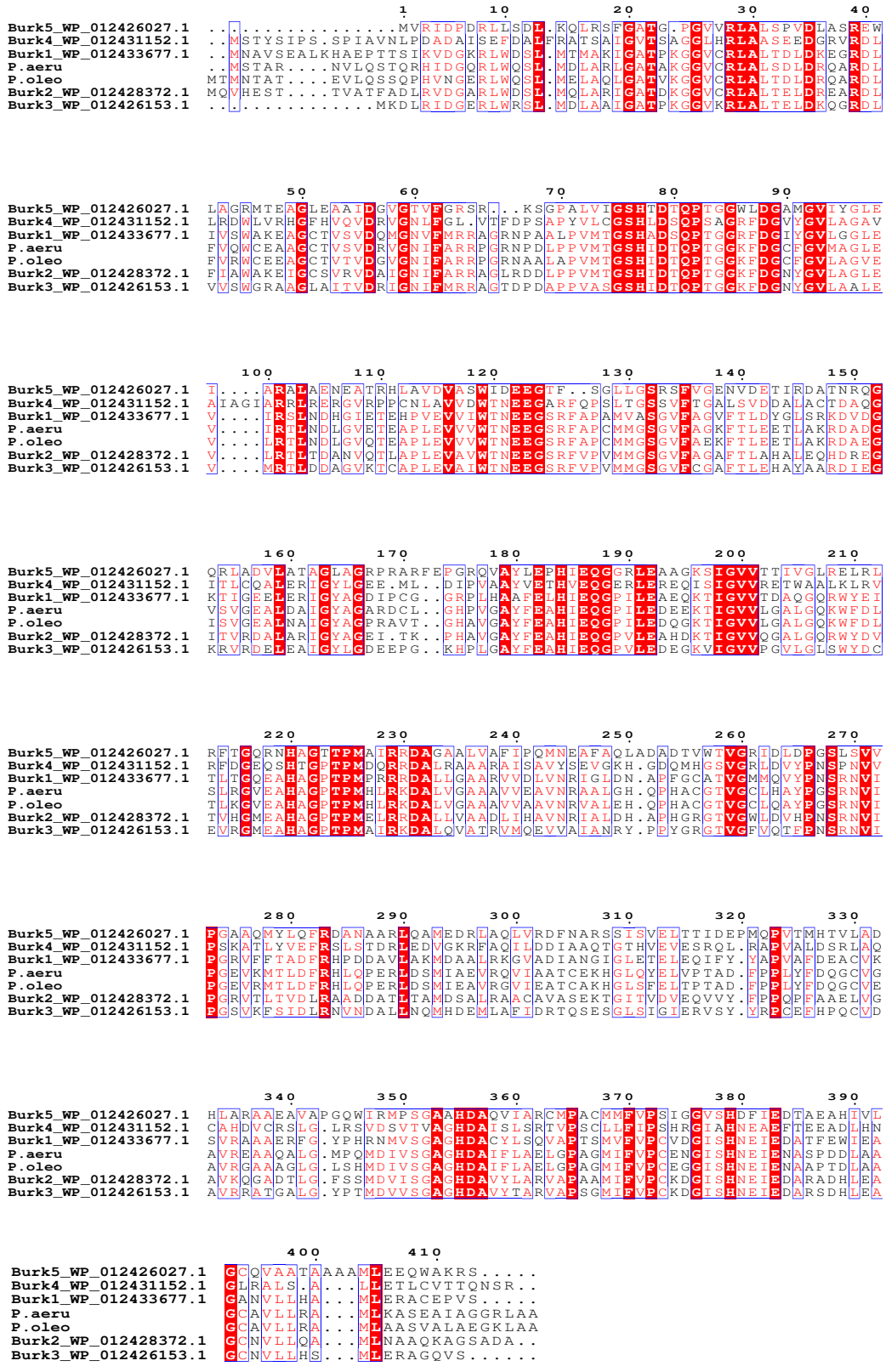

Figure 42: Multiple sequence alignment of all seven identified proteins.
MSA of protein sequences of Burk1 (WP_012433677.1), Burk2 (WP_012428372.1), Burk3 (WP_012426153.1), Burk4 (WP_012431152.1), Burk5 (WP_012426027.1), P. oleo (OWK49263.1) and P.aeru (AAG03833.1) aligned to βUp from *L. kluyveri* (Q96W94, not shown) was conducted using ESPript 3.0. Highly conserved amino which are similar in each sequence are highlighted in red. Less conserved amino acids are circled in blue.

For Burk2 an identity of 59.01 % and Burk 3 an identity of 56.3% in overall comparison to Burk1 was found. However Burk4 and Burk5 showed a lower percentage identity of 37.26 % and 35.06 %. Comparing solely Burk4 and Burk5 to each other a sequence percentage identity of 34.39 % was determined. A comparison of the five protein sequences from *B. phytofirmans* is shown in Figure 43 (p. 107).

Comparing only the proteins P.aeru and P.oleo to each other a query cover of 99 % and a percentage identity of 85.01 % was found. Burk1 showed a sequence homology to P.aeru of 58.37 % and to P.oleo 56.46 % (Figure 44, p. 108).

Relative to Burk1 a sequence percentage identity can be ranked starting with the highest identity: Burk2 > P.aeru > Burk3 > P.oleo > Burk4 > Burk 5. An overview is given in Table 43.

Table 43: Multiple sequence alignment scores of novel decarbamoylating enzymes.
A global alignment was performed using NCBI BLASTp with BLOSUM62 matrix. All protein sequences were aligned to the sequence of Burk1. E-value = expect value (random background noise).

Protein	Sequence length (amino acids)	Query coverage	E-value	Percentage identity
Burk1	426	-	-	-
Burk2	426	95 %	8e-176	59.01 %
Burk3	412	95 %	2e-166	56.30 %
Burk4	430	96 %	4e-71	37.26 %
Burk5	413	92 %	3e-53	35.06 %
P.aeru	427	95 %	2e-167	58.37 %
P.oleo	429	98 %	1e-161	56.46 %

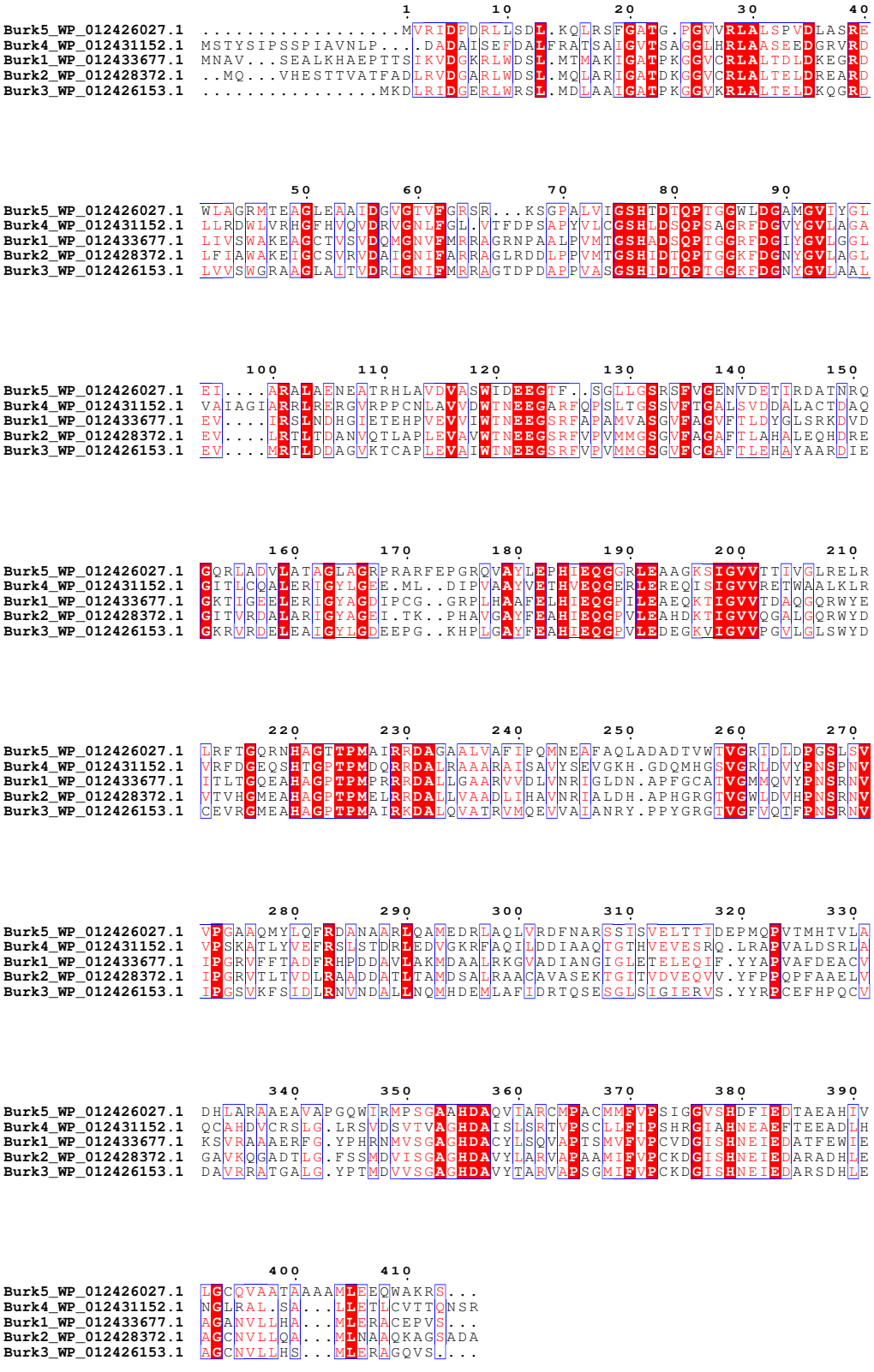

Figure 43: Multiple sequence alignment of identified proteins from *B. phytofirmans*.
MSA of protein sequences of Burk1-5 aligned to L-carb of *G. stearothermophilus* (NCBI Q53389.1, not displayed) was conducted using ESPript 3.0. Highly conserved amino which are similar in each sequence are highlighted in red. Less conserved amino acids are circled in blue.

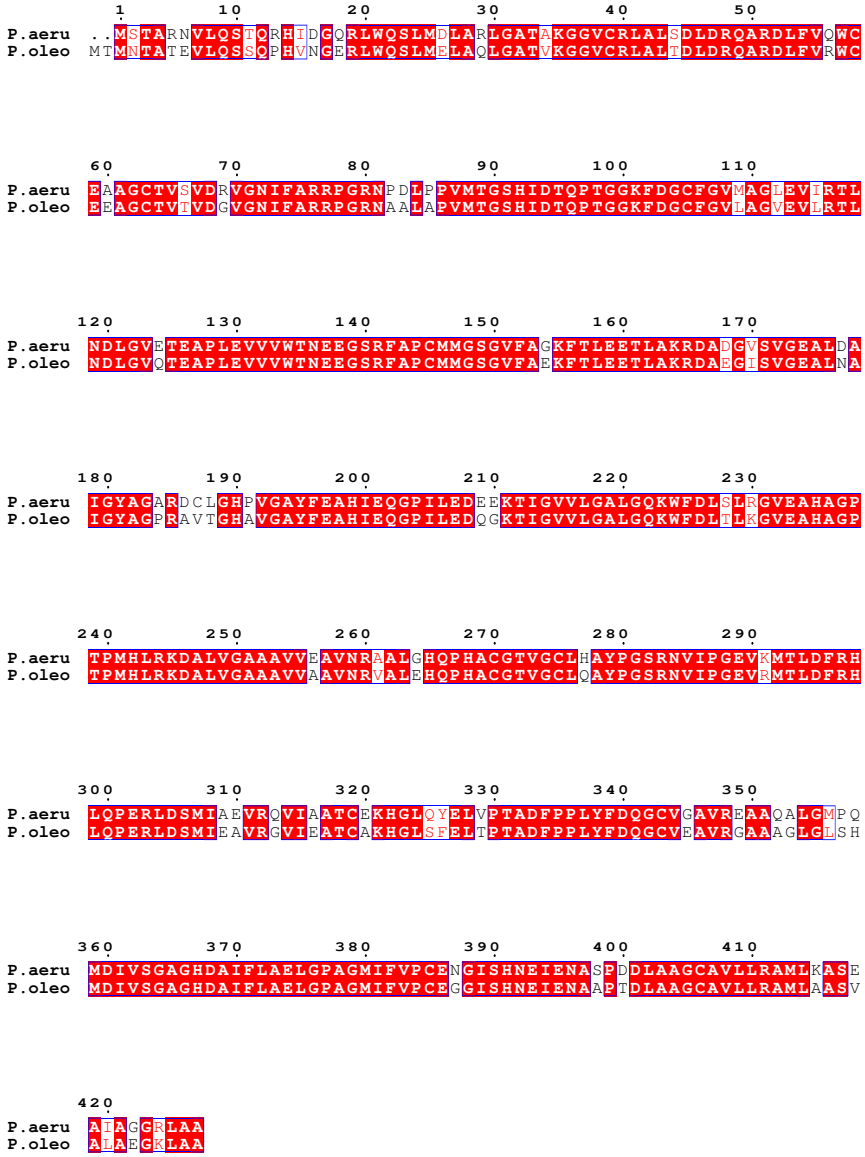

Figure 44: Multiple sequence alignment of identified proteins from *Pseudomonas sp*.
MSA of protein sequences of P. oleo (OWK49263.1) and P.aeru (AAG03833.1) aligned to L-carb of *G. stearothermophilus* (NCBI Q53389.1, not displayed) was conducted using ESPript 3.0. Highly conserved amino which are similar in each sequence are highlighted in red. Less conserved amino acids are circled in blue.

To evaluate the class affiliation the amino acid sequences of Burk1-5, P.oleo and P.aeru were aligned to selected representatives of each class of decarbamoylating enzymes. The corresponding percentage identities are given in Table 44. For protein accession numbers see Table 4 (p. 48).

Table 44: Multiple sequence alignment matrix of novel to classified decarbamoylating enzymes.
βUp = β-ureidopropionase; SklβUp = βUp from L- kluyveri; AaHyd = allantoate amidohydrolases; L-Carb = L-carbamoylase; D-Carb = D-carbamoylase.

Protein ID (PDB)	2V8H (SklβUp)		1Z2L		3N5F		1FO6	
Class	βUp		AaHyd		L-Carb		D-Carb	
	Query cover (%)	Identity (%)	Query cover (%)	Identity (%)	Query cover (%)	Identity (%)	Query cover (%)	Identity (%)
Burk1	84	42.53	97	31.93	99	37.35	-	-
Burk2	92	39.07	94	32.99	99	38.24	7	39.13
Burk3	84	39.43	96	33.42	99	38.93	15	46.15
Burk4	83	31.12	95	31.14	93	33.51	-	-
Burk5	83	30.51	91	33.86	97	33.25	7	33.33
P.aeru	90	40.87	95	31.99	99	38.24	-	-
P.oleo	90	41.06	94	32.32	97	40.85	21	39.13

Burk1-3, Burk5 and P.aeru and P. oleo possessed the highest query cover towards L-Carb 3N5F. However Burk1, P.oleo and P.aeru had the highest percentage identity towards βUp from *L. kluyveri* (2V8H). Burk4 showed the highest sequence homology also to 3N5F but had the highest query cover to AaHyd 1Z2L. None of the seven proteins had a similar query cover or percentage identity to D-Carb 1FO6. The highest query cover to 1FO6 with 21 % and a percentage identity of almost 40 %. Burk1, Burk4 and P.aeru showed no homology to 1FO6.

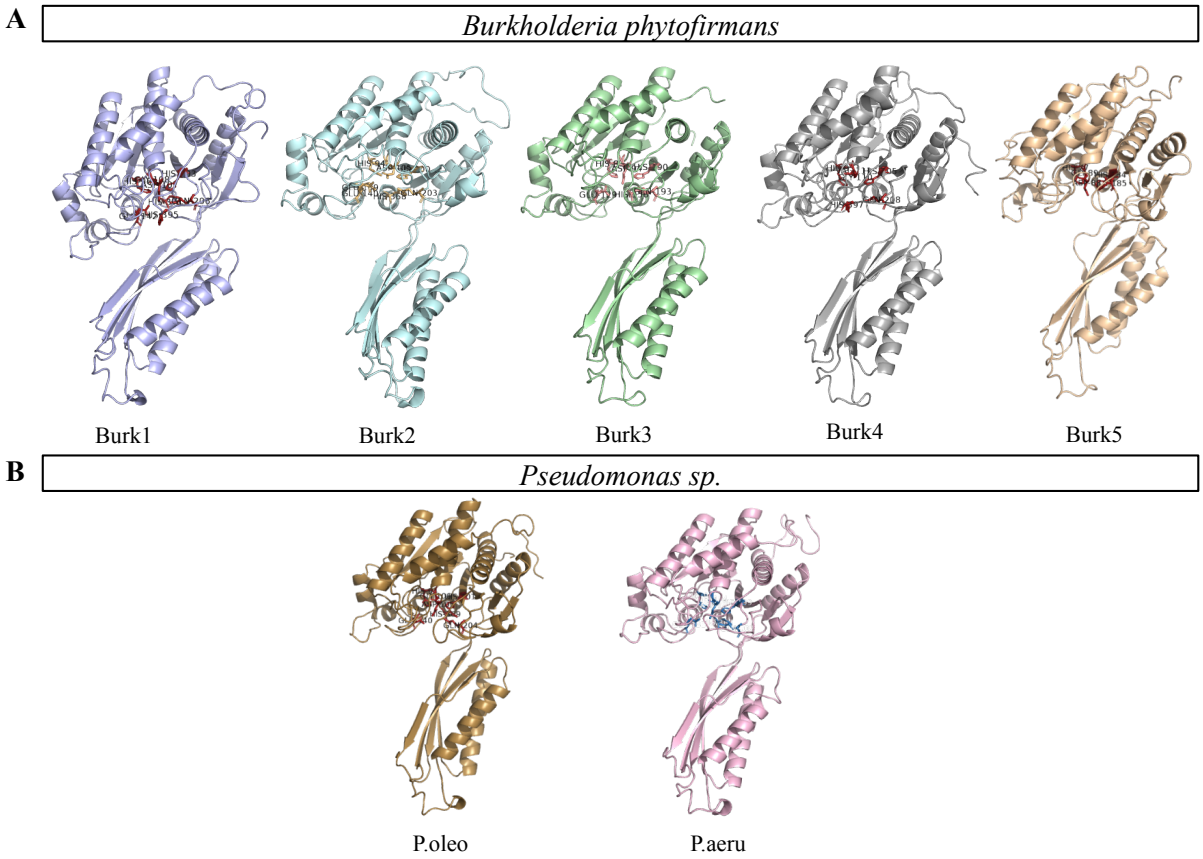

Figure 45: Monomer structure models of identified proteins.
Models were generated using the protein sequences obtained from NCBI and using Phyre[2] server. A) Models of proteins from strain *B. phytofirmans*. B) Models generated for the two different *Pseudomonas sp*. *P. oleovorans* and *P.aeruginosa*. For protein accession numbers see **Table 4** (p. 48).

As mentioned earlier L-Carbs, AaHyds and βUps can be distinguished from D-Carbs because they possess a different tertiary structure. To identify which tertiary structure the novel enzymes form a structure homology model was generated using Phyre[2] algorithm as described in section 3.2.6.1. An overview of the formed protein-model structures is given in Figure 45. 3D-tertiary models were based on 120 other protein structures of the PDB data bank.

P.oleo, P.aeru and Burk1-4 showed a high structure homology to the protein structure 5I4M (*B. vietnamiensis*) that is annotated as member of the hydantoinase/carbamoylases family. In contrast to that Burk5 showed the highest structural similarity to L-Carb 6C0D from *Parabulkholderia phytomatum*. All generated models show the typical monomer-structure of L-Carbs, AaHyds and βUps. One monomer is composed of two domains, whereby the bigger domain harbours the active site. E.g. like in 3N5F the monomer consists of dimerization domain formed by a long four-stranded antiparallel β-sheet and two long α-helices on one side of the β-sheet. The active-site domain consists of several shorter α-helices and β-sheets.

The prognosticated highly conserved amino acids of each enzyme model generated by Phyre[2] algorithm are given in Table 50 on p. 125. Additionally for Burk3 and P.oleo transmembrane-helices were identified. A sequence homology to D-Carbs was not observed for any of the seven enzymes.

4.4.1 Cloning, expression and purification

Genes of the seven identified proteins were ordered and synthesized from Thermo Fisher Scientific GENEART GmbH in a cloning vector. Plasmids were transferred to competent *E. coli* XL1 blue cells for DNA multiplication. Genes and expression vector (pLJSRSF7) were cut by using restriction enzymes BamHI and HindIII and subsequently ligated according to section 3.2.1.2. The plasmid was transformed into *E. coli* BL21 DE3 expression host by heat shock. For all enzymes suitable expression conditions were determined (see 3.2.3.2). Enzyme activity studies were either performed with fresh lysate or FPLC-purified enzyme. For all enzymes a FPLC purification *via* their MBP-tag was conducted. Figure 46 shows each enzyme after FPLC-purification. Expected protein bands of 98 kDa are present in every line. Additionally a band of ~40 kDa is more or less visible on the gel, as well as some slight other protein bands of higher size. Purification procedures of every protein with additional Äkta-chromatogram can be found in the appendix (8.9).

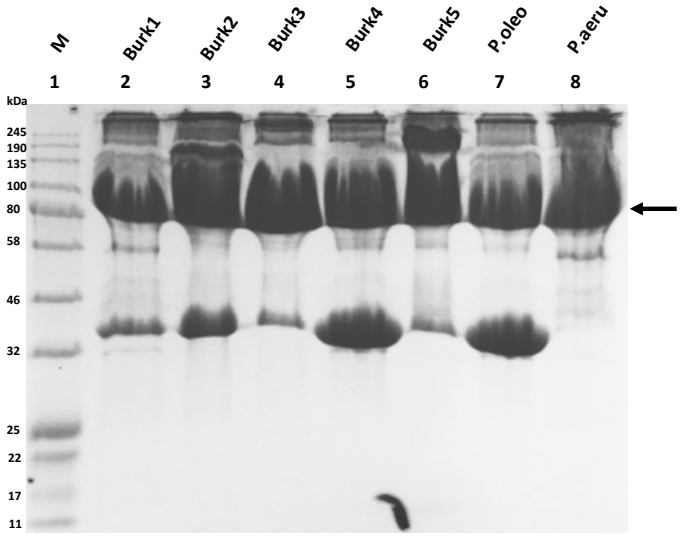

Figure 46: Verification of expression of identified proteins.
1: Marker: Color Prestained Protein Standard Broad Range (NEB); 2: 20 µg purified Burk1 (98.2 kDa); 3: 20 µg purified Burk2 (97.6 kDa); 4: 20 µg purified Burk3 (96.95 kDa); 5: 20 µg purified Burk4 (98.82 kDa); 6: 20 µg purified Burk5 (96.5 kDa); 7: 20 µg purified P.oleo (97.3 kDa); 8: 20 µg purified P.aeru (97.33 kDa).

4.4.2 Classification of novel decarbamoylating enzymes

The seven novel enzymes were classified. The four classes of decarbamoylating enzymes focused on in this work are defined by conversion of different substrates: D- or L-NCαAAs, NCβAla and allantoic acid. Since no structural similarity to D-Carbs was shown (see section 4.4) all seven enzymes were tested towards their degradation of a small NCLαAA such as NCLαSer, NCβAla and allantoic acid. Cells with expressed protein were resuspended in a 50 mM HEPES buffer pH 7 and disrupted by sonification. Activity studies were performed mixing 400 µl 10 mM substrate/product solution (dissolved in 50 mM HEPES buffer pH 7) with 100 µl protein lysate and incubated at 30 °C and 1000 rpm over night (see also 3.2.3.6). The temperature of 30 °C was chosen since the optimal growth temperature of *B. phytofirmans*, *P. oleovorans* and *P.aeruginosa* is 30 °C according to DMSZ. In addition the bivalent metal cofactors $CoCl_2$, $MnCl_2$, $NiCl_2$ (2 mM final concentration each) were tested. Several controls, such as substrate controls (without lysate) and product controls were carried out to exclude thermal decay of the substrate or enzymatic product degradation. All reactions were conducted in triplicate and reactions were stopped by denaturation at 95 °C for 5 min. Substrate concentrations were determined by Ehrlich-assay and product concentrations were detected through OPA/IBLC-derivatization in the HPLC (reaction product of allantoic acid excluded).

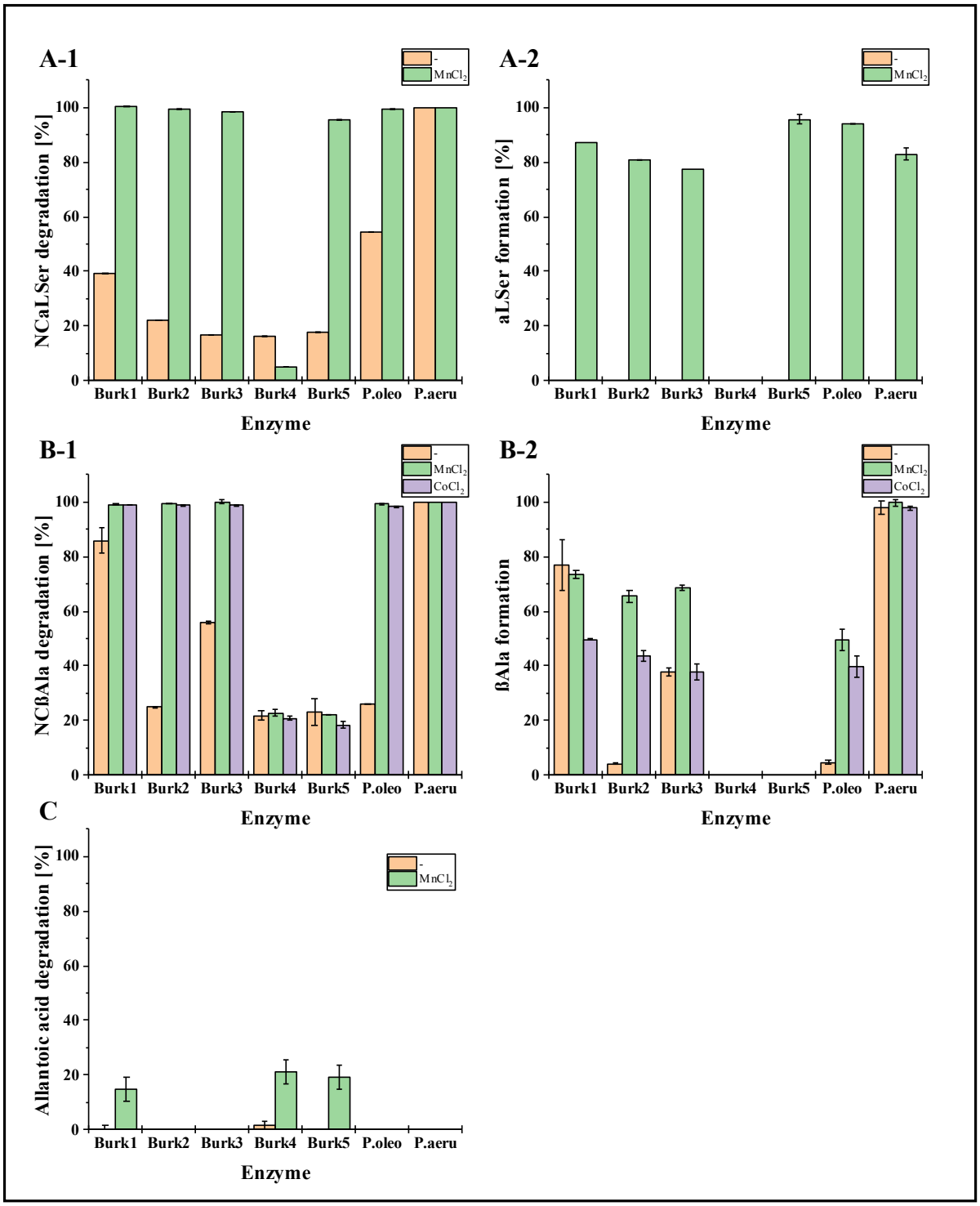

Figure 47: Classification of novel enzymes.
Burk1-5, P.oleo and P.aeru were investigated towards their conversion and product formation of A1&2) NCLαSer, B1&2) NCβAla and C) allantoic acid (only substrate degradation). Reactions were performed without and with cofactors $CoCl_2$, $MnCl_2$, $NiCl_2$. Activity studies were performed mixing 400 µl 10 mM substrate/product solution (dissolved in 50 mM HEPES buffer pH 7) with 100 µl protein lysate and incubated at 30 °C and 1000 rpm over night. All substrate degradations and product formations were calculated in relation to detected amount of substrate in substrate controls.

All enzymes were tested towards their conversion of a small NCαLAA to examine whether they exhibited L-Carb activity. Therefore NCLαSer was chosen as model substrate (Figure 47 A1). Reactions for P.aeru were performed at 37 °C, all other reactions were incubated at 30 °C over night. Burk1-3, P. oleo and P.aeru possessed activity towards NCLαSer. The strongest activity was observed for P.oleo and P.aeru, which converted approximately 50-100% of the initially present substrate concentration. Burk3 degraded only 16 % NCLαSer. The presence of $MnCl_2$ enhanced the activity to 98-100 % substrate conversion. Burk 4 and Burk5 showed almost the same activity towards NCLαSer without cofactor, however, in reactions with $MnCl_2$ Burk 4 had a lower conversion of 5% but Burk 5 a much higher of 95 % conversion of NCLαSer. Strong product degradation was observed in product controls (data not shown). A degradation of product by heat denaturation was excluded. 100 % of product was degraded in reactions without cofactor. In reactions containing $MnCl_2$ approximately 50 % product were converted in product control reactions. A formation of αSer was still observed of 77-94 % for all enzymes except Burk4 (Figure 47 A 2).

In Figure 47 B-1 the substrate degradation and in Figure 47 B 2 the product formation is displayed for reactions with NCβAla. For enzymes Burk1-5, P.oleo and P.aeru a decrease of NCβAla was measured without any cofactor. The strongest substrate conversion was observed for P.aeru without cofactor. Addition of metal cofactors, especially $CoCl_2$ and $MnCl_2$ had a strong influence on the substrate degradation. E.g. for Burk2 and Burk3 the addition of these cofactors led to increase to almost 100 % conversion. Other non-metal cofactors did not increase the substrate depletion. By adding NAD/NADH the substrate degradation was even lower compared to the substrate concentrations without cofactor (data not shown). In contrast to the other enzymes for Burk4 and Burk5 only a slight conversion of NCβAla of ~20 % but no production of βAla could be detected. The detected product formation concentration was not equally to the substrate depletion. In all product controls less product was detected after incubation with lysate. In substrate controls no product formation was observed.

To investigate whether enzymes possess AaHyd-activity also lysate-reactions with allantoic acid were performed (Figure 47 C). Conversion of allantoic acid was monitored by incubating reactions at 40 °C for Burk1, Burk4 and Burk5 and 30 °C for Burk2, Burk3, P.oleo and P.aeru. Degradation of allantoic acid was observed for Burk1, Burk4 and Burk5 but only for reactions containing $MnCl_2$. Thereby Burk 4 showed the highest degradation with 21 % calculated relatively to the substrate controls containing $MnCl_2$. Burk 5 was able to convert 19 % and Burk1 14 % of the initial allantoic acid concentration. For the other enzymes no

degradation was detected. The product of allantoic acid, (*S*)-ureidoglycine, was not investigated in the experiment since it spontaneously decays to (*S*)-ureidoglycolate.

Standard deviations were very small and therefore negligible. In summary all novel enzymes showed activity towards at least two substrates, which are representative for their enzyme class. Furthermore a strong influence for bivalent metal cofactors like $MnCl_2$ was observed. Burk1 in fact had activity for all three representative substrate classes and was therefore of particular interest in further experiments.

4.4.3 Characterization of novel enzymes

All novel enzymes were examined for their conversion of natural substrates of different enzyme classes. After an activity towards NCβAla had been determined it was tested whether the recombinantly expressed enzymes were able to convert NCβPhe to βPhe. Therefor enzyme lysate or FPLC enriched and concentrated enzyme was used in combination with several bivalent metal cofactors. Also influences of NAD/NADH towards their conversion of NCβPhe were tested. However, no enzyme or suitable condition tested led to detectable degradation of NCβPhe. Neither significant substrate degradation nor product formation was detected.

Therefor the focus was set on three novel questions: (1): what parameters influence the substrate acceptance (in terms of size) in the active centre? (2): are the enzymes able to cleave smaller aliphatic NCβ(h)AAs to their corresponding β(h)AA? And (3): do they show activity towards non-canonical NCαAAs?

To determine the limits for residue size towards the acceptance in the active site several aliphatic and aromatic canonical NCαAAs were tested. P.aeru und Burk1 were chosen for a more intensive investigation, whereby mostly reactions with enzyme lysate were performed. In Table 45 (p. 116) investigated conversions towards non-canonical α-substrates of P.aeru are shown, sorted by the amino acid residue size. Four different metal cofactors were tested. The reactions were conducted with enzyme lysate at 37 °C and 1000 rpm over night. All substrate degradations and product formations were calculated in relation to detected amount of substrate in substrate controls. For all investigated NCαAAs a conversion of 60-100 % was detected. The product formation of α-L-serine was highly depended on cofactor presence. No product formation was detected for α-L-valine and α-L-isoleucine. In presence of $NiCl_2$, $CoCl_2$ and $MnCl_2$ higher substrate conversion and product formation was observed.

Table 45: Substrate scope of P.aeru towards *N*-carbamoyl-derivates of canonical α-L-amino acids.
Reactions were performed with enzyme lysate at 37 °C and 1000 rpm over night. All substrate degradations and product formations were calculated in relation to detected amount of substrate in substrate controls. Con. [%] Substrate = Amount of converted substrate in %. Form. [%] Product = detected formed product. "-" = Amount of converted substrate / formation of product without additional cofactor; $MnCl_2$ or $CoCl_2$ or $NiCl_2$ or $ZnCl_2$ = Amount of converted substrate / formation of product with 2 mM $MnCl_2$ or $CoCl_2$ or $NiCl_2$ or $ZnCl_2$ used as cofactor. NCα-L-Gly = *N*-carbamoyl-α-L-glycine; α-L-Gly = α-L-glycine; NCα-L-ABA = *N*-carbamoyl-α-L-aminobutyric acid; α-L-ABA = α-L-aminobutyric acid; NCα-L-Ser = *N*-carbamoyl-α-L-serine; α-L-Ser = α-L-serine; NCα-L-Cys = *N*-carbamoyl-α-L-cysteine; α-L-Cys = α-L-cysteine; NCα-L-Val = *N*-carbamoyl-α-L-valine; α-L-Val = α-L-valine; NCα-L-Iso = *N*-carbamoyl-α-L-isoleucine; α-L-Iso = α-L-isoleucine; NCα-L-Leu = *N*-carbamoyl-α-L-leucine; α-L-Leu = α-L-leucine; NCα-L-Met = *N*-carbamoyl-α-L-methionine; α-L-Met = α-L-methionine.

70-100% | 40-70% | 20-40% | 0.1-20 % | 0 % | *n.d.* = not determined

Substrate	Product	P.aeru									
		Con. [%] Substrate					Form. [%] Product				
	Cofactor	-	$ZnCl_2$	$NiCl_2$	$MnCl_2$	$CoCl_2$	-	$ZnCl_2$	$NiCl_2$	$MnCl_2$	$CoCl_2$
NCα-L-Gly	α-L-Gly	78.9 ± 16	62.8 ± 0.6	98.1 ± 0.69	100 ± 0.1	100 ± 0.1	27.6 ± 33.3	1.5 ± 0.1	91.4 ± 2.7	97.3 ± 9.0	92.7 ± 6.0
NCα-L-ABA	α-L-ABA	63.7 ± 0.1	20.3 ± 0.2	63.8 ± 0	63 ± 0	64.6 ± 0.1	87.3 ± 0.4	5.8 ± 0	93 ± 2.5	97.2 ± 10	90.3 ± 4.8
NCα-L-Ser	α-L-Ser	100 ± 0.2	64.4 ± 0.9	100 ± 0.4	100 ± 0.3	100 ± 0.4	0	1.9 ± 0.1	68.2 ± 1.2	77.8 ± 2.1	77.3 ± 2.3
NCα-L-Cys	α-L-Cys	90 ± 0.4	76.1 ± 2	89 ± 1.1	98.8 ± 0.7	68.6 ± 7	24.1 ± 1.1	0	0	96.5 ± 4.6	26.9 ± 6.4
NCα-L-Val	α-L-Val	66.8 ± 1.4	68.8 ± 0.4	66.1 ± 0.2	68.2 ± 3.8	67.2 ± 2.6	0	0	0	0	0
NCα-L-Iso	NCα-L-Iso	65.2 ± 0.1	66 ± 0	64.4 ± 0.1	63.1 ± 0.1	62.8 ± 0	0	0	0	0	0
NCα-L-Leu	α-L-Leu	63.7 ± 0.9	64.9 ± 1.6	65.7 ± 5.2	66.4 ± 1	61 ± 1.3	0	0	0.7 ± 0.2	5.4 ± 0.8	0.4 ±0.3
NCα-L-Met	α-L-Met	63.7 ± 0.7	63.2 ± 0.7	69.7 ± 0.9	95.3 ± 1	62.7 ± 1.9	0	0	15.2 ± 2.6	88.1 ± 1.9	3.7 ± 0.5

The highest product formation for all tested substrates was obtained in the presence of $MnCl_2$. In comparison to that the presence of $ZnCl_2$ inhibited the conversion of several substrates. For NCα-L-Gly, NCα-L-Ser and NCα-L-Cys a higher conversion was observed than for NCα-L-ABA (*N*-carbamoyl-α-L-amino butyric acid), NCα-L-Val, NCα-L-Iso, NCα-L-Leu and NCα-L-Met. Only a slight formation of α-L-Leu was detected. Without addition of a metal cofactor no product formation was observed for α-L-Ser, α-L-Val, α-L-Iso, α-L-Leu and α-L-Met. Product controls showed a strong degradation of several reaction products.

Several lysate experiments were performed to investigate whether the novel enzymes are also able to cleave non-canonical NCαAAs. First Burk1 was intensively examined for its conversion of *N*-carbamoyl-derivates of non-canonical α-L-amino acids in lysate experiments. The results are given in Table 46 (p. 118). Reactions were performed without and with $MnCl_2$ as additional cofactor. $MnCl_2$ was selected as best cofactor, since previous activity studies proved $MnCl_2$ to have the highest effect towards substrate conversion for Burk1. Two aliphatic substrates, related to canonical substrates and several aromatic *N*-carbamoyl-derivates were tested. Reactions were performed at 30 °C and 1000 rpm over night. Results show that slight conversions were detected for NCα-L-neopentylglycine and NCα-L-tert-Leu. The presence of $MnCl_2$ had an impact on product formation. Especially for the degradation of NCβ-2-L-thienylalanine the product formation increased from 2 % to 97 %. Burk1 did not degrade other substrates with aromatic substituents with six C-atoms. Neither substrate conversion nor product formation was detected for NCα-L-naphtylalanine, NCαL-phenylglyine and NCα-L-hydroxy-phenylglycine.

Since most enzymes showed strong activity of towards NCα-L-Ser and NCα-L-Met, several aliphatic NCβAAs, such as NCLβhSer and NCLβhMet were investigated on their conversion by Burk1 and P.aeru (Table 47, p. 119). The shown results are a compilation of different experiments for each enzyme. FPLC purified enzymes where used, whereby for Burk1 a final protein concentration of 0.23 µg/µl and for P.aeru a final protein concentration of 2.14 µg/µl was used. Reactions were performed at 30 °C and 1000 rpm over night and stopped after 20 h by denaturation at 95 °C for 5 min. Substrate degradation was analysed using Ehrlich-Assay and product concentrations were either detected *via* HPLC or fluorescence assay (see 3.2.5).

Table 46: Activity of Burk1 towards non-canonical *N*-carbamoyl-α-amino acids.
Reactions were performed using enzyme lysate of expressed Burk1 and incubated at 30 °C for 20 h. All substrate degradations and product formations were calculated in relation to detected amount of substrate in substrate controls. Con. [%] Substrate = Amount of converted substrate in %. Form. [%] Product = detected formed product. Without cofactor = Amount of converted substrate / formation of product without additional cofactor; $MnCl_2$ = Amount of converted substrate / formation of product with 2 mM $MnCl_2$ used as cofactor. NCα-L-NeoGly = *N*-carbamoyl-α-L-neopentylglycine; α-L-NeoGly = α-L-neopentylglycine; NCα-L-tert-Leu = *N*-carbamoyl-α-L-tertiary-leucine; α-L-tert-Leu = α-L-tertiary-leucine; NCβ-2-L-ThieAla = *N*-carbamoyl-β-2-L-thienylalanine; β-2-L-ThieAla = β-2-L-thienylalanine; NCα-L-NaphtAla = *N*-carbamoyl-α-L-naphtylalanine; α-L-NaphtAla = α-L-naphtylalanine; NCα-L-PheGly = *N*-carbamoyl-α-L-phenylglycine; α-L-PheGly = α-L-phenylglycine; NCα-L-p-H-PheGly = *N*-carbamoyl-α-L-hydroxy-phenylglycine; α-L-p-H-PheGly = α-L-hydroxy-phenylglycine.

70-100% | 40-70% | 20-40% | 0.1-20 % | 0 % | *n.d.* = not determined

Substrate	Product	Burk1 Con. [%] Substrate	Burk1 Form. [%] Product
		Aliphatic	
NCα-L-NeoGly 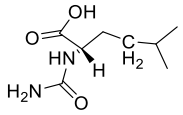	**α-L-NeoGly** 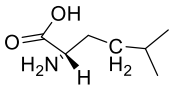	**Without cofactor**	
		10.1 ± 0.7	8.4 ± 0.4
		$MnCl_2$	
		9.8 ± 2.8	10.6 ± 0.5
NCα-L-tert-Leu 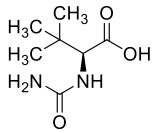	**α-L-tert-Leu** 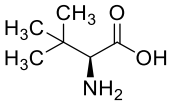	**Without cofactor**	
		4.6 ± 0.8	8.7 ± 0.3
		$MnCl_2$	
		5 ± 3	14.1 ± 0.4
		Aromatic	
NCβ-2-L-ThieAla 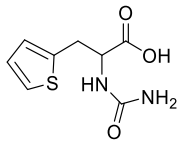	**β-2-L-ThieAla** 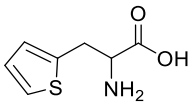	**Without cofactor**	
		0.8 ± 1.4	2 ± 0
		$MnCl_2$	
		90.2 ± 1.6	97.1 ± 0.6
NCα-L-NaphtAla 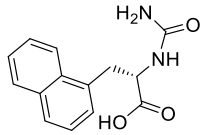	**α-L-NaphtAla** 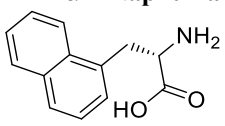	**Without cofactor**	
		0	0
		$MnCl_2$	
		0	0
NCα-L-PheGly 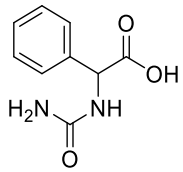	**α-L-PheGly** 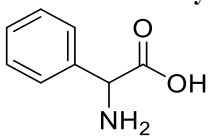	**Without cofactor**	
		0	0
		$MnCl_2$	
		0	0
NCα-L-p-H-PheGly 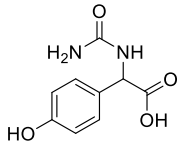	**α-L-p-H-PheGly** 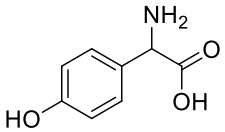	**Without cofactor**	
		0	0
		$MnCl_2$	
		0	0

Table 47: Substrate scope of Burk1 and P.aeru towards *N*-carbamoyl-β-amino acids.
Reactions were conducted with FPLC enrieched enzymes. Burk1 was used with a final concentration of 0.23 µg/µl and P.aeru with a final concentration of 2.14 µg/µl in each reaction. Reactions were incubated at 30 °C for 20 h. All substrate degradations and product formations were calculated in relation to detected amount of substrate in substrate controls. Con. [%] Substrate = Amount of converted substrate in %. Form. [%] Product = detected formed product. Without cofactor = Amount of converted substrate / formation of product without additional cofactor; $MnCl_2$ or $CoCl_2$ or $NiCl_2$ or $ZnCl_2$ = Amount of converted substrate / formation of product with 2 mM $MnCl_2$ or $CoCl_2$ or $NiCl_2$ or $ZnCl_2$ used as cofactor. NCβAla = *N*-carbamoyl-β-alanine; βAla = β-alanine; NCβ-L-hAla = *N*-carbamoyl-β-L-homo-alanine; β-L-hAla = β-L-homo-alanine; NCβ-L-hSer = *N*-carbamoyl-β-L-homo-serine; β-L-hSer = β-L-homo-serine; NCβ-D-hSer = *N*-carbamoyl-β-D-homo-serine; β-D-hSer = β-D-homo-serine; NCβ-L-hMet = *N*-carbamoyl-β-L-homo-methionine; β-L-hMet = β-L-homo-methionine; NCβ-*rac*-Leu = *N*-carbamoyl-β-*rac*-leucine; β-*rac*-Leu = β-*rac*-leucine; NCβ-Hep = *N*-carbamoyl-L-3-aminoheptanoic acid; β-Hep = L-3-aminoheptanoic acid; NCβ-*rac*-Phe = *N*-carbamoyl-β-*rac*-phenylalanine; β-*rac*-Phe = β-*rac*-phenylalanine.

70-100% | 40-70% | 20-40% | 0.1-20 % | 0 % | *n.d.* = not determined

Substrate	Product	Burk1 (0.23 µg/µl) Con. [%] Substrate	Burk1 (0.23 µg/µl) Form. [%] Product	P.aeru (2.14 µg/µl) Con. [%] Substrate	P.aeru (2.14 µg/µl) Form. [%] Product
		Aliphatic			
NCβAla 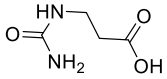	**βAla** 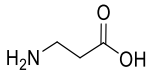	**Without cofactor**			
		85.9 ± 4.8	76.8 ± 9.2	100	100
		$MnCl_2$			
		99.1 ± 0.1	73.3 ± 1.4	100	100
		$CoCl_2$			
		98.8 ± 0.1	49.6 ± 0.2	*n.d.*	*n.d.*
		$ZnCl_2$			
		29.9 ± 6.3	20.1 ± 0.9	*n.d.*	*n.d.*
NCβ-L-hAla 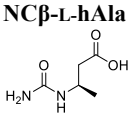	**β-L-hAla** 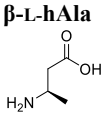	**Without cofactor**			
		18.7 ± 0.3	0.3 ± 0.2	45.5 ± 2.9	0.4 ± 0.1
		$MnCl_2$			
		22 ± 3.5	3.4 ± 0.4	93.7 ± 0.1	33.7 ± 2.5
NCβ-L-hSer 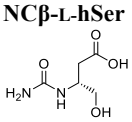	**β-L-hSer** 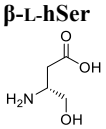	**Without cofactor**			
		14.5 ± 0.6	0.6 ± 0	29.7 ± 0.1	0
		$MnCl_2$			
		20.6 ± 1.1	1.1 ± 0.1	93 ± 1.3	100 ± 2.1
NCβ-D-hSer 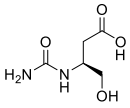	**β-D-hSer** 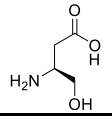	**Without cofactor**			
		10.5 ± 0.3	0.3 ± 0.2	37.2 ± 0.5	0.3 ± 0.2
		$MnCl_2$			
		9.7 ± 0.1	0.1 ± 0	37.2 ± 3.5	0.7 ± 0
NCβ-L-hMet 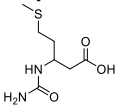	**β-L-hMet** 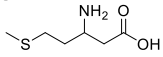	**Without cofactor**			
		14.4 ± 0.1	0	40.2 ± 1.4	0
		$MnCl_2$			
		8.8 ± 0	0	36.4± 4.2	1.8 ± 3
NCβ-*rac*-Leu 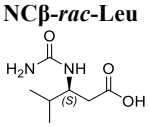	**β-*rac*-Leu** 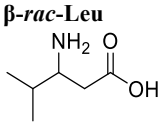	**Without cofactor**			
		12.6 ± 0.1	0	38.9 ± 4	0.2 ± 0.1
		$MnCl_2$			
		9.8 ± 0	0	35.7 ± 0.2	0.1 ± 0.1
NCβ-Hep 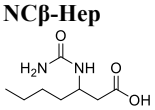	**β-Hep** 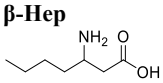	**Without cofactor**			
		19 ± 1	1 ± 0	40.7 ± 2.1	0.1 ± 0.1
		$MnCl_2$			
		5.1 ± 1.1	1 ± 0.1	36.6 ± 2.2	0.5 ± 0.8
NCβ-*rac*-Phe 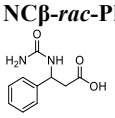	**β-*rac*-Phe** 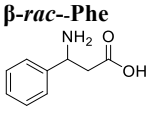	**Without cofactor**			
		0	0	0	0
		$MnCl_2$ / $CoCl_2$ / $NiCl_2$ / $ZnCl_2$			
		0	0	0	0

Both Burk1 and P.aeru were able to convert aliphatic *N*-carbamoyl-β-(homo)-amino acids. However a significant amount of product was only detected for L-β-homo-alanine and L-β-homo-serine. Here, too, an addition of $MnCl_2$ increased the amount of converted substrate and formed product. For Burk1 a decrease of NCβHep and NCβLhMet of 18 % and 14 % respectively but no product formation was detected. Furthermore Burk1 showed activity towards NCDβhSer of 10 %, but only a slight product formation was detected (< 1 mM). Even though reactions were performed with previously enriched enzyme strong product degradation for βhMet about 50 % was observed for Burk1. In contrast to that no product degradation was detected for βHep and DβhSer.

For P.aeru a ten times higher protein concentration was used in the reactions as for Burk1. P.aeru shows a strong degradation of NCLβhAla and NCLβhSer especially when $MnCl_2$ was present. The only βhAAs that were verifiable were LβhAla and LβhSer. Also for NCβ-D/L-Hep, NCLβhMet and NCDβhSer a degradation of up to 40 % was measured, but no significant product formation was observed. Substrate controls showed no significant substrate decay or product formation, but degradation of product was detected in product controls. For DβhSer up to 38 %, for LβhMet up to 8 %, for D/LβLeu up to 11 % and for βHep up to 18 % product degradation were observed.

For direct comparison of all seven enzymes activity was studied using selected non-canonical amino acid substrates with proven activity in former experiments with Burk1 and P.aeru. Therefor the same protein concentrations (final concentration of 1 µg/µl) and parameters for each enzyme were used (30 °C, 1000 rpm, over night). After purification of the enzymes *via* FPLC they were stored at -20 °C until use (activity after freezing had been proven earlier). The results in Table 48 (p. 122) revealed that all enzymes possessed decarbamoylating activity towards non-canonical amino acid derivates. The highest substrate affinity was detected for the conversion of *N*-carbamoyl-β-2-thienylalanine (*N*Cβ-2-ThieAla). As shown previously for Burk1, a conversion of other substrates with an aromatic C6-ring substitutent was not observed. In contrast to that for the *N*Cβ-2-ThieAla substituent (aromatic C5-ring with incorporated sulphur atom) a substrate conversion and product formation of up to 100 % was detected for Burk1-3, Burk5 and P.aeru was observed. For P. oleo only a conversion of 27 % was measured. In contrast to this no degradation of NCβ-2-ThieAla was detected for Burk4. Also other enzymes than Burk1 showed activity towards non-canonical α-substrates. E.g. *N*-carbamoyl-α-L-neopentylglycine (NCα-L-NeoGly) was approximately degraded up to 20 % but usually only a slight product formation was observed. The only exception is Burk5 for which a high conversion of NCα-L-NeoGly was observed. Especially when $MnCl_2$ was

present in the reaction a product concentration (α-L-neopentylglycine) of 60 % was obtained. Substrate controls showed no thermal degradation of NCα-L-NeoGly and no product formation of α-L-NeoGly. However especially for Burk4 a product degradation of α-L-NeoGly was detected in product controls of 25 %. For other enzymes almost no product degradation was detected. Overall the conversion of *N*-carbamoyl-α-L-tertiary-leucine (NCα-L-tertLeu) was lower with conversion rates of up to 20 % (P. oleo) but only a slight product formation of maximum 3 % was detected. Substrate controls showed no significant substrate degradation for NCα-L-tertLeu but a product degradation of 10-20 % approximately was observed. Furthermore Burk1, P.oleo and P.aeru showed a strong affinity towards conversion of *N*-carbamoyl-L-β-homo-serine (*N*CLβhSer) of up to 66 % with $MnCl_2$ as cofactor. But only a product formation of L-β-h-serine of up to 20 % was measured.

A thermal or cofactor dependent degradation of *N*CLβhSer can be excluded, since no significant product was detected in substrate controls without enzyme. However product degradation was observed in product controls of up to 30 % for LβhSer (data not shown).

Table 48: Overall comparison of seven novel decarbamoylating enzymes.
All reactions were conducted using 1 µg/µl final concentration of each enzyme. Reactions were incubated at 30 °C and 1000 rpm for 20 h. All substrate degradations and product formations were calculated in relation to detected amount of substrate in substrate controls. Con. [%] Substrate = Amount of converted substrate in %. Form. [%] Product = detected formed product. Without cofactor = Amount of converted substrate / formation of product without additional cofactor; $MnCl_2$ or $CoCl_2$ or $NiCl_2$ or $ZnCl_2$ = Amount of converted substrate / formation of product with 2 mM $MnCl_2$ or $CoCl_2$ or $NiCl_2$ or $ZnCl_2$ used as cofactor.

70-100%	40-70%	20-40%	0.1-20 %	0 %	*n.d.* (not determined)

Substrate	Product	Burk1		Burk2		Burk3		Burk4		Burk5		P. oleo		P.aeru	
		Con. [%] Substrate	Form. [%] Product	Con. [%] Substrate	Form. [%] Product	Con. [%] Substrate	Form. [%] Product	Con. [%] Substrate	Form. [%] Product	Con. [%] Substrate	Form. [%] Product	Con. [%] Substrate	Form. [%] Product	Con. [%] Substrate	Form. [%] Product
Aliphatic															
NCβAla 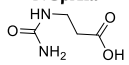	βAla 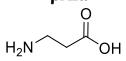	**Without cofactor**													
		100 ± 0	100 ± 0	93.2 ± 0.5	60.9 ± 42.1	92.9 ± 0.1	100 ± 0	8.4 ± 0.2	0	10.7 ± 0.1	0	99 ± 0	100 ± 0	99.8 ± 0.0	100 ± 0
		$MnCl_2$													
		100 ± 0	100 ± 0	100 ± 0	100 ± 0	100 ± 0	100 ± 0	24.7 ± 0.4	12.98 ± 0	41.0 ± 0.3	33.7 ± 0	100 ± 0	100 ± 0	100 ± 0	100 ± 0
NCβ-L-hSer 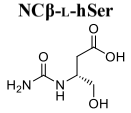	β-L-hSer 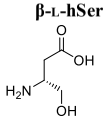	**Without cofactor**													
		24.8 ± 2.5	1.7 ± 0.2	18 ± 0.9	1.5 ± 0.2	5.9 ± 4.04	1.5 ± 0.0	3.50 ± 4.30	1.6 ± 0.1	16.6 ± 1	2.2 ± 0.4	11.4 ± 0.52	2.3 ± 0.3	17.1 ± 1.7	2.9 ± 0.4
		$MnCl_2$													
		66.6 ± 28	19.1 ± 8	27.5 ± 4	3.8 ± 1.6	29.2 ± 1.7	6.4 ± 6.8	15.4 ± 7.97	1.5 ± 0.4	16.9 ± 5.2	1.6 ± 0.3	51.2 ± 1.2	24.2 ± 19.4	36.4 ± 19.3	14.9 ± 0.7
NCα-L-NeoGly 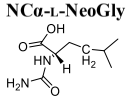	α-L-NeoGly 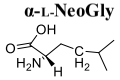	**Without cofactor**													
		20.1 ± 1.3	0.4 ± 0.1	17.96 ± 0.1	0.3 ± 0.2	13 ± 3.4	0.36 ± 0	11.8 ± 5.7	0.79 ± 0.8	51.6 ± 7	46.3 ± 8	15.2 ± 7	1.4 ± 0.7	17.7 ± 1	3.3 ± 0.9
		$MnCl_2$													
		21.4 ± 2.1	4.3 ± 0.3	21.4 ± 0.5	0.2 ± 0	15.1 ± 2.1	0.57 ± 0	17.6 ± 3.4	0.23 ± 0	100 ± 0.8	61.5± 0	24.2 ± 1.6	2.5 ± 0.5	27.5 ± 2	13.1 ± 1.7
NCα-L-tert-Leu 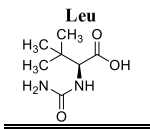	α-L-tert-Leu 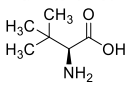	**Without cofactor**													
		19.2 ± 1.8	1.8 ± 0.1	12.1 ± 1.9	1.3 ± 0	3.3 ± 2.1	1.87 ± 0	8.8 ± 2	2.14 ± 0.3	0	2.6 ± 0.5	15.9 ± 1.4	3.9 ± 0.6	13.8 ± 2.4	5.02 ± 0.9
		$MnCl_2$													
		17.1 ± 1.5	1.4 ± 0.1	17.9 ± 2	1.7 ± 0.8	12.2 ± 1.3	2.09 ± 0.7	18.2 ± 2.7	2.18 ± 0.4	14.2 ± 4.8	3.6 ± 1.0	20.5 ± 1	3.1 ± 1	17.6 ± 2.7	3.3 ± 1.0
Aromatic															
NCβ-2-L-ThieAla 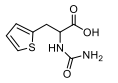	β-2-L-ThieAla 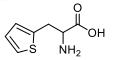	**Without cofactor**													
		95.2 ± 0.3	91.2 ± 0.7	0	0.1 ± 0.0	0	0	0	0	96.5 ± 0.0	92.7 ± 0.4	16.3 ± 0.9	17.9± 0.5	3.3 ± 0.5	5.5 ± 0.3
		$MnCl_2$													
		100 ± 0	95 ± 1.1	100 ± 0	95.0 ± 1.0	100 ± 0	95.8 ± 0.7	0	0.1 ± 0.0	98.7 ± 1.9	96.8 ± 0.6	27.5 ± 11.4	49.8 ± 31.1	99.5 ± 0.5	93.6 ± 0.1
NCβ-*rac*-Phe 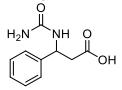	β-*rac*-Phe 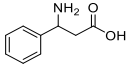	**Without cofactor**													
		0	0	0	0	0	0	0	0	0	0	0	0	0	0
		$MnCl_2$ / $CoCl_2$ / $NiCl_2$ / $ZnCl_2$													
		0	0	0	0	0	0	0	0	0	0	0	0	0	0

For Burk1 and P.aeru the optimal pH- and temperature range was determined in 50 mM HEPES buffer. Therefor purified enzyme was incubated with 10 mM NCβAla at different temperatures and pH-values. The reaction was stopped after 1 h with 10 % (v/v) 2 M HCl. The final protein concentration in each reaction was 0.23 mg/ml. Previous to analytics the sample was neutralized by the corresponding amount of 2 M NaOH. The concentration of produced βAla was determined *via* HPLC analysis. All reactions were performed in triplicate whereby substrate and product controls were carried as well. The results for Burk1 (Figure 48 A) show that the highest amount of βAla was obtained at a pH of 6.8 at 40 °C. However, in general the enzyme revealed activity in a wide temperature and pH range. Also P.aeru possesses its highest activity at these conditions (Figure 48 B). Whereby P.aeru possesses quite high activity at pH 6.8 in general. A higher temperatures of 50 °C led to a very low or no activity respectively. For none of the enzymes a degradation of βAla was observed in product controls. No thermal degradation of the initial substrate concentration of 10 mM NCβAla was observed in substrate controls at the investigated temperatures.

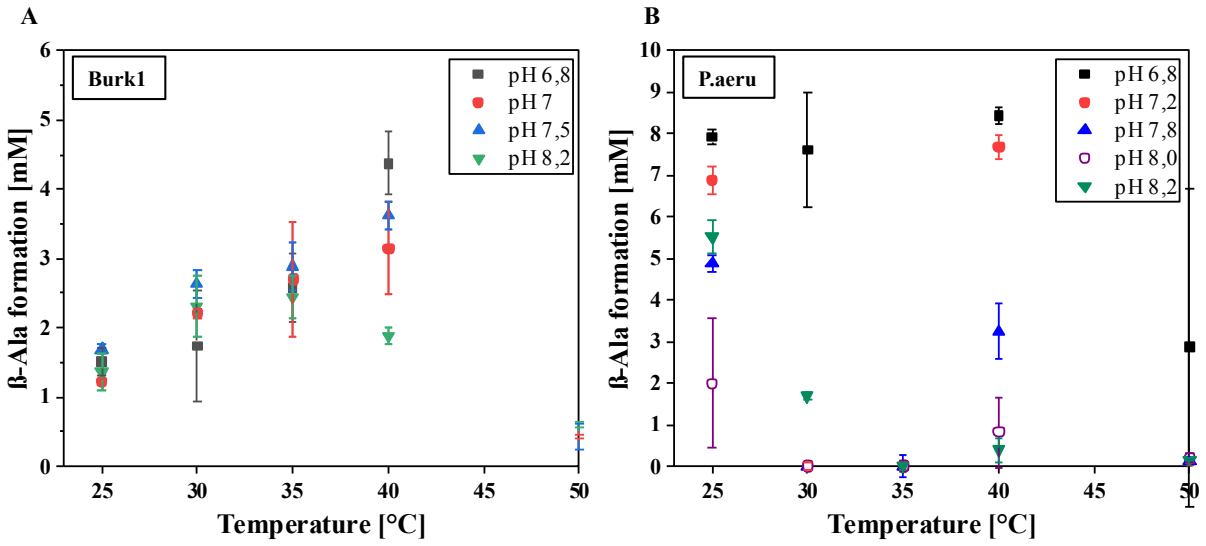

Figure 48: Temperature and pH optimum of Burk1 and P.aeru.
Detected βAla concentrations after incubation with 10 mM NCβAla at different pH values and temperatures for 1 h. Reactions were stopped with 2 M HCl and neutralized with 2 M NaOH prior analysing. A) βAla concentrations after incubation with Burk1. B) βAla concentration after incubation with P.aeru.

For determination of optimal reaction conditions, stability tests for Burk1 were performed. Therefor purified and concentrated enzymes were stored at -80 °C with and without addition of 10-20 % glycerol, at -20 °C and at 4 °C for 5 days. Subsequently the activity was tested by incubation of 0.7 µg/µl enzyme with 10 mM NCβAla over night at 30 °C and 1000 rpm. It was observed that Burk1 showed approximately the same activity after storage at mentioned

conditions compared to activities obtained with fresh enzyme. Also for Burk2, Burk3, Burk4, Burk5, P. oleo and P.aeru still the same activity towards NCβAla after previous storage at -20 °C or -80°C could be observed. An addition of glycerol or sudden freezing with liquid nitrogen was not necessary to preserve the enzyme activity required for over night biotransformation experiments.

Since Burk 1, 2 and 3 have a very homologue amino acid sequences and exhibit similar activities towards several substrates they were directly compared to each other. Therefor kinetic parameters for the conversion of NCβAla without cofactor were determined. Reactions were performed with purified enzyme with an initial protein concentration of 0.23 mg/ml final concentration in each reaction. All reactions were incubated with the previously determined optimal reaction conditions at 40 °C and at a pH of 6.8. NCβAla concentrations of 0, 3, 6 and 10 mM were used and samples were taken after 0, 5 15 and 60 min and stopped by addition of 2 M HCl. All reactions were performed in triplicate. All three enzymes showed a high conversion of NCβAla after one hour. For all enzymes a kinetic progression according to Michaelis-Menten kinetics (Figure 49) could be assumed. The corresponding kinetic parameters were calculated as described in section 3.2.3.7 and are given in Table 49. In contrast to Burk2 and Burk3 a significant lower K_m-value was observed for Burk1 (5.71 mM). The K_m-values for Burk2 and Burk3 were higher with 22.3 mM and 27.8 mM respectively. The highest turnover rate was also observed for Burk1 (66.4 s^{-1}), followed by Burk3 (34.8 s^{-1}) and Burk2 (6.9 s^{-1}). These results correlate with those found in lysate experiments (see Figure 47).

Table 49: Kinetic parameters of Burk1-3.
K_M: Michaelis-Menten constant (mM); A_{max}: maximum specific activity; k_{cat}: turnover number (s-1).

Enzyme	A_{max} [µmol/min/mg]	K_m [mM]	A_{max}/K_m [µmol/(min•mg•mM)]	k_{cat} [1/s]	Turnover rate [1/(s •M]
Burk 1	0.5	5.71	0.088	0.38	66.4
Burk 2	0.2	22.36	0.009	0.15	6.9
Burk 3	1.3	27.8	0.047	0.97	34.8

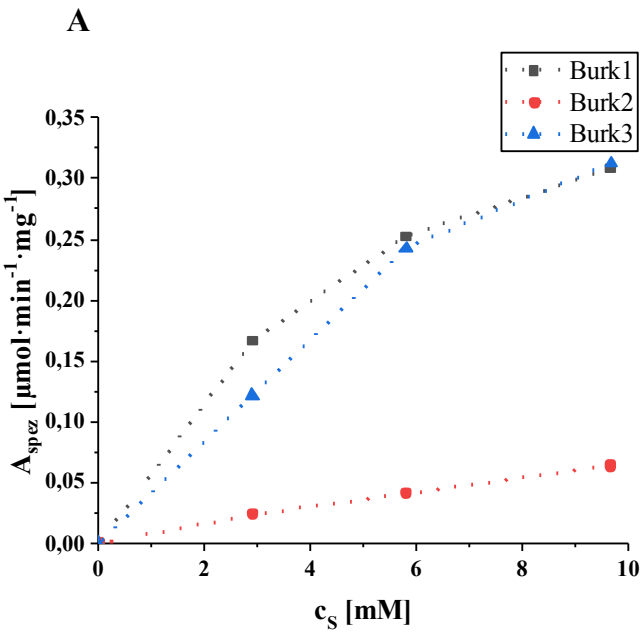

Figure 49: Michaelis-Menten kinetic of Burk1-3.
Linearization was performed using Lineweaver-Burk method. A_{spez}: specific activity U/mg (µmol/(min*mg); c_S: substrate concentration (mM).

4.4.4 Structural analysis of enzyme-models

As mentioned in section 4.4.2 an enzyme model was generated for all enzymes used within this work using Phyre[2] algorithm (see Figure 45, p. 110). At the same time the highly conserved amino acids of the active site were proposed, by performing a Clustal Ω multiple sequence alignment and comparisons to other known protein structures (Table 50).

Table 50: Identified highly conserved amino acids in enzyme-model active sites.
Amino acid residues found in every of the seven enzymes are marked in red. Other common amino acids, present in most but not in all enzymes are marked as follows: Asp (green), Glu (light blue), Gln (dark blue), second His (orange). Additional amino acids that occur only in one enzyme are black and marked in bold.

Burk1	Burk2	Burk3	Burk4	Burk5	P.oleo	P.aeru
Highly Conserved amino acids (calculated with Phyre[2]server)						
96 His	94 His	83 His	95 His	77 His	94 His	92 His
107 Asp	105 Asp	94 Asp	110 Gly	88 Asp	105 Asp	103 Asp
108 Gly	106 Gly	95 Gly	**111 Val**	89 Gly	106 Gly	104 Gly
142 Glu	139 Glu	129 Glu	205 His	184 His	140 Glu	138 Glu
203 His	**140 Glu**	190 His	208 Gln	**185 ILE**	201 His	199 His
206 Gln	200 His	193 Gln	397 His		204 Gln	202 Gln
371 His	203 Gln	358 His			369 His	367 His
395 His	368 His					

In all proposed actives sites of the seven enzyme models at least two histidines and one glycine are present (red). However, several differences exist. One of the most common other amino acid residues is aspartate (Asp, green), present in all enzymes showing a high affinity

towards NCβAla. Burk1-3, P.oleo and P.aeru showing the highest affinity towards NCβAla (100 % without additional cofactor) harbour also a glutamate residue (Glu, light blue). A glutamine residue (Gln, dark blue) is proposed for the active site of all enzymes except Burk5. Additionally all enzymes but Burk5 harbour a second histidine, whereby Burk1 possesses the most with four histidines. Burk2 is the only enzymes with a proposed second glutamate (Glu) residue. Furthermore Burk4 and Burk5 are the only enzymes, which harbour a valine (Val) and an isoleucine (ILE) respectively. The active sites of P.oleo and P.aeru seem to be similar with regard to the proposed highly conserved amino acids. This fits to their high sequence homology of 85 % (see MSA Figure 44, p. 108). An insight into the arrangement of the conserved amino acids of the corresponding proposed actives sites is given in (Figure 50 A-G).

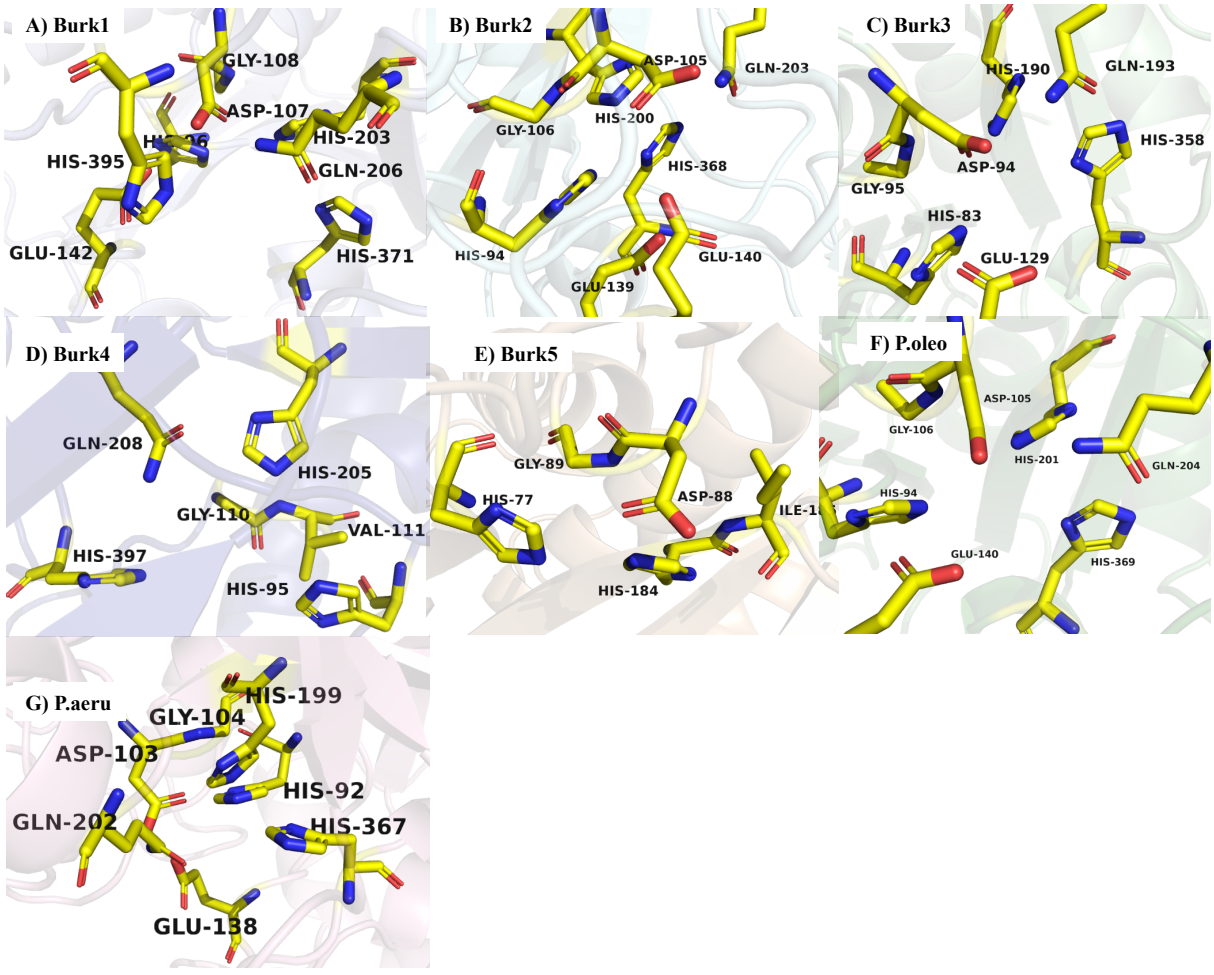

Figure 50: Models of proposed actives sites of Burk1-5, P.oleo and P.aeru.
Marked active sites of A) Burk1 B) Burk2 C) Burk3 D) Burk4 E) Burk5 F) P.oleo G) P.aeru. Highly conserved amino acids are highlighted in yellow, nitrogen atoms highlighted in blue, oxygen atoms in red. Figure was made using PDB-files of the models generated by Phyre[2] algorithm (see 3.2.6.1) and edited using PyMol.

To investigate whether the results of *in vitro* experiments may be explained through structure analysis several *in silico* ligand-dockings were performed with the corresponding models

generated by Phyre[2]. Since enzyme models were designed through structural alignments to existing homologue enzymes structures, they did not contain a substrate molecule. For docking experiments starting coordinates had to be determined. This was performed as explained in section 3.2.6.3 by transferring a co-crystallized substrate from a known structure to an enzyme model *via* alignment of the catalytic domains in PyMol. For Burk1-5, P.oleo and P.aeru starting coordinates were generated by transferring the NCβAla-molecule of 2V8H (named as "URP" in the PDB-file) or 3-PG-molecule of 5I4M to the relevant model. As mentioned earlier the highest structural homology for the generated enzyme models was enzyme 5I4M from *B. vietnamiensis*. Substrate dockings were performed as described in section 3.2.6.4. Of the 500 generated models only the top 10 models were analysed in PyMol. To investigate whether hydrogen bond forming may be possible distances in Å were determined between certain residues. Since different enzyme models are embedded in a different coordinate system they cannot be compared to each other. Only various docked substrates of one enzyme can be compared to each other. Dockings for Burk1, Burk4 and P.aeru were performed to propose possible binding and catalysis of different substrates with verified activity (see section 4.4.3). As mentioned earlier the energy score interface delta (IΔ) represents a measure of binding energy between the ligand and the enzyme molecule. Thus the lower the energy scores obtained from the docking experiment using ROSIE the better the fit of the ligand into the model (see section 3.2.6.4). However a low energy cannot be equated to being the most realistic docking model.

Starting coordinates for Burk1 were generated through alignment with 5I4M. Figure 51 shows a possible binding of NCβAla and NCβLhAla in the active site of Burk1 model. Since Burk1 showed a higher activity towards NCβAla the model with the lowest energy was set as reference docking with an interface delta (I Δ) of -12.78. The carbamoyl group of both dockings is oriented towards the metal ions (Figure 51). Distance measurements in Å of the carbonyl-O-atom (3.3 Å) and the N-atom of the *N*-carbamoyl group (3.2 Å) show a possible interaction with His395 and Gln206. These residues may be involved in the catalytic mechanism of Burk1. Regarding to Table 44 the highest amino acid sequence identity was found to 2V8H. His-395 is an additional fourth His that the other enzymes do not possess. Figure 51 B shows the possible binding of NCβLhAla. Most of the 10 models for NCβLhAla showed a completely different direction than NCβAla. Thus a model showing a similar coordination than NCβAla but higher energy was chosen (I Δ -10.41).

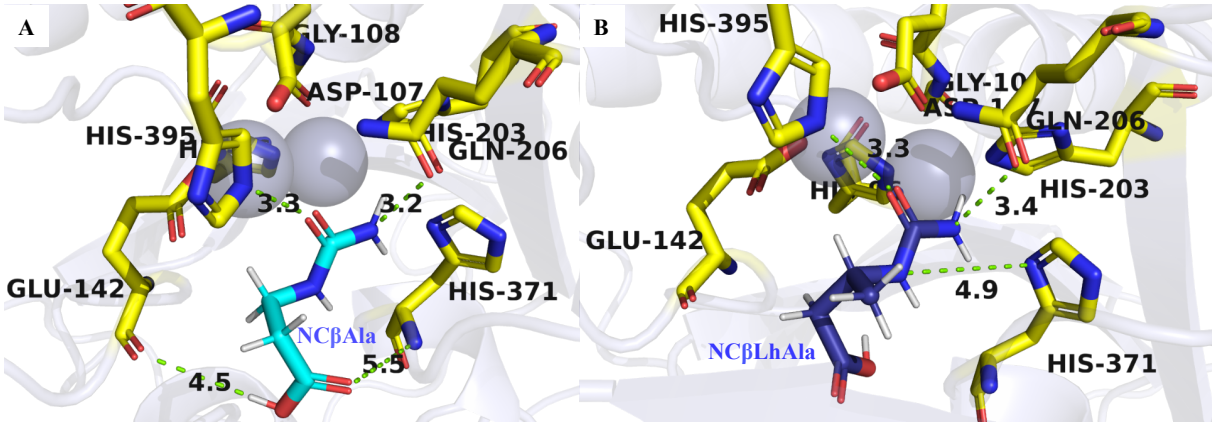

Figure 51: Dockings generated for model of Burk1.
A) Model of Burk1 with docked NCβAla B) Model of Burk1 with docked NCβLhAla. Highly conserved amino acid residues of the active site are highlighted in yellow. Nitrogen atoms highlighted in blue, oxygen atoms in red. Docking-models generated by ROSIE were edited with PyMol. Metal cofactor ions are shown as grey balls.

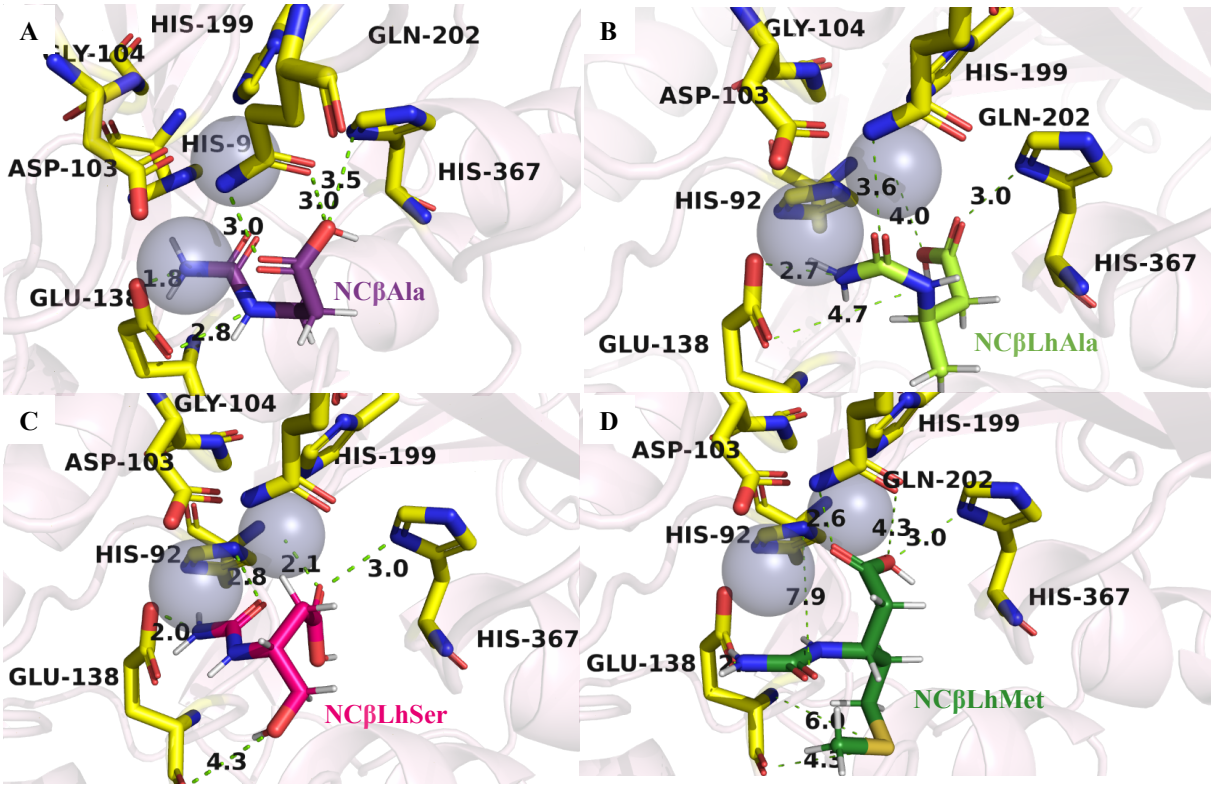

Figure 52: Dockings generated for model of P.aeru.
A) Model of P.aeru with docked NCβAla B) Model of P.aeru with docked NCβLhAla C) Model of P.aeru with docked NCβLhSer D) Model of P.aeru with docked NCβLhMet. Highly conserved amino acid residues of the active site are highlighted in yellow. Nitrogen atoms highlighted in blue, oxygen atoms in red. Docking-models generated by ROSIE were edited with PyMol. Metal cofactor ions are shown as grey balls.

The starting coordinates for P.aeru were generated through alignment with 2V8H. Figure 52 A shows the model of NCβAla with the lowest energy (I Δ -12.83) and thus was used as reference docking. The *N*-carbamoyl group of NCβAla was oriented towards the metal ions. The length of hydrogen bonds in a protein can be up to 3 Å. For the N-atoms of the *N*-

carbamoyl group low distances of 1.8 and 2.8 Å were measured to Glu-138. The oxygen of the *N*-carbamoyl group showed a distance of 3 Å to Gln-202. Furthermore a distance of 3 Å to Gln-202 and 3.5 Å to His-367 was found for the acid group of the substrate. For the docking of NCβLhAla a similar oriented model was selected (I Δ -9.57) but longer distances to Glu-138 and Gln-202 were found (Figure 52 B). For NCβLhSer only one model with the same orientation than NCβAla was identified (I Δ -10.18) (Figure 52 C). It possesses a distance of 2 Å from its N-atom of the *N*-carbamoyl group to Glu-138 and a shorter distance to His-92 for the oxygen of the *N*-carbamoyl group. In contrast to that no model of NCβLMet was identified with a similar orientation like NCβAla. Longer distances to His-92, Gln202 and His 367 were observed. The chosen model had an I Δ of -11.09.

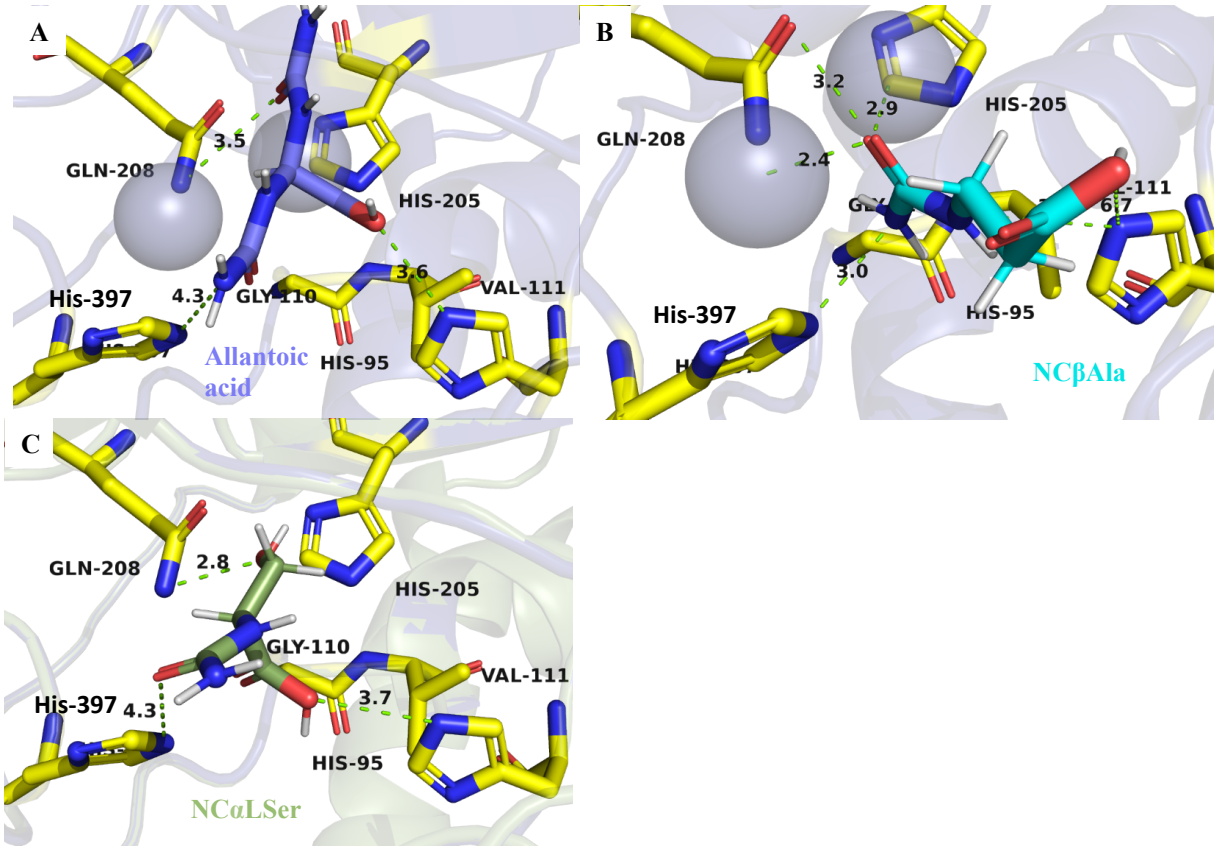

Figure 53: Dockings generated for Burk4.
A) Model of Burk4 with docked allantoic acid B) Model of Burk4 with docked NCβAla C) Model of Burk4 with docked NCαLSer. Highly conserved amino acid residues of the active site are highlighted in yellow. Nitrogen atoms highlighted in blue, oxygen atoms in red. Docking-models generated by ROSIE were edited with PyMol. Metal cofactor ions are shown as grey balls.

Coordinates for Burk4 were generated through alignment with 5I4M. Allantoic acid was set as reference docking (I Δ -9.76). Contacts of approximately 3-4 Å were found to His-397, Gln-208 and His-95. The most suiting model of NCβAla (I Δ -9.44) possessed shorter

distances to His-397 and Gln-208 and His-205. Whereby the acid group had higher distances to His-95. The carbamoyl group in the dockings of NCαLSer (I Δ -9.02) was oriented away from the metal ions. However distances of 2.8 Å for the acid group to Gln-208 and 3.7 Å of the OH-group of the residue to His-95 were measured. Also the Gly-110 residue is close. For all three substrates of Burk4 approximately the same conversion had been observed (20 % relative activity) in previous experiments (see 4.4.2.).

These performed docking experiments based on enzyme models by Phyre[2] may give an idea of residues involved in the catalytic mechanisms and possible intra-molecular interactions.

4.5 Decarbamoylating enzymes with 3D-tertiary structures

As described in section 1.5.2 there are several decarbamoylating enzymes known with *via* x-ray crystallography determined crystal structures. Four enzymes from each class of decarbamoylating enzymes were chosen: 1R3N (βUp from *L. kluyveri*), 1Z2L (AaHyd from E. coli K12), 1F06 (D-Carb from *R. radiobacter*) and 3N5F (L-Carb from *G. stearothermophilus*). Additionally the uncharacterized enzyme 5I4M, isolated from *Burkholderia vietnamiensis* was found through structural alignment studies. Due to its structural similarity to the other mentioned enzymes it was assumed that it might also exhibits a decarbamoylating activity. A comparison of all x-ray structures is given in Figure 54. So far for 5I4M only a crystal structure is known, but no biochemical data or proven enzyme activities are available yet. None of the other mentioned crystallized enzymes was ever investigated towards their conversion of other NCβAAs than NCβAla. This section deals with three questions: (1): Is a decarbamoylating enzyme from one enzyme class able to convert the natural substrates of another enzyme class? (2): Are these enzymes able to convert other NCβAAs than NCβAla? And (3): Can important amino acid residues which are responsible for the enzyme activity be identified through ligand-docking simulations and do these *in silico* studies reflect the results from *in vitro* experiments?

An overview on the activities found for these five enzymes towards aliphatic and aromatic NCβAAs in combination with *in silico* computational studies to investigate their functionality is given in this section. By using the ConSurf-Server (see section 3.2.6.5) highly conserved amino acids of each enzyme were identified and additional docking experiments gave an indication of preserved residues that are putatively important for the catalytic activity of the enzymes. Within this task several residues were identified for mutations using rational protein engineering.

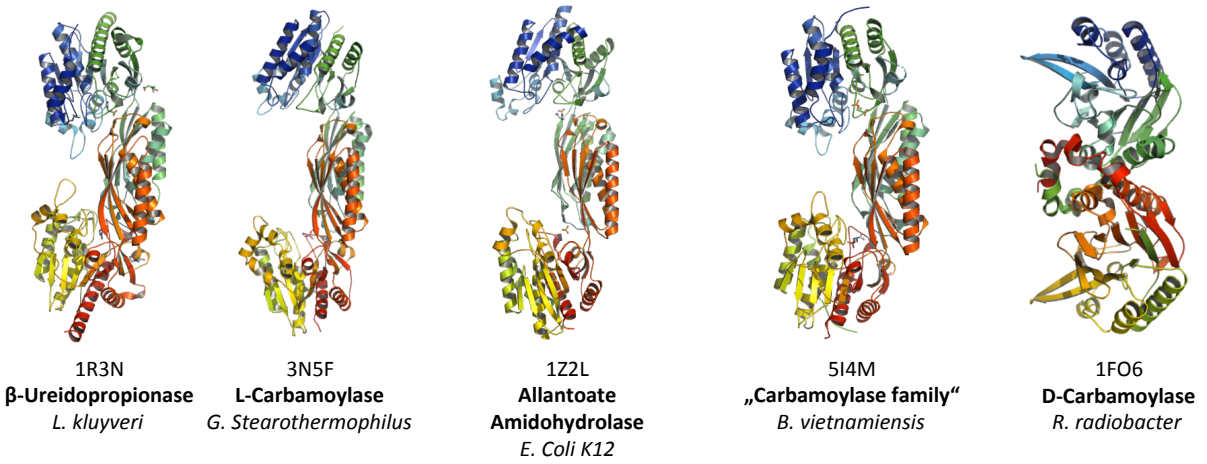

Figure 54: Homodimer comparison of 1R3N, 3N5F, 1Z2L, 5I4M and 1FO6.
Enzyme classifications were obtained from PDB-database. 1R3N, 3N5F, 1Z2L, 5I4M, 1FO6 = PDB identifier. Each homodimers consists of two identical monomers.

Table 51: Sequence alignment matrix of 1FO6, 1R3N, 5I4M, 1Z2L and 3N5F.
The amino acid sequence of each enzyme was compared to every other enzyme by conducting a multiple sequence alignment using Clustal Ω tool. Shown is the percentage identity.

	1FO6	**1R3N**	**5I4M**	**1Z2L**	**3N5F**
1FO6	100 %	46.04 %	49.61 %	47.99 %	46.65 %
1R3N	46.04 %	100 %	59.54 %	51.47 %	53.23 %
5I4M	49.61 %	59.54 %	100 %	53.80 %	58.56 %
1Z2L	47.99 %	51.47 %	53.8 %	100 %	58.9 %
3N5F	46.65 %	53.23 %	58.56 %	58.9 %	100 %

All five enzymes are homologues to each other and share a certain sequence similarity. In Table 51 enzymes are compared to each other regarding their percentage identity generated by Clustal Ω multiple sequence alignment of their amino acid sequence.

Genes of all proteins were ordered from Proteogenix in expression vector pET19 (Table 6, p. 49). In the first step enzymes 1R3N, 5I4M, 1Z2L, 3N5F and 1FO6 were transformed into *E. coli* BL21 DE3 cells and a suitable expression condition was determined for every enzyme (see Table 34, p. 70). Subsequently a purification method was established for each enzyme. Exemplary FLPC chromatograms and SDS-gels are shown in section 8.9.

Enzymes were investigated towards their stability and storing conditions using optimal enzyme activity conditions given in Table 35 (p. 72). Reactions were always conducted over night and 1000 rpm. 3N5F showed a 50 % and 1Z2L 13 % activity loss after been frozen at -20 °C and thawed again (without glycerine) in comparison to their activity directly after

purification. Also for 1FO6 a decrease of activity of 60 % (stored at -20°C) and 13 % (stored with glycerine at -80°C) was observed. Thus in further experiments 3N5F, 1Z2L and 1FO6 were directly used for enzyme reactions after FPLC purification. 1R3N and 5I4M exhibited the same activity after storage at -20 °C for 5 days. If already known from literature reactions of the various enzymes were performed at their respective optimal temperature and pH value. Thus the following conditions were applied: reactions with 1Z2L were incubated at 37 °C and pH 8 [182], with 3N5F at 65 °C and pH 7.5 [176] and with 1FO6 at 37 °C and a pH 7 [224]. Reactions with 5I4M were incubated at the optimal growth temperature of *B. vietnamiensis* (30 °C) and pH 7 since no information was known from literature (see also Table 35 p. 72). All activity studies were performed under the mentioned conditions over night and 1000 rpm. Reactions were stopped by denaturation at 95 °C for 5 min. All reactions were performed with 180 µl substrate solution and 20 µl previously purified enzyme of various concentrations. If needed metal cofactors with a final concentration of 2 mM were added to the reaction.

4.5.1 Evaluation of current classification

The enzyme 1R3N is classified as βUp and proven to convert NCβAla to βAla [233]. It was investigated whether enzymes that are not classified as βUps are also able to convert NCβAla. Other βUps are described to be able to convert some aliphatic proteinogenic NCαAAs like L-Carbs do [169]. In contrast to that for described L-Carbs and D-Carbs almost no information on their conversion of NCβAla is available. Moreover AaHyds like 1Z2L are only described to exhibit activity towards allantoic acid [182]. It has never been examined whether other chemical similar substrates are also accepted. Since AaHyds show a high structural homology to defined βUps and L-Carbs it was tested whether AaHyds are also able to convert NCβAla or NCαAAs to their corresponding amino acids. It was also investigated whether L-Carbs are able to convert NCβAla or allantoic acid.

Thus all enzymes (1R3N, 1Z2L, 5I4M, 1FO6, 3N5F) were investigated on the following substrates: allantoic acid to detect allantoate amidohydrolases activity, NCβAla to evaluate βUp activity, NCαLSer to examine the L-Carb activity. To investigate whether expressed enzymes possessed activity biotransformations with in literature described substrates were performed as control reactions. All enzymes were found to be active with these substrates under published conditions (see Table 53, p. 135). In each experiment a substrate with described activity was carried along as activity-control to exclude inactivity of the enzymes. Table 52 gives an overview of the described activities for each enzyme.

Table 52: Overview of described activities and cofactor dependencies for 5I4M, 1Z2L, 3N5F, 1FO6 and 2V8H.
Reactions with the named substrates were carried as activity controls to exclude an inactivity of the enzymes after FPLC purification.

Enzyme (PDB ID)	Enzyme class	Substrate with known activity	Cofactor dependency
5I4M	*Unknown*	*Unknown*	*Unknown*
1Z2L	AaHyd	Allantoic acid [182]	*Unknown*
3N5F	L-Carb	NCαLVal NCαLMet (and other NCαLAAs) [176]	$CoCl_2$ best
1FO6	D-Carb	NCαD-hydroxy-phenylglycine [156]	No
1R3N	βUp	NCβAla [233]	$ZnCl_2$

Table 53 (p. 135) shows all novel observed activities for the five enzymes in comparison to their already described activities.

Only for 5I4M no biochemical data are available e.g. concerning substrate spectra and reaction conditions. Activity tests with purified enzyme (1.9 µg/µl final concentration) revealed a conversion of NCβAla to βAla of approximately 100 % with or without cofactor $MnCl_2$. A lower degradation was observed towards allantoic acid of 41 % and 48 % with and without cofactor. Additional lysate experiments showed an almost full conversion of NCαLSer to αLSer when $MnCl_2$ was present. But also without cofactor 66 % αLSer were catalysed.

For 1Z2L only an activity towards allantoic acid is described. This was confirmed by 95 % degradation of allantoic acid with 0.2 µg/µl final enzyme concentration present in each reaction. With additional 2 mM $MnCl_2$ the degradation was similar (99%) but. 1Z2L was also found to convert NCβAla to βAla and NCαLSer to αLSer of 66 % and 55 % respectively when incubated with $MnCl_2$. Without cofactor only a conversion of 24 % NCβAla was detected.

The known activity of L-Carb 3N5F towards NCα-amino acids like NCα-L-Val or NCα-L-Met was confirmed (Table 59, p. 198) as well as the strong cofactor dependency towards Co^{2+}. Besides, an activity towards NCβAla and allantoic acid was detected. For these substrates also a higher conversion was achieved by adding $CoCl_2$ to the reaction. Thus about 90% βAla were formed and about 22 % allantoic acid where degraded by 3N5F.

The βUp 1R3N has a high affinity towards NCβAla and is supposed to be Zn^{2+} dependent. It was examined towards its conversion of several aliphatic and aromatic NCα-amino acids and

strong activities towards NCα-L-Met, NCα-L-Val, NCα-L-Cys, NCα-glycine (NCαGly) and NCα-ABA could be observed (Table 56, p. 196). 90 % of NCα-L-Ser were converted using enzyme lysate and $MnCl_2$ thereby 60 % α-L-Ser could be produced. Aromatic non-canonical NCα-amino acids were not converted. Only a slight activity towards the canonical NCα-phenylalanine was observed (Table 56, p. 196). It was also found that that Zn^{2+} decreased the enzyme activity in contrast to $Ni^{2+,}$ Co^{2+} or Mn^{2+}. The enzyme activity was found to be enhanced most using $MnCl_2$ as cofactor. Additionally this enzyme possesses a slight activity towards allantoic acid (35 %) but $MnCl_2$ did not increase the degradation of allantoic acid.

1FO6 is described as a D-Carb exhibiting no cofactor dependency. Its activity known from literature was validated by the conversion of NCα-D-hydroxy-phenylglycine whereby almost 100 % D-hydroxy-phenylglycine was formed (Table 58, p.197). Also non-canonical α-D-tryptophan could be generated in a high ratio, whereby a higher amount of product was obtained without cofactor. In contrast to that only a slight activity of 18 % degradation towards aliphatic NCα-D-Ser to α-D-Ser was observed without cofactor. Furthermore a slight conversion of 33 % allantoic acid was observed for 1FO6 without cofactor but only 17 % with cofactor. A reaction using enzyme lysate showed no degradation of NCβAla.

Table 53: Evaluation of classification of 2V8H, 5I4M, 3N5F, 1Z2L and 1FO6 (PDB).
All reactions were conducted using lysate (L) or 1 µg/µl indicated enzyme concentration (E). Used reaction temperature was different depending on the enzyme (see Table 35, p. 72) and 1000 rpm for 20 h. All substrate degradations and product formations were calculated in relation to detected amount of substrate in substrate controls. Con. [%] Substrate = Amount of converted substrate in %. Form. [%] Product = detected formed product. Without cofactor = Amount of converted substrate / formation of product without additional cofactor; $MnCl_2$ or $CoCl_2$ = Amount of converted substrate / formation of product with 2 mM $MnCl_2$ or $CoCl_2$ used as cofactor. NCβAla = *N*-carbamoyl-β-alanine; βAla = β-alanine; NCα-L-Ser = *N*-carbamoyl-α-L-Ser; α-L-Ser = α-L-Ser; NCα-D-Ser = *N*-carbamoyl-α-D-Ser; α-D-Ser = α-D-Ser; NCα-D-p-H-PheGly = *N*-carbamoyl-α-D-para-hydroxy-phenylglycine; α-D-p-H-PheGly = α-D-para-hydroxy-phenylglycine.

70-100% | 40-70% | 20-40% | 0.1-20 % | 0 % | *n.d.* (not determined)

Substrate	Product	1R3N		5I4M		3N5F		1Z2L		1FO6	
		Con. [%] Substrate	Form. [%] Product	Con. [%] Substrate	Form. [%] Product	Con. [%] Substrate	Form. [%] Product	Con. [%] Substrate	Form. [%] Product	Con. [%] Substrate	Form. [%] Product
NCβAla 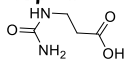	**βAla** 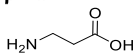	**E (0.64 µg/µl) Without cofactor**		**E (1.9 µg/µl) Without cofactor**		**E (0.9 µg/µl) Without cofactor**		**E (0.22 µg/µl) Without cofactor**		**L Without cofactor**	
		100	86.3 ± 5.6	100	97.6 ± 0.3	9.2 ± 1.2	5.6 ± 0.6	24.0 ± 3.7	29.6 ± 0.2	0	0
		$MnCl_2$		**$MnCl_2$**		**$CoCl_2$**		**$MnCl_2$**			
		100	90.3 ± 5.5	100	98.5 ± 0.5	96.6 ± 1.2	90.9 ± 0.1	66.9 ± 2.7	63.9 ± 3.4	0	0
Allantoic acid 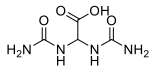	-	**E (0.64 µg/µl) Without cofactor**		**E (1.9 µg/µl) Without cofactor**		**E (0.37 µg/µl) Without cofactor**		**E (0.22 µg/µl) Without cofactor**		**E (4.9 µg/µl) Without cofactor**	
		35.3 ± 2.5	*n.d.*	48.9 ± 1.6	*n.d.*	16.3 ± 3.8	*n.d.*	95.8 ± 3.6	*n.d.*	33.9 ± 1.3	*n.d.*
		$MnCl_2$		**$MnCl_2$**		**$CoCl_2$**		**$MnCl_2$**			
		32.0 ± 2.2	*n.d.*	41.3 ± 4.2	*n.d.*	22.9 ± 4.6	*n.d.*	99.0 ± 4.0	*n.d.*	17.6 ± 0.6	*n.d.*
NCα-L-Ser 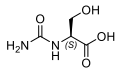	**α-L-Ser** 	**L Without cofactor**		**L Without cofactor**		**E (0.37 µg/µl) Without cofactor**		**E (0.22 µg/µl) Without cofactor**			
		50.4 ± 0.2	23.5 ± 0.1	72.8 ± 0.4	66.2 ± 0.5	0	0	0	0	*n.d.*	*n.d.*
		$MnCl_2$		**$MnCl_2$**		**$CoCl_2$**		**$MnCl_2$**			
		90 ± 0.5	61.3 ± 0.2	96.7 ± 0.8	99.8 ± 0.6	100	100	55.4 ± 5.9	43.1 ± 1.8	*n.d.*	*n.d.*
NCα-D-Ser 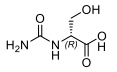	**α-D-Ser** 									**E (4.9 µg/µl) Without cofactor**	
		n.d.	*n.d.*	*n.d.*	*n.d.*	*n.d.*	*n.d.*	*n.d.*	*n.d.*	18.1 ± 6.6	21.5 ± 0.5
										$CoCl_2$	
		n.d.	*n.d.*	*n.d.*	*n.d.*	*n.d.*	*n.d.*	*n.d.*	*n.d.*	18.0 ± 5.6	20.1 ± 0.6
NCα-D-p-H-PheGly 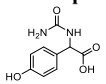	**α-D-p-H-PheGly** 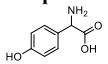									**Without cofactor**	
		n.d.	*n.d.*	*n.d.*	*n.d.*	*n.d.*	*n.d.*	*n.d.*	*n.d.*	100	100
										$CoCl_2$	
		n.d.	*n.d.*	*n.d.*	*n.d.*	*n.d.*	*n.d.*	*n.d.*	*n.d.*	100	100

4.5.2 Activity towards aliphatic *N*-carbamoyl-β-homo-amino acids

All five enzymes (1R3N, 5I4M, 1Z2L, 1FO6 and 3N5F) were compared to each other towards their conversion of aliphatic NCβhAAs. Therefor three substrates with different residue sizes and polarity were tested: unpolar NCβhAla quite similar to the natural substrate NCβAla of βUps, polar NCβhSer for which activity has already been observed for the newly found decarbamoylating enzymes and unpolar NCβhMet, which possesses a slightly bigger residue size, but also incorporates a hetero atom. Additionally conversion of NCβPhe and NCβTyr was tested for some of the enzymes. In general no thermal or cofactor influenced substrate degradation was observed in substrate controls. However slight product degradation was often observed in product controls. A summary of all results is given in Table 54 (p. 138).

5I4M shows a significant degradation of NCβLhAla and NCβhSer of 14 % and 21 % respectively and approximately the same amount was converted into product without cofactor. Addition of $MnCl_2$ increased the degradation of NCβLhAla to 25 % whereby 18 % product formation was detected. For NCβLhMet a degradation of 6 % without cofactor was observed, but only 2 % product of βLhMet was detected. With $MnCl_2$ being present in the reaction a substrate conversion of 16 % to 4 % βLhMet was measured.

The AaHyd 1Z2L is able to degrade approximately 100 % of allantoic acid with an enzyme concentration of 0.2 µg/µl also showed activity towards all aliphatic NCβhAAs. However only product formation for βLhSer was detected when $MnCl_2$ was present. Also substrate degradations of NCβLhAla (6.6 %) and NCβLhMet (13 %) were observed but no product was measured even though no product degradation was observed in product controls.

According to literature L-Carb 3N5F usually shows a much higher activity when $CoCl_2$ is present. In contrast to this a high degradation of NCβLhSer was detected without cofactor (48 %) and approximately the same amount of product was generated at a final enzyme concentration of 2.5 µg/µl. Also for degradation of NCβLhAla a slightly higher product amount was formed without cofactor (63 %) than with $CoCl_2$ present (56 %). For NCβLhMet no significant degradation was observed.

Similar activities towards degradation of aliphatic NCβhAAs were observed for βUp 1R3N. A cofactor independent conversion of NCβAla had been shown already. A higher enzyme activity towards NCβhAAs was observed without additional cofactor. NCβLhAla and NCβLhSer were converted in a similar amount using 0.6 µg/µl final enzyme concentration. However a much higher product concentration was detected for βLhSer of up to 26 %

compared to 15 % of βLhAla. In contrast to that of 16 % degraded NCβLhMet only 4.4 % βLhMet were detected. Furthermore no product degradation for βLhAAs was observed in product controls.

Additionally the influence of different bivalent metal ions on the conversion of NCβhAAs was investigated in more detail for 2V8H. Therefor reactions with 0.6 µg/µl final enzyme concentration and 2 mM final concentration of $CoCl_2$, $MnCl_2$, $ZnCl_2$ or $NiCl_2$ were performed. The highest amount of βLhAla was detected using $NiCl_2$ as cofactor. The production of βLhSer was not increased *via* cofactor addition. It was found that the presence of $ZnCl_2$ led to lowest detected substrate degradations and product concentrations of the corresponding amino acid. $MnCl_2$ and $CoCl_2$ did not show an increase on the enzyme activity (data not shown).

Since 1FO6 is a D-Carb the corresponding D-enantiomers of aliphatic NCβhAAs were used in the enzyme reactions with a final 1FO6 concentration of 0.9 µg/µl. However, no D-enantiomer of NCβhMet was available in this work. The enzyme, which is known to be cofactor independent with regard to its catalysis, exhibited a degradation of 59 % NCβhDSer without cofactor but only 50 % of βhDSer were detected in HPLC. The conversion of NCβhDAla was higher with up to 65 % without cofactor and a slightly lower amount of 57 % βhDAla was measured. In general the degradation was not increased by addition of cofactors, sometimes even an inhibiting effect was assumed. Slight product degradation was detected for βhDAla and βhDSer.

For none of the enzymes an activity towards aromatic NCβAAs was observed.

Table 54: Substrate scope of 2V8H, 5I4M, 3N5F, 1Z2L and 1FO6 towards *N*-carbamoyl-β-(homo)-amino acids.

All reactions were conducted using lysate (L) or indicated enzyme concentration (E). Used reaction temperature was different depending on the enzyme (see Table 35, p. 72) and 1000 rpm for 20 h. All substrate degradations and product formations were calculated in relation to detected amount of substrate in substrate controls. Con. [%] Substrate = Amount of converted substrate in %. Form. [%] Product = detected formed product. Without cofactor = Amount of converted substrate / formation of product without additional cofactor; $MnCl_2$ or $CoCl_2$ or $NiCl_2$ or $ZnCl_2$ = Amount of converted substrate / formation of product with 2 mM $MnCl_2$ or $CoCl_2$ or $NiCl_2$ or $ZnCl_2$ used as cofactor.

70-100%	40-70%	20-40%	0.1-20 %	0 %	*n.d. (not determined)*

Substrate	Product	2V8H		5I4M		3N5F		1Z2L		1FO6	
		Con. [%] Substrate	Form. [%] Product	Con. [%] Substrate	Form. [%] Product	Con. [%] Substrate	Form. [%] Product	Con. [%] Substrate	Form. [%] Product	Con. [%] Substrate	Form. [%] Product
Aliphatic											
NCβAla 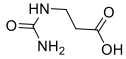	**βAla** 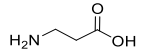	**E (0.64 µg/µl) Without cofactor**		**E (1.9 µg/µl) Without cofactor**		**E (0.9 µg/µl) Without cofactor**		**E (0.22 µg/µl) Without cofactor**		**E (55 µg/µl) Without cofactor**	
		100	86.3 ± 6.1	100	97.6 ± 0.3	9.2 ± 1.2	5.6 ± 0.6	24.0 ± 3.7	29.6 ± 0.2	0	0
		$MnCl_2$				**$CoCl_2$**				**$CoCl_2$**	
		100	90.3 ± 5.5	100	98.5 ± 0.5	96.6 ± 1.2	90.9 ± 0.1	66.9 ± 2.7	63.9 ± 3.4	0	0
NCβ-L-hAla 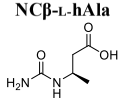	**β-L-hAla** 	**E (0.64 µg/µl) Without cofactor**		**E (1.9 µg/µl) Without cofactor**		**E (2.5 µg/µl) Without cofactor**		**E (0.22 µg/µl) Without cofactor**			
		59.3 ± 0.5	15.8 ± 0.8	14.1 ± 3.7	18.9 ± 0.4	63.3 ± 0.7	56.2 ± 0.0	0	0	*n.d.*	*n.d.*
		$MnCl_2$		**$MnCl_2$**		**$CoCl_2$**		**$MnCl_2$**			
		48.7 ± 3.5	11.7 ± 0.3	25.7 ± 4.0	17.7 ± 0.2	60.6 ± 0.8	51.1 ± 0.4	6.6 ± 1.3	0	*n.d.*	*n.d.*
NCβ-D-hAla 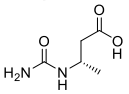	**β-D-hAla** 									**E (0.9 µg/µl) Without cofactor**	
		n.d.	*n.d.*	*n.d.*	*n.d.*	*n.d.*	*n.d.*	*n.d.*	*n.d.*	64.9 ± 5.0	57.4 ± 0.6
										$CoCl_2$	
		n.d.	*n.d.*	*n.d.*	*n.d.*	*n.d.*	*n.d.*	*n.d.*	*n.d.*	59.7 ± 6.5	45.4 ± 1.5
NCβ-L-hSer 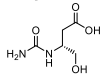	**β-L-hSer** 	**E (0.64 µg/µl) Without cofactor**		**E (1.9 µg/µl) Without cofactor**		**E (2.5 µg/µl) Without cofactor**		**E (0.22 µg/µl) Without cofactor**		**Without cofactor**	
		57.6 ± 1.2	26.8 ± 1.2	21.5 ± 3.6	12.3 ± 0.2	48.9 ± 1.6	48 ± 0.6	6.5 ± 2.7	0	*n.d.*	*n.d.*
		$MnCl_2$		**$MnCl_2$**		**$CoCl_2$**		**$MnCl_2$**			
		54.5 ± 1.5	20.5 ± 4.1	20.6 ± 3.5	12.0 ± 0.3	64.3 ± 0.7	28.2 ± 0.1	14.9 ± 4.9	11.8 ± 1.3	*n.d.*	*n.d.*
NCβ-D-hSer 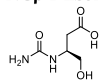	**β-D-hSer** 									**E (0.9 µg/µl) Without cofactor**	
		n.d.	*n.d.*	*n.d.*	*n.d.*	*n.d.*	*n.d.*	*n.d.*	*n.d.*	59.2 ± 3.8	50.0 ± 2.1
										$CoCl_2$	
		n.d.	*n.d.*	*n.d.*	*n.d.*	*n.d.*	*n.d.*	*n.d.*	*n.d.*	60.05 ± 0.2	47.5 ± 1.7
NCβ-L-hMet 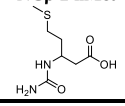	**β-L-hMet** 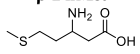	**E (0.64 µg/µl) Without cofactor**		**E (1.9 µg/µl) Without cofactor**		**E (2.5 µg/µl) Without cofactor**		**E (0.22 µg/µl) Without cofactor**			
		11.2 ± 3.9	0.2 ± 0.1	6.6 ± 5.7	1.7± 1.3	1.1 ± 8.4	5.2 ± 1.2	0	0	*n.d.*	*n.d.*
		$MnCl_2$		**$MnCl_2$**		**$CoCl_2$**		**$MnCl_2$**			
		4.7 ± 4.1	0.4 ± 0.6	16.2 ± 3.5	4.4 ± 0.6	1.6 ± 4.8	0.5 ± 0.4	13.0 ± 1.0	0	*n.d.*	*n.d.*
Aromatic											
NCβ-*rac*-PheAla 	**β-*rac*-PheAla** 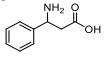	**L Without cofactor**				**L Without cofactor**				**E (1.3 µg/µl) Without cofactor**	
		0	0	*n.d.*	*n.d.*	0	0	*n.d.*	*n.d.*	0	0
		$MnCl_2$/$CoCl_2$/$NiCl_2$/$ZnCl_2$				**$CoCl_2$**				**$ZnCl_2$**	
		0	0	*n.d.*	*n.d.*	0	0	*n.d.*	*n.d.*	0	0
NCβ-*rac*-Tyr 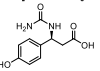	**β-*rac*-Tyr** 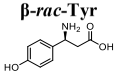									**Without cofactor**	
		n.d.	*n.d.*	*n.d.*	*n.d.*	*n.d.*	*n.d.*	*n.d.*	*n.d.*	0	0
										$ZnCl_2$	
		n.d.	*n.d.*	*n.d.*	*n.d.*	*n.d.*	*n.d.*	*n.d.*	*n.d.*	0	0

4.5.3 Docking experiments with ROSIE

In the protein data bank x-ray crystal structures of 1R3N and 1Z2L with co-crystallized substrate molecule are available. 2V8H is the structure of 1R3N with bound NCβAla. In the following section the PDB code 2V8H will be used. The structure of 5I4M harvests a 3-phosoglyceric acid molecule in its active site. Thus starting coordinates can be obtained from these coordinated molecules in their active site. Since 2V8H and 3N5F share a high sequence and structure similarity starting coordinates were generated through transfer of the NCβAla molecule of 2V8H to 3N5F (see section 3.2.6.3). Starting coordinates for docking experiments of enzyme 1FO6 were generated by transfer of NCα-D-Met from 1UF5 to structure 1FO6. Several docking experiments shall be spotlighted in this section that give an idea of how substrates may be located in the active centre of the enzymes and how this may influences their activity especially towards conversion of NCβ-amino acids. It was investigated whether these *in silico* enzyme-ligand dockings reflect the results gained from *in vitro* experiments. In contrast to dockings performed with generated models of Burk1-5, P.oleo and P.aeru these dockings are way more significant since an official x-ray structure is available. The crystal structures were visualized and edited with PyMol. For all enzymes highly conserved amino acid residues were determined with ConSurf server. Thus Table 55 was generated that gives an overview of the highly conserved residues (> 80 %) of each enzyme.

Table 55: Highly conserved residues determined with ConSurf-Server.
2V8H, 1Z2L, 3N5F, 5I4M, 1FO6 = PDB code.

2V8H	1Z2L	3N5F	5I4M	1FO6
62 R	31 R	79 H	44 R	11 G
70 D	59 D	81 D	94 G	25 R
74 R	62 G	87 G	95 S	45 E
91 D	81 G	90 D	96 G	52 F
94 G	82 S	91 G	98 D	72 P
112 G	83 H	125 E	100 Q	79 L
113 S	85 D	187 E	104 G	96 E
114 H	86 T	189 H	107 D	108 N
116 D	87 V	191 E	108 G	125 K
117 T	91 G	192 Q	109 I	127 H
118 Q	93 L	204 G	110 Y	129 P
121 A	94 D	221 G	111 G	130 G
122 G	95 G	225 H	118 V	144 E
122 G	98 G	227 G	142 E	148 F
125 D	102 A	234 R	146 F	170 C
125 D	128 E		148 P	172 D
126 G	129 E		201 E	173 R
129 G	190 E		203 H	174 R
135 E	192 H		204 I	175 W
159 A	194 E		205 E	177 E
160 E	195 Q		206 Q	180 R
160 E	199 L		210 L	193 G
161 G	207 G		235 G	225 N
163 R	224 G		241 G	234 K
223 E	228 H		248 R	236 G
224 E	230 G		301 R	238 E
226H	237 R		371 H	252 P
226 H	239 D		372 D	254 G
227 E	267 G		392 G	265 D
228 E	279 V		395 H	
229 Q	290 R		399 E	
230 P	358 A			
233 L	360 H			
241 G	361 D			
242 V	375 F			
258 G	381 G			
258 G	383 S			
262 H	384 H			
262 H	228 H			
264 G	230 G			
270 R	237 R			
271 R	239 D			
299 G	267 G			
322 R	279 V			
367 F	290 R			
397 H	358 A			
398 D	360 H			
410 M	361 D			
418 G	375 F			
420 S	381 G			
421 H	383 S			
421 H	384 H			
425 E				

Out of the five examined enzymes 2V8H was the most studied enzyme in this work. For all in *vitro* tested substrates an additional ligand docking was performed. In 2V8H NCβAla is bound thus the enzyme is present in its closed conformation. *In silico* ligand dockings were assessed through their energy scores interface delta ($I\Delta$) and total score (see section 3.2.6.4). In each docking run 500 energy models were generated for one substrate. Only the top 10 models with the lowest energies obtained from each substrate docking were used for further analysis. For each docking run the average energy scores of the top 10 models were calculated.

Ligand dockings for 2V8H are visualized in Figure 55 A. As reference docking energy scores obtained from an additional NCβAla docking were used. Regarding the average energy scores of the ligand docking experiments a trend emerged for docked substrates of 2V8H. Substrates with no or low observed activity tended to have a higher energy and thus a worse fit in the active centre of 2V8H. NCαGly and NCαLSer as well as NCβhLSer (for which a good activity had been detected in biotransformation studies) the energy scores are similar to those of the natural substrate NCβAla. Energy scores for substrates with less conversion like NCβhLMet and NCαLLeu possessed way higher interface scores. For aromatic NCβPhe no activity had been observed *in vitro* and *in silico* higher interface delta and total scores were obtained than for all other docked substrates of 2V8H.

The AaHyd 1Z2L is the sole enzyme with a high activity towards the conversion of allantoic acid. Thus energy scores obtained from an additional docking of allantoic acid were used as reference. Since the tertiary structure is available with co-crystallized allantoic acid the enzyme represents the closed conformation. NCβAla, NCβhLAla, NCβhLSer and NCβhLMet with lower detected conversions compared to the conversion of allantoic acid energy scores possess a higher total or interface delta score compared to scores of allantoic acid (Figure 55 B).

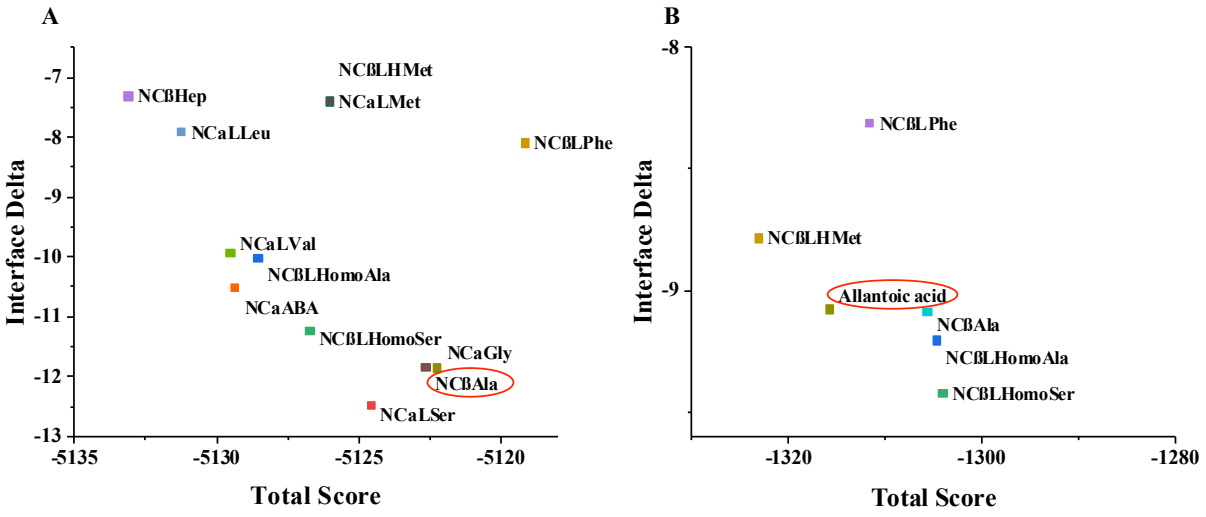

Figure 55: Determined energy scores for docked substrates for 2V8H and 1Z2L.
Each data point was obtained through generating 500 models of each substrate docking. Of these 500 models the top 10 models were used to calculate average interface delta and total scores. Substrates for which a high turnover was detected *in vitro* tend to show similar energy scores in comparison to the reference docking with their natural substrate *in silico*. Other substrates with lower or no detected turnover in vitro show higher energy score in comparison to the reference docking with their natural substrate *in silico*. A) Average energy scores of substrates docked into 2V8H. Reference substrate NCβAla is circled in red. B) Average energy scores of substrates docked into 1Z2L. The reference substrate allantoic acid is circled in red.

A closer look into generated dockings for 2V8H for substrates of different activities is given in Figure 56. Although NCβAla is already incorporated in the PDB-structure of 2V8H it was also docked with the same coordinates (x = 27.611; y = 14.253; z = 40.865) as the other ligands to obtain reference energy score values. All further dockings with other substrates were oriented in the same way like NCβAla (Figure 56 A). In this case the *N*-carbamoyl group faced towards the metal ion molecules. The acid group in turn is oriented in the opposite direction. Distances to the catalysing amino acid residues Arg-322, Asn-309, His-262, Gly-396, Gln-229 and His-397 known from literature were determined. They had lengths between 2.1 and 3.2 Å. The lowest energy model of NCβAla (I Δ -13.4) is similar oriented as in the original crystal structure. The comparison is shown in Figure 56 B. In Figure 56C the docked model of NCβLhSer (I Δ -10.9) was oriented similar to NCβAla and thus its *N*-carbamoyl and acid group possessed similar distances to Arg-322 and Gln-229. The OH-group of the serine residue was oriented towards Gly-396. The same orientation was observed for docked NCβLhMet (I Δ -8.84) but the methionine residue possessed a higher distance to Gly-396 and His-397. Energy scores for docking of NCβPhe were higher with an average I Δ of -8.1. One opportunity for docking of NCβPhe was an orientation similar to NCβAla but thus the ligand was shifted in the active site compared to NCβAla (Figure 56 E). The phenyl residue faced towards His-397 and Gly-396. Another opportunity was that the *N*-carbamoyl residue stayed approximately at the same place but then the acid group was found to be oriented in a complete other direction with a big distance to Arg-322. Under these conditions the phenyl residue was oriented to Arg-322 (Figure 56 F).

Since no information about the active site is reported for 5I4M it was proposed by analysing the conversed residues generated with ConSurf (Table 55 p. 140). NCβAla was docked using coordinates of co-crystallized 3-phosphoglycerid acid (x = 6.415; y = 9.479; x = 19.824). NCβAla (I Δ -14.9) was coordinated by Gln-206, His-371 and Arg-301 (Figure 57 A). The *N*-carbamoyl group was coordinated by Gln-206 and His-371 and the acid group was coordinated by Arg-301. These findings are similar to substrate coordination of 2V8H. In the docking of NCβLhMet (Figure 57 B) the molecule is oriented in a similar direction compared to NCβAla. His-371 may coordinates the methionine residue. However, a distance of 4.2 Å of the methionine residue to His-371 was determined. The I Δ -9.48 correlates to the lower activity observed towards NCβLhMet. The docking of NCβPhe (I Δ -12.25) shows a similar orientation of the *N*-carbamoyl group but higher distances were measured (~ 5 Å) (Figure 57

C). The acid group in turn faces into the opposite direction. The phenyl residue is oriented towards Arg-301.

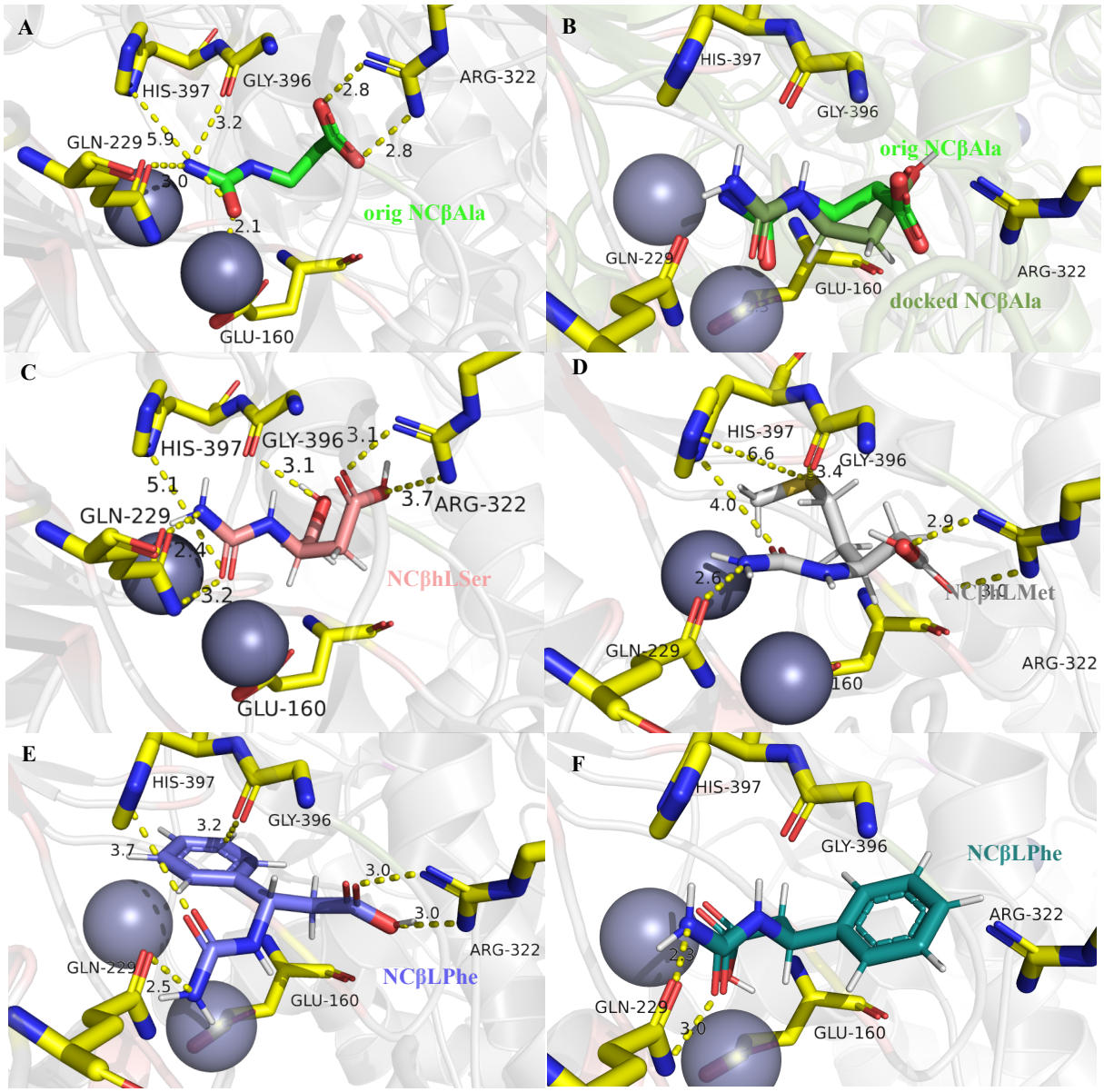

Figure 56: Dockings generated for 2V8H.
A) Orientation of the original co-crystallized NCβAla molecule of 2V8H. B) Comparison of the original NCβAla molecule (light green) with the best docking model of NCβAla (dark green). C) Docking of NCβhLSer with similar orientation to NCβAla reference. D) Docking of NCβhLMet with similar orientation to NCβAla reference. E) Option one for docking of NCβLPhe with similar orientation to NCβAla reference. F) Option two for docking of NCβLPhe with similar orientation of the *N*-carbamoyl group compared to NCβAla reference. Highly conserved amino acid residues of the active site are highlighted in yellow. Nitrogen atoms highlighted in blue, oxygen atoms in red. Docking-models generated by ROSIE were edited with PyMol. Metal cofactor ions are shown as grey balls.

Coordinates for docking NCβAla (I Δ -11.62) into 3N5F were generated by structural alignment with 2V8H (x = 26.388; y = 14.248; z = 40.316). Residues of the active site reported from literature were not found close to the active centre determined through docking of NCβAla reference (Arg-286, His225, Asn 273). The oxygen of the *N*-carbamoyl group of NCβAla showed a distance of 2.8 Å to Gln-192 (Figure 58 A, p. 146). Docking of NCβhLSer (I Δ -11.94) resulted in longer distances to Gln-192 but a shorter distance to Glu-125 (Figure 58 B). A docking of NCβPhe led to no generation of models. These findings are in accordance with *in vitro* observations with no detectable activity for NCβPhe.

The docking of allantoic acid into the active site of 1Z2L (x = 61.486; y = 32.453; z = 22.665) led to a slightly different orientation of allantoic acid (I Δ -8.71). Instead of a coordination of the acid group by His-384 (as reported from literature) a shorter distance was measured to Arg-290 (Figure 59 A, p. 146). For Gln-195 and Arg-217 longer distances to allantoic acid were measured. The docking of NCβLhMet (I Δ -8.71) showed a similar orientation than the original position of allantoic acid with lower distances (Figure 59 B). Even if both substrates show a similar I Δ value the interface score was more positive for NCβLhMet reflecting the lower degradation compared to allantoic acid. The average I Δ values were lower for allantoic acid than for the docked substrates.

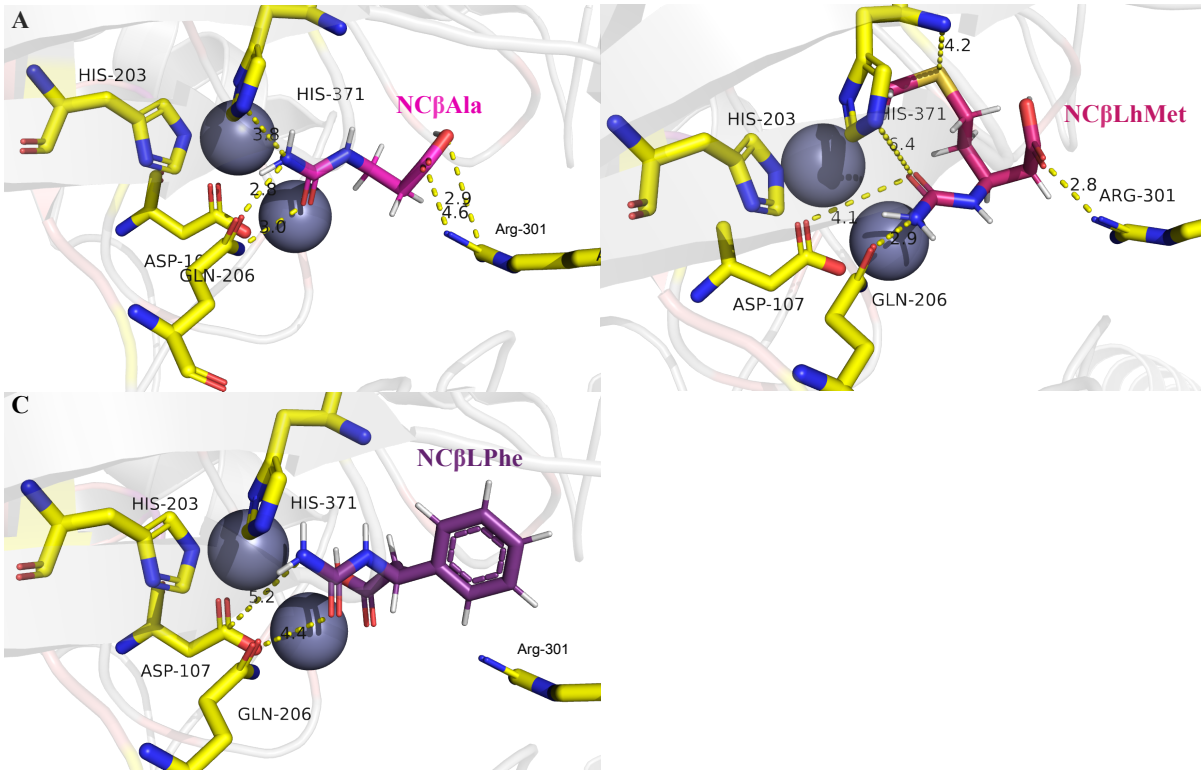

Figure 57: Dockings generated for 5I4M.
A) Reference docking with NCβAla. B) Docking of NCβLhMet C) Docking of NCβPhe. Highly conserved amino acid residues of the active site are highlighted in yellow. Nitrogen atoms highlighted in blue, oxygen atoms in red. Docking-models generated by ROSIE were edited with PyMol. Metal cofactor ions are shown as grey balls.

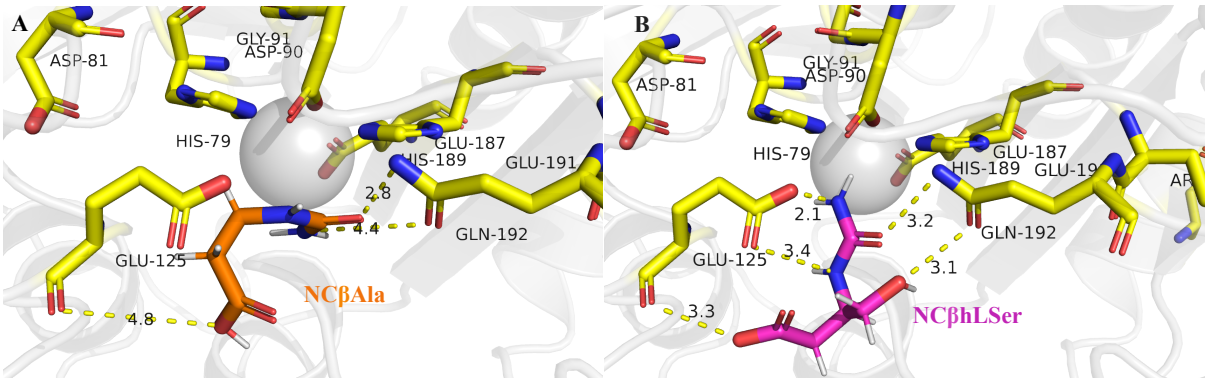

Figure 58: Dockings generated for 3N5F.
Highly conserved residues were obtained through ConSurf A) Docking of NCβAla B) Docking of NCβhLSer. Highly conserved amino acid residues of the active site are highlighted in yellow. Nitrogen atoms highlighted in blue, oxygen atoms in red. Docking-models generated by ROSIE were edited with PyMol. Metal cofactor ions are shown as grey balls.

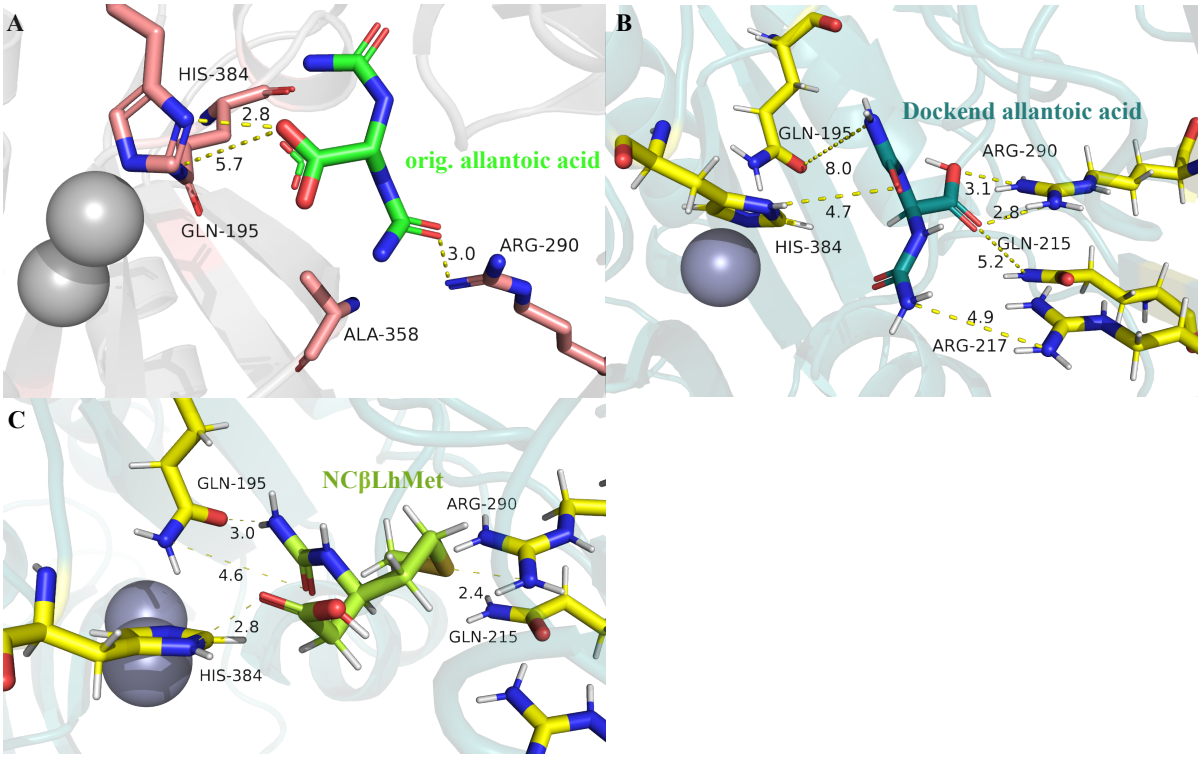

Figure 59: Dockings generated for 1Z2L.
A) Original orientation of allantoic acid in the structure. B) Control reference docking of allantoic acid. C) Docking of NCβLhMet with partly similar orientation to reference. Highly conserved amino acid residues of the active site are highlighted in yellow. Nitrogen atoms highlighted in blue, oxygen atoms in red. Docking-models generated by ROSIE were edited with PyMol. Metal cofactor ions are shown as grey balls.

No co-crystallized ligand was bound in the original tertiary structure of 1FO6. Thus coordinates were obtained from structural alignment with 1UF5 (x = 7.501; y = 18.173; z = 18.777) and transfer of the co-crystallized substrate NCαDMet of 1UF5. Because of the known activity towards *N*-carbamoyl-α-D-hydroxy-phenylglycine (NCαDhydPheGly) this substrate was docked as reference (I Δ -13.75). The closest distances were found to Glu-146 and His-144 (Figure 60 A). Distance of the acid group to Cys-172 was longer with 6.2 Å. In the docking of NCβDhSer (I Δ -15.05) a lower distance to Cys-172 was measured (Figure 60 B). The *N*-carbamoyl group was found to be oriented towards His-144 with 3 Å distance. The determined energy scores of NCβDhSer with lower values than for NCαDhydPheGly do not correspond to the observed activities of these substrates. NCβPhe was oriented slightly different. The *N*-carbamoyl group was closer to Cys-172 whereby the acid group was faced towards His-144 (Figure 60 C) (I Δ -8.71).

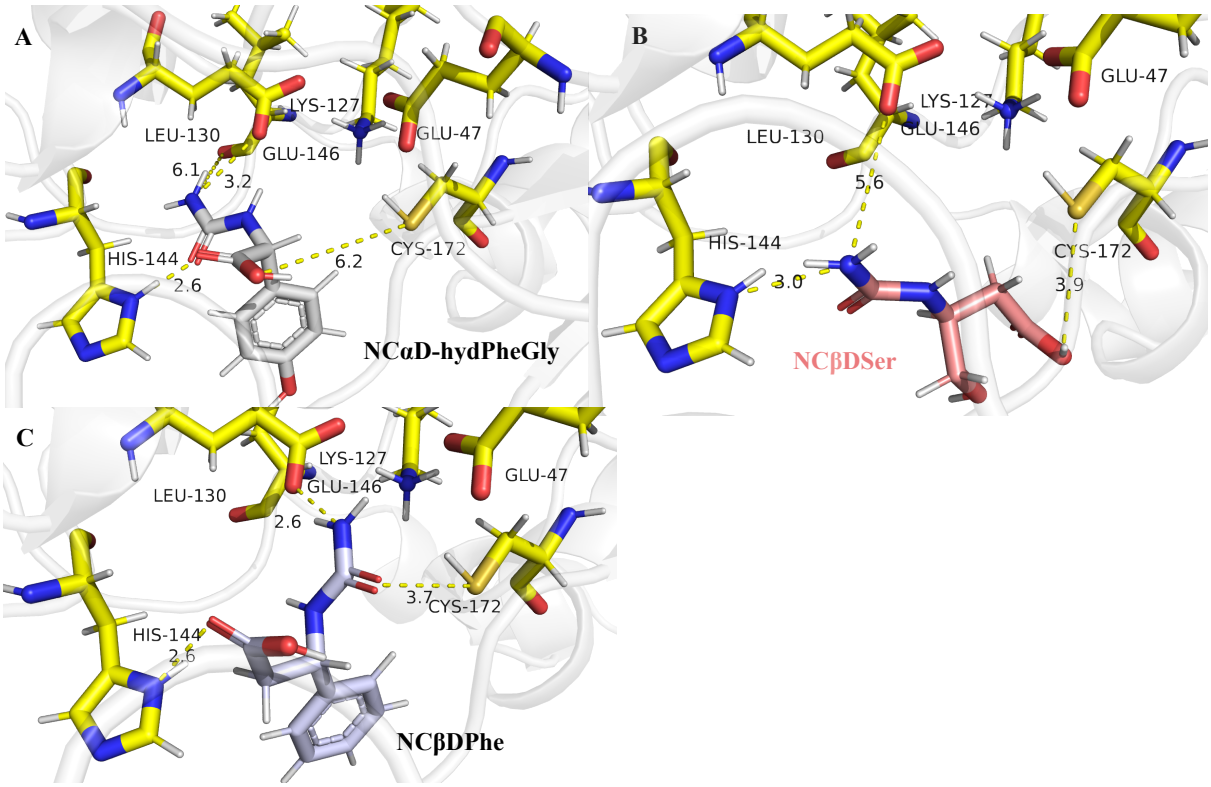

Figure 60: Dockings generated for 1FO6.
A) Docking of NCαDhydPheGly as reference B) Docking of NCβDhSer C) Docking of NCβDPhe. Highly conserved amino acid residues of the active site are highlighted in yellow. Nitrogen atoms highlighted in blue, oxygen atoms in red.

4.5.4 Rational Protein Engineering

Since enzymes 2V8H, 3N5F 1Z2L and 5I4M showed degradation of NCLβHSer but only a low activity towards NCLβHMet several approaches of rational protein engineering were carried out to enhance the activity towards NCLβHMet. Two residues for 2V8H and three residues of 5I4M were selected for a rational protein engineering approach (Figure 61, p. 148). The selected residues are located close to the active site but are not highly conserved. To investigate their influence on enzyme activity they were selected for mutation to alanine. Mutation Primers were designed as explained in 3.2.7 (see also Table 27). A Touch-Down-PCR protocol was conducted to insert the mutation into the plasmid DNA. To find a suitable PCR condition a screening was performed including addition of different supplements (Figure 62, p. 149).

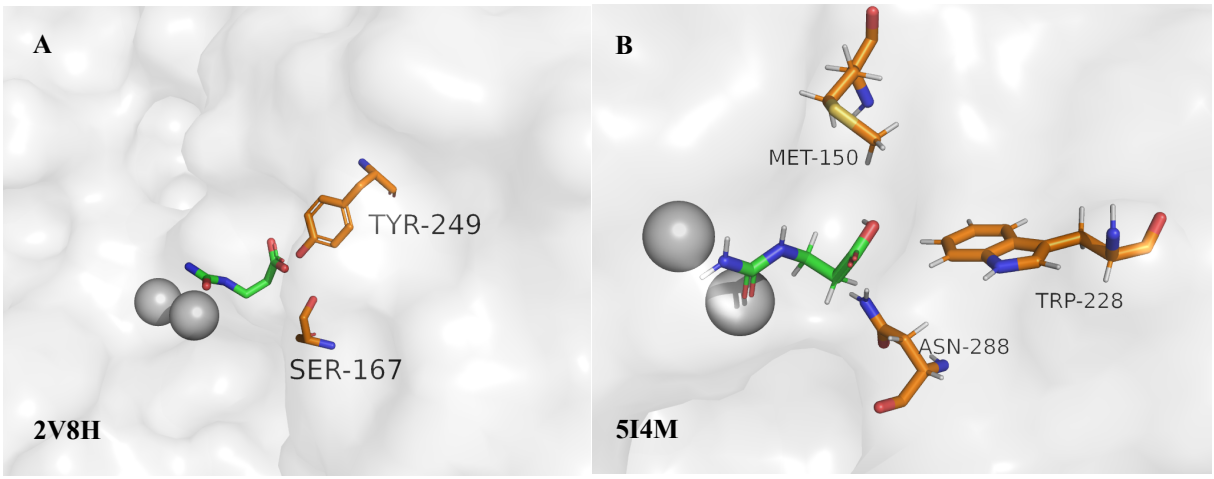

Figure 61: Overview of selected mutations for 2V8H and 5I4M.
Figures were made using PDB-files of 2V8H and 5I4M edited with PyMol. Metal cofactor ions are shown as grey balls. A) Active site of 2V8H with co-crystallized NCβAla (green) and unconserved residues Tyr-249 and Ser-167 selected for mutations (orange). B) Active site of 5I4M with docked NCβAla (green) and unconserved residues Met-150, Trp-228, Asn-288 (orange).

The agarose gel of the PCR-screening shows several PCR conditions leading to an amplification of products with the corresponding plasmid size of 2V8H (7253 kb) and 5I4M (6278 kb). Of the conducted PCR screening PCR-products with only one single band were selected for DpnI template DNA digestion and transformation into *E. coli* XL1 blue cells: PCR products of line 9 (mutation W228A), 25 (mutation N288A), 30 (mutation M150A), 35, 36, 39 and 40 for (mutation S167A) were selected to continue. However only mutation S167A could be correctly amplified. The corresponding plasmid was transferred into *E. coli* BL21 DE3 cells and subsequently expressed under the same conditions as the wild-type enzyme and purified *via* FPLC (MBP tag). The freshly purified enzyme (1.78 µg/µl final concentration) was then tested towards its conversion of 10 mM NCLβHMet and additionally NCLβHSer over night. The enzyme was found to still possess activity. However the conversion of the substrates was found to be lower as for the wild-type enzyme.

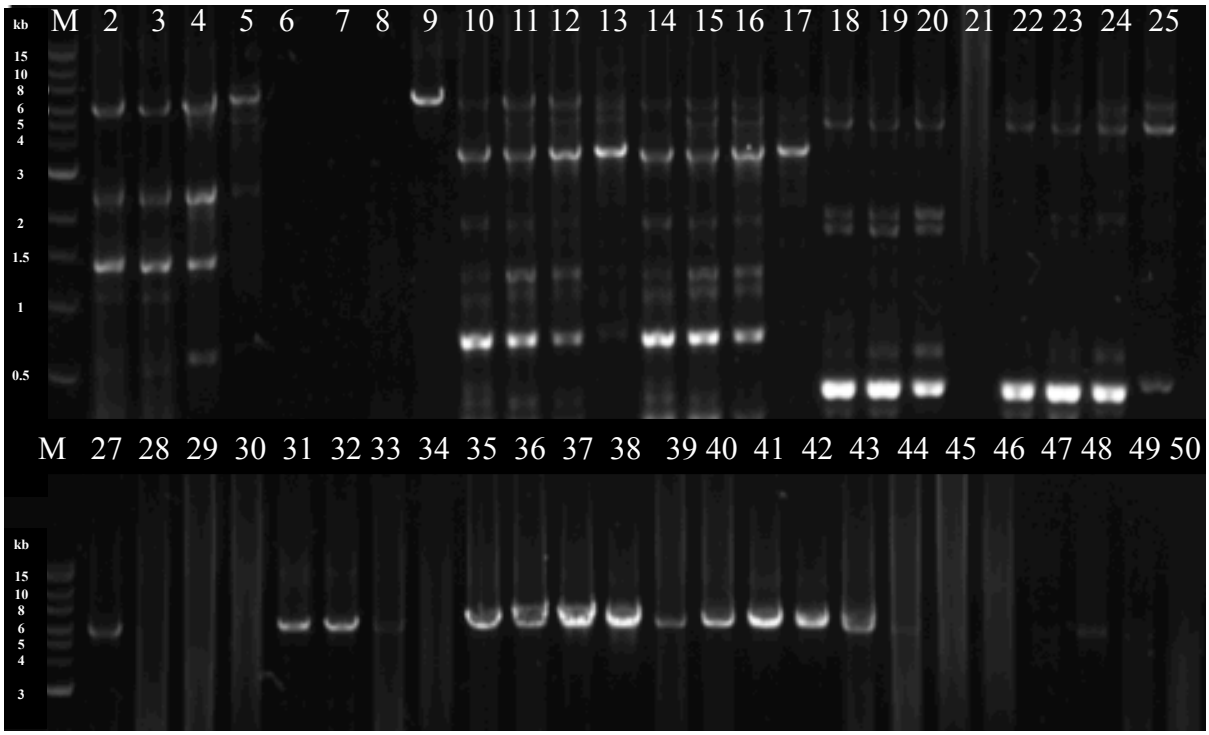

Figure 62: TD-PCR screening for amplification of point mutations of 2V8H and 5I4M.
Used Primers are given in **Table 27** p. 60; M: Marker (Quick-Load® 1 kb Extend DNA Ladder), 2: Mutation W228A - 5I4M GC Buffer Phusion Polymerase 0 ml DMSO, 3: Mutation W228A - 5I4M GC Buffer Phusion Polymerase 1 ml DMSO, 4:Mutation W228A - 5I4M GC Buffer Phusion Polymerase 2 ml DMSO, 5: Mutation W228A - 5I4M GC Buffer Phusion Polymerase 3 ml DMSO, 6: Mutation W228A - 5I4M HF Buffer Phusion Polymerase 0 ml DMSO, 7:Mutation W228A - 5I4M HF Buffer Phusion Polymerase 1 ml DMSO, 8; Mutation W228A - 5I4M HF Buffer Phusion Polymerase 2 ml DMSO, 9: Mutation W228A - 5I4M HF Buffer Phusion Polymerase 3 ml DMSO, 10: Mutation Y249A - 2V8H GC Buffer Phusion Polymerase 0 ml DMSO, 11: Mutation Y249A - 2V8H GC Buffer Phusion Polymerase 1 ml DMSO, 12: Mutation Y249A - 2V8H GC Buffer Phusion Polymerase 2 ml DMSO, 13: Mutation Y249A - 2V8H GC Buffer Phusion Polymerase 3 ml DMSO, 14: Mutation Y249A - 2V8H HF Buffer Phusion Polymerase 0 ml DMSO, 15: Mutation Y249A - 2V8H HF Buffer Phusion Polymerase 1 ml DMSO, 16: Mutation Y249A - 2V8H HF Buffer Phusion Polymerase 2 ml DMSO, 17: Mutation Y249A - 2V8H HF Buffer Phusion Polymerase 3 ml DMSO, 18: Mutation N288A - 5I4M GC Buffer Phusion Polymerase 0 ml DMSO, 19: Mutation N288A - 5I4M GC Buffer Phusion Polymerase 1 ml DMSO, 20: Mutation N288A - 5I4M GC Buffer Phusion Polymerase 2 ml DMSO, 21: Mutation N288A - 5I4M GC Buffer Phusion Polymerase 3 ml DMSO, 22: Mutation N288A - 5I4M HF Buffer Phusion Polymerase 0 ml DMSO, 23: Mutation N288A - 5I4M HF Buffer Phusion Polymerase 1 ml DMSO, 24: Mutation N288A - 5I4M HF Buffer Phusion Polymerase 2 ml DMSO, 25: Mutation N288A - 5I4M HF Buffer Phusion Polymerase 3 ml DMSO, M: Marker (Quick-Load® 1 kb Extend DNA Ladder), 27: Mutation M150A 2.0 - 5I4M GC Buffer Phusion Polymerase 0 ml DMSO, 28: Mutation M150A 2.0 - 5I4M GC Buffer Phusion Polymerase 1 ml DMSO, 29: Mutation M150A 2.0 - 5I4M GC Buffer Phusion Polymerase 2 ml DMSO, 30: Mutation M150A 2.0 - 5I4M GC Buffer Phusion Polymerase 3 ml DMSO, 31: Mutation M150A 2.0 - 5I4M HF Buffer Phusion Polymerase 0 ml DMSO, 32: Mutation M150A 2.0 - 5I4M HF Buffer Phusion Polymerase 1 ml DMSO, 33: Mutation M150A 2.0 - 5I4M HF Buffer Phusion Polymerase 2 ml DMSO, 34: Mutation M150A 2.0 - 5I4M HF Buffer Phusion Polymerase 3 ml DMSO, 35: Mutation S - 2V8H GC Buffer Phusion Polymerase 0 ml DMSO, 36: Mutation S - 2V8H GC Buffer Phusion Polymerase 1 ml DMSO, 37: Mutation S - 2V8H GC Buffer Phusion Polymerase 2 ml DMSO, 38: Mutation S - 2V8H GC Buffer Phusion Polymerase 3 ml DMSO, 39: Mutation S - 2V8H HF Buffer Phusion Polymerase 0 ml DMSO, 40: Mutation S - 2V8H HF Buffer Phusion Polymerase 1 ml DMSO, 41: Mutation S - 2V8H HF Buffer Phusion Polymerase 2 ml DMSO, 42: Mutation S - 2V8H HF Buffer Phusion Polymerase 3 ml DMSO, 43: Mutation M150A - 5I4M GC Buffer Phusion Polymerase 0 ml DMSO, 44: Mutation M150A - 5I4M GC Buffer Phusion Polymerase 1 ml DMSO, 45: Mutation M150A - 5I4M GC Buffer Phusion Polymerase 2 ml DMSO, 46: Mutation M150A - 5I4M GC Buffer Phusion Polymerase 3 ml DMSO, 47: Mutation M150A - 5I4M HF Buffer Phusion Polymerase 0 ml DMSO, 48: Mutation M150A - 5I4M HF Buffer Phusion Polymerase 1 ml DMSO, 49: Mutation M150A - 5I4M HF Buffer Phusion Polymerase 2 ml DMSO, 50: Mutation M150A - 5I4M HF Buffer Phusion.

5 Discussion

5.1 Screening of *N*-carbamoyl-β-phenylalanine degrading strains

One of the aims of this work was the identification of wild-type strains able to grow on NCβPhe as sole nitrogen source. Slight growth was observed for several strains on solid minimal medium containing NCβPhe. To validate an enzymatic conversion of NCβPhe NCβPhe were grown in minimal medium containing $(NH_4)_2SO_4$ and NCβAla respectively. Cells were harvested and used for biotransformations investigating the conversion of NCβAla and NCβPhe.

Regarding to the results it can be assumed that pre-cultivation with NCβAla induced the protein biosynthesis of genes coding for decarbamoylating enzymes in the wild-type strains. Several strains previously cultivated in medium containing NCβAla as nitrogen source showed a partly strong increase for the conversion of NCβAla of up to 80 % in lysate experiments. Compared to cells cultivated in medium containing $(NH_4)_2SO_4$ the conversion of NCβAla was generally lower. Additionally in lysate controls of cells previously cultivated in NCβAla no formation of βAla was observed. Probably the expression of βUps present in the pyrimidine catabolism of each organism was enhanced, since NCβAla is their natural substrate [1], [234]. The sole exception was strain M19 (*Ochrobactrum* sp.) with visible growth on agarose plates but did not grow in liquid medium containing NCβAla. *Ochrobactrum* sp. are described as nodulation bacteria and perform symbiotic nitrogen fixation for plants [235], [236]. Thus it may be that strain M19 was not able to use NCβAla as nitrogen source but fixed nitrogen from air. Control strain G (*P. glucosidasius*) that had not previously been induced by cultivation in NCβAla containing medium and strain 80 (*L. kluyveri*) verified that a decarbamoylating activity was present. For strain 80 a βUp activity is known from literature [172]. Strain G also possesses a gene coding for a putative decarbamoylating enzyme (GenBank: CP012712.1). However, even if the approximately same amount of cells was used for lysate experiments it could be possible that the protein expression and present amount of decarbamoylating enzymes varied in every strain. Thus results can only give an indication of existing activity of decarbamoylating enzymes. Especially results for lysate biotransformations of strain 80 (*L. kluyveri*) correlate with the results of its overexpressed and purified βUp (SklβUp / 2V8H). In both cases a full conversion of NCβAla to βAla was achieved when using $MnCl_2$ as a cofactor. Furthermore it can be assumed that all other strains showing a high conversion of NCβAla to βAla possess

genes coding for decarbamoylating enzymes, e.g. βUps that are known to catalyse this reaction and are present in almost all bacteria in the pyrimidine catabolism [151]. Additionally it can be assumed their activity is enhanced with bivalent metal cofactors, which is common for decarbamoylating enzymes [147], [175], [237]. This was proven with the overexpression of the corresponding genes from strain 37 (*B. phytofirmans*) and 71 (*P. oleovorans*) (see section 4.4.2.). This in turn will be discussed later in this section.

A significant growth on agarose-plates containing NCβPhe as sole nitrogen source was shown for several strains. However, due to high standard deviations a significant conversion of NCβPhe was not fully proven in biotransformation experiments. But for control strain 80 detected amounts of degraded NCβPhe are higher than the HPLC standards deviation. In contrast to the strong degradation of NCβAla a conversion of NCβPhe was not increased through induction with NCβAla. Control strain 80 showed NCβPhe degradation of 7 % with $NiCl_2$ present (corresponds to 0.5 mM of the initial 8 mM substrate concentration). This is contrary to the results obtained for the recombinantly overexpressed SklβUp of strain 80 for which a degradation of NCβPhe had never been observed. This arises the assumption that different enzymes may be present in the lysate, which could be responsible for the slight degradation of NCβPhe. A thermal decay of NCβPhe can be excluded since no βPhe concentration was detected in substrate controls. There are many other enzyme classes likely to exhibit an activity towards NCβPhe such as ammonia lyases or aminomutases, which transfer the amino group of an amino acid [117]. Later results of investigated novel enzymes, obtained from the wild-type strain screening (Burk1-5, P.oleo and P.aeru), proved that the conversion of NCβPhe to βPhe was not catalysed by these decarbamoylating enzymes (see section 4.4.3). Until now no decarbamoylating enzyme is known from literature that can catalyse this reaction.

Product degradation in product controls of 2-4 mM suggest the assumption that other enzymes present in the lysate caused this decrease of βPhe. This is likely since degradation of βPhe was recently is reported for ω-transaminases [238].

However it cannot be excluded that other microorganisms may possess genes coding for decarbamoylating enzymes that are able to perform a conversion of NCβPhe to βPhe. Further investigations towards the tertiary structures of decarbamoylating enzymes of this work suggested that the constitution of the active site might lead to repulsion of the phenyl residue of βPhe. This will be discussed in more detail in section 4.5.3.

In the screening conducted in this work only a very small fraction of known bacteria and eukaryotic organisms was investigated. The number of unknown microorganisms is even higher [239]. It is known that the highest amount of βAAs can be found in marine cyanobacteria mostly as part of natural products with polyketidic origin [15], [102], [240]. Cyanobacteria especially produce βAAs that have no proteinogenic α-amino acid counterpart [15]. It is likely that they possess metabolic pathways for their production. The screened institute's strain collection did not include cyanobacteria. Thus it could be an approach to screen cyanobacteria towards their degradation of NCβPhe. Therefore a screening based on liquid cultures could be more appropriate since some cyanobacteria are able to fix nitrogen [241]. Also the media will have to be adapted to the demands of these bacteria. A difficulty of cultivation of cyanobacteria is that they perform photosynthesis and thus need sun light for their growth [242]. Thus a combination of bioinformatic and biochemical screening approach with subsequent recombinantly protein expression would be easier. A BLASTp search by using the protein sequence of Burk1 as template sequence (since a high decarbamoylating activity was proven for this enzyme) revealed several putative decarbamoylating enzymes in cyanobacteria (data not shown).

5.2 Novel decarbamoylating enzymes

5.2.1 Classification of novel decarbamoylating enzymes

Seven novel enzymes (Burk1-5, P.oleo and P.aeru) have been identified through wild-type strain screening. A classification was proposed regarding to their potential tertiary structures (Figure 45, p. 110), their catalytic activity (see Figure 47, p. 113) and protein sequence homologies (Figure 42, p. 105).

Their decarbamoylating activity was proven by their ability to convert NCβAla to βAla. All enzymes were able to catalyse this reaction; hence they possess βUp activity. For Burk 4 and Burk 5 a formation of βAla was only observed using purified enzyme and $MnCl_2$ as a cofactor. The other novel decarbamoylating enzymes also showed a high cofactor dependency since the formation of βAla was highest using $MnCl_2$. In view of the fact that βUps can also possess activity towards NCαAAs, e.g. βUps from *A. tumefaciens* and *P. putida* [169][52], NCαLSer was used as model substrate to investigate the L-Carb activity of the enzymes. The results revealed that all enzymes except Burk 4 were able to fully convert NCαLSer to αLSer but exclusively with $MnCl_2$ present. A cofactor dependency is not mentioned for βUp from *A. tumefaciens* but NCαLSer has not been tested for this enzyme. According to literature the βUp

from *P. putida* also showed activity towards 10 mM NCαLSer of 33.9 % but 0.6 µmol $CoCl_2$ had been present in the reaction mixture, a conversion without additional cofactor is not reported [52]. Compared to this the activities of the novel enzymes towards NCαLSer presented in this work were much higher. However the influence of $CoCl_2$ towards the conversion of NCαLSer was not tested for them.

Burk1, Burk4 and Burk5 also showed activity towards allantoic acid when $MnCl_2$ was present. There is no information known about βUps possessing AaHyd-activity. Burk 4 exhibited the strongest activity towards allantoic acid and the lowest towards NCβAla and NCαLSer. Thus Burk4 may more likely be an AaHyd. Burk2, Burk3, P.oleo and P.aeru could be classified as βUps with additional L-Carb activity like the βUp from *P. putida.* Additionally P.aeru was found to have activity towards conversion of NCβDhSer and thus may also possess D-Carb activity. However, acceptance of both enantiomers has been reported for several L- and D-carbamoylases [52], [157], [243]. In contrast to this some carbamoylases are strictly L- or D-specific [154], [180]. On the basis of the available results, no conclusion can be drawn as to whether the enzymes are enantioselective, since only pure enantiomers of the substrates and no racemic mixtures were used. Burk1 and Burk5 cannot clearly be assigned to one of the existing classes of decarbamoylating enzymes because they exhibit activity of at least three of the four classes of decarbamoylating enzymes at the same time. Burk1 showed activity towards NCβDhSer whereby is exhibits activity of all four classes of decarbamoylating enzymes: βUp (NCβAla), L-Carb (NCαLSer), D-Carb and AaHyd activity. But since Burk1 possesses its highest activity towards NCβAla and NCαLSer it can rather be classified as βUp with additional L-Carb/D-Carb activity. Burk5 may be classified as L-Carb with additional AaHyd activity since no formation of βAla was observed.

However the conversion of NCβDAAs has never been reported before. Officially only the conversion of NCαD-amino acids is defined as D-Carb activity. It is worth mentioning that not all of the novel enzymes were tested towards their conversion of a NCα- or β-D-amino acid. Thus it could be possible that also other enzymes exhibit D-enantiomer activity.

The observed enzyme activities may be partly explained by their sequence alignments (Table 44, p. 24). Even if Burk4 showed the highest activity towards allantoic acid Burk1 possesses the highest percentage sequence identity to the AaHyd 1Z2L in contrast to the other enzymes. Compared to enzymes of the different classes Burk4 exhibits the highest identity to AaHyd 1Z2L. Burk1 has an even higher identity to the L-Carb 3N5F and a lower to βUp 2V8H. This is contrary to the results in the experiments since Burk1 showed a higher conversion of

NCβAla than NCαLSer. No sequence identity was found in comparison with D-Carb 1FO6, even if Burk1 converted NCβDhSer. Thus it could be assumed that the D-Carb activity does not arrive from a D-Carb-like sequence. Burk4 and Burk5 showing the lowest activity towards NCβAla, also showed the lowest sequence identity to βUp 2V8H. P.aeru, for which broad activity towards NCα-amino acids was observed showed also the highest sequence identity to L-Carb 3N5F. Homology can be assumed from 30 % sequence identity already [244] thus all of the identified seven enzymes show homology to AaHyds, βUps and L-Carbs but not to D-Carbs. This corresponds to sequence alignments known from literature [163], revealing that AaHyds, βUps and L-Carbs share homologous amino acid sequences and even homologous enzyme structures. This in turn corresponds to the structures of the generated models of Burk1-5, P. oleo and P.aeru which are structurally related to AaHyds, βUps and L-Carbs but not to D-Carbs. A classification of the novel enzymes on the basis of the existing definitions of the literature is therefore not clearly possible.

It had never been shown before that decarbamoylating enzymes possess that many cross-class activities as shown in this work. Only βUps are described to possess an additional activity towards NCαL-amino acids [52]. However by protein sequence similarity alone the enzymes cannot be classified also their tertiary structures have to be analysed. This will be discussed in more detail in 5.2.4.

5.2.2 Characterization of novel enzymes

Regarding to the results in this work many substrate conversions of the novel enzymes have been found to be highly cofactor dependent (see Figure 47, p. 113; Table 45, p. 116; Table 46, p. 118; Table 47, p. 119; Table 48, p. 122). This property of decarbamoylating enzymes has often been widely described [148], [163], [176]. For the seven novel enzymes especially Mn^{2+} and Co^{2+} had a strong influence on the enzyme activity. The found results do not exactly correlate with literature. Due to results from literature it can be assumed that each enzyme and substrate possesses a slightly different cofactor dependency [52], [148], [163], [175], [176]. However several cofactors seem to have a stronger effect than others. Ni^{2+}, Mn^{2+}, Co^{2+} and Fe^{2+} usually lead to an increase of activity whereas for other metal ions such as Mg^{2+}, Cu^{2+}, Ca^{2+}, Hg^{2+}, Fe^{2+}, Fe^{3+}, K^{+}, Na^{+} or Li^{+} no beneficial effect was observed regarding to the conversion of NCβAla or NCαAAs [52], [175], [176]. These findings have also been observed in experiments of this work. With regard to the seven novel enzymes mostly Mn^{2+} led to a higher yield of the corresponding amino acid. In contrast to that the best cofactors in literature are Co^{2+} and Ni^{2+}. For βUp P.aeru most of the common cofactors were tested (Zn^{2+},

Ni^{2+}, Mn^{2+}, Co^{2+}). It can be assumed for βUp P.aeru that Mn^{2+} enhances the enzyme activity towards NCαAAs with unpolar and more steric residues such as NCαL-Leu or NCαLMet. A weaker influence was observed for Ni^{2+} in contrast Zn^{2+} led to an inhibition especially for smaller NCαAAs (see Table 45). Thus is can be assumed that the seven novel enzymes are Mn^{2+} dependent enzymes whereas Zn^{2+} leads to their inhibition. This inhibiting effect of Zn^{2+} had also been observed for βUp from *A. tumefaciens* [148], L-Carb from *G. stearothermophilus* (3N5F) [176] and L-Carb from *Sinorhizobium meliloti* [175]. A connection between the atomic size and the catalytic effect of an ion may be assumed, since Mn^{2+} is the smallest and Zn^{2+} the biggest ion. The hypothesis can be proposed that too big ions inhibit or disturb ionic or polar interactions present in the active site during substrate catalysis.

There are several K_M-values known for the conversion of NCβAla in literature. The βUp from *Rattus rattus* exhibits the lowest K_M-value of 0.0065 mM [245] and βUp from *L. kluyveri* (2V8H) of 70 mM [246]. However the K_M-value of *L. kluyveri* was determined under the inhibiting effect of Zn^{2+} (no other cofactor had ever been tested for this enzyme). The fastest conversion of NCβAla of bacterial βUps was observed for *Clostridium uracilicum* with a K_M-value of 0.634 [234] followed by βUp from *P. putida* with a K_M-value 1.56 [52]. However it has to be mentioned that all known K_M-values were determined when the corresponding best metal cofactor was present in the reaction. K_M-values obtained for βUp Burk1 (5.71 mM), βUp Burk2 (22.36 mM) and βUp Burk3 (27.8 mM) are much higher, but they were generated without the addition of a cofactor. Especially K_M-value of βUp Burk1 is only approximately four times higher than the K_M-value obtained for *P. putida*. If kinetic parameters would be determined with cofactor $MnCl_2$ they may be in the range of *P. putida* or *C. uracilicum*. For instance for βUp P.aeru (0.9 µg/µl final concentration) an almost full conversion of 10 mM NCβAla was observed after five minutes with 2 mM $MnCl_2$ present at its optimal temperature (40 °C) and pH 6.8 (see Table 57, p. 197). Furthermore the optimal pH and temperature conditions, which had been used to generate the kinetic parameters for βUps Burk1-3 were only investigated in detail for Burk1.

Novel enzymes were active in a broad range regarding to pH-value and temperature (see Figure 48, p.123). The optimal pH of 6.8 and temperature of 40 °C was found to be same for the investigated enzymes βUp Burk1 and βUp P.aeru. In contrast to that many described decarbamoylating enzyme, like βUp from *A. tumefaciens* and L-Carb from *S. meliloti* have a pH optimum of 8 [148], [175]. However, a different buffer system (HEPES) was used for enzyme reactions in contrast to most publications Tris/HCl or sodium phosphate buffer was

used. The buffer system can have an influence on the enzyme stability through buffer-component binding, proton transfer, metal or substrate binding effects directly or indirectly mediated by buffers or by buffers acting as pseudo substrates [247].

Not only do Burk1-5, P.oleo and P.aeru possess a broad activity range in regard to their pH and temperature, they also show a high activity after storage at -80 °C, -20 °C for several days. βUp Burk1 still showed the activity after 5 days storage at 4°C compared to fresh enzyme. This indicates certain enzyme stability and would be an important feature regarding to enzyme application for the production of chiral noncAAs. Other enzymes known from literature showed a broad range of stabilities. Some of them are only stable for 30 to 60 min at their optimal temperature, e.g. βUp from *P. putida*, L-Carb from *S. meliloti*, βUp from *A. tumefaciens* or L-Carb from *Pseudomonas sp.* NS671 [52][175][147], [174]. Others are known to be stable for several days, e.g. the L-Carb from *Bacillus kaustophilus* still possessed 100 % activity after 15 days and 6 % activity after 36 days incubation at 50 °C when 3 mM Mn^{2+} were present [248]. L-Carb from *B. kaustophilus* showed no high sequence similarity to βUp Burk1 (37 % sequence identity).

5.2.3 Production of non-canonical amino acids

Goal of this work was the identification of novel enzymes applicable in a modified hydantoinase process for the production of non-canonical amino acids. For the seven novel enzymes βUps Burk1-3, P. oleo and P.aeru, AaHyd Burk4 and L-Carb Burk5 activity towards the production of at least four of the following non-canonical amino acids was observed: αL-NeoGly, αL-tert-Leu, β-2-L-ThieAla, βAla, βL-hAla and β-L-hSer. It was observed that each enzyme exhibits a different activity towards the production of these noncAAs.

As already mentioned previously the production of non-canonical α-amino acids has been studied extensively between 1980 and 2000s and thus several processes are already known [153], [179], [180], [243], [249], [250], [251], [139]. For L-Carb Burk5 the highest conversion of 100 % of NCαL-NeoGly (with 2 mM Mn^{2+} present) was observed with a product yield of 61 % after 20 h of incubation. The enzymes still converted 50 % without any cofactor present. In contrast to that the process for the production of αL-NeoGly of Gröger *et al.* is dependent on the costly cofactor NADH and the reaction needs 25 h [120]. It was not investigated how fast the reaction of LCarb Burk5 towards NCαL-NeoGly was and if the enzyme is enantioselective. This would be an important question for further examinations and further optimizations of the enzyme e.g. due to protein engineering.

βUp Burk1 and L-Carb Burk5 showed the highest activity towards NCβ-2-L-ThieAla with approximately 95 % conversion without additional cofactor. βUps Burk2, Burk3 and P.aeru were also able to form >93 % of β-2-L-ThieAla. In literature a substrate acceptance of NCβ-2-L-ThieAla with a high yield after 24 h has already been mentioned for *Arthrobacter aurescens* DSM 3747 regarding the hydantoinase process [140] and is catalysed by a L-Carb (k_{cat} / K_M (s^{-1} mM)) [252]. Especially for βUp Burk1 and L-Carb Burk5 kinetic parameters towards this substrate should be determined. It may be possible that these enzymes a smaller K_M-values for this substrate. Especially Burk1 has already a quite low K_M-value without additional cofactor.

The highest conversion of NCαL-tert-Leu of 20 % was shown for βUp P.oleo. However, only 3 % product was formed. This may be due product degradation caused by remaining impurities after enzyme purification, since a product degradation of 10-20 % approximately had been observed. However, the enzyme may be a perfect candidate for protein engineering. A suitable hydantoinase able to convert tert-butylhydantoin to *N*-carbamoyl-(*R*)-tert-Leu is already known in literature [115] [253]. Also a process for (S)-tert-Leu was described but only due to chemical catalysis [115] [253]. Further optimization and investigation of βUp P.oleo towards the production of αL-tert-Leu by the hydantoinase process could be completed if a suiting hydantoinase with (*S*)-enantioselectivity is available.

As described earlier, several approaches for the enzymatic production of optically pure βPhe have been published in the last years [124], [127]. The molecule is especially interesting because of its presence as building block in several pharmaceutical drugs [61]. For the production of chiral βPhe with a modified hydantoinase process a chemical synthesis route for 6-phenyl-5,6-dihydrouracil (PheDU) and a corresponding hydantoinase for the production of NCβPhe are already known [146]. However, in this work no enzyme for the second step of this process was discovered through the microbial screening. Degradation of chiral NCβPhe and NCβLeu using a decarbamoylating enzyme and the modified hydantoinase process has been tested but never been achieved according to literature [169]. E.g. for βUp from *A. tumefaciens* (βcar_{At}) the conversion of *N*-carbamoyl-β^3-amino acids was only achieved with a methyl-group but not with a phenyl-resdiue in the β-positions. Due to analysis of a modelled tertiary structure of βcar_{At} Martínez-Gómez and co-workers assumed that substituents larger than a single atom group are impossible to be accepted by the active site because of possible steric clashes and disturbance of polar interactions of catalytic residues [169].

Also no conversion of substrates with other aromatic residues like chiral NCβTyr (*N*-carbamoyl-β-tyrosine), NCαLPheGly (*N*-carbamoyl-α-L-phenylglycine) or NCαLpHPheGly

(*N*-carbamoyl-α-L-para-hydroxy-phenylglycine) was detected for investigated βUp Burk1. In contrast to that noncAA D-hydroxy-phenylglycine is synthesized by a D-Carb from *Agrobacterium* sp. using the hydantoinase process [180]. Also for other D-Carbs from *Agrobacterium* sp. KNK712 or *Flavobacterium* sp. AJ11199[a] high conversion (100 %) of NCαLpHPheGly was reported [179][249]. In contrast to this for L-Carbs only a conversion of *N*-carbamoyl-α-L-phenylalanine is reported with lower conversions, e.g. 31 % for L-Carb from *A. aurescens* (31 %) [252] or *S. meliloti* (25 %) [254] leading to the canonical α-L-phenylalanine. For the βUp from *P. putida* no activity towards *N*-carbamoyl-α-L-phenylalanine (NCαLPhe) or other substrates with aromatic residues was observed [52]. This is reflected by the results obtained for βUp Burk1 showing only a low formation of αLPhe of 16 % and only when $MnCl_2$ was present (see Table 60, p. 199).

Interestingly NCβ-2-L-ThieAla, which constitutes of a five-ring residue including a heteroatom, is converted in a high ratio even without cofactor by several of the novel enzymes, e.g. by βUp Burk1 and L-Carb Burk5. However, the amino group of NCβ-2-L-ThieAla is located at the α-position, which may influences the conversion of this substrate. Despite this it should be investigated whether a corresponding NCβ-histidine or NCβ-thienylalanine is degraded by βUp Burk1 or L-Carb Burk5. Eventually the presence of the heteroatom in NCβ-2-L-ThieAla and the slightly lower size of the amino acid residue (in comparison to NCβPhe) promote interactions of physical forces present in the active site.

Since not even a slight activity towards NCβPhe was observed for Burk1-5, P.oleo or P.aeru a protein engineering approach for its conversion could turn out to be difficult. Especially rational protein engineering would not be possible because of the missing information about 3D-tertiary structures of the identified decarbamoylating enzymes. Furthermore protein engineering has more potential if at least a slight activity towards a substrate is present [3]. One possibility could be error prone PCR to build a big mutant library. More detailed investigations on the conversion of NCβPhe are probably pointless, since already several metal cofactors and NADH were investigated, also lysate as well as high protein concentrations were studied. As mentioned for βUp from *A. tumefaciens* (βcar_{AT}) substituents with larger residue sizes may lead to sterical clashes [169]. This may also occur for newly identified βUps Burk1, 2, 3, P. oleo and P.aeru.

The aim of this thesis was the production of β^3-amino acids. These have their amino group and substituents at the β-position. As already mentioned several routes for the enzymatic production of the aromatic optically pure β^3Phe have been developed [124], [127]. In contrast

to this nothing is known about the biotechnological production of aliphatic β^3-amino acids and β-homo-amino acids (β(h)AAs). Small aliphatic β(h)AAs are building blocks in many natural products with biological activity [71]. They are especially interesting for their application in peptide drugs because the substitution of α-amino acids with their β-isomers may result in increased enzyme stability [255] and influence the peptide conformation [256]. The only enzyme ever to be investigated towards its activity of NCβ(h)AAs is the βUp from *A. tumefaciens* C58 (βcar_{AT}) [148]. In this study a K_M-value of 3.44 is determined for the conversion of *N*-carbamoyl-β-L-homo-alanine (NCβhAla). However, no information about the formed amount of the product β-L-homo-alanine is reported. The conversion of chiral *N*-carbamoyl-β-homo-serine (NCLβhSer or NCDβhSer) or *N*-carbamoyl-β-homo-methionine (NCLβhMet) was never tested [169].

Since no other information is known about decarbamoylating activity of other enzymes towards aliphatic NCβAAs it can be assumed that the first biocatalytic production of the aliphatic βhAAs β-L-homo-alanine and β-L-homo-serine was achieved in this work using the novel decarbamoylating enzymes (with exception of the naturally occurring βAla). By using βUp P.aeru with a final enzyme concentration of ~2 µg/µl with presence of Mn^{2+} a synthesis of 100 % βLhSer and 33 % βLhAla was achieved within 20 h (Table 47, p.119). Contrary to the assumption for βUp βcar_{AT} to only be able to convert NCβAAs with a substituent consisting of only one single atom group [169] NCβLhSer with a bigger substituent was also converted by βUp P.aeru. Hence βLhSer enzymatically synthesized in this work is the largest β^3-amino acids ever produced.
In Table 48 (p. 122) it is noticeable that for most conversions the amount of NCβLhSer is higher than the detected amount of corresponding amino acid βLhSer. This could be due to the fact that product degradation was observed in product controls, probably caused by remaining impurities after FPLC purification. Another option could be that decarbamoylating enzymes are able to further convert the formed amino acid. However, such an activity has not been observed for other of the novel enzymes.

As shown in the docking experiments generated for model of βUp P.aeru it can be assumed that NCβLhAla and NCβLhSer are coordinated by Gln-202, His-367, Glu-138 and His-92 as reference substrate NCβAla (Figure 52, p.128). No molecular clashes were observed for substrates with bigger substituents like NCβLhSer and NCβLhMet in these dockings, like they had been reported for dockings of βcar_{AT} [148]. The higher conversion may be due to the polar serine residue coordinated by Glu-138. His-92 may coordinate the carbonyl-C-atom of the *N*-carbamoyl-group. The docking for NCβLhMet shows a larger distance to His-92 than

NCβAla, NCβLhAla and NCβLhSer. This could explain why βLhMet was degraded but no βLhMet was formed. The essential reaction groups like *N*-carbamoyl-group and acid group are oriented differently for docking of NCβLhMet and may have led to a different conversion. βUps as well as L-Carbs, D-Carbs are classified in the E.C. class 3.5.1 of linear amides. They are hydrolases acting on carbon-nitrogen bonds other than peptide bonds (information obtained from BRENDA database [257]). Thus other possible hydrolysation reactions regarding to NCβLhMet could be e.g. the cleaving of formate ($HCOO^-$), ammonium (NH_3) or acetate (CH_3COO^-).

Comparing the seven novel enzymes in Table 48 (p. 122) the highest conversion of NCβLhSer with a final enzyme concentration of 1 µg/µl was detected for βUp Burk1 (with Mn^{2+}), followed by L-Carb Burk5 (with Mn^{2+}) and βUp P.oleo, showing a relative conversion of 51 % without any additional cofactor. Due to this results it can be assumed that the conversion of aliphatic NCβhAAs is not necessarily cofactor dependent, but highly enhanced by addition of metal ion Mn^{2+}. The same observations were made for conversion of NCβAla, the natural substrate of βUps. In literature βUps as part of the pyrimidine catabolism are not described to be mandatory cofactor or coenzyme dependent [234].

Several aliphatic and aromatic *N*-carbamoyl-β^3-amino acids with different sizes and polarities of their residues have been tested for the first time in this work. βUp P.aeru was intensively investigated towards its conversion of both NCαL-amino acids and NCβAAs (see Table 45 p. 116 and Table 47 p. 119). The more unpolar and larger the residues are the lower is the formation of the corresponding αL-amino acid. E.g. no formation of αL-valine and αL-isoleucine was observed. For αL-leucine only a slight product formation was observed. Of substrates with small residues like NCαL-Gly, NCαL-ABA or incorporated heteroatom and thus polar residues like NCαL-Ser, NCαL-Cys, NCαL-Met the corresponding amino acids were formed. With larger size of the residue a higher cofactor-dependency can be assumed in regard to the results. Similar observations are reported for βUp from *P. putida* [52] showing the showed best conversion for NCαL-Gly (K_M 0.68 mM), NCαL-Ala K_M (1.56 mM), followed by NCβAla (K_M 3.74 mM) and the slowest conversion for NCαL-Ser (K_M 75.1 mM). However, only few data about conversion of NCαL-amino acids by βUps is known. A similar trend may be transferred to the conversion of NCβhAAs. An activity of βUps Burk1 and P.aeru towards aliphatic NCβ(h)AAs with sterically larger and unpolar residues such as NCβLhMet, chiral NCβLeu or NCβHep of 35-40 % was observed. However, no significant product formation could be detected. For chiral NCβPhe neither conversion nor product formation was observed for βUps Burk1 and P.aeru. The reason for this may be that the amino

acid residues larger than for NCβhLSer are sterically hindered in the active centre. This will be discussed in more detail in the following section. For βUp βcar_{AT} conversion of chiral *N*-carbamoyl-β-leucine (NCβLeu) and *N*-carbamoyl-β-phenylalanine (NCβPhe) is not reported and the conversion of chiral *N*-carbamoyl-β-homo-serine (NCLβhSer or NCDβhSer) or *N*-carbamoyl-β-homo-methionine (NCLβhMet) was never tested [169].

5.2.4 Suggestions of active centres

The *in silico* dockings conducted for βUps Burk1-3, P.oleo and P.aeru, AaHyd Burk4 and L-Carb Burk5 were based on enzyme models previously generated by Phyre^2, which in turn were generated on the basis of 120 other models with a high confidence of 100 %. The template for most of the enzyme models in this work was the tertiary structure of *B. vietnamiensis,* which had a high identity of 57 %. If two proteins share 50 % or higher sequence identity their backbones differ by less than 1 Å deviation [258]. Other templates had lower identities but also with a confidence of 100 %. The generated models can be assumed as good if the model confidence is > 90 % [205]. An identity of > 55 % can also be assumed as good since in general enzyme models can be generated from a structural homology higher than 30 % [259]. This high confidence of the generated enzyme models makes them good indicator for structure analyses since no enzyme crystal structure was available for the novel enzymes.

The overall tertiary structure of the generated enzyme models of βUps Burk1-3, P.oleo and P.aeru, AaHyd Burk4 and L-Carb Burk5 are very similar. This tertiary structure homology between βUps, L-Carbs and AaHyds has already been reported [233] [182]. However, each active site was found to be different. The conducted *in silico* dockings were performed based on the generated models to give an idea of the substrate orientation in each active site of the novel enzymes (see Figure 51-Figure 53, p. 128 ff.). Nothing is known from literature in regard to docking of NCAAs into models of decarbamoylating enzymes using ROSIE ligand docking, but studies on other enzymes using a similar method, choosing the best-fitting model out of the top ten models generated by ligand docking tool ROSIE, has been reported [260]. The procedure of performing docking experiments with a previously generated enzyme model was reported for a ω-transaminase and nitrilase using other algorithms (SIWSS-Model for model generation and Autodock4.2 for docking of the ligand). In this case the active site was predicted by superimposing the modeled structure with a strucuture template co-crystallized with its substrate [128].

Homolog model SklβUp from *L. kluyveri* (2V8H) with co-crystallized substrate NCβAla (= ligand) was used as template for the coordinate generation (see 3.2.6.3) and reference, since all of the novel enzymes except AaHyd Burk4 showed a good βUp activity. The orientation of co-crystallized NCβAla in 2V8H was studied to get an idea of the natural orientation of the ligand in the active site of a βUp. In the structure of 2V8H it was observed that the *N*-carbamoyl group was oriented towards the ion molecules (see Figure 23 C) [170]. The acid group of the amino group faces in the opposite direction.

Regarding the dockings performed for novel βUps Burk1 and P.aeru showing 100 % activity towards conversion of NCβAla to βAla, all performed dockings for other substrates than NCβAla were based on the docking of NCβAla providing the lowest energy. In this reference docking the *N*-carbamoyl group of NCβAla was oriented towards the ion molecules as reported for SklβUp [173]. As described earlier the NCβAla molecule in SklβUp (2V8H) is coordinated by a glutamine residue (Gln-229), histidines residue (His-397) and arginine residue (Arg-322): The Arg residue provides the coordination of the acid group of NCβAla, the glutamine and histidine coordinate the transition state formed after nucleophilic attack of a OH^- molecule until the amid bond is cleaved [173]. The mechanism is described in more detail in section 1.5.2. (see Figure 24, p. 34).

The closest residues to docked NCβAla in the proposed active site of Burk1 are Glu-142, His-395 and Gln-226. As reported for SklβUp in Burk1 also a histidines residue (His-395) may coordinates the oxygen of the carbamoyl group. Furthermore a glutamine residue (Gln-206) may coordinates the outer amino group of the *N*-carbamoyl group. The docking of Burk1 suggests that a glutamic acid residue (Glu-142) may is responsible to orient the acid group instead of an arginine residue like in 2V8H. Hydrogen bonds can also form between two groups of carboxylic acid with an average distance of 2.65 Å [261], but the Arg residue is basic and polar and the Glu residue is acid and polar. A coordination of an acid group is more likely coordinated by a basic group from the chemical point of view. However, the distance in the docking model of 4.5 Å is way higher than 2.65 Å and would be too long to form a hydrogen bond between these two carboxylic groups. With distances of ~3 Å a forming of hydrogen bonds would be possible since hydrogen bonds were found to be of a maximum length of 3.2 Å. But most hydrogen bonds usually are even shorter (1- 2.7 Å) [262]. The model of similar docked NCβLhAla was the only model of the top 10 models to be oriented in that way. This could be a sign that this ligand does not fit very well into the proposed active site. Also the activity of Burk1 towards NCβLhAla was way lower than towards NCβAla. According to this the energy scores for NCβLhAla (-10.41) was higher as for NCβAla (-

12.78) and thus the affinity of NCβLhAla to the active site of Burk1 is lower than for NCβAla [184]. The higher energy score obtained in the docking experiments in turn may explain the lower conversion of NCβLhAla compared to NCβAla. From the biochemically perspective this result could be explained due to the slightly more sterical and unpolar residue of NCβLhAla, since it is known for polar residues in the active site to clearly favour polar residues during catalysis [263].

As already mentioned the Phyre^2 algorithm uses different known enzymes structures to modulate an enzyme model. For the most part the model of βUp P.aeru was based on the structure of *B. vietnamiensis* (5I4M). However official information about the activity in its active has not been reported. The third best template for βUp P.aeru model was the structure of 3N5F. As mentioned in the introduction the catalytic triade of 3N5F includes an Arg, His and Asn [177]. In contrast to this the dockings for P.aeru showed that residues Glu-138, Gln-202 and His-367 probably would be close enough to coordinate the ligand (see Figure 52, p.128). This residue arrangement would also rather fit to the proposed catalytic triade of 2V8H (Gln, His, Arg). The similarity to the catalytic triade of 2V8H in turn fits to the high activity of βUp P.aeru towards NCβAla equally to 2V8H. According to the measured distances NCβAla and NCβLhSer would most probably be coordinated by hydrogen bonds [261]. The highest distances to the residues of the proposed active site were found for NCβLhMet, which may explain the lower activity towards this substrate because a higher distance than 3 Å does not lead to formation of hydrogen bonds [261]. Compared to polar NCβLhSer the residue of NCβLhMet is unpolar and thus a good coordination through formation of hydrogen bonds is more unlikely, since Glu, Gln and His are all polar residues [263].

All mentioned earlier βUps belong to the enzyme class of hydrolases using water to cleave a bond. For hydrolases the most common mechanisms are based on acid/base chemistry with histidines and glutamate being two of the most common catalytic residues of this class [263]. Furthermore for most of the known hydrolases the reaction includes covalent attachment of a residue to the substrate to be able to cleave the bond to be cleaved [263]. For SklβUp (2V8H) a similar mechanism has been reported by Lundgren and co-workers (see Figure 24, p. 34) [173]. Thus is can be assumed for βUps P.aeru and Burk1 to form hydrogen bonds and thus a binding of the substrate to stabilize transition states is likely. The most observed catalytic triad for the class of hydrolases is serine-histidine-aspartatic acid (Ser-His-Asp). This triad was not proposed for βUps P.aeru and Burk1, however it has also not be described for other decarbamoylating enzymes e.g. SklβUp (2V8H) [173], L-Carb 3N5F [178] or D-Carb 1FO6

[181]. However in all novel enzymes but AaHyd Burk4 at least two histidines and one aspartate residue was proposed to be part of the active site (Table 49, p. 124). A serine was not prognosticated for any of the novel enzymes. Thus it can be assumed that proposed βUps Burk1-3, P. oleo and P.aeru as well as L-Carb Burk5 and AaHyd Burk 4 may belong to the class of hydrolases [E.C. 3.]. Also the highly conserved Gly, present in each proposed active centre of the seven novel enzymes probably is able to coordinate the outer amino group of the *N*-carbamoyl group with its acid group. This has also been reported for the coordination of NCβAla in 2V8H [264].

In the structure of AaHyd 1Z2L the co-crystallized allantoic acid is oriented in a different way compared to NCβAla in 2V8H. Here the acid group faces the metal ions and distance between ligand and catalytic residues are longer compared to ligand binding in 2V8H [265]. As proposed earlier Burk4 that possesses the highest amino acid query cover towards AaHyd 1Z2L and is most likely an AaHyd. For 1Z2L it is reported that an Arg/Asn, His and Gln coordinate allantoic acid [182]. Because of missing data and tertiary structures of other AaHyds, 1Z2L is the only enzyme available for comparison to AaHyd Burk4. The proposed active site of AaHyd Burk4 demonstrates that allantoic acid could probably be coordinated by residues glutamine (Gln-208), two histidines (His-397 and His-95) (see Figure 53, p. 129). Like in 1Z2L the oxygen of the acid group of allantoic acid was found to be coordinated by a histidines residue (His-95) and one *N*-carbamoyl group by a glutamine residue (Gln-208). To both residues the distances are in a range of 3 Å, which is similar to distances of possible hydrogen bonds [261]. AaHyd Burk4 showed approximately the same activity towards NCβAla, allantoic acid and NCαLSer, which is reflected in approximately same energy scores of dockings and also similar distances towards proposed residues of the active site. Like in the structure of allantoic acid also NCαLSer possesses polar heteroatoms, which are able to form hydrogen bonds. This and low distances to the proposed active site residues may be responsible for the similar activities for these substrates.

In every proposed model of the novel enzymes also metal ions may play an important role as cofactors since decarbamoylating enzymes tend to be cofactor dependent [176], [264], [265]. In general for one third of all known enzymes a metal ion is required for the catalysis. Metal ions are mostly involved in three kinds of catalytic processes: (1) binding of substrates to ensure a suiting conformation of it; (2) Redox-reactions by change of the oxidation state and (3) electrostatic stabilisation or negative charge shielding [1]. In known hydrolases 39 % required a metal ion for their catalysis [266]. As already mentioned regarding to the observations made for the novel enzymes a metal dependency towards their catalysis can be

assumed. For other decarbamoylating enzymes an interaction of metal ions between polar and charged groups, e.g. acid and *N*-carbamoyl group and the acid group of the substrates is reported, e.g. for SklβUp (2V8H) [173]. According to this it can be assumed for the novel enzymes that metal ions like Mn^{2+} may function in the activation and/or in the electrostatic stabilization of the transition state of the of the *N*-carbamoyl-substrate. This influence has been reported in case metal ions are not involved in redox-catalysis, which is the case for decarbamoylating enzymes [266]. Since metal ions are known to provide electrostatic stabilisation a positive influence towards substrates with tiny or polar residues may be suggested, since substrates with unpolar and more sterical residues tended to be less converted by the novel enzymes. The lower conversion of unpolar and more sterical residues has already been discussed earlier.

It is noteworthy that the results obtained from ConSurf fit to those of the enzyme models generated with Phyre^2 and the performed dockings. All docked substrates were found to be very close to the identified highly conserved amino acids. Algorithms of ConSurf and Phyre^2 perform multiple sequence alignments based on different sources. Thus it is a good indicator if their results correlate. It is also conspicuous that all proposed active sites of the novel enzymes constitute of exclusively polar residues. The only enzymes for which a single unpolar residue was proposed to be in the active site are Burk4 (with Val) and Burk5 (with Ile). The Ile residue present in L-Carb Burk5 could be the reason for its good conversion of the unpolar substrate NCαL-NeoGly. The missing of unpolar groups in the proposed active sites of decarbamoylating enzymes suggests repulsion between polar residues of the catalytic cleft and the unpolar phenyl residue of NCβPhe. This would correspond to the fact that no activity towards NCβPhe could be observed.

All of the seven novel enzymes exhibited an activity towards aliphatic NCβAAs even though they possess several differences in their amino acid sequence and tertiary structure. Thus it can be assumed that the scope of possible variations in regard towards mutations for protein engineering is available.

5.3 Decarbamoylating enzymes with 3D-tertiary structures

5.3.1 Evaluation of current classification

Like the new identified enzymes βUps Burk1-3, P.oleo and P.aeru, L-Carb Burk5 and AaHyd Burk4 also the enzymes 2V8H, 5I4M, 3N5F, 1Z2L and 1FO6 were investigated on their activity towards representative substrates of different enzyme classes. In contrast to the novel enzymes four of the five mentioned enzymes with known 3D-tertiary structure have been already classified in previous publications (see Figure 54, p.131) [173], [178], [181], [182]. In addition to this to this at least three cross-class activities were detected for each of these enzymes in this work (Table 53, p. 135). As mentioned previously only βUps have been discussed to possess an additional activity towards proteinogenic NCαL-amino acids and thus L-Carb activity [169][52]. As discussed earlier the novel enzymes βUps Burk1-3, P.oleo and P.aeru, L-Carb Burk5 and AaHyd Burk4 cross-class activities have been detected.

For 2V8H, 5I4M, 3N5F, 1Z2L sharing a high amino acid sequence and structural similarity were found to possess activity towards NCβAla, allantoic acid and NCαLSer but with different activities towards each substrate. Until today no activity for 5I4M has been reported. The full conversion of NCβAla for βUp 2V8H and 5I4M (class not defined) was found to be cofactor independent. Thereby it can be suggested that 5I4M can be classified as βUp. Like other known βUps they also possess L-Carb activity, which appeared to be cofactor dependent, since a much higher conversion was achieved using $MnCl_2$ as cofactor. Enantioselectivity of these enzymes was not investigated in in this work. The novel found activity towards allantoic acid for βUps 2V8H and 5I4M has never been reported and appeared to be cofactor independent. However only $MnCl_2$ was tested in this work. The higher relative activity of 5I4M compared to 2V8H towards allantoic acid can be caused due to a higher final enzyme concentration. To relatively compare the enzymes they should be tested with the same enzyme concentration each in the same experiments, which was not done for the results presented Table 53 (p. 135).

In contrast to cofactor independent conversion of NCβAla by βUps 2V8H and 5I4M and the as L-Carb classified enzyme 3N5F showed a high cofactor dependency towards conversion of NCβAla. The high cofactor dependency towards $CoCl_2$ has been reported for several NCαAAs in literature but a βUp activity has never been shown before [176]. Also the newfound activity towards allantoic acid could be slightly cofactor dependent, but no other cofactors than $CoCl_2$ were investigated in this work. Interestingly also the activity towards

NCαLSer appeared to be completely cofactor dependent, since no αLSer was detected when no cofactor was present. This has not been pointed out in literature, but activity towards NCαLSer has also not been reported yet [176].

Even if for 1Z2L a low enzyme concentration of 0.22 µg/µl had been present in the reactions (compared to concentrations of other enzymes) a much higher (> 95 %) relative conversion of allantoic acid was observed. This observation suits the reported AaHyd activity of 1Z2L [265]. However the reaction seems to be cofactor independent. No specific cofactor dependency is reported for 1Z2L but it was mentioned that the enzyme can be activated by adding substrate and Mn^{2+} [151]. Contrary to that a cofactor dependent activity was observed for NCβAla and NCαLSer. Thus the enzyme can be identified as AaHyd with additional βUp and L-Carb activity, which has never been reported before. Beyond that AaHyd 1Z2L possesses a high activity even at low concentrations thus low K_M can be assumed.

Even if no activity towards NCβAla was found for D-Carb 1FO6 in lysate experiments an activity towards allantoic acid and NCαDSer could be detected for the first time. Regarding to literature 1FO6 possesses activity towards aromatic D-enantiomeric substrates (e.g. NCαD-hydroxyphenylglycine) but apparently also towards aliphatic D-substrates like NCαDSer. However the activity towards NCαDSer was only moderate (~20 %) in contrast to the high enzyme concentration of 4.9 µg/µl used. Regarding to the results of this work aromatic substrates were converted completely, such as the natural substrate NCαD-hydroxy-phenylglycine. Furthermore neither cofactor dependency was observed in this work nor is reported for D-Carb 1FO6 [267]. Moreover activity and stability of this enzyme are known to be negatively affected by metal ions [268]. This was also observed in some experiments with 1FO6. The activity towards allantoic acid is surprisingly since 1FO6 exhibits a different tertiary structure. However as displayed in Table 51 (p. 131) the enzyme still possesses a sequence similarity of > 45 % to 2V8H, 5I4M, 1Z2L and 3N5F. Thus 1FO6 is a quite homologue protein to 1Z2L. In general all other investigated enzymes have a sequence similarity of > 50 % towards 1Z2L and possess an activity towards allantoic acid.

Together with the results from Burk1-5, P.oleo and P.aeru it can be assumed that most decarbamoylating enzymes possess not only a high structural and sequential similarity to each other but also a similar substrate scope regarding NCβAla, allantoic acid and small NCαAAs.

5.3.2 Production of aliphatic β-amino acids

βUps 2V8H and 5I4M, L-Carb 3N5F, AaHyd 1Z2L and D-Carb 1FO6 were investigated and compared to each other towards their conversion of different aromatic and aliphatic NCβ-homo-amino acids (see Table 54 p. 24). All investigated enzymes were able to produce aliphatic βAAs, but an activity towards aromatic NCβAAs was not observed. βhDAla, βhLSer, βhDSer and βhLMet were enzymatically produced for the first time in this work since no information can be found in literature.

The best conversions of NCβhLAla were detected for βUps 2V8H and 5I4M and L-Carb 3N5F. This fits to the fact that these enzymes also obtained the best activity towards the structurally similar NCβAla (Table 54, p. 138). However the activities towards NCβhLAla were about 40-80 % lower compared to NCβAla conversion. This could be due to the additional C-atom of NCβhLAla that may cause a different orientation or steric clashes in the active site, which in turn may result in the lower conversion rate. As already discussed earlier steric clashes of NCβhLAla and lower conversion rates in comparison to NCβAla have also been reported for the model structure of βcar_{At} [169].

Almost no activity towards NCβhLAla (with $MnCl_2$) was observed for AaHyd 1Z2L showing a relative conversion of > 60 % of NCβAla when Mn^{2+} is present. This leads to the assumption that 1Z2L may catalyses the degradation of NCβhLAla differently than 2V8H, 5I4M and 3N5F. Using 3N5F the best yield was achieved for βhLAla of 56 %. Almost the whole converted substrate amount was detected as product. For 2V8H way lower product concentrations than converted substrate concentrations were detected. Maybe the substrate is cleaved in a different way as mentioned earlier.

2V8H, 5I4M and 3N5F showed approximately the same activity towards NCβhLSer. For 2V8H more product was obtained for βhLSer than for βhLAla. This may be due to the heteroatom in the serine residue. For the sterically larger NCβhLMet only low conversions of maximum 16 % and 4 % formed product were detected. Compared to the good converted NCβhLSer it also possesses a heteroatom, which may influences the coordination in enzymes active sites. However NCβhLMet may be more sterically hindered in the active site. To explain this observation several docking experiments were performed which will be discussed in more detail in the following section.

1FO6 exhibits a remarkable activity towards NCβhDAla and NCβhDSer. Almost the same amount of degraded substrate was converted into the corresponding product with a final

enzyme concentration of 0.9 µg/ml. This is the first time a D-β-amino acids has been enzymatically produced. Surprisingly the enzyme exhibits a higher activity towards NCβhDAla and NCβhDSer than towards NCαDSer. A reason for this may be the shifted position of the amino group, leading to a better positioning in the active site. The reactions of 1FO6 appeared to be cofactor independent which has been reported for this enzyme [268]. Thus 1FO6 may be a good candidate for further investigations towards the production of βhD-amino acids. D-Carbs like 1FO6 tend to be more instable than βUps but investigations on enhancing their stability have already been reported [224].

Therefor substrates may be tested again with an available mutant of 1FO6 to investigate whether the activity maintains while the enzyme stability is increased at the same time.

Also 3N5F might be interesting for further investigations since this enzyme possesses a high thermal stability and an optimal reaction temperature of 65 °C [176]. Since it exhibits a good activity towards NCβhLAla and NCβhLSer it may be a potential candidate for the biotechnological production of aliphatic β-amino acids *via* a modified hydantoinase process.

βUps 2V8H and 5I4M, L-Carb 3N5F, AaHyd 1Z2L and D-Carb 1FO6 did not convert aromatic NCβAAs like NCβD/LPhe and NCβD/LTyr. By 1FO6 a high conversion of aromatic NCαD-amino acids was reported [180]. It may be possible that the β-position of the amino group of the β-substrate drastically influences the enzyme activity. Here for also docking experiments were performed which are discussed in the following section. However 1FO6 may also be a good candidate for protein engineering approaches to produce βDPhe, because this enzyme already offers the ability to accept bulky and sterically large amino acid residues.

5.3.3 *In silico* docking experiments *versus in vitro* experiments

It is possible to establish some connections between the experimentally and computationally obtained results. The conserved amino acid residues obtained from analysing ConSurf results led so similar results as reported literature.

As described earlier for βUp 2V8H the amino acids Arg-322, Asn-309, His-397, Gln229 and Gly-396 are described to be involved in the catalytically degradation of NCβAla [173]. Almost all these residues were also identified through the ConSurf Server. The observed energy scores for docked substrates of βUp 2V8H reflect the results determined by *in vitro* experiments conducted in this thesis. Substrates that showed a high activity tend to have low energy scores close to those of NCβAla. Lower energy scores are equal to a low binding

energy between ligand and enzyme molecule and thus a better fit of the docked substrate into the active site. It becomes apparent that substrates showing good activity *in vitro* and a corresponding low energy in docking experiments are either unpolar and very small or polar. The much higher energy scores determined *in silico* for NCβPhe correlate with the fact that no degradation of this substrate was observed *in vitro*. The high energy scores for NCβPhe are interpreted as a bad binding of NCβPhe to the active site of 2V8H. Virtual investigations of this docking revealed that sterical clashes might appear. This has also been reported for βUp from *A. tumefaciens* (βcar_{AT}) [169] as already mentioned earlier. Other docking approaches for βUps except for βcar_{AT} and 2V8H in this work are not known.

Regarding to the *in vitro* and *in silico* results obtained for 2V8H it is assumed that ligand-docking results can give an impression on the activity of βUp 2V8H. Since for 2V8H a 3D-tertiary structure with a co-crystallized substrate is available to find appropriate starting coordinates good docking results were obtained. When comparing the dockings of different substrates conducted for 2V8H it was found that the phenyl residue of NCβPhe faced either to His-397 or towards Arg-322. The aromatic phenyl residue is completely unpolar. In contrast to that all residues of the active site possess very polar side chains. There could be repulsion between polar and nonpolar groups. In general substrates can be coordinated in the active site through different physical forces. For instance Van der Waal forces, hydrogen bonds or ionic interactions [1]. To form a hydrogen bond, a hydrogen donor and acceptor group is required. Short and strong hydrogen bonds usually possess a length of < 3 Å and can be build between polar groups [261]. Thus it could be assumed that the phenyl residue cannot build hydrogen bonds because of missing polarity and cannot form Van der Waals or ionic interactions because of missing dipoles and charges. For example a phenol residue can form hydrogen bonds because of its OH-group [261]. For βUp 2V8H also several other aromatic NCαAAs such as NCαLPhe were tested *in vitro* but no significant activity was detected (see Table 56, p.196). Thus it can be assumed that the β-position of the amino group of the corresponding amino acid is not the sole reason that no degradation was observed towards NCβPhe. It can be assumed that 2V8H is not able to coordinate unpolar (especially phenyl-) residues due to the amino acids composition in its active site. This presumption may also explain why a conversion of NCβHep has never been observed, because it also possesses an unpolar and long side chain. E.g the phenylalanine side chain is known to form only weak hydrogen bonds of the types OH-π and CH-O [269] but to form van der Waals type interactions. Distances of the phenyl residue to catalytic residues in the active site were measured of ~3 Å for performed *in silico* dockings in this work. Van der Waals interactions e.g. between aromatic residues are

optimally 5-7.5 Å [270]. The large size of the phenylalanine side chain and the low distance to the catalytic residues may lead to repulsion reaction since the optimal distance for van der Waals interactions is not possible according to the results of the NCβPhe docking. For smaller substrates with unpolar side chains like NCαGly or NCαVal a conversion has been observed *in vitro*. However with increasing sterical size of the residue the activity towards the substrate decreased. E.g. for NCαLeu a worse degradation was observed than for NCαGly. A reason for this may be that the polar and charged *N*-carbamoyl- and acid groups of each amino acid are able to equalize the unpolarity of smaller side chains. According to the dockings of NCβAla, NCβhLSer *N*-carbamoyl- and acid groups have ~3 Å distance and are able to build hydrogen bonds. A good activity towards aliphatic NCβAAs was observed for NCβhLAla and NCβhLSer, possessing only a small unpolar side chain and a polar side chains. For all enzymes investigated in this work a lower activity towards NCβhLMet, which possesses also an unpolar side chain was observed. The docking of NCβhLSer in 2V8H revealed that it may be possible that the CH_2-OH group builds a hydrogen bond to Gly-396 (see Figure 56, p.143). NCβhLMet with its unpolar side chain probably is not able to form hydrogen bonds, but it may be able to build weaker van der Waals forces through its sulphur heteroatom. This could be the reason for the lower degradation of NCβhLMet compared to NCβhLSer.

βUp 5I4M possesses a similar activity as 2V8H regarding NCβAla but no information about the amino acid residues responsible for the activity, is available in literature. Decarbamoylating enzymes were described to be able to switch back and forth between an active and inactive conformation dependent on whether a substrate is bound to the active site or not [170], [182]. If no substrate is bound, the enzyme is present in its open conformation. Since 5I4M was not co-crystallized with bound substrate it can be assumed that the structure available from PDB data bank represents its inactive (open) conformation. Through analysis with the ConSurf Server and comparison with the PDB-structure of βUp 5I4M it can be assumed that His-371, Gln-206 and Arg-301 are responsible for the catalytic activity of the enzyme. Asp-107 and His-203 may be essential for the coordination of the cofactor metal ions. These findings perfectly reflect the results obtained from *in vitro* studies regarding the high activity of βUps 5I4M and 2V8H towards NCβAla. In 2V8H the coordination is also performed by a His, Gln and Arg residue *via* hydrogen bonds [173]. The structure of 5I4M reveals that the *N*-carbamoyl-group is coordinated by Gln-206 and His-371 and the acid-group by Arg-301 similar to the mechanism in 2V8H. The methionine side chain of NCβhLMet is located towards His-371 with a distance of 4 Å thus polar interactions might be weaker and thus may explain the slight conversion of this substrate. While the *N*-carbamoyl-group and the

acid group of NCβhLMet are oriented in the same way as for NCβAla, the acid-group of NCβPhe is completely shifted. A building of hydrogen bonds to Arg-301 is thus impossible. Here additionally a repulsion of the unpolar phenyl residue of NCβPhe and Arg-301 can be assumed.

Compared to βUps 2V8H and 5I4M the active site of L-Carb 3N5F looks slightly different. From the reported catalytic triade of Arg-286, His-225 and Asn-273 [178] only His-225 was identified by ConSurf analysis. Arg-286 and Asn-273 were not found to be close to the active. However the active site was defined by transferring NCβAla from 2V8H to 3N5F. It may be possible that this led to wrong assumptions of the location of the active site due to unrealistic starting coordinates. But usually the active site for decarbamoylating enzymes was found to be close to the metal ions in the structure. The active site for 3N5F in this work is thus proposed to constitute of Glu-125 and Gln-192 and His-225 to coordinate NCβAla (see Figure 58, p. 145). The other identified highly conserved residues Asp-81, Asp-90, Gly.91, Glu-187 and His-189 probably coordinate the metal atoms. The conversion of NCβhLSer may be explained due to the fact that it is most likely oriented as NCβAla. A docking of NCβPhe was not executable by ROSIE reflecting the experimental result that no conversion of NCβPhe was observed. Apparently no possible orientation for NCβPhe in the active site of 3N5F was found under the set conditions.

AaHyd 1Z2L was co-crystallized with allantoic acid. Thus is has to be assumed that the displayed enzyme was in its closed (active) conformation [182]. According to literature 1Z2L possesses also a His (His-384), Gln (Gln-195) and Arg residue (Arg-290) to coordinate the substrates like βUps 2V8H and 5I4M [182]. But through taking a closer look into the structure, the highly conserved residues seem to be further away from each other (see Figure 59, p. 146). This could be because allantoic acid is bigger than NCβAla. These findings could explain why AaHyd 1Z2L also possesses an activity towards NCβAla but a lower one compared to βUps 2V8H and 5I4M. Docked NCβhLMet is oriented differently than docked allantoic acid. A polar interaction of the methionine side chain with Arg-290 may be present, but may also lead to a different degradation of NCβhLMet. This might explains the slight substrate conversion and no product detection obtained for *in vitro* experiments.

The active site of 1FO6 is very different than the active sites of the other four enzymes. This has also been reported in literature. For example a Cys and a Lys can be found in the active site of 1FO6 that are not present in the other enzymes active sites. Glu-47 and Cys-172 are supposed to coordinate the substrate in the catalytic cleft [181]. The acyl group of the *N*-

carbamoyl-group is supposed to be coordinated by Cys-172. This was not observed in the conducted dockings. However the starting coordinates were generated by alignment with a mutant of 1FO6 may possess a different structure and thus other coordinates than the original 1FO6 structure. It is possible that the chosen starting coordinates to perform docking experiments were not optimal. The docking should be repeated using more plausible coordinates. This example shows the limitations of the ligand docking if no optimal starting coordinates are available. However, no other D-Carb with co-crystallized substrate was found in the protein database (PDB). The high activity towards NCαhydPheGly may be a result of the OH-group that gives its residue the ability to form stronger hydrogen bonds and polar interactions to other amino acid residues. In contrast to that no polar group is present in NCβPhe. This and the shifted position of the amino group could be the reason that NCβPhe is not converted by 1FO6, which usually possesses activity towards many aromatic substrates. Dockings conducted for D-Carb from Agrobacterium sp. strain KNK712 (PDB code 1ERZ) have been reported in order to investigate the catalytic mechanisms of the enzyme using Affinity program [271].

Regarding these observations it can be assumed that probably other NCβAAs can be converted to the corresponding amino acids by one of these enzymes. However, according to *in vitro* and *in silico* experiments the residue should not be too large and bulky. A substrate with a polar side chain or a charged group is probably preferred. Thus substrates like *N*-carbamoyl-β-histidine, *N*-carbamoyl-β-threonine, *N*-carbamoyl-β-asparagine, *N*-carbamoyl-β-aspartic acid or *N*-carbamoyl-β-glutamic acid should be chemically synthesized and tested. A high probability for their conversion can be assumed.

6 Conclusion and Outlook

Aim of this project was to identify enzymes for the production of β^3-amino acids that are to be used in a modified hydantoinase process. The identification of a *N*-carbamoyl-β-phenylalanine degrading wild-type strain possessing an enzyme to produce β-phenylalanine by the conducted microbial screening was not achieved. However, since only slightly more than 200 strains were screened, it is possible that a suitable enzyme may be found in another organism. Identified strains with slight growth on *N*-carbamoyl-β-phenylalanine as sole nitrogen source should be further investigated. In order to make screening more systematic, additional wild-type strains have to be examined in combination with computational bioinformatic high-throughput methods. Since computational algorithms can only be used to analyse already known sequences, *in vitro* screening is still essential. For example, cyanobacteria should be investigated since they are known producers of β-amino acids. Other methods, such as artificial evolution, should also be considered. However several biocatalytically approaches for the production of β-phenylalanine on a gram scale have been already developed over the past years (see section 1.4.3.).

Although no enzyme was identified for the production of β-phenylalanine aliphatic β^3-amino acids β-L-homo-alanine and β-L-homo-serine were biocatalytically produced for the first time using seven newly identified and classified decarbamoylating enzymes βUps Burk1-3, P.oleo and P.aeru, AaHyd Burk4 and L-Carb Burk5. Additionally also the non-canonical α-amino acids L-neopentylglycine and β-2-thienylalanine were produced using these enzymes. The use of five enzymes known from literature (βUps 2V8H and 5I4M, L-Carb 3N5F, D-Carb 1FO6 and AaHyd 1Z2L) led to the synthesis of β-L-homo-alanine, β-L-homo-serine, β-D-homo-alanine and β-D-homo-serine. Also a slight formation of β-L-homo-methionine was detected using these enzymes. This is the first time β^3-amino acids having a larger side chain than a methyl-group and D-β^3-amino acids were enzymatically produced. Several novel cross-class activities were identified for all twelve enzymes. A preference towards conversion of substrates with polar or charged side chains can be assumed due observations of *in vitro* experiments and *in silico* dockings. In turn a degradation of substrates with large, sterical and unpolar side chains seemed to be inhibited through the amino acid residues present in the active sites of the enzymes. Thus other *N*-carbamoyl-β-amino acids like *N*-carbamoyl-β-threonine, *N*-carbamoyl-β-lysine or *N*-carbamoyl-β-asparagine should be investigated for their conversion by decarbamoylating enzyme used in this work to enzymatically synthesize the corresponding β-amino acid.

Like aromatic β-amino acids also aliphatic β-homo-amino acids show a broad application area [71]. One of the biggest challenges of the modified hydantoinase process is the low solubility of PheDU (up to 4 mM) and NCβPhe (up to 20 mM). In this work it was found that especially β-homo-amino acids are more soluble (> 100 mM). Additional heating to 40 °C to the optimal activity of newly identified enzymes would increase the solubility even more. The influence of other bivalent metal cofactors on the conversion of non-canonical *N*-carbamoyl-β-substrates is to be investigated more intensively since almost no information is available regarding this topic. Furthermore the newly identified cross-class activities, the enantioselectivity and the enantiospecificity of the novel identified enzymes should be investigated since this was not examined in this work. Also a more detailed characterization regarding their thermal and physical sustainability should be performed. Additionally the required enzyme concentration to fully convert *N*-carbamoyl-β-homo amino acids should be determined.

All enzymes investigated in this work possess a wild-type activity towards chiral non-canonical *N*-carbamoyl-β-homo amino acids and thus offer particular potential for rational protein engineering, especially if a tertiary structure is available. Using the latest techniques, mutants can be produced and tested within a few weeks or months. Thus the already started protein engineering experiments for βUps 2V8H and 5I4M presented in this work should be continued. Docking experiments conducted in this work can be used as the basis for these protein engineering experiments. A more detailed analysis of these ligand dockings, e.g. calculation of van der Waals energies may give a deeper insight into the enzymatic catalysis.

The twelve enzymes investigated in this work may be used in a modified hydantoinase process for the production of β^3-amino acids. In order to complete the enzyme cascade attempts could be made to chemically produce corresponding hydantoins leading to βhAla, βhSer or βhMet. In a further step, suitable hydantoinases should be identified.

Like aromatic β-amino acids also aliphatic β-homo-amino acids show a broad application area [71]. One of the biggest challenges of the modified hydantoinase process is the low solubility of PheDU (up to 4 mM) and NCβPhe (up to 20 mM). In this work it was found that especially β-homo-amino acids are more soluble (> 100 mM). Additional heating to 40 °C to the optimal activity of newly identified enzymes would increase the solubility even more. The influence of other bivalent metal cofactors on the conversion of non-canonical *N*-carbamoyl-β-substrates is to be investigated more intensively since almost no information is available regarding this topic. Furthermore the newly identified cross-class activities, the

enantioselectivity and the enantiospecificity of the novel identified enzymes should be investigated since this was not examined in this work. Also a more detailed characterization regarding their thermal and physical sustainability should be performed. Additionally the required enzyme concentration to fully convert *N*-carbamoyl-β-homo amino acids should be determined.

All enzymes investigated in this work possess a wild-type activity towards chiral non-canonical *N*-carbamoyl-β-homo amino acids and thus offer particular potential for rational protein engineering, especially if a tertiary structure is available. Using the latest techniques, mutants can be produced and tested within a few weeks or months. Thus the already started protein engineering experiments for βUps 2V8H and 5I4M presented in this work should be continued. Docking experiments conducted in this work can be used as the basis for these protein engineering experiments. A more detailed analysis of these ligand dockings, e.g. calculation of van der Waals energies may give a deeper insight into the enzymatic catalysis.

The twelve enzymes investigated in this work may be used in a modified hydantoinase process for the production of β^3-amino acids. In order to complete the enzyme cascade attempts could be made to chemically produce corresponding hydantoins leading to βhAla, βhSer or βhMet. In a further step, suitable hydantoinases should be identified.

7 References

[1] C. Voet, Donald, Voet, Judith, Pratt, *Lehrbuch der Biochemie*, Zweite Auf. 2008.

[2] „Nomenclature and Symbolism for Amino Acids and Peptides: Recommendations 1983“, *Eur. J. Biochem.*, Bd. 138, Nr. 1, S. 9–37, 1984.

[3] P. J. Almhjell, C. E. Boville, and F. H. Arnold, „Engineering enzymes for noncanonical amino acid synthesis“, *Chem. Soc. Rev.*, Bd. 47, Nr. 24, S. 8980–8997, 2018.

[4] A. Stevenazzi, M. Marchini, G. Sandrone, B. Vergani, and M. Lattanzio, „Amino acidic scaffolds bearing unnatural side chains: An old idea generates new and versatile tools for the life sciences, *Bioorganic Med. Chem. Lett.*, Bd. 24, Nr. 23, S. 5349–5356, 2014.

[5] M. LaPlante, K., Rybak, „Daptomycin: a novel lipopeptide antibiotic against Gram-positive pathogens, *Infect. Drug Resist.*, Bd. 5, S. 2321–2331, 2004.

[6] H. Schmuck, Carsten, Wennemers, *Highlights in Bioorganic Chemistry*. 2004.

[7] L. BUCHWALDT and H. GREEN, „Phytotoxicity of destruxin B and its possible role in the pathogenesis of Alternaria brassicae, *Plant Pathol.*, Bd. 41, Nr. 1, S. 55–63, 1992.

[8] S. Engel, P. R. Jensen, and W. Fenical, „Chemical ecology of marine microbial defense, *J. Chem. Ecol.*, Bd. 28, Nr. 10, S. 1971–1985, 2002.

[9] M.-I. Steer, David, Lew, Rebecca, Perlmutter, Patrick, Smith, Ian, Aguilar, „Beta-Amino Acids: Versatile peptidomimetics, *Curr. Med. Chem.*, Bd. Volume 9, 2002.

[10] B. Ballerd, C. E.; Yu, H.; Wang, „Recent Developments in Depsipeptide Research, in *Current Medicinal Chemistry*, Volume 9,., Bentham Science Publishers, 2002.

[11] C. Shih *u. a.*, „Synthesis and biological evaluation of novel cryptophycin analogs with modification in the betaalanine region, Bd. 9, S. 69–74, 1999.

[12] K. C. Nicolaou, W. -M Dai, and R. K. Guy, „Chemistry and Biology of Taxol, *Angew. Chemie Int. Ed. English*, Bd. 33, Nr. 1, S. 15–44, 1994.

[13] D. G. I. Kingston, „Taxol, a molecule for all seasons, *Chem. Commun.*, Nr. 10, S. 867–880, 2001.

[14] D. L. Boger and H. Cai, „The binding and cleavage of DNA by bleomycin A 2 was investigated through the use of synthetic analogues.

[15] C. A. Bewley and D. J. Faulkner, „Lithistid sponges: Star performers or hosts to the stars, *Angew. Chemie - Int. Ed.*, Bd. 37, Nr. 16, S. 2162–2178, 1998.

[16] Y. Kodaira, „Taxol, *Agric. Biol. Chem.*, Bd. 25, 261–26, 1961.

[17] S. T. A. Suzuki, S. Kuyama, Y. Kodaira, „Taxol, *Agric. Biol. Chem.*, Bd. 30, 517–51, 1966.

[18] T. Ast *u. a.*, „Synthesis and biological evaluation of destruxin A and related analogs, *J. Pept. Res.*, Bd. 58, Nr. 1, S. 1–11, 2001.

[19] N. K. Gulavita, S. A. Pomponi, A. E. Wright, D. Yarwood, and M. A. Sills, „Isolation and structure elucidation of perthamide B, a novel peptide from the sponge Theonella sp., *Tetrahedron Lett.*, Bd. 35, Nr. 37, S. 6815–6818, 1994.

[20] „R. E. Summons, Phytochemistry, 20, 1125–1127 (1981).

[21] „C. J. Schofield, M. W. Walter, Amino Acids, Peptides, and Proteins, 30, 335–397 (1999).

[22] „T. H. Haskell, S. A. Fusari, R. P. Frohardt, Q. R. Bartz, J. Am. Chem. Soc., 74, 599–602

(1952).

[23] „Y. Mori, M. Tsuboi, M. Suzuki, K. Fukushima, T. Arai, J. Antibiot., 35, 543–544 (1982).

[24] „J. C. French, Q. R. Bartz, H. W. Dion, J. Antibiot., 26, 272–283 (1973.

[25] „D. E. Robertson, D. Noll, M. F. Roberts, J. Biol. Chem., 267, 14893–14901 (1992).

[26] „H. Wojciechawska, J. Ciarkowski, H. Chmara, E. Borowski, Experientia, 28, 1423–1424 (1972).

[27] „Okino, T.; Matsuda, H.; Murakami, M.; Yamaguchi, K. Tetrahedron Lett., 1993, 34, 501.

[28] N. Mimoto, T., Imai, J., Kisanuki, S., Enomoto, H., Hattori, „Kynostatin (KNI)-227 and -272, Highly Potent Anti-HIV Agents: Conformationally Constrained Tripeptide Inhibitors of HIV Protease Containing Allophenylnorstatine, *Chem. Pharm. Bull.*, Nr. 40 (8) 2251-2253 (1992), 1992.

[29] „M. C. Roy, I. I. Ohtani, J. Tanaka, T. Higa, R. Satari, Tetrahedron Lett., 40, 5373–5376 (1999).

[30] „Carter, D. C.; Moore, R. E.; Mynderse, J. S.; Niemczura, N. P.; Todd, J. S. J. Org. Chem., 1984, 49, 236.

[31] „Fülöp, F. In Studies in Natural Product Chemistry, Vol. 22, Atta-ur-Rahman, Ed., Elsevier, New York, 2000, pp. 273–306.

[32] „Crews, P.; Manes, L. V.; Boehler, M. Tetrahedron Lett., 1986, 27, 2797.

[33] „Zabriskie, T. M.; Klocke, J. A.; Ireland, C. M.; Marcus, A. H.; Molinski, T. F.; Faulkner, D. J.; Xu, C.; Clardy, J. C. J. Am. Chem. Soc., 1986, 108, 3123.

[34] „Jung, M. J. In Chemistry and Biochemistry of the Amino Acids, G. C. Barrett, Ed., Chapman and Hall, New York, 1985, p. 227.

[35] „Roers, R.; Verdine, G. L. Tetrahedron Lett., 2001, 42, 3563.

[36] „Nagai, M.; Kojima, F.; Naganawa, H.; Hamada, M.; Aoyagi, T.; Takeuchi, T. J. Antibiot., 1997, 50, 82.

[37] „Rodriguez, J.; Fernandez, R.; Quinoa, E.; Riguera, R.; Debitus, C.; Bouchet, P. Tetrahedron Lett., 1994, 35, 9239.

[38] E. Juaristi and V. A. Soloshonok, *Enantioselective Synthesis of beta-Amino Acids*, Second Edi. Wiley-Interscience, 2005.

[39] D. Seebach and J. L. Matthews, „β-Peptides: a surprise at every turn, *Chem. Commun.*, Bd. 1, S. 2015–2022, 1997.

[40] D. Seebach, A. K. Beck, and D. J. Bierbaum, „The world of β- And γ-Peptides comprised of homologated proteinogenic amino acids and other components, *Chem. Biodivers.*, Bd. 1, Nr. 8, S. 1111–1239, 2004.

[41] H. Zou *u. a.*, „Biosynthesis and biotechnological application of non-canonical amino acids: Complex and unclear, *Biotechnol. Adv.*, Bd. 36, Nr. 7, S. 1917–1927, 2018.

[42] R. Gopalakrishnakone, P., Carlini, C., Ligabue-Braun, *Plant Toxins*. Springer rederence, 2017.

[43] J. Krakauer, Y. Long, A. Kolbert, S. Thanedar, and J. Southard, „Presence of L-canavanine in hedysarum alpinum seeds and its potential role in the death of chris mccandless, *Wilderness Environ. Med.*, Bd. 26, Nr. 1, S. 36–42, 2015.

[44] V. N. Mishra *u. a.*, „Lathyrism: has the scenario changed in 2013?, *Neurol. Res.*, Bd. 36, Nr. 1, S. 38–40, 2014.

[45] W. W. Deng, S. Ogita, and H. Ashihara, „Biosynthesis of theanine-(γ-ethylamino-l-glutamic acid) in seedlings of Camellia sinensis, *Phytochem. Lett.*, Bd. 1, Nr. 2, S. 115–119, 2008.

[46] T. T. H. Nguyen, X. Bai, and H. Shim, „Next generation antibody therapeutics : bispecific antibodies and antibody-drug conjugates, *Biodesign*, Bd. 3, Nr. 4, S. 154–161, 2015.

[47] J. Horn, „Isolation of a new sulfur-containing amino acid (Lanthionine) from soduium carbonate-treated wool, *J. Biol. Chem.*, 1940.

[48] N. Sewald, „Synthetic Routes towards Enantiomerically Pure Beta-Amino Acids, *Angew. Chemie - Int. Ed.*, Bd. 42, Nr. 47, S. 5794–5795, 2003.

[49]. „R. Engeland, Ber. Dtsch. Chem. Ges., 42, 2457–2462 (1909).

[50] „H. R. Crumpler, C. E. Dent, H. Harris, R. G. Westall, Nature, 167, 307–308 (1951).

[51] „K. Fink, R. B. Henderson, R. M. Fink, Proc. Soc. Exp. Biol. Med., 78, 135–141 (1951).

[52] J. Ogawa and S. Shimizu, „β-Ureidopropionase with N-carbamoyl-α-L-amino acid amidohydrolase activity from an aerobic bacterium, Pseudomonas putida IFO 12996, *Eur. J. Biochem.*, Bd. 223, Nr. 2, S. 625–630, 1994.

[53] B. Rathinasabapathi, W. M. Fouad, and C. A. Sigua, „beta-Alanine betaine synthesis in the Plumbaginaceae. Purification and characterization of a trifunctional, S-adenosyl-L-methionine-dependent N-methyltransferase from Limonium latifolium leaves., *Plant Physiol.*, Bd. 126, Nr. 3, S. 1241–9, 2001.

[54] O. Griffith, „Beta-Amino Acids: Mammalian Metabolism and Utility as alpha-Amino Acid Analogues, *Annu. Rev. Biochem.*, Bd. 55, Nr. 1, S. 855–878, 2002.

[55] H. A. Chirpich, T., Zappia, V., Cistilow, R. N., Barker, „Lysine 2,3-Aminomutase - Purification and Properties of a Pyridixal Phosphate and S-Adenosylmethionine-activated Enzymes, *J. Biol. Chem.*, Bd. 245, Nr. 7, 1970.

[56] J. J. Fox and K. A. Watanabe, „On the Structure of Blasticidin S, a Nucleoside Antibiotic, *Tetrahedron Lett.*, Nr. 9, S. 897–904, 1966.

[57] T. P. Hettinger, Z. Kurylo-Borowska, and L. C. Craig, „the Chemistry of the Edeine Polyamine Antibiotics, *Ann. N. Y. Acad. Sci.*, Bd. 171, Nr. 3, S. 1002–1009, 1970.

[58] R. E. Summons, „Occurcence, structure and synthesis of 3-(N-Mehtylamino)glutatic acid, an amino acid from Prochloron DidemNII, Bd. 20, Nr. 5, S. 1125–1127, 1981.

[59] W. T. Ojima, I,. Lin, S., „Recent advances in the medicinal chemistry of taxoids with novel beta-amino acid side chains., *Curr. Med. Chem.*, Bd. 6, S. 927–54, 1999.

[60] M. J. Turner, W. W., & Rodriguez, *Recent advances in the medicinal chemistry of antifungal agents*, Bd. 4. 1996.

[61] Wani et al., „Plant antitumo ragents. VI. The Isolation and structure of taxol, a novel antileukemic and antitumor agent from Taxus brevifolia, 1971.

[62] N. Tanaka, H. Yamaguchi, and H. Umezawa, „Mechanism of kasugamycin action on polypeptide synthesis, *J. Biochem.*, Bd. 60, Nr. 4, S. 429–434, 1966.

[63] Z. Czajgucki, M. Zimecki, and R. Andruszkiewicz, „The immunoregulatory effects of edeine analogues in mice, *Cell. Mol. Biol. Lett.*, Bd. 12, Nr. 2, S. 149–161, 2007.

[64] L. Nezbedová, K. Drandarov, N. Deschamps, C. Werner, and M. Hesse, „Biogenesis and function of macrocyclic spermine alkaloids, *Arkivoc*, Bd. 2001, Nr. 8, S. 154, 2001.

[65] E. A. Evans, C.S., Qureshi, M.Y., Bell, *Phytochemistry*, Bd. 16, S. 565–570, 1977.

[66] S. Calve, A. J. Witten, A. R. Ocken, and T. L. Kinzer-Ursem, „Incorporation of non-canonical

amino acids into the developing murine proteome, *Sci. Rep.*, Bd. 6, Nr. March, S. 1–7, 2016.

[67] T. Baumann, J. H. Nickling, M. Bartholomae, A. Buivydas, O. P. Kuipers, and N. Budisa, „Prospects of in vivo incorporation of non-canonical amino acids for the chemical diversification of antimicrobial peptides, *Front. Microbiol.*, Bd. 8, Nr. FEB, S. 1–9, 2017.

[68] J. M. Waisvisz, M. G. Van Der Hoeven, J. Van Peppen, and W. C. M. Zwennis, „Bottromycin. I. A New Sulfur-containing Antibiotic, *J. Am. Chem. Soc.*, Bd. 79, Nr. 16, S. 4520–4521, 1957.

[69] Y. Kobayashi *u. a.*, „Bottromycin derivatives: Efficient chemical modifications of the ester moiety and evaluation of anti-MRSA and anti-VRE activities, *Bioorganic Med. Chem. Lett.*, Bd. 20, Nr. 20, S. 6116–6120, 2010.

[70] M. Igarashi *u. a.*, „Cremimycin, a Novel 19-Membered Macrocyclic Lactam Antibiotic, from Streptomyces sp., *Scanning*, Bd. 51, Nr. 2.

[71] F. Kudo, A. Miyanaga, and T. Eguchi, „Biosynthesis of natural products containing β-amino acids, *Nat. Prod. Rep.*, Bd. 31, Nr. 8, S. 1056–1073, 2014.

[72] K. SHINDO, M. KAMISHOHARA, A. ODAGAWA, M. MATSUOKA, and H. KAWAI, „Vicenistatin, a novel 20-membered macrocyclic lactam antitumor antibiotic., *J. Antibiot. (Tokyo).*, Bd. 46, Nr. 7, S. 1076–1081, 2012.

[73] Y. Huang and T. Liu, „Therapeutic applications of genetic code expansion, *Synthetic and Systems Biotechnology*. 2018.

[74] E. L. Sievers and P. D. Senter, „Antibody-Drug Conjugates in Cancer Therapy, *Annu. Rev. Med.*, Bd. 64, Nr. 1, S. 15–29, 2013.

[75] C. Yuan and R. M. Williams, „Total synthesis of the anti methicillin-resistant Staphylococcus aureus peptide antibiotics TAN-1057A-D, *J. Am. Chem. Soc.*, Bd. 119, Nr. 49, S. 11777–11784, 1997.

[76] M. Krátký *u. a.*, „Synthesis of readily available fluorophenylalanine derivatives and investigation of their biological activity, *Bioorg. Chem.*, Bd. 71, S. 244–256, 2017.

[77] J. A. Johnson, Y. Y. Lu, J. A. Van Deventer, and D. A. Tirrell, „Residue-specific incorporation of non-canonical amino acids into proteins: Recent developments and applications, *Curr. Opin. Chem. Biol.*, Bd. 14, Nr. 6, S. 774–780, 2010.

[78] P. Neumann-Staubitz and H. Neumann, „The use of unnatural amino acids to study and engineer protein function, *Curr. Opin. Struct. Biol.*, 2016.

[79] J. H. Nickling *u. a.*, „Antimicrobial Peptides Produced by Selective Pressure Incorporation of Non-canonical Amino Acids, *J. Vis. Exp.*, Nr. 135, S. 1–12, 2018.

[80] M. J. Lajoie, D. Söll, and G. M. Church, „Overcoming Challenges in Engineering the Genetic Code, *Journal of Molecular Biology*. 2016.

[81] A. Dumas, L. Lercher, C. D. Spicer, and B. G. Davis, „Designing logical codon reassignment - Expanding the chemistry in biology., *Chem. Sci.*, Bd. 6, Nr. 1, S. 50–69, 2015.

[82] M. Suchanek, A. Radzikowska, and C. Thiele, „Photo-leucine and photo-methionine allow identification of protein-protein interactions in living cells, *Nat. Methods*, Bd. 2, Nr. 4, S. 261–267, 2005.

[83] F. Li, H. Zhang, Y. Sun, Y. Pan, J. Zhou, and J. Wang, „Expanding the genetic code for photoclick chemistry in E. coli, Mammalian Cells, and A. thaliana, *Angew. Chemie - Int. Ed.*, Bd. 52, Nr. 37, S. 9700–9704, 2013.

[84] B. Wiltschi, „Incorporation of non-canonical amino acids into proteins in yeast, *Fungal Genet. Biol.*, 2016.

[85] Y. Fan, C. R. Evans, and J. Ling, „Rewiring protein synthesis: From natural to synthetic amino acids, *Biochimica et Biophysica Acta - General Subjects*. 2017.

[86] J. C. Anderson, N. Wu, S. W. Santoro, V. Lakshman, D. S. King, and P. G. Schultz, „An expanded genetic code with a funtional quadruplet codon, *PNAS*, S. 1–6, 2004.

[87] S. Bain, J.D., Switzer, C., Chamberlin, A., Benner, „Ribosome-Mediated Incorporation of a Non-Standard Amino Acid into a Peptide through expansion of the genetic code, *Lett. to Nat.*, Bd. 356, Nr. April, S. 537–539, 1992.

[88] H. Ma, X. Yang, Z. Lu, N. Liu, and Y. Chen, „The ‚gate keeper' role of Trp222 determines the enantiopreference of diketoreductase toward 2-chloro-1-phenylethanone, *PLoS One*, Bd. 9, Nr. 7, 2014.

[89] J. N. Kolev, J. M. Zaengle, R. Ravikumar, and R. Fasan, „Enhancing the efficiency and regioselectivity of P450 oxidation catalysts by unnatural amino acid mutagenesis, *ChemBioChem*, Bd. 15, Nr. 7, S. 1001–1010, 2014.

[90] Y. Ravikumar, S. P. Nadarajan, T. Hyeon Yoo, C. S. Lee, and H. Yun, „Unnatural amino acid mutagenesis-based enzyme engineering, *Trends in Biotechnology*. 2015.

[91] J. Frackenpohl, P. I. Arvidsson, J. V. Schreiber, and D. Seebach, „The Outstanding Biological Stability of β- and γ-Peptides toward Proteolytic Enzymes: An In Vitro Investigation with Fifteen Peptidases, *ChemBioChem*, Bd. 2, Nr. 6, S. 445–455, 2001.

[92] G. Guichard *u. a.*, „Melanoma peptide MART-1(27-35) analogues with enhanced binding capacity to the human class I histocompatibility molecule HLA-A2 by introduction of a β-amino acid residue: Implications for recognition by tumor-infiltrating lymphocytes, *J. Med. Chem.*, Bd. 43, Nr. 20, S. 3803–3808, 2000.

[93] C. Melo Czekster, W. E. Robertson, A. S. Walker, D. Söll, and A. Schepartz, „In Vivo Biosynthesis of a β-Amino Acid-Containing Protein, *J. Am. Chem. Soc.*, Bd. 138, Nr. 16, S. 5194–5197, 2016.

[94] K. D. Stigers, M. J. Soth, and J. S. Nowick, „Designed molecules that fold to mimic protein secondary structures, *Curr. Opin. Chem. Biol.*, Bd. 3, S. 714–723, 1999.

[95] D. Seebach, D., Ciceri, P., Overhand, M. Jaun, B., Rigo, „Probing the Helical Secondary Structure of Short-Chain-beta-Peptides, *Helv. Chim. Ac*, Bd. 79, Nr. 1, S. 2848–2856, 1996.

[96] G. Lelais and D. Seebach, „β2-Amino acids-syntheses, occurrence in natural products, and components of β-peptides, *Biopolym. - Pept. Sci. Sect.*, Bd. 76, Nr. 3, S. 206–243, 2004.

[97] E. T. Kaiser and F. J. Kezdy, „Secondary structures of proteins and peptides in amphiphilic environments (A Review), *Rev. Lit. Arts Am.*, Bd. 80, Nr. February, S. 1137–1143, 1983.

[98] Y. Hamuro, J. P. Schneider, and W. F. DeGrado, „De novo design of antibacterial β-peptides, *J. Am. Chem. Soc.*, Bd. 121, Nr. 51, S. 12200–12201, 1999.

[99] A. Oja, S., Saransaari, P., Schousboe, *Handbook of Neurochemistry and Molecular Neurobiology*. New York, 2007.

[100] K. Sasaoka, M. Kito, and Y. Onishi, „Some properties of the theanine synthesizing enzyme in tea seedlings, *Agric. Biol. Chem.*, Bd. 29, Nr. 11, S. 984–988, 1965.

[101] T. HASHIMOTO, Y. SHINOHARA, and H. HASEGAWA, „Homocysteine Metabolism, *Yakugaku Zasshi*, Bd. 127, Nr. 10, S. 1579–1592, 2007.

[102] P. Spiteller and F. Von Nussbaum, „Biosynthesis of beta-Amino Acids, in *Highlights in Bioorganic Chemistry: Methods and Applications*, 2004, S. 90–106.

[103] B. Weiner, W. Szymański, D. B. Janssen, A. J. Minnaard, and B. L. Feringa, „Recent advances in the catalytic asymmetric synthesis of beta-amino acids., *Chem. Soc. Rev.*, Bd. 39, Nr. 5, S.

1656–91, 2010.

[104] D. C. Blakemore *u. a.*, „Organic synthesis provides opportunities to transform drug discovery, *Nat. Chem.*, Bd. 10, Nr. 4, S. 383–394, 2018.

[105] „Shiraiwa, T., Shinjo, K., Kurokawa, H., Bulletin of the Chemical Society of Japan, 1991, 64.

[106] „Shiraiwa, T., Shinjo, K., Kurokawa, H., Chemistry Letters, 1989, 1413.

[107] M. J. Burk, „Handbook of Chiral Chemicals, 2nd Editio., 2005, S. 249–82.

[108] M. J. Burk, „C2-Symmetric Bis(phospholanes) and Their Use in Highly Enantioselective Hydrogenation Reactions, *J. Am. Chem. Soc.*, Bd. 113, Nr. 8518, 1991.

[109] Y. Hsiao *u. a.*, „Highly efficient synthesis of β-amino acid derivatives via asymmetric hydrogenation of unprotected enamines, *J. Am. Chem. Soc.*, Bd. 126, Nr. 32, S. 9918–9919, 2004.

[110] Y. Hamashima, N. Sasamoto, D. Hotta, H. Somei, N. Umebayashi, and M. Sodeoka, „Catalytic asymmetric addition of β-ketoesters to various imines by using chiral palladium complexes, *Angew. Chemie - Int. Ed.*, Bd. 44, Nr. 10, S. 1525–1529, 2005.

[111] U. T. Bornscheuer, G. W. Huisman, R. J. Kazlauskas, S. Lutz, J. C. Moore, and K. Robins, „Engineering the third wave of biocatalysis, *Nature*, Bd. 485, Nr. 7397, S. 185–194, 2012.

[112] A. & A. Sanchez, S., Rodriguez-Sanoja, R., Demain, „Our microbes not only produce antibiotics, they also overproduce amino acids, *J. Antibiot. (Tokyo).*, 2017.

[113] C. Reitz, Q. Fan, and P. Neubauer, „Synthesis of non-canonical branched-chain amino acids in Escherichia coli and approaches to avoid their incorporation into recombinant proteins, *Curr. Opin. Biotechnol.*, Bd. 53, S. 248–253, 2018.

[114] T. Lütke-Eversloh, C. N. S. Santos, and G. Stephanopoulos, „Perspectives of biotechnological production of L-tyrosine and its applications, *Appl. Microbiol. Biotechnol.*, Bd. 77, Nr. 4, S. 751–762, 2007.

[115] A. S. Bommarius, M. Schwarm, K. Stingl, M. Kottenhahn, K. Huthmacher, and K. Drauz, „Synthesis and use of enantiomerically pure tert-leucine, *Tetrahedron: Asymmetry*, Bd. 6, Nr. 12, S. 2851–2888, 1995.

[116] Hoechst, „Verfahren zur Biotechnischen Herstellung von L-Thienylalaninen in enantiomerenreiner Form aus 2-Hydroxy-3-thienyl-acrylsäuren and ihre Verwendung, 1999.

[117] N. J. Turner, „Ammonia lyases and aminomutases as biocatalysts for the synthesis of α-amino and β-amino acids, *Curr. Opin. Chem. Biol.*, Bd. 15, Nr. 2, S. 234–240, 2011.

[118] H. Raj *u. a.*, „Engineering methylaspartate ammonia lyase for the asymmetric synthesis of unnatural amino acids, *Nat. Chem.*, Bd. 4, Nr. 6, S. 478–484, 2012.

[119] Q. Zhou *u. a.*, „Probing the function of the Tyr-Cys cross-link in metalloenzymes by the genetic incorporation of 3-methylthiotyrosine, *Angew. Chemie - Int. Ed.*, Bd. 52, Nr. 4, S. 1203–1207, 2013.

[120] H. Gröger, O. May, H. Werner, A. Menzel, and J. Altenbuchner, „A ‚second-generation process' for the synthesis of L-neopentylglycine: Asymmetric reductive amination using a recombinant whole cell catalyst, *Org. Process Res. Dev.*, Bd. 10, Nr. 3, S. 666–669, 2006.

[121] D. Zhang, X. Chen, R. Zhang, P. Yao, Q. Wu, and D. Zhu, „Development of β-Amino Acid Dehydrogenase for the Synthesis of β-Amino Acids via Reductive Amination of β-Keto Acids, *ACS Catal.*, Bd. 5, Nr. 4, S. 2220–2224, 2015.

[122] A. Vogel, R. Schmiedel, U. Hofmann, K. Gruber, and K. Zangger, „Converting aspartase into a β-amino acid lyase by cluster screening, *ChemCatChem*, Bd. 6, Nr. 4, S. 965–968, 2014.

[123] Y. Kawata *u. a.*, „Cloning and over-expression of thermostable Bacillus sp. YM55-1 aspartase and site-directed mutagenesis for probing a catalytic residue, *Eur. J. Biochem.*, Bd. 267, Nr. 6, S. 1847–1857, 2000.

[124] R. Li *u. a.*, „Computational redesign of enzymes for regio- and enantioselective hydroamination article, *Nat. Chem. Biol.*, Bd. 14, Nr. 7, S. 664–670, 2018.

[125] B. Wu *u. a.*, „Enzymatic synthesis of enantiopure α- and β-amino acids by phenylalanine aminomutase-catalysed amination of cinnamic acid derivatives, *ChemBioChem*, Bd. 10, Nr. 2, S. 338–344, 2009.

[126] N. D. Ratnayake, C. Theisen, T. Walter, and K. D. Walker, „Whole-cell biocatalytic production of variously substituted β-aryl- and β-heteroaryl-β-amino acids, *J. Biotechnol.*, 2016.

[127] O. Buß *u. a.*, „β-Phenylalanine Ester Synthesis From Stable β-Keto Ester Substrate Using Engineered Ω-Transaminases, *Molecules*, Bd. 23, Nr. 5, S. 1–11, 2018.

[128] S. Mathew, S. P. Nadarajan, U. Sandaramoorthy, H. Jeon, T. Chung, and H. Yun, „Biotransformation of β-keto nitriles to chiral (S)-β-amino acids using nitrilase and ω-transaminase, *Biotechnol. Lett.*, Bd. 39, Nr. 4, S. 535–543, 2017.

[129] S. Mathew, H. Bea, S. P. Nadarajan, T. Chung, and H. Yun, „Production of chiral β-amino acids using ω-transaminase from Burkholderia graminis, *J. Biotechnol.*, Bd. 196–197, S. 1–8, 2015.

[130] H. Gröger, H. Trauthwein, S. Buchholz, K. Drauz, C. Sacherer, and H. Werner, „The first aminoacylase-catalyzed enantioselective synthesis of aromatic beta-amino acids, S. 1977–1978, 2004.

[131] J. Ogawa, J. Mano, and S. Shimizu, „Microbial production of optically active β-phenylalanine ethyl ester through stereoselective hydrolysis of racemic β-phenylalanine ethyl ester, *Appl. Microbiol. Biotechnol.*, Bd. 70, Nr. 6, S. 663–669, 2006.

[132] P. Anastas and N. Eghbali, „Green chemistry: Principles and practice, *Chem. Soc. Rev.*, Bd. 39, Nr. 1, S. 301–312, 2010.

[133] R. A. Sheldon and J. M. Woodley, „Role of Biocatalysis in Sustainable Chemistry, *Chem. Rev.*, Bd. 118, Nr. 2, S. 801–838, 2018.

[134] U. Engel, J. Rudat, and C. Syldatk, „The Hydantoinase Process: Recent developments for the production of non-canonical amino acids, in *Industrial biocatalysis. Ed.: P. Grunwald*, 2014.

[135] J. M. Clemente-Jiménez, S. Martínez-Rodríguez, F. Rodríguez-Vico, and F. J. L. Heras-Vázquez, „Optically pure α-amino acids production by the ‚Hydantoinase Process‘, *Recent Pat. Biotechnol.*, Bd. 2, Nr. 1, S. 35–46, 2008.

[136] M. J. Rodríguez-Alonso, J. M. Clemente-Jiménez, F. Rodríguez-Vico, and F. J. Las Heras-Vázquez, „Rational re-design of the ‚double-racemase hydantoinase process‘ for optically pure production of natural and non-natural l-amino acids, *Biochem. Eng. J.*, Bd. 101, S. 68–76, 2015.

[137] K.-E. Jaeger, A. Liese, and C. Syldatk, *Einführung in die Enzymtechnologie*. 2018.

[138] J. Ogawa and S. Shimizu, „Industrial microbial enzymes: Their discovery by screening and use in large-scale production of useful chemicals in Japan, *Curr. Opin. Biotechnol.*, Bd. 13, Nr. 4, S. 367–375, 2002.

[139] B. Wilms, A. Wiese, C. Syldatk, R. Mattes, and J. Altenbuchner, „Development of an Escherichia coli whole cell biocatalyst for the production of L-amino acids, *J. Biotechnol.*, Bd. 86, Nr. 1, S. 19–30, 2001.

[140] C. Pietzsch, Markus, Syldatk, „Hydrolysis and Formation of Hydantoins, *Enzym. Catal. Org.*

Synth., 2002.

[141] K. Makryaleas K., Drauz, „Method of Preparing D-alpha-amino acids, 4,980,284, 1990.

[142] I. Aranaz, N. Acosta, and A. Heras, „Enzymatic d-p-hydrophenyl glycine synthesis using chitin and chitosan as supports for biocatalyst immobilization, *Biocatal. Biotransformation*, Bd. 36, Nr. 2, S. 89–101, 2018.

[143] E. Ware, „The chemistry of the hydantoins, *Chem. Rev.*, Bd. 46, Nr. 3, S. 403–470, 1950.

[144] „Syldatk, C., Miller, R., Wagner, F., Biocatalytic Production of Amino Acids and Derivates Hanser Publishers, 1992, 75-128.

[145] U. Engel, „Towards a modified hydantoinase process for the chemoenzymatic production of chiral β -amino acids Substrate synthesis , screening , and characterization of novel biocatalysts.

[146] U. Engel, C. Syldatk, and J. Rudat, „Stereoselective hydrolysis of aryl-substituted dihydropyrimidines by hydantoinases, *Appl. Microbiol. Biotechnol.*, Bd. 94, Nr. 5, S. 1221–1231, 2012.

[147] A. I. Martínez-Gómez *u. a.*, „N-Carbamoyl-β-alanine amidohydrolase from Agrobacterium tumefaciens C58: A promiscuous enzyme for the production of amino acids, *J. Chromatogr. B Anal. Technol. Biomed. Life Sci.*, Bd. 879, Nr. 29, S. 3277–3282, 2011.

[148] A. I. Martinez-Gomez *u. a.*, „Potential application of N-carbamoyl-beta-alanine amidohydrolase from Agrobacterium tumefaciens C58 for beta-amino acid production, *Appl. Environ. Microbiol.*, Bd. 75, Nr. 2, S. 514–520, 2009.

[149] L. Holm and C. Sander, „An evolutionary treasure - Vast set of amido hydrolases related to urease, *Proteins Struct. Funct. Genet.*, Bd. 28, Nr. 061/20, S. 72–82, 1997.

[150] J. Ogawa and S. Shimizu, „Diversity and versatility of microbial hydantoin-transforming enzymes, *J. Mol. Catal. B Enzym.*, Bd. 2, Nr. 4–5, S. 163–176, 1997.

[151] G. D. Vogels and C. Van der Drift, „Degradation of purines and pyrimidines by microorganisms., *Bacteriol. Rev.*, Bd. 40, Nr. 2, S. 403–468, 1976.

[152] F. Groß, C., Syldatk, C., Wagner, „Screening Method For Microorganisms Producing L-Amino Acids From D,L-5-Monosubstituted Hydantoins, *Biotechnol. Tech.*, Bd. 1, Nr. 2, S. 85–90, 1987.

[153] C. Syldatk and F. Wagner, „Biotechnological production of d-or l-amino acids from 5-monosubstituted hydantoins, *Food Biotechnol.*, Bd. 4, Nr. 1, S. 87–95, 1990.

[154] R. Olivieri, E. Fascetti, L. Angelini, and L. Degen, „Microbial transformation of racemic hydantoins to D-amino acids, *Biotechnol. Bioeng.*, Bd. 23, Nr. 10, S. 2173–2183, 1981.

[155] A. Möller, C. Syldatk, M. Schulze, and F. Wagner, „Stereo- and substrate-specificity of a d-hydantoinase and a d-N-carbamyl-amino acid amidohydrolase of Arthrobacter crystallopoietes AM 2, *Enzyme Microb. Technol.*, Bd. 10, Nr. 10, S. 618–625, 1988.

[156] C. K. Lee, Z. S. Lee, and P. F. Yang, „Effect of cell membrane of Agrobacterium radiobacter on enhancing D-amino acids production from racemic hydantoins, *Enzyme Microb. Technol.*, Bd. 28, Nr. 9–10, S. 806–814, 2001.

[157] S. Wu, L. Yang, Y. Liu, G. Zhao, J. Wang, and W. Sun, „Enzymatic production of D-p-hydroxyphenylglycine from DL-5-p- hydroxyphenylhydantoin by Sinorhizobium morelens S-5, *Enzyme Microb. Technol.*, Bd. 36, Nr. 4, S. 520–526, 2005.

[158] O. May, M. Siemann, M. Pietzsch, M. Kiess, R. Mattes, and C. Syldatk, „Substrate-dependent enantioselectivity of a novel hydantoinase from Arthrobacter aurescens DSM 3745: Purification and characterization as new member of cyclic amidases, *J. Biotechnol.*, Bd. 61, Nr.

1, S. 1–13, 1998.

[159] S. Sanchez, R. Rodríguez-Sanoja, A. Ramos, and A. L. Demain, „Our microbes not only produce antibiotics, they also overproduce amino acids, *J. Antibiot. (Tokyo).*, Bd. 71, Nr. 1, S. 26–36, 2018.

[160] C. Slomka *u. a.*, „Chemical synthesis and enzymatic, stereoselective hydrolysis of a functionalized dihydropyrimidine for the synthesis of β-amino acids, *AMB Express*, Bd. 5, Nr. 1, S. 85, 2015.

[161] J. Abendroth, K. Niefind, O. May, M. Siemann, C. Syldatk, and D. Schomburg, „The structure of L-hydantoinase from Arthobacter aurescens leads to an anderstanding of dihydropyrimidinase substrate and enantio specificity, *Biochemistry*, Bd. 41, Nr. 27, S. 8589–8597, 2002.

[162] Y. H. Cheon *u. a.*, „Crystal structure of D-hydantoinase from Bacillus stearothermophilus: Insight into the stereochemistry of enantioselectivity, *Biochemistry*, Bd. 41, Nr. 30, S. 9410–9417, 2002.

[163] S. Martínez-Rodríguez and et al. Martínez-Gómez, „Carbamoylases: Characteristics and applications in biotechnological processes, *Appl. Microbiol. Biotechnol.*, Bd. 85, Nr. 3, S. 441–458, 2010.

[164] T. W. Traut, *β-Alanine Synthase an Enzyme Involved in Catabolism of Uracil and Thymine*, Bd. 324, Nr. 1987. Elsevier Masson SAS, 2000.

[165] T. Kuhara, M. Ohse, Y. Inoue, and T. Shinka, „Five cases of β-ureidopropionase deficiency detected by GC/MS analysis of urine metabolome, *J. Mass Spectrom.*, Bd. 44, Nr. 2, S. 214–221, 2009.

[166] P. Vreken *u. a.*, „cDNA cloning, genomic structure and chromosomal localization of the human BUP-1 gene encoding beta-ureidopropionase, *Biochim. Biophys. Acta*, Bd. 1447, Nr. 2–3, S. 251–257, 1999.

[167] N. Tamaki, N. Mizutani, M. Kikugawa, S. Fujimoto, and C. Mizota, „Purification and properties of beta-ureidopropionase from the rat liver., *Eur. J. Biochem.*, Bd. 169, Nr. 1, S. 21–6, 1987.

[168] a B. Van Kuilenburg, H. Van Lenthe, and a H. Van Gennip, „A radiochemical assay for beta-ureidopropionase using radiolabeled N-carbamyl-beta-alanine obtained via hydrolysis of [2-(14)C]5, 6-dihydrouracil., *Anal. Biochem.*, Bd. 272, Nr. 2, S. 250–3, 1999.

[169] A. I. Martínez-Gómez *u. a.*, „Potential application of N-carbamoyl-β-alanine amidohydrolase from Agrobacterium tumefaciens C58 for β-amino acid production, *Appl. Environ. Microbiol.*, Bd. 75, Nr. 2, S. 514–520, 2009.

[170] S. Landgren, B. Andersen, J. Piškur, and D. Dobritzsch, „Crystal structures of yeast β-alanine synthase complexes reveal the mode of substrate binding and large scale domain closure movements, *J. Biol. Chem.*, Bd. 282, Nr. 49, S. 36037–36047, 2007.

[171] S. Landgren, B. Andersen, J. Piškur, and D. Dobritzsch, „Crystal structures of yeast beta-alanine synthase complexes reveal the mode of substrate binding and large scale domain closure movements, *J. Biol. Chem.*, Bd. 282, Nr. 49, S. 36037–36047, 2007.

[172] S. Landgren, *β -Alanine Synthase : One Reaction , Two Folds and Mechanisms*. 2007.

[173] S. Landgren, Z. Gojković, J. Piškur, and D. Dobritzsch, „Yeast β-Alanine Synthase Shares A Structural Scaffold and Origin with Dizinc-dependent Exopeptidases, *J. Biol. Chem.*, Bd. 278, Nr. 51, S. 51851–51862, 2003.

[174] T. Ishikawa, K. Watabe, Y. Mukohara, and H. Nakamura, „N -Carbamyl- L -Amino Acid Amidohydrolase of Pseudomonas sp. Strain NS671: Purification and Some Properties of the

Enzyme Expressed in Escherichia coli , *Biosci. Biotechnol. Biochem.*, Bd. 60, Nr. 4, S. 612–615, 2009.

[175] S. Martínez-Rodríguez, J. M. Clemente-Jiménez, F. Rodríguez-Vico, and F. J. Las Heras-Vázquez, „Molecular cloning and biochemical characterization of L-N-carbamoylase from Sinorhizobium meliloti CECT4114, *J. Mol. Microbiol. Biotechnol.*, Bd. 9, Nr. 1, S. 16–25, 2005.

[176] J. Pozo-Dengra, A. I. Martínez-Gómez, S. Martínez-Rodríguez, J. M. Clemente-Jiménez, F. Rodríguez-Vico, and F. J. Las Heras-Vázquez, „Evaluation of substrate promiscuity of an L-carbamoyl amino acid amidohydrolase from Geobacillus stearothermophilus CECT43, *Biotechnol. Prog.*, Bd. 26, Nr. 4, S. 954–959, 2010.

[177] S. Martínez-Rodríguez *u. a.*, „Crystallization and preliminary crystallographic studies of the recombinant L-N-carbamoylase from Geobacillus stearothermophilus CECT43, *Acta Crystallogr. Sect. F Struct. Biol. Cryst. Commun.*, Bd. 64, Nr. 12, S. 1135–1138, 2008.

[178] S. Martínez-Rodríguez *u. a.*, „Mutational and structural analysis of l-N-carbamoylase reveals new insights into a peptidase M20/M25/M40 family member, *J. Bacteriol.*, Bd. 194, Nr. 21, S. 5759–5768, 2012.

[179] H. Nozaki, I. Kira, K. Watanabe, and K. Yokozeki, „Purification and properties of d-hydantoin hydrolase and N-carbamoyl-d-amino acid amidohydrolase from Flavobacterium sp. AJ11199 and Pasteurella sp. AJ11221, *J. Mol. Catal. B Enzym.*, Bd. 32, Nr. 5–6, S. 205–211, 2005.

[180] A. Louwrier and C. J. Knowles, „The purification and characterization of a novel D(-)-specific carbamoylase enzyme from an Agrobacterium sp., *Enzyme Microb. Technol.*, Bd. 19, Nr. 8, S. 562–571, 1996.

[181] W. C. Wang, W. H. Hsu, F. T. Chien, and C. Y. Chen, „Crystal structure and site-directed mutagenesis studies of N-carbamoyl-D-amino-acid amidohydrolase from Agrobacterium radiobacter reveals a homotetramer and insight into a catalytic cleft, *J. Mol. Biol.*, Bd. 306, Nr. 2, S. 251–261, 2001.

[182] R. Agarwal, S. K. Burley, and S. Swaminathan, „Structural Analysis of a Ternary Complex of Allantoate Amidohydrolase from Escherichia coli Reveals its Mechanics, *J. Mol. Biol.*, Bd. 368, Nr. 2, S. 450–463, 2007.

[183] M. Cui, M. Mihaly, Z. Hong-Xing, and X.-Y. Meng, „Molecular Docking: A powerful approach for structure-based drug discovery, *Curr. Comput. Aided. Drug Des.*, Bd. 7, Nr. 2, S. 146–157, 2011.

[184] J. Combs, S., DeLuca, S. L., DeLuca, S. H., Lemmon, G., Nannemann, D.P., Nguyen, E., Willis, J., Sheehan, J., Meiler, „Small-molecule ligand docking into comparative models with Rosetta, *Nat. Protoc.*, Bd. 8, S. 1277–1298, 2013.

[185] R. Moretti, S. Lyskov, R. Das, J. Meiler, and J. J. Gray, „Web-accessible molecular modeling with Rosetta: The Rosetta Online Server that Includes Everyone (ROSIE), *Protein Sci.*, Bd. 27, Nr. 1, S. 259–268, 2018.

[186] N. Moitessier, P. Englebienne, D. Lee, J. Lawandi, and C. R. Corbeil, „Towards the development of universal, fast and highly accurate docking/scoring methods: A long way to go, *Br. J. Pharmacol.*, Bd. 153, Nr. SUPPL. 1, S. 7–26, 2008.

[187] B. D. Rohl CA, Strauss CEM, Misura KMS, „Protein structure prediction using Rosetta, *Methods Enzym.*, Bd. 383, S. 66–93, 2004.

[188] J. Siegel, „Computational design of an enzyme catalyst for a stereoselective bimolecular Diels-Alder reaction, *Science (80-.).*, Bd. 329, S. 309–313, 2010.

[189] B. Kuhlman, „Design of a novel globular protein fold with atomic-level accuracy, *Science (80-.*

)., Bd. 302, S. 1364–1368, 2003.

[190] B. D. Davis IW, „RosettaLigand docking with full ligand and receptor flexibility., *J. Mol. Biol.*, Bd. 385, S. 381–392, 2009.

[191] B. D. Misura KMS, Chivian D, Rohl CA, Kim DE, „Physically realistic homology models built with ROSETTA can be more accurate than their templates., *Proc Natl Acad Sci USA*, Bd. 103, S. 5361–5366, 2006.

[192] B. D. Davis IW, Raha K, Head MS, „Blind docking of pharmaceutically relevant compoands using RosettaLigand, *Protein Sci.*, Bd. 18, S. 1998–2002, 2009.

[193] B. D. Das R, „Macromolecular modeling with Rosetta., *Annu Rev Biochem.*, Bd. 77, S. 363–382, 2008.

[194] J. Murciano-Calles, D. K. Romney, S. Brinkmann-Chen, A. R. Buller, and F. H. Arnold, „A Panel of TrpB Biocatalysts Derived from Tryptophan Synthase through the Transfer of Mutations that Mimic Allosteric Activation, *Angew. Chemie - Int. Ed.*, Bd. 55, Nr. 38, S. 11577–11581, 2016.

[195] U. T. Bornscheuer, „The fourth wave of biocatalysis is approaching, *Philos. Trans. R. Soc. A Math. Phys. Eng. Sci.*, Bd. 376, Nr. 2110, S. 1–7, 2018.

[196] M. Goldsmith and D. S. Tawfik, „Directed enzyme evolution: Beyond the low-hanging fruit, *Curr. Opin. Struct. Biol.*, Bd. 22, Nr. 4, S. 406–412, 2012.

[197] J. D. Bloom, M. M. Meyer, P. Meinhold, C. R. Otey, D. MacMillan, and F. H. Arnold, „Evolving strategies for enzyme engineering, *Curr. Opin. Struct. Biol.*, Bd. 15, Nr. 4, S. 447–452, 2005.

[198] C. A. Denard, H. Ren, and H. Zhao, „Improving and repurposing biocatalysts via directed evolution, *Curr. Opin. Chem. Biol.*, Bd. 25, S. 55–64, 2015.

[199] S. Lutz, „Beyond directed evolution-semi-rational protein engineering and design, *Curr. Opin. Biotechnol.*, Bd. 21, Nr. 6, S. 734–743, 2010.

[200] F. Guerrero, A. Ciragan, and H. Iwaï, „Tandem SUMO fusion vectors for improving soluble protein expression and purification, *Protein Expr. Purif.*, Bd. 116, S. 42–49, 2015.

[201] S. F. Altschul, W. Gish, W. Miller, E. W. Myers, and D. J. Lipman, „Basic local alignment search tool, *J. Mol. Biol.*, Bd. 215, Nr. 3, S. 403–410, 1990.

[202] R. Amirav-Drory, Omri, Debbi, Yogev, Nevo, „Genome Compiler. [Online]. Verfügbar unter: http://www.genomecompiler.com/.

[203] M. R. Willcott, „MestRe Nova, *J. Am. Chem. Soc.*, Bd. 131, Nr. 36, S. 13180, Sep. 2009.

[204] P. Berman, H., Westbrook, J., Feng, z., Gilliland, G., Bhat, T., Weissig, H., Shindyalov, I., Bourne, „The Protein Data Bank, *Nucleid Acids Reasearch*, Bd. 28, Nr. 1, 200n. Chr.

[205] L. A. Kelley, S. Mezulis, C. M. Yates, M. N. Wass, and M. J. E. Sternberg, „The Phyre2 web portal for protein modeling, prediction and analysis, *Nat. Protoc.*, Bd. 10, Nr. 6, S. 845–858, Juni 2015.

[206] E. Gasteiger, A. Gattiker, C. Hoogland, I. Ivanyi, R. D. Appel, and A. Bairoch, „ExPASy: The proteomics server for in-depth protein knowledge and analysis, *Nucleic Acids Res.*, Bd. 31, Nr. 13, S. 3784–3788, 2003.

[207] „PyMOL. The PyMOL Molecular Graphics System, Version 1.2r3pre, Schrödinger, LLC.

[208] „Reverse Complement. [Online]. Verfügbar unter: http://reverse-complement.com/.

[209] „SeeMS. SeeMS (64-bit) 3.0.18240.0 (28.08.2018) © 2018 Vanderbilt University.

[210] J. J. Almagro Armenteros *u. a.*, „SignalP 5.0 improves signal peptide predictions using deep neural networks, *Nat. Biotechnol.*, Bd. 37, Nr. April, 2019.

[211] „SnapGene, Nr. SnapGene® software (from GSL Biotech; available at snapgene.com).

[212] C. Notredame, D. G. Higgins, and J. Heringa, „T-coffee: A novel method for fast and accurate multiple sequence alignment, *J. Mol. Biol.*, Bd. 302, Nr. 1, S. 205–217, 2000.

[213] R. Apweiler, „The universal protein resource (UniProt) in 2010, *Nucleic Acids Res.*, Bd. 38, Nr. SUPPL.1, S. 142–148, 2009.

[214] G. Celniker *u. a.*, „ConSurf: Using evolutionary data to raise testable hypotheses about protein function, *Isr. J. Chem.*, Bd. 53, Nr. 3–4, S. 199–206, 2013.

[215] H. Ashkenazy *u. a.*, „ConSurf 2016: an improved methodology to estimate and visualize evolutionary conservation in macromolecules, *Nucleic Acids Res.*, Bd. 44, Nr. W1, S. W344–W350, 2016.

[216] H. Ashkenazy, E. Erez, E. Martz, T. Pupko, and N. Ben-Tal, „ConSurf 2010: Calculating evolutionary conservation in sequence and structure of proteins and nucleic acids, *Nucleic Acids Res.*, Bd. 38, Nr. SUPPL. 2, S. 529–533, 2010.

[217] M. Landau *u. a.*, „ConSurf 2005: The projection of evolutionary conservation scores of residues on protein structures, *Nucleic Acids Res.*, Bd. 33, Nr. SUPPL. 2, S. 299–302, 2005.

[218] F. Glaser *u. a.*, „ConSurf: Identification of functional regions in proteins by surface-mapping of phylogenetic information, *Bioinformatics*, Bd. 19, Nr. 1, S. 163–164, 2003.

[219] C. Berezin *u. a.*, „ConSeq: The identification of functionally and structurally important residues in protein sequences, *Bioinformatics*, Bd. 20, Nr. 8, S. 1322–1324, 2004.

[220] X. Robert and P. Gouet, „Deciphering key features in protein structures with the new ENDscript server, *Nucleic Acids Res.*, Bd. 42, Nr. W1, S. 320–324, 2014.

[221] T. Invitrogen, „Related products Anza ™ T4 DNA Ligase Master Mix DNA ligation protocol, Nr. May, S. 4–5, 2016.

[222] „Anza Restriction Enzyme Cloning System Cloning has never been simpler.

[223] D. J. Korbie and J. S. Mattick, „Touchdown PCR for increased specificity and sensitivity in PCR amplification, *Nat. Protoc.*, Bd. 3, Nr. 9, S. 13–15, 2008.

[224] C. J. Chiang, J. T. Chern, J. Y. Wang, and Y. P. Chao, „Facile immobilization of evolved Agrobacterium radiobacter carbamoylase with high thermal and oxidative stability, *J. Agric. Food Chem.*, Bd. 56, Nr. 15, S. 6348–6354, 2008.

[225] B. Brucher, J. Rudat, C. Syldatk, and O. Vielhauer, „Enantioseparation of Aromatic beta(A3)-Amino acid by Precolumn Derivatization with o-Phthaldialdehyde and N-Isobutyryl-l-cysteine, *Chromatographia*, Bd. 71, Nr. 11–12, S. 1063–1067, 2010.

[226] J. S. S. Clapp C. H. and J. L. Peochmann, „Identification of amino acids in unknown dipeptides: A derivatization with 9-fluorenylmethyl chloroformate and HPLC, *J. Chem. Educ.*, Bd. 69, Nr. 4, S. 122–126, 1992.

[227] J. Taillades *u. a.*, „A pH-dependent cyanate reactivity model: application to preparative N-carbamoylation of amino acids, *J. Chem. Soc. Perkin Trans. 2*, Nr. 7, S. 1247–1254, 2001.

[228] H. M. Berman *u. a.*, „The Protein Data Bank Helen, *Nucleic Acids Res.*, Bd. 28, Nr. 1, S. 235–242, 2000.

[229] M. Calull, J. Fábregas, R. M. Marcé, and F. Borrull, „Determination of free amino acids by precolumn derivatization with phenylisothiocyanate. Application to wine samples, *Chromatographia*, Bd. 31, Nr. 5–6, S. 272–276, 1991.

[230] A. Poehlein, R. Daniel, A. Bollinger, S. Thies, N. Katzke, and K. Jaeger, „First Insights into the Genome Sequence of Pseudomonas oleovorans DSM 1045, Bd. 5, Nr. 32, S. 10–11, 2017.

[231] A. Weilharter, B. Mitter, M. V. Shin, P. S. G. Chain, J. Nowak, and A. Sessitsch, „Complete genome sequence of the plant growth-promoting endophyte burkholderia phytofirmans strain PsJN, *J. Bacteriol.*, Bd. 193, Nr. 13, S. 3383–3384, 2011.

[232] C. K. Stover *u. a.*, „Complete genome sequence of Pseudomonas aeruginosa PAO1, an opportunistic pathogen., *Nature*, Bd. 406, Nr. 6799, S. 959–64, 2000.

[233] Z. Gojkovic, M. P. Sandrini, and J. Piskur, „Eukaryotic beta-alanine synthases are functionally related but have a high degree of structural diversity, *Genetics*, Bd. 158, Nr. 3, S. 999–1011, 2001.

[234] C. Wasternack, G. Lippmann, and H. Reinbotte, „Pyrimidine-degrading enzymes. Purification and properties of β-ureidopropionase of Euglena gracilis, *BBA - Enzymol.*, Bd. 570, Nr. 2, S. 341–351, 1979.

[235] M. E. Trujillo *u. a.*, „Nodulation of *Lupinus albus* by Strains of *Ochrobactrum lupini*sp . nov ., *Appl. Environ. Microbiol.*, Bd. 71, Nr. 3, S. 1318–1327, 2005.

[236] A. Ngom *u. a.*, „A novel symbiotic nitrogen-fixing member of the Ochrobactrum clade isolated from root nodules of Acacia mangiu, *J. Gen. Appl. Microbiol.*, Bd. 50, Nr. 1, S. 17–27, 2006.

[237] P. Soriano-Maldonado, F. J. Las Heras-Vazquez, J. M. Clemente-Jimenez, F. Rodriguez-Vico, and S. Martínez-Rodríguez, „Enzymatic dynamic kinetic resolution of racemic N-formyl- and N-carbamoyl-amino acids using immobilized l-N-carbamoylase and N-succinyl-amino acid racemase, *Appl. Microbiol. Biotechnol.*, Bd. 99, Nr. 1, S. 283–291, 2014.

[238] O. Buß *u. a.*, „Enantiomer discrimination in β-phenylalanine degradation by a newly isolated Paraburkholderia strain BS115 and type strain PsJN, *AMB Express*, Bd. 8, Nr. 1, 2018.

[239] P. Calero and P. I. Nikel, „Chasing bacterial chassis for metabolic engineering: a perspective review from classical to non-traditional microorganisms, *Microb. Biotechnol.*, Bd. 12, Nr. 1, S. 98–124, 2019.

[240] N. Fusetani and S. Matsunaga, „Bioactive Sponge Peptides, *Chem. Rev.*, Bd. 93, Nr. 5, S. 1793–1806, 1993.

[241] A. A., M. Hemida, and T. Ohyam, „Nitrogen Fixing Cyanobacteria: Future Prospect, *Adv. Biol. Ecol. Nitrogen Fixat.*, 2014.

[242] N. Schuergers *u. a.*, „Cyanobacteria use micro-optics to sense light direction, *Elife*, Bd. 5, S. 1–16, 2016.

[243] Y. Ikenaka, H. Nanba, Y. Yamada, K. Yajima, M. Takano, and S. Takahashi, „Screening, characterization, and cloning of the gene for N-carbamyl-D-amino acid amidohydrolase from thermotolerant soil bacteria, *Biosci. Biotechnol. Biochem.*, Bd. 62, Nr. 5, S. 882–886, 1998.

[244] M. Pearson, W., Sierk, „The limits of protein sequence comparison?, *Curr. Opin. Struct. Biol.*, Bd. 15, Nr. 3, S. 254–260, 2005.

[245] M. M. Matthews, T. W. Trauts, and N. Carolina, „Regulation of N-Carbamoyl-bet-alanine Amidohydrolase, the Terminal Enzyme in Pyrimidine Catabolism, by Ligand-induced Change in Polymerization, *Biol. Chem.*, Bd. 262, Nr. 15, S. 7232–7237, 1987.

[246] K. D. Schnackerz and D. Dobritzsch, „Amidohydrolases of the reductive pyrimidine catabolic pathway. Purification, characterization, structure, reaction mechanisms and enzyme deficiency, *Biochim. Biophys. Acta - Proteins Proteomics*, Bd. 1784, Nr. 3, S. 431–444, 2008.

[247] S. O. Ugwu and S. P. Apte, „The Effect of Buffers on Protein Conformational Stability Buffer effects on freeze drying, *86 Pharm. Technol. MARCH*, Nr. March, 2004.

[248] H. Y. Hu, W. H. Hsu, and H. R. Chien, „Characterization and phylogenetic analysis of a thermostable N-carbamoyl-L-amino acid amidohydrolase from Bacillus kaustophilus CCRC11223, *Arch. Microbiol.*, Bd. 179, Nr. 4, S. 250–257, 2003.

[249] H. Nanba, Y. Ikenaka, Y. Yamada, K. Yajima, M. Takano, and S. Takahashi, „Isolation of Agrobacterium sp. strain KNK712 that produces N-carbamyl-D-amino acid amidohydrolase, cloning of the gene for this enzyme, and properties of the enzyme, *Biosci. Biotech. Biochem.*, Bd. 62, Nr. 5. S. 875–881, 1998.

[250] S. Wu, Y. Liu, G. Zhao, J. Wang, and W. Sun, „Thermostable d-carbamoylase from Sinorhizobium morelens S-5: purification, characterization and gene expression in Escherichia coli, *Biochimie*, Bd. 88, Nr. 3–4, S. 237–244, 2006.

[251] M. Pietzsch *u. a.*, „Purification of recombinant hydantoinase and L-N-carbamoylase from Arthrobacter aurescens expressed in Escherichia coli: comparison of wild-type and genetically modified proteins, *J. Chromatogr. B Biomed. Sci. Appl.*, Bd. 737, Nr. 1–2, S. 179–186, 2000.

[252] B. Wilms, A. Wiese, C. Syldatk, R. Mattes, J. Altenbuchner, and M. Pietzsch, „Cloning, nucleotide sequence and expression of a new L-N-carbamoylase gene from Arthrobacter aurescens DSM 3747 in E. coli, *J. Biotechnol.*, Bd. 68, Nr. 2–3, S. 101–113, 1999.

[253] M. Bommarius, A., Drauz, K., Kottenhan, „Verfahren zur Herstellung von (R)-tertiär-Leucin (Degussa), 1997.

[254] S. Martínez-Rodríguez, M. Andújar-Sánchez, J. M. Clemente Jiménez, V. Jara-Pérez, F. Rodríguez-Vico, and F. J. Las Heras-Vázquez, „Thermodynamic and mutational studies of l-N-carbamoylase from Sinorhizobium meliloti CECT 4114 catalytic centre, *Biochimie*, Bd. 88, Nr. 7, S. 837–847, 2006.

[255] T. Heck *u. a.*, „Enzymatic degradation of β- and mixed α,β-oligopeptides, *Chem. Biodivers.*, Bd. 3, Nr. 12, S. 1325–1348, 2006.

[256] L. M. Johnson and S. H. Gellman, *α-Helix mimicry with α/β-peptides*, 1. Aufl., Bd. 523. Elsevier Inc., 2013.

[257] L. Jeske, S. Placzek, I. Schomburg, A. Chang, and D. Schomburg, „BRENDA in 2019: A European ELIXIR core data resource, *Nucleic Acids Res.*, Bd. 47, Nr. D1, S. D542–D549, 2019.

[258] S. Y. Chung and S. Subbiah, „A structural explanation for the twilight zone of protein sequence homology, *Structure*, Bd. 4, Nr. 10, S. 1123–1127, 1996.

[259] A. I. Gilson, A. Marshall-Christensen, J. M. Choi, and E. I. Shakhnovich, „The Role of Evolutionary Selection in the Dynamics of Protein Structure Evolution, *Biophys. J.*, Bd. 112, Nr. 7, S. 1350–1365, 2017.

[260] Q. Tang, S. Chakraborty, and G. Xu, „Mechanism of vaccinia viral protein B14-mediated inhibition of IκB kinase β activation, *J. Biol. Chem.*, Bd. 293, Nr. 26, S. 10344–10352, 2018.

[261] A. Langkilde *u. a.*, „Short strong hydrogen bonds in proteins: A case study of rhamnogalacturonan acetylesterase, *Acta Crystallogr. Sect. D Biol. Crystallogr.*, Bd. 64, Nr. 8, S. 851–863, 2008.

[262] P. A. Frey, „Review: Strong hydrogen bonding in molecules and enzymatic complexes, *Magn. Reson. Chem.*, Bd. 39, Nr. S1, S. S190–S198, 2001.

[263] G. L. Holliday, J. B. O. Mitchell, and J. M. Thornton, „Anderstanding the Functional Roles of Amino Acid Residues in Enzyme Catalysis, *J. Mol. Biol.*, Bd. 390, Nr. 3, S. 560–577, 2009.

[264] S. Landgren, Z. Gojkovic, J. Piskur, and D. Dobritzsch, „Yeast beta-Alanine Synthase Shares A Structural Scaffold and Origin with Dizinc-dependent Exopeptidases, *J. Biol. Chem.*, Bd. 278, Nr. 51, S. 51851–51862, 2003.

[265] R. Agarwal, S. K. Burley, and S. Swaminathan, „Structural Analysis of a Ternary Complex of Allantoate Amidohydrolase from Escherichia coli Reveals its Mechanics, *J. Mol. Biol.*, Bd. 368, Nr. 2, S. 450–463, 2007.

[266] C. Andreini, I. Bertini, G. Cavallaro, G. L. Holliday, and J. M. Thornton, „Metal ions in biological catalysis: From enzyme databases to general principles, *J. Biol. Inorg. Chem.*, Bd. 13, Nr. 8, S. 1205–1218, 2008.

[267] A. Buson *u. a.*, „Identification, sequencing and mutagenesis of the gene for a D-carbamoylase from Agrobacterium radiobacter, *FEMS Microbiol. Lett.*, Bd. 145, Nr. 1, S. 55–62, 1996.

[268] W. H. Hsu, F. T. Chien, C. L. Hsu, T. C. Wang, H. S. Yuan, and W. C. Wang, „Expression, crystallization and preliminary X-ray diffraction studies of N-carbamyl-D-amino-acid amidohydrolase from Agrobacterium radiobacter, *Acta Crystallogr. Sect. D Biol. Crystallogr.*, Bd. 55, Nr. 3, S. 694–695, 1999.

[269] S. Scheiner, T. Kar, and J. Pattanayak, „Comparison of various types of hydrogen bonds involving aromatic amino acids, *J. Am. Chem. Soc.*, Bd. 124, Nr. 44, S. 13257–13264, 2002.

[270] Anjana, R., Vaishnavi, M., Sherlin, D. et. al. „Aromatic-aromatic interactions in structures of proteins and protein-DNA complexes: a study based on orientation and distance, *Bioinformation*, Bd. 8, Nr. 24, S. 1220–1224, 2012.

[271] W. W. Han *u. a.*, „The substrate specificity and the catalytic mechanism of N-carbamyl-d-amino acid amidohydrolase: A theoretical investigation, *Chem. Phys. Lett.*, Bd. 472, Nr. 1–3, S. 107–112, 2009.

[272] C. Werle, „Biochemical Characterization and Structural Analysis of Decarbamoylating Enzymes for the Biocatalytic Production of Non-Canonical-Amino Acids, 2019.

8 Appendix

8.1 Figure legend

8.2 Table legend

8.3 Additionally detected enzyme activities

All biotransformations described in this section were conducted according to 3.2.3.6. Lysate was obtained resuspending 1 g wet biomass of expressed cells with 5 ml HEPES buffer. Cells were disrupted using sonification (see 3.2.3.1).

8.3.1 βUp from *L. kluyveri* (PDB: 1R3N or 2V8H*)*

βUp from *L. kluyveri* was additionally tested on activity towards several *N*-carbamoyl-α-L-amino acids using enzyme lysate. Initial substrate concentration was 5 mM each. Reactions were performed over night at 30 °C pH 8 and 1000 rpm and stopped after 20 h by protein denaturation at 95 °C for 5 min. An overview of the results is given in Table 56. The bigger and more unpolar the amino acid residue the lower was the detected activity.

Table 56: Activity of βUp from *L. kluyveri* towards *N*-carbamoyl-α-L-amino acids.
"+" = 0.1-1 mM substrate conversion; "++" = 1-4 mM substrate conversion; "+++" = > 4 mM substrate conversion. Reactions were performed over night at 30 °C and 1000 rpm with enzyme lysate and stopped after 20 h by protein denaturation at 95 °C for 5 min. Initial substrate concentration was 5 mM. "-" = Without additional cofactor.

Substrate	Tested Cofactors	Substrate degradation
Aliphatic		
N-carbamoyl-α-L-glycine		+++ (all conditions)
N-carbamoyl-α-L-serine		+++ (all conditions)
N-carbamoyl-α-L-aminobutyric acid		+++ (all conditions)
N-carbamoyl-α-L-cysteine	-, $ZnCl_2$, $NiCl_2$,	+++ (-)
N-carbamoyl-α-L-valine	$MnCl_2$, $CoCl_2$	++ ($NiCl_2$, $MnCl_2$)
N-carbamoyl-α-L-isoleucine		++ ($NiCl_2$, $MnCl_2$)
N-carbamoyl-α-L-leucine		+ ($CoCl_2$)
N-carbamoyl-α-L-methionine		++ ($MnCl_2$)
Aromatic		
N-carbamoyl-α-L-phenylalanine	-, $ZnCl_2$, $CoCl_2$	-
N-carbamoyl-α-L-phenyglycine	-, $ZnCl_2$, $CoCl_2$	-
N-carbamoyl-α-L-hydroxy phenyglycine	-, $ZnCl_2$, $CoCl_2$	-
Rac N-carbamoyl-α-L-Tryptophan	-, $ZnCl_2$, $CoCl_2$	-

8.3.2 βUp from *P. aeruginosa*

Additionally for P.aeru the conversion of NCβAla was investigated regarding to its velocity. Therefore 10 mM of NCβAla were dissolved in 100 mM HEPES buffer pH 8. Reactions were

performed at 40 °C and 1000 rpm in a volume of 700 µl with a final concentration of 2 mM $MnCl_2$ in triplicates. Reactions were mixed using a liquid handling station. P.aeru was FPLC-purified with a final concentration of 0.9 µg/µl in the reaction. Reactions were started by manually addition of the enzyme. As negative control a reaction without enzyme was carried in triplicate. A product control with 10 mM was also carried in triplicate. After 5, 10 and 15 min 100 µl of the reaction solution were mixed with 10 µl of 2 M HCl and analysed *via* Ehrlich-assay and HPLC. Results are given in

Table 57: Turnover of NCβAla by P.aeru after 5, 10 and 15 min.
Reactions were incubated at 40 °C and pH 8 in 100 mM HEPES buffer with 2 mM $MnCl_2$ and 0.9 µg/µl purified P.aeru final concentration. Reactions were stopped by mixing 100 µl of the reaction mixture with 10 µl 2 M HCl. Samples were taken after 5, 10 and 15 min.

Substrate	**Cofactor**	**Substrate concentration (mM) after**			
		0 min	**5 min**	**10 min**	**15 min**
N-carbamoyl-β-alanine	$MnCl_2$	9.59 ± 0,03	0.52 ± 0.08	0 ± 0	0 ± 0
Product		**Product concentration (mM) after**			
β-alanine	$MnCl_2$	**0 min**	**5 min**	**10 min**	**15 min**
		9.36 ± 0.1	5.45 ± 0.1	9.31± 0.2	9.65 ± 0.1

8.3.3 D-Carb from *R. radiobacter* (PDB: 1FO6)

1FO6 (PDB) from *R. radiobacter* was tested on activity towards *N*-carbamoyl-α-D-amino acids using enzyme lysate. Initial substrate concentration was 10 mM each. Reactions were performed over night at 37 °C pH 7 and 1000 rpm and stopped after 20 h by protein denaturation at 95 °C for 5 min. An overview of the results is given in Table 58.

Table 58: Activity of 1FO6 from *R. radiobacter* towards *N*-carbamoyl-α-D-amino acids.
"+++" = Full conversion of 10 mM substrate. Reactions were performed over night at 37 °C and 1000 rpm with enzyme lysate and stopped after 20 h by protein denaturation at 95 °C for 5 min. Initial substrate concentration was 10 mM. "-" = Without additional cofactor.

Substrate	**Tested Cofactors**	**Substrate degradation**
N-carbamoyl-α-D-para-hydroxy-phenylglycine	-, $CoCl_2$	+++ (-)
N-carbamoyl-α-D-tyrosine		+++ (-)

8.3.4 L-Carb from *G. stearothermophilus* (PDB: 3N5F)

3N5F (PDB) from *G. stearothermophilus* was tested on activity towards *N*-carbamoyl-α-L-amino acids using enzyme lysate. Initial substrate concentration was 5 mM each. Reactions were performed over night at 65 °C pH 7 and 1000 rpm and stopped after 20 h by protein denaturation at 95 °C for 5 min. An overview of the results is given in Table 59.

Table 59: Activity of 3N5F from *G. stearothermophilus* towards *N*-carbamoyl-α-L-amino acids.
"+" = 0.1-1 mM substrate conversion; "++" = 1-3 mM substrate conversion; "+++" = > 4 mM substrate conversion. Reactions were performed over night at 65 °C and 1000 rpm with enzyme lysate and stopped after 20 h by protein denaturation at 95 °C for 5 min. Initial substrate concentration was 5 mM.

Substrate	Tested Cofactors	Substrate degradation
N-carbamoyl-α-L-valine	$CoCl_2$	+++
N-carbamoyl-α-L-methionine		++

8.3.5 βUps Burk1, Burk 2 and Burk 3 from *B. phytofirmans* and βUp P.oleo from *P. oleovorans*

βUps Burk1, Burk 2 and Burk 3 from *B. phytofirmans* and βUp P.oleo from *P. oleovorans* were additionally investigated on their conversion of several chiral *N*-carbamoyl-α-substrates using enzyme lysate. Reactions were performed dissolving 10 mM of each substrate in 50 mM HEPES pH7 and incubating reactions at 30 °C and 1000 rpm for 20 h. Substrate controls without enzyme and product controls for monitoring product degradation by the corresponding enzyme were also carried. Reactions were performed without and with MnCl2 as cofactor (2 mM final concentration). Reactions were conducted mixing 400 µl of substrate solution with 100 µl lysate in duplicates using a liquid handling station. Reactions were stopped by 5 min denaturation at 95 °C. After centrifugation for 10 min at 13.000 rpm supernatant was analysed with Ehrlich-Assay and HPLC. An overview of the tested chiral N-carbamoyl-α-substrates for βUps Burk1, Burk 2 and Burk 3 P.oleo is given in Table 60. Percentage amounts of converted substrate and formed product were calculated in relation to the detected amount of substrate in substrate controls after 20 h. Standard deviations were lower than 0.1 % and thus negligible. For canonical amino acids α-L-serine and α-L-methionine strong product degradation in product controls was observed. Substrate decay was not observed in substrate controls.

Table 60: Activity of βUps Burk1, Burk 2 and Burk 3 and P.oleo towards chiral *N*-carbamoyl-α-substrates.
Reactions were performed dissolving 10 mM of each substrate in 50 mM HEPES pH 7 and incubating reactions at 30 °C and 1000 rpm for 20 h. $MnCl_2$ was added with 2 mM final concentration. Converted amount of substrate and formed product was calculated in relation to amount of substrate in substrate controls detected after 20 h.

		Enzyme			
Substrate / product	**Cofactor**	**Burk1**	**Burk2**	**Burk3**	**P. oleo**
		Converted substrate [%]			
N-carbamoyl-α-L-phenylalanine	-	0	0	3 ± 0	5 ± 0
	$MnCl_2$	22 ± 0	17 ± 0	9 ± 0	18 ± 0
N-carbamoyl-α-L-tryptophan	-	5 ± 0	2 ± 0	5 ± 0	3 ± 0
	$MnCl_2$	14 ± 0	15 ± 0	16 ± 0	11 ± 0
N-carbamoyl-α-L-serine	-	40 ± 0	22 ± 0	17 ± 0	54 ± 0
	$MnCl_2$	100 ± 0	99 ± 0	98 ± 0	99 ± 0
N-carbamoyl-α-L-methionine	-	12 ± 0	12 ± 0	8 ± 0	8 ± 0
	$MnCl_2$	99 ± 0	98 ± 0	91 ± 0	53 ± 0
N-carbamoyl-α-L-leucine	-	8 ± 0	9 ± 0	11 ± 0	11 ± 0
	$MnCl_2$	8 ± 0	9 ± 0	16 ± 0	15 ± 0
		Formed product [%]			
α-L-phenylalanine	-	0	0	0	0
	$MnCl_2$	16 ± 0	3 ± 0	0	1 ± 0
α-L-tryptophan	-	0	0	0	0
	$MnCl_2$	0	0	0	0
α-L-serine	-	0	0	0	0
	$MnCl_2$	100 ± 0	99 ± 0	98 ± 0	99 ± 0
α-L-methionine	-	0	0	0	0
	$MnCl_2$	69 ±	74 ± 0	66 ± 0	38 ± 0
α-L-leucine	-	0	0.5 ± 0	0	0.3 ± 0
	$MnCl_2$	3 ± 0	1 ± 0	1 ± 0	2 ± 0

8.4 Gene sequences

Gene sequences of novel decarbamoylating enzymes used in this work (see Table 4 p. 48 for accession numbers). Restriction site marked for BamHI (GGATCC) and HindIII (AAGCTT) marked in grey.

>Burk 1 (Acc.: NC_010681.1:304 1700-3042980, Chromosome 1; 95749.51 Da.):

GCACTCTGGTGGATCCATGAATGCAGTTAGCGAAGCACTGAAACATGCAGAACCGACCACCAGTATTAAAGTT
GATGGTAAACGTCTGTGGGATAGCCTGATGACCATGGCAAAAATTGGTGCAACCCCGAAAGGTGGTGTTTGTC
GTCTGGCACTGACCGATCTGGATAAAGAAGGTCGCGATCTGATTGTTAGCTGGGCAAAAGAAGCAGGTTGTAC
CGTTAGCGTTGATCAGATGGGTAATGTTTTTATGCGTCGTGCAGGTCGTAATCCGGCAGCACTGCCGGTTATGA
CCGGTAGCCATGCAGATAGCCAGCCGACCGGTGGTCGTTTTGATGGTATTTATGGTGTTTTAGGTGGCCTGGAA
GTTATTCGTAGCCTGAACGATCATGGTATTGAAACCGAACATCCGGTTGAAGTTGTTATTTGGACCAATGAAGA
AGGTAGCCGTTTTGCACCGGCAATGGTTGCAAGCGGTGTTTTTGCGGGTGTTTTTACCCTGGATTATGGTCTGA
GCCGTAAAGATGTGGATGGTAAAACCATTGGTGAAGAACTGGAACGTATTGGTTATGCCGGTGATATTCCGTG
TGGTGGTCGTCCGCTGCATGCCGCATTTGAACTGCATATTGAACAGGGTCCGATTCTGGAAGCAGAACAGAAA
ACAATTGGTGTTGTTACCGATGCACAGGGTCAGCGTTGGTATGAAATTACCCTGACAGGTCAAGAAGCACACG
CAGGTCCGACACCGATGCCTCGTCGTCGTGATGCACTGCTGGGTGCAGCACGTGTTGTTGATCTGGTTAATCGT
ATTGGTCTGGATAATGCACCGTTTGGTTGTGCAACCGTGGGTATGATGCAGGTTTATCCGAATAGCCGTAATGT
TATTCCGGGTCGTGTGTTTTTTACCGCAGATTTTCGTCATCCTGATGATGCAGTTCTGGCCAAAATGGATGCAGC
CCTGCGTAAAGGTGTTGCAGATATTGCAAATGGTATCGGTCTGGAAACCGAGCTGGAACAAATTTTCTATTATG
CACCGGTTGCATTTGATGAAGCCTGTGTTAAAAGCGTTCGTGCAGCAGCAGAACGTTTTGGCTATCCGCATCGT
AATATGGTTAGCGGTGCAGGTCATGATGCATGTTATCTGAGCCAGGTTGCACCGACCAGCATGGTTTTTGTTCC
GTGTGTTGATGGCATTAGCCATAACGAAATTGAAGATGCAACCTTTGAATGGATTGAAGCGGGTGCAAATGTA
CTGCTGCATGCAATGCTGGAACGTGCATGTGAACCGGTTAGCTAAAAGCTTAATGCATATG

>Burk 2 (Acc.: NC_010676.1:286 1449-2862729, Chromosome 2; 95115.88 Da.):

GCACTCTGGTGGATCCATGCAGGTTCATGAAAGCACCACCGTTGCAACCTTTGCCGATCTGCGTGTTGATGGTG
CACGTCTGTGGGATAGCCTGATGCAGCTGGCACGTATTGGTGCAACCGATAAAGGTGGTGTTTGTCGTCTGGCA
CTGACCGAACTGGATCGTGAAGCACGTGACCTGTTTATTGCATGGGCAAAAGAAATTGGTTGTAGCGTTCGTGT
GGATGCCATTGGTAACATTTTTGCACGTCGTGCAGGTCTGCGTGATGATCTGCCTCCGGTTATGACCGGTAGCC
ATATTGATACCCAGCCGACCGGTGGTAAATTTGATGGTAATTATGGTGTTCTGGCAGGTCTGGAAGTTCTGCGT
ACCCTGACCGATGCAAATGTTCAGACCCTGGCACCGCTGGAAGTTGCAGTTTGGACCAATGAAGAAGGTAGCC
GTTTTGTTCCGGTGATGATGGGTAGCGGTGTTTTTGCCGGTGCATTTACCCTGGCGCATGCACTGGAACAGCAT
GATCGCGAAGGTATTACCGTTCGTGATGCCCTGGCTCGCATTGGTTATGCCGGTGAAATTACCAAACCGCATGC
AGTTGGTGCATATTTTGAAGCCCATATTGAACAGGGTCCTGTTCTGGAAGCACATGATAAAACCATTGGTGTTG
TTCAGGGTGCACTGGGTCAGCGTTGGTATGATGTTACCGTTCATGGTATGGAAGCGCATGCAGGTCCGACACC
GATGGAACTGCGTCGTGATGCACTGCTGGTTGCAGCAGATCTGATTCATGCAGTTAATCGTATTGCACTGGATC
ATGCACCGCATGGTCGTGGCACCGTTGGTTGGCTGGATGTTCATCCGAATAGCCGTAATGTTATTCCGGGTCGT
GTTACCCTGACAGTTGACCTGCGTGCAGCCGATGATGCAACACTGACCGCCATGGATAGCGCACTGCGTGCCG
CATGTGCAGTTGCAAGCGAAAAAACCGGCATTACCGTTGATGTTGAACAGGTTGTTTATTTTCCGCCTCAGCCG
TTTGCAGCCGAACTGGTTGGTGCAGTTAAACAGGGTGCAGATACCCTGGGTTTTAGCAGCATGGATGTTATTAG
CGGTGCAGGTCATGATGCAGTTTATCTGGCACGTGTGGCACCGGCAGCAATGATTTTTGTGCCGTGTAAAGATG
GCATTAGCCACAACGAAATTGAAGATGCACGTGCCGATCATCTGGAAGCCGGTTGTAATGTTCTGCTGCAGGC
AATGCTGAATGCAGCACAGAAAGCAGGTAGCGCAGATGCATAAAAGCTTAATGCATATG

>Burk 3 (Acc.: NC_010676.1:304 405-305643, Chromosome 2; 92691.08 Da.):

GCACTCTGGTGGATCCATGAAAGATCTGCGTATTGATGGTGAACGTCTGTGGCGTAGCCTGATGGATCTGGCA
GCAATTGGTGCAACCCCGAAAGGTGGTGTTAAACGTCTGGCACTGACCGAACTGGATAAACAGGGTCGTGATC
TGGTTGTTAGCTGGGGTCGTGCAGCAGGTCTGGCAATTACCGTTGATCGTATTGGTAACATTTTTATGCGTCGT
GCAGGCACCGATCCGGATGCACCGCCTGTTGCAAGCGGTAGCCATATTGATACCCAGCCGACCGGTGGTAAAT
TTGATGGTAATTATGGTGTTCTGGCAGCCCTGGAAGTTATGCGTACCCTGGATGATGCCGGTGTTAAAACCTGT
GCACCGCTGGAAGTTGCAATTTGGACCAATGAAGAAGGTAGCCGTTTTGTTCCGGTTATGATGGGTAGCGGTG

TTTTTTGTGGTGCATTTACCCTGGAACATGCATATGCCGCACGTGATATTGAAGGTAAACGTGTTCGTGATGAA
CTGGAAGCCATTGGTTATCTGGGTGATGAAGAACCGGGTAAACATCCGCTGGGTGCATATTTTGAAGCACATA
TTGAACAGGGTCCAGTGCTGGAAGATGAAGGCAAAGTTATTGGTGTTGTTCCGGGTGTGCTGGGTCTGAGCTG
GTATGATTGTGAAGTTCGTGGTATGGAAGCACATGCAGGTCCGACACCGATGGCAATTCGTAAAGATGCACTG
CAGGTTGCGACCCGTGTTATGCAAGAAGTTGTTGCAATTGCCAATCGTTATCCGCCTTATGGTCGTGGCACCGT
TGGTTTTGTTCAGACCTTTCCGAATAGCCGTAATGTTATTCCGGGTAGCGTGAAATTTTCAATTGATCTGCGCAA
TGTTAATGACGCACTGCTGAATCAGATGCATGATGAAATGCTGGCATTTATTGATCGTACCCAGAGCGAAAGC
GGTCTGAGCATTGGTATTGAACGTGTTAGCTATTATCGTCCGTGTGAATTTCATCCGCAGTGTGTTGATGCAGTT
CGTCGTGCAACCGGTGCACTGGGTTATCCGACCATGGATGTTGTTAGCGGTGCAGGTCATGATGCCGTTTATAC
CGCACGTGTTGCACCGTCAGGTATGATTTTTGTGCCGTGTAAAGATGGCATTAGCCACAACGAAATTGAAGAT
GCACGTAGCGATCATCTGGAAGCAGGTTGTAATGTTCTGCTGCATAGCATGCTGGAACGTGCCGGTCAGGTTA
GCTAAAAGCTTAATGCATATG

>Burk 4 (Acc.: NC_010681.1:554 74-56766, Chromosome 1; 95129.54 Da.):

GCACTCTGGTGGATCCATGAGCACCTATAGCATTCCGAGCAGCCCGATTGCAGTTAATCTGCCGGATGCAGAT
GCAATTAGCGAATTTGATGCACTGTTTCGTGCAACCAGCGCAATTGGTGTTACCAGTGCCGGTGGTCTGCATCG
TCTGGCAGCAAGCGAAGAGGATGGTCGTGTTCGTGATCTGCTGCGTGATTGGCTGGTTCGTCATGGTTTTCATG
TTCAGGTTGATCGTGTTGGTAACCTGTTTGGTCTGGTTACCTTTGATCCGAGCGCACCGTATGTGCTGTGTGGTA
GCCATCTGGATAGCCAGCCGAGCGCAGGTCGTTTTGATGGTGTTTATGGTGTTCTGGCAGGCGCAGTTGCAATT
GCCGGTATTGCACGTCGTCTGCGTGAACGTGGTGTTCGTCCGCCTTGTAATCTGGCAGTTGTTGATTGGACCAA
TGAAGAAGGTGCACGTTTTCAGCCGAGCCTGACCGGTAGCAGCGTTTTTACCGGTGCACTGAGCGTTGATGAT
GCCCTGGCATGTACCGATGCACAGGGCATTACCCTGTGTCAGGCACTGGAACGTATTGGTTATCTGGGTGAAG
AAATGCTGGATATTCCGGTTGCAGCATATGTTGAAACCCATGTTGAACAGGGTGAACGTCTGGAACGTGAGCA
GATTAGCATTGGTGTTGTTCGTGAAACCTGGGCAGCACTGAAACTGCGTGTTCGCTTTGATGGCGAACAGAGCC
ATACCGGTCCGACACCGATGGATCAGCGTCGTGACGCACTGCGTGCAGCAGCACGTGCCATTAGCGCAGTTTA
TAGCGAAGTTGGTAAACATGGTGATCAGATGCATGGTAGCGTTGGTCGTCTGGATGTTTATCCGAATAGCCCG
AATGTTGTTCCGAGCAAAGCAACCCTGTATGTTGAATTTCGTAGCCTGAGCACCGATCGTCTGGAAGATGTGGG
TAAACGTTTTGCACAGATTCTGGATGATATTGCAGCACAGACCGGTACACATGTTGAAGTTGAAAGCCGTCAG
CTGCGTGCTCCGGTTGCGCTGGATTCACGTCTGGCACAGTGTGCACATGATGTTTGCCGTAGCCTGGGTCTGCG
TAGCGTTGATAGCGTTACCGTTGCAGGTCATGATGCAATTTCACTGAGCCGTACCGTTCCGAGCTGTCTGCTGT
TTATTCCGAGCCATCGTGGTATTGCCCATAATGAAGCAGAATTTACCGAAGAGGCCGATCTGCATAATGGTCTG
CGTGCCCTGAGCGCACTGCTGGAAACCCTGTGTGTTACAACCCAGAATAGCCGTTAAAAGCTTAATGCATATG

>Burk 5 (Acc.: NC_010676.1:169 451-170692; 94032.05 Da.):

GCACTCTGGTGGATCCATGGTTCGTATTGATCCTGATCGTCTGCTGAGCGATCTGAAACAGCTGCGTAGCTTTG
GTGCAACCGGTCCGGGTGTTGTTCGTCTGGCACTGAGTCCGGTTGATCTGGCAAGCCGTGAATGGCTGGCAGGT
CGTATGACCGAAGCAGGTCTGGAAGCAGCAATTGATGGTGTTGGCACCGTTTTTGGTCGTAGCCGTAAAAGCG
GTCCGGCACTGGTTATTGGTAGCCATACCGATACACAGCCGACCGGTGGTTGGCTGGATGGTGCAATGGGTGT
TATTTATGGTCTGGAAATTGCACGTGCCCTGGCAGAAAATGAAGCAACCCGTCATCTGGCAGTTGATGTTGCAA
GCTGGATTGATGAAGAAGGCACCTTTAGCGGTCTGCTGGGTAGCCGTAGTTTTGTTGGTGAAAATGTTGATGAA
ACCATTCGTGATGCAACCAATCGTCAGGGTCAGCGTCTGGCAGATGTTCTGGCAACCGCAGGCCTGGCAGGCC
GTCCGCGTGCACGTTTTGAACCGGGTCGTCAGGTTGCATATCTGGAACCGCATATTGAACAAGGTGGTCGCCTG
GAAGCCGCAGGTAAAAGCATTGGTGTTGTTACCACCATTGTTGGTCTGCGTGAACTGCGTCTGCGTTTTACCGG
TCAGCGTAATCATGCAGGTACAACCCCGATGGCAATTCGTCGTGATGCCGGTGCAGCACTGGTTGCATTTATTC
CGCAGATGAATGAAGCATTTGCACAGCTGGCCGATGCAGATACCGTTTGGACCGTTGGTCGCATTGATTTAGAT
CCGGGTAGCCTGAGCGTTGTTCCGGGTGCAGCCCAGATGTATCTGCAGTTTCGTGACGCAAATGCAGCACGTCT
GCAGGCAATGGAAGATCGTCTGGCCCAGCTGGTTCGTGATTTTAATGCACGTAGCAGCATTAGCGTTGAACTG
ACCACAATTGATGAACCGATGCAGCCGGTTACCATGCATACCGTTCTGGCCGATCACCTGGCACGTGCGGCAG
AAGCAGTTGCACCTGGTCAGTGGATTCGTATGCCGAGCGGTGCCGCACATGATGCACAGGTTATTGCACGTTGT
ATGCCTGCATGTATGATGTTTGTTCCGAGTATTGGTGGTGTGAGCCATGATTTTATTGAAGATACCGCAGAAGC
CCATATTGTTCTGGGTTGCCAGGTTGCAGCCACCGCAGCAGCAGCAATGCTGGAAGAACAGTGGGCAAAACGT
AGCTAAAAGCTTAATGCATATG

>P.oleo (Acc.: NIUB01000001.1: 76233-77522; 96139.55 Da.):

GCACTCTGGTGGATCCATGACCATGAATACCGCAACCGAAGTTCTGCAGAGCAGCCAGCCGCATGTTAATGGT
GAACGTCTGTGGCAGAGCCTGATGGAACTGGCACAGCTGGGTGCAACCGTTAAAGGTGGTGTTTGTCGTCTGG
CACTGACCGATCTGGATCGTCAGGCACGTGACCTGTTTGTTCGTTGGTGTGAAGAAGCAGGTTGTACCGTTACC

GTTGATGGTGTTGGTAACATTTTTGCACGTCGTCCGGGTCGTAATGCAGCACTGGCACCGGTTATGACCGGTAG
TCATATTGATACCCAGCCGACCGGTGGTAAATTTGATGGTTGTTTTGGTGTTCTGGCAGGCGTTGAAGTGCTGC
GTACCCTGAATGATCTGGGTGTTCAGACCGAAGCACCGCTGGAAGTTGTTGTTTGGACCAATGAAGAAGGTAG
CCGTTTTGCACCGTGTATGATGGGTAGCGGTGTTTTTGCAGAAAAATTCACCCTGGAAGAAACCCTGGCAAAA
CGTGATGCCGAAGGTATTAGCGTTGGTGAAGCACTGAATGCAATTGGTTATGCAGGTCCGCGTGCAGTTACAG
GTCATGCAGTTGGTGCATATTTCGAAGCACATATTGAACAGGGTCCGATTCTGGAAGATCAGGGTAAAACCAT
TGGTGTTGTTCTGGGTGCACTGGGTCAGAAATGGTTTGATCTGACCCTGAAAGGTGTTGAAGCACATGCCGGTC
CGACACCGATGCATCTGCGTAAAGATGCACTGGTTGGTGCAGCAGCAGTTGTTGCAGCAGTTAATCGTGTTGC
ACTGGAACATCAGCCTCATGCATGTGGCACCGTTGGTTGTCTGCAGGCATATCCGGGTAGCCGTAATGTTATTC
CGGGTGAAGTTCGTATGACCCTGGATTTTCGTCATCTGCAGCCGGAACGTCTGGATAGCATGATTGAAGCAGTT
CGTGGTGTTATTGAAGCAACCTGTGCAAAACATGGTCTGTCATTTGAACTGACCCCGACCGCAGATTTTCCGCC
TCTGTATTTTGATCAGGGTTGTGTGGAAGCCGTGCGTGGTGCCGCAGCCGGTCTGGGTCTGAGCCATATGGATA
TTGTTAGCGGTGCAGGTCATGATGCCATTTTTCTGGCAGAACTGGGTCCTGCAGGTATGATTTTTGTTCCGTGTG
AAGGTGGTATTAGCCACAACGAAATTGAAAATGCCGCACCGACAGATCTGGCAGCCGGTTGTGCAGTTCTGCT
GCGTGCAATGCTGGCAGCAAGCGTTGCCCTGGCAGAAGGTAAACTGGCAGCATAAAAGCTTAATGCATATG

>P.aeru (Acc.: NC_002516.2:498420-499703 Pseudomonas aeruginosa PAO1 chromosome, complete genome)

ATGAGCACTGCCCGGAACGTCCTGCAATCCACCCAGCGACACATCGATGGCCAGCGCCTCTGGCAATCGC
TGATGGATCTCGCCCGCCTCGGCGCCACCGCCAAGGGTGGGGTCTGCCGCCTGGCCCTGAGCGATCTCGA
CCGCCAGGCCCGCGATCTCTTCGTGCAATGGTGCGAAGCGGCCGGCTGCACGGTCAGCGTCGATCGGGTC
GGCAACATCTTCGCCCGTCGTCCCGGGCGTAACCCGGACTTGCCCCCGGTGATGACCGGTAGCCACATCG
ACACCCAGCCCACCGGTGGCAAGTTCGACGGCTGCTTCGGGGTGATGGCCGGCCTCGAGGTGATCCGCAC
CCTCAACGACCTCGGGGTGGAAACCGAGGCGCCGCTGGAGGTGGTGGTGTGGACCAACGAGGAAGGCTCG
CGCTTCGCGCCCTGCATGATGGGCTCGGGCGTATTCGCCGGGAAGTTCACCCTGGAGGAGACCCTGGCCA
AGCGCGATGCCGACGGTGTCAGCGTAGGCGAGGCGCTGGACGCCATCGGCTACGCGGGAGCGCGCGATTG
TCTCGGACATCCGGTGGGCGCCTATTTCGAGGCGCACATCGAACAGGGGCCGATCCTCGAGGACGAGGAG
AAGACCATCGGCGTGGTGCTCGGCGCGCTCGGGCAGAAATGGTTCGACCTGTCCCTGCGCGGCGTCGAGG
CACACGCCGGGCCAACGCCGATGCACCTGCGCAAGGATGCCCTGGTCGGTGCCGCGGCGGTGGTCGAGGC
GGTCAATCGCGCGGCCCTCGGCCATCAGCCGCATGCTTGCGGCACGGTCGGCTGCCTGCACGCCTATCCC
GGTTCGCGCAACGTGATACCCGGCGAAGTGAAGATGACCCTGGACTTCCGCCATCTGCAACCGGAGCGCC
TGGACTCGATGATCGCCGAGGTCCGCCAGGTGATCGCCGCTACCTGCGAGAAGCATGGCTTGCAATACGA
GCTGGTGCCGACCGCCGATTTCCCGCCGCTGTACTTCGACCAGGGATGCGTCGGCGCGGTGCGCGAGGCG
GCGCAGGCGCTGGGCATGCCGCAGATGGACATCGTCAGCGGCGCCGGCCACGACGCGATCTTCCTCGCCG
AACTCGGTCCGGCGGGGATGATCTTCGTGCCCTGCGAGAACGGCATCAGCCACAACGAGATCGAGAACGC
CAGCCCCGACGACCTGGCCGCCGGCTGCGCGGTGCTGTTGCGGGCCATGCTCAAGGCCTCCGAGGCGATC
GCCGGCGGCCGCCTGGCGGCCTGA

>3N5F (UniProt Q53389.1)

ATTCAGGGTGAACGTCTGTGGCAGCGTCTGATGGAACTGGGTGAAGTTGGTAAACAGCCGAGCGGTGGTGTTA
CCCGTCTGAGCTTTACAGCCGAAGAACGTCGTGCAAAAGATCTGGTTGCAAGCTATATGCGTGAAGCAGGTCT
GTTTGTTTATGAAGATGCAGCAGGTAATCTGATCGGTCGTAAAGAAGGCACCAATCCGGACGCAACCGTTGTT
CTGGTTGGTAGCCATCTGGATAGCGTTTATAATGGTGGTTGTTTTGATGGTCCGCTGGGTGTTCTGGCAGGCGT
TGAAGTTGTTCAGACCATGAATGAACATGGTGTTGTTACCCATCATCCGATTGAAGTGGTTGCATTTACCGATG
AAGAAGGTGCACGTTTTCGTTTTGGTATGATTGGTAGCCGTGCAATGGCAGGCACCCTGCCTCCGGAAGCACTG
GAATGTCGTGATGCAGAAGGTATTAGCCTGGCAGAAGCAATGAAACAGGCAGGTCTGGACCCGGATCGTCTGC
CGCAGGCAGCACGTAAACCGGGTACAGTTAAAGCATATGTTGAACTGCATATTGAACAGGGTCGTGTTCTGGA
AGAAACCGGTCTGCCGGTTGGTATTGTTACCGGTATTGCCGGTCTGATTTGGGTGAAATTTACCATTGAAGGTA
AAGCAGAACATGCCGGTGCAACCCCGATGAGCCTGCGTCGTGATCCGATGGCAGCAGCAGCACAGATTATTAT
CGTTATTGAAGAAGAAGCACGTCGTACCGGCACCACCGTTGGTACAGTTGGTCAGCTGCATGTTTATCCTGGTG
GTATTAATGTTATTCCGGAACGTGTTGAATTTGTGCTGGATCTGCGTGATCTGAAAGCCGAAGTTCGTGATCAG
GTTTGGAAAGCAATTGCAGTTCGTGCAGAAACCATTGCCAAAGAACGTAATGTTCGTGTTACCACCGAACGTC
TGCAAGAAATGCCTCCGGTTCTGTGTAGTGATGAAGTTAAACGTGCAGCAGAAGCAGCCTGTCAGAAACTGGG
TTATCCGAGCTTTTGGCTGCCGAGTGGTGCAGCACATGATAGCGTTCAGCTGGCACCGATTTGTCCGATTGGCA
TGATTTTTGTTCGTAGCCAGGATGGTGTTAGCCATAGTCCGGCAGAATGGTCAACCAAAGAAGATTGCGCAGC
AGGCGCAGAAGTTCTGTATCATACCGTTTGGCAGCTGGCCCAGGGTTAA

>1FO6 (UniProt Q44185)

ACCCGCCAGATGATTCTGGCCGTGGGTCAGCAGGGCCCGATTGCACGTGCAGAAACCCGTGAACAGGTGGTGG
GTCGTCTGCTGGATATGCTGACCAATGCAGCCAGTCGTGGTGTTAATTTTATTGTGTTTCCGGAACTGGCCCTG
ACCACCTTTTTCCCGCGTTGGCATTTTACCGATGAAGCAGAACTGGATAGTTTTTATGAAACCGAAATGCCGGG
CCCGGTTGTGCGCCCGCTGTTTGAAACCGCAGCCGAACTGGGTATTGGCTTTAATCTGGGTTATGCCGAACTGG
TTGTTGAAGGCGGTGTGAAACGTCGTTTTAATACCAGTATTCTGGTTGATAAAAGCGGTAAAATTGTTGGTAAA
TACCGCAAAATTCACCTGCCGGGTCATAAAGAATATGAAGCATATCGCCCGTTTCAGCATCTGGAAAAACGCT
ATTTTGAACCGGGCGATCTGGGTTTTCCGGTTTATGATGTTGATGCAGCCAAAATGGGCATGTTTATTTGCAAT
GATCGTCGTTGGCCGGAAACCTGGCGTGTGATGGGTCTGAAAGGTGCAGAAATTATTTGTGGCGGCTATAATA
CCCCGACCCATAATCCGCCGGTGCCGCAGCATGATCATCTGACCAGCTTTCATCATCTGCTGAGCATGCAGGCA
GGTAGCTATCAGAATGGTGCCTGGAGTGCAGCAGCAGGTAAAGTTGGCATGGAAGAAGGCTGTATGCTGCTGG
GCCATAGTTGTATTGTGGCCCCGACCGGTGAAATTGTTGCACTGACCACCACCCTGGAAGATGAAGTGATTACC
GCAGCCCTGGATCTGGATCGTTGCCGTGAACTGCGTGAACATATTTTTAATTTTAAGGCACACCGTCAGCCGCA
GCATTATGGTCTGATTGCCGAATTTTAA

>2V8H (Acc.: AF333185.1:1207- 2574)

GGATCCATGAGCAAAGATGTTAGCAGCACCATTACCACCGTTAGCGCAAGTCCGGATGGCACCCTGAATCTGC
CTGCAGCAGCACCGCTGAGCATTGCAAGCGGTCGTCTGAATCAGACCATTCTGGAAACCGGTAGCCAGTTTGG
TGGTGTTGCACGTTGGGGTCAAGAAAGCCATGAATTTGGTATGCGTCGTCTGGCAGGCACCGCACTGGATGGT
GCAATGCGTGATTGGTTTACCAATGAATGTGAAAGCCTGGGTTGCAAAGTGAAAGTGGATAAAATTGGCAATA
TGTTCGCAGTGTATCCGGGTAAAAATGGTGGTAAACCGACCGCAACCGGTAGTCATCTGGATACCCAGCCGGA
AGCAGGTAAATATGATGGTATTCTGGGTGTTCTGGCAGGTCTGGAAGTTCTGCGTACCTTTAAAGATAATAACT
ACGTGCCGAACTATGATGTTTGCGTTGTTGTGTGGTTTAATGAAGAAGGTGCACGTTTTGCACGTAGCTGTACC
GGTAGCAGTGTTTGGAGCCATGATCTGAGCCTGGAAGAGGCATATGGCCTGATGAGCGTTGGTGAAGATAAAC
CGGAAAGCGTTTATGATAGCCTGAAAAACATTGGCTATATTGGTGATACACCGGCAAGCTATAAAGAAAACGA
AATCGATGCACACTTTGAGCTGCATATTGAACAGGGTCCGATTCTGGAAGATGAAAACAAAGCAATTGGTATT
GTTACCGGTGTGCAGGCATATAATTGGCAGAAAGTTACCGTTCATGGTGTTGGTGCACATGCAGGTACAACCC
CGTGGCGTCTGCGTAAAGATGCACTGCTGATGAGCAGCAAAATGATTGTTGCAGCAAGCGAAATTGCACAGCG
TCATAATGGTCTGTTTACCTGCGGTATTATTGATGCAAAACCGTATAGCGTGAACATCATTCCGGGTGAAGTTA
GCTTTACCCTGGATTTTCGTCATCCGAGTGATGATGTTCTGGCCACCATGCTGAAAGAAGCAGCAGCAGAATTT
GATCGCCTGATCAAAATTAACGATGGTGGTGCACTGAGCTATGAAAGCGAAACCCTGCAGGTTAGTCCGGCAG
TTAATTTTCATGAAGTTTGCATTGAATGCGTTAGCCGTAGCGCATTTGCACAGTTCAAAAAAGATCAGGTTCGT
CAGATTTGGAGCGGTGCAGGTCATGATAGCTGCCAGACCGCACCGCATGTTCCGACCAGCATGATTTTTATCCC
GAGTAAAGATGGTCTGAGCCACAACTATTATGAATATAGCAGTCCGGAAGAAATCGAGAACGGTTTTAAAGTT
CTGCTGCAAGCCATCATCAACTATGATAACTATCGTGTGATTCGCGGTCATAAGCTT

>5I4M (Acc.: CP020395.1:51154 1-512821)

CATGGACGCAGTTAGCGAAACCGCAAAACGTGCAGCACTGGATACCAGCATTAAAGTTGATGGTCGTCGTCTG
TGGGATAGCCTGATGGAAGTTGCAAAAATTGGTGCAACCCCGAAAGGTGGTGTTTGTCGTCTGGCACTGACCG
ATCTGGATAAAGCAGCACGTGATCTGATTGTTGGTTGGGCAAAAGCAGCAGGTTGTACCGTTACCGTTGATAC
CATGGGTAATGTTTTTATGCGTCGTGCAGGTCGTGTTGCAGATGCAGCACCGGTTGTTACCGGTAGCCATGCAG
ATAGCCAGCCGACCGGTGGTCGTTTTGATGGTATTTATGGTGTTTTAGGTGGCCTGGAAGTTATTCGTAGCCTG
AATGATCATGGTATCGAAACCGAACATCCGGTTGAAGTTGTTATTTGGACCAATGAAGAAGGTAGCCGTTTTG
CACCGGCAATGGTTGCAAGCGGTGTTTTTGCGGGTGTTTTTCCGCTGGAATATGGTCTGAGCCGTAAAGATGTT
GATGGTAAAACCATTGGTGAAGAACTGGCACGTATTGGTTATGCCGGTGATGCACCGTGTGGTGGTCGTAAAC
TGCATGCCGCATTTGAACTGCATATTGAACAGGGTCCGATTCTGGAAGCAGAATGCAAAACAATTGGTGTTGT
GACCGATGCACAGGGTCAGCGTTGGTATGAAATTACCTTTACCGGTCAAGAAGCACACGCAGGTCCGACACCG
ATGCCTCGTCGTCGTGATGCACTGCTGGGTGCAAGCCGTGTTGTTGATCTGGTTAATCGTATTGGTCTGGATCA
TGCACCGTATGGCTGTGCAACCGTGGGTATGATGCAGGTTCATCCGAATAGCCGTAATGTTATTCCGGGTCGTG
TGTTTTTTACCGTGGATTTTCGTCATCCTGATGATGCAGTTCTGGCAAAAATGGATGCAGCCCTGCGTGATGGT
GTTGCCCGTATTGCAGCAGATATTGGCCTGGATACCGCACTGGAACAAATTTTCTATTATGCACCGATTGCATT
TGATAGCGCATGTGTTGCAGCAGTTCGTGCAGCAGCAGATCGTTTTGGTTATAGCCATCGTGATATTGTTAGCG
GTGCAGGTCATGATGCATGTTATCTGGCACAGGTTGCACCGACCAGCATGGTTTTTGTTCCGTGTATTGATGGC
ATTAGCCACAACGAAATTGAAGATGCCACACCGGCATGGATTGAAGCAGGCGCAAATGTTCTGCTGCATGCAA
TGCTGAGCCGTGCATGTGAACCGGTTAGCTAAA

>1Z2L (UniProt: P77425)

ATTACCCATTTTCGTCAGGCAATTGAAGAAACCCTGCCGTGGCTGAGCAGCTTTGGTGCAGATCCGGCAGGCG
GTATGACCCGTCTGCTGTATAGTCCGGAATGGCTGGAAACCCAGCAGCAGTTCAAAAAACGTATGGCAGCAAG
CGGTCTGGAAACACGTTTTGATGAAGTTGGTAATCTGTATGGTCGTCTGAATGGCACCGAATATCCGCAAGAA
GTTGTTCTGAGCGGTAGCCATATTGATACCGTTGTTAATGGTGGCAATCTGGATGGTCAGTTTGGTGCACTGGC
AGCATGGCTGGCAATTGATTGGCTGAAAACACAGTATGGTGCACCGCTGCGTACCGTTGAAGTTGTTGCAATG

GCAGAAGAAGAAGGTAGCCGTTTTCCGTATGTTTTTTGGGGTAGCAAAAACATTTTTGGTCTGGCAAATCCGGA
TGATGTGCGCAATATTTGTGATGCAAAAGGCAATAGCTTTGTGGATGCAATGAAAGCATGTGGTTTTACCCTGC
CGAACGCACCGCTGACACCGCGTCAGGATATTAAAGCATTTGTTGAACTGCATATTGAACAGGGTTGTGTGCT
GGAAAGCAATGGTCAGAGCATTGGTGTTGTGAATGCAATTGTTGGTCAGCGTCGTTATACCGTTACACTGAATG
GTGAAAGCAATCATGCAGGTACAACCCCGATGGGTTATCGTCGCGATACCGTTTATGCATTTAGCCGTATTTGT
CATCAGAGCGTGGAAAAAGCAAAACGCATGGGTGATCCGCTGGTTCTGACCTTTGGTAAAGTTGAACCGCGTC
CGAATACCGTTAATGTTGTTCCGGGTAAAACAACCTTTACCATTGATTGTCGTCATACCGATGCAGCCGTTCTG
CGTGATTTTACACAGCAGCTGGAAAATGATATGCGTGCAATCTGTGATGAAATGGATATTGGCATTGATATCG
ATCTGTGGATGGATGAAGAACCGGTGCCGATGAATAAAGAACTGGTTGCGACCCTGACCGAACTGTGTGAACG
TGAAAAACTGAATTATCGTGTTATGCATAGCGGTGCAGGTCATGATGCACAGATTTTTGCACCGCGTGTTCCGA
CCTGTATGATTTTTATCCCGAGCATTAATGGCATCAGCCATAATCCGGCAGAACGTACCAATATCACCGATCTG
GCAGAAGGTGTTAAAACCCTGGCACTGATGCTGTATCAGCTGGCATGGCAGAAATAA

8.5 Protein sequences

Amino acids sequences of all investigated enzymes (see Table 4 p. 48 for accession numbers).

>Poleo_OWK49263.1 Hydantoin utilization protein C [Pseudomonas oleovorans subsp. oleovorans]

MTMNTATEVLQSSQPHVNGERLWQSLMELAQLGATVKGGVCRLALTDLDRQARDLFVRWCEEAGCTVTVDGVG
NIFARRPGRNAALAPVMTGSHIDTQPTGGKFDGCFGVLAGVEVLRTLNDLGVQTEAPLEVVVWTNEEGSRFAPCM
MGSGVFAEKFTLEETLAKRDAEGISVGEALNAIGYAGPRAVTGHAVGAYFEAHIEQGPILEDQGKTIGVVLGALGQ
KWFDLTLKGVEAHAGPTPMHLRKDALVGAAAVVAAVNRVALEHQPHACGTVGCLQAYPGSRNVIPGEVRMTLD
FRHLQPERLDSMIEAVRGVIEATCAKHGLSFELTPTADFPPLYFDQGCVEAVRGAAAGLGLSHMDIVSGAGHDAIFL
AELGPAGMIFVPCEGGISHNEIENAAPTDLAAGCAVLLRAMLAASVALAEGKLAA

>Burk1_WP_012433677.1 Zn-dependent hydrolase [Paraburkholderia phytofirmans]
MNAVSEALKHAEPTTSIKVDGKRLWDSLMTMAKIGATPKGGVCRLALTDLDKEGRDLIVSWAKEAGCTVSVDQM
GNVFMRRAGRNPAALPVMTGSHADSQPTGGRFDGIYGVLGGLEVIRSLNDHGIETEHPVEVVIWTNEEGSRFAPAM
VASGVFAGVFTLDYGLSRKDVDGKTIGEELERIGYAGDIPCGGRPLHAAFELHIEQGPILEAEQKTIGVVTDAQGQR
WYEITLTGQEAHAGPTPMPRRRDALLGAARVVDLVNRIGLDNAPFGCATVGMMQVYPNSRNVIPGRVFFTADFRH
PDDAVLAKMDAALRKGVADIANGIGLETELEQIFYYAPVAFDEACVKSVRAAAERFGYPHRNMVSGAGHDACYLS
QVAPTSMVFVPCVDGISHNEIEDATFEWIEAGANVLLHAMLERACEPVS

>Burk2_WP_012428372.1 Zn-dependent hydrolase [Paraburkholderia phytofirmans] beta-alanine synthase
MQVHESTTVATFADLRVDGARLWDSLMQLARIGATDKGGVCRLALTELDREARDLFIAWAKEIGCSVRVDAIGNIF
ARRAGLRDDLPPVMTGSHIDTQPTGGKFDGNYGVLAGLEVLRTLTDANVQTLAPLEVAVWTNEEGSRFVPVMMG
SGVFAGAFTLAHALEQHDREGITVRDALARIGYAGEITKPHAVGAYFEAHIEQGPVLEAHDKTIGVVQGALGQRWY
DVTVHGMEAHAGPTPMELRRDALLVAADLIHAVNRIALDHAPHGRGTVGWLDVHPNSRNVIPGRVTLTVDLRAA
DDATLTAMDSALRAACAVASEKTGITVDVEQVVYFPPQPFAAELVGAVKQGADTLGFSSMDVISGAGHDAVYLAR
VAPAAMIFVPCKDGISHNEIEDARADHLEAGCNVLLQAMLNAAQKAGSADA

>Burk3_WP_012426153.1 Zn-dependent hydrolase [Paraburkholderia phytofirmans]
MKDLRIDGERLWRSLMDLAAIGATPKGGVKRLALTELDKQGRDLVVSWGRAAGLAITVDRIGNIFMRRAGTDPDA
PPVASGSHIDTQPTGGKFDGNYGVLAALEVMRTLDDAGVKTCAPLEVAIWTNEEGSRFVPVMMGSGVFCGAFTLE
HAYAARDIEGKRVRDELEAIGYLGDEEPGKHPLGAYFEAHIEQGPVLEDEGKVIGVVPGVLGLSWYDCEVRGMEA
HAGPTPMAIRKDALQVATRVMQEVVAIANRYPPYGRGTVGFVQTFPNSRNVIPGSVKFSIDLRNVNDALLNQMHD
EMLAFIDRTQSESGLSIGIERVSYYRPCEFHPQCVDAVRRATGALGYPTMDVVSGAGHDAVYTARVAPSGMIFVPC
KDGISHNEIEDARSDHLEAGCNVLLHSMLERAGQVS

>Burk4_WP_012431152.1 Allantoate Amidohydrolase
MSTYSIPSSPIAVNLPDADAISEFDALFRATSAIGVTSAGGLHRLAASEEDGRVRDLLRDWLVRHGFHVQVDRVGNL
FGLVTFDPSAPYVLCGSHLDSQPSAGRFDGVYGVLAGAVAIAGIARRLRERGVRPPCNLAVVDWTNEEGARFQPSL
TGSSVFTGALSVDDALACTDAQGITLCQALERIGYLGEEMLDIPVAAYVETHVEQGERLEREQISIGVVRETWAALK
LRVRFDGEQSHTGPTPMDQRRDALRAAARAISAVYSEVGKHGDQMHGSVGRLDVYPNSPNVVPSKATLYVEFRSL
STDRLEDVGKRFAQILDDIAAQTGTHVEVESRQLRAPVALDSRLAQCAHDVCRSLGLRSVDSVTVAGHDAISLSRT
VPSCLLFIPSHRGIAHNEAEFTEEADLHNGLRALSALLETLCVTTQNSR

>Burk5_WP_012426027.1 Zn-dependent hydrolase [Paraburkholderia phytofirmans] Allantoate amidohydrolase, beta-alanine synthase
MVRIDPDRLLSDLKQLRSFGATGPGVVRLALSPVDLASREWLAGRMTEAGLEAAIDGVGTVFGRSRKSGPALVIGS
HTDTQPTGGWLDGAMGVIYGLEIARALAENEATRHLAVDVASWIDEEGTFSGLLGSRSFVGENVDETIRDATNRQG
QRLADVLATAGLAGRPRARFEPGRQVAYLEPHIEQGGRLEAAGKSIGVVTTIVGLRELRLRFTGQRNHAGTTPMAIR
RDAGAALVAFIPQMNEAFAQLADADTVWTVGRIDLDPGSLSVVPGAAQMYLQFRDANAARLQAMEDRLAQLVR
DFNARSSISVELTTIDEPMQPVTMHTVLADHLARAAEAVAPGQWIRMPSGAAHDAQVIARCMPACMMFVPSIGGV
SHDFIEDTAEAHIVLGCQVAATAAAAMLEEQWAKRS

>Paeru_AAG03833.1 N-carbamoyl-beta-alanine amidohydrolase [Pseudomonas aeruginosa PAO1]
MSTARNVLQSTQRHIDGQRLWQSLMDLARLGATAKGGVCRLALSDLDRQARDLFVQWCEAAGCTVSVDRVGNIF
ARRPGRNPDLPPVMTGSHIDTQPTGGKFDGCFGVMAGLEVIRTLNDLGVETEAPLEVVVWTNEEGSRFAPCMMGS
GVFAGKFTLEETLAKRDADGVSVGEALDAIGYAGARDCLGHPVGAYFEAHIEQGPILEDEEKTIGVVLGALGQKWF
DLSLRGVEAHAGPTPMHLRKDALVGAAAVVEAVNRAALGHQPHACGTVGCLHAYPGSRNVIPGEVKMTLDFRHL
QPERLDSMIAEVRQVIAATCEKHGLQYELVPTADFPPLYFDQGCVGAVREAAQALGMPQMDIVSGAGHDAIFLAEL
GPAGMIFVPCENGISHNEIENASPDDLAAGCAVLLRAMLKASEAIAGGRLAA

>SklβUp_Q96W94
GSMSKDVSSTITTVSASPDGTLNLPAAAPLSIASGRLNQTILETGSQFGGVARWGQESHEFGMRRLAGTALDGAMR
DWFTNECESLGCKVKVDKIGNMFAVYPGKNGGKPTATGSHLDTQPEAGKYDGILGVLAGLEVLRTFKDNNYVPN
YDVCVVVWFNEEGARFARSCTGSSVWSHDLSLEEAYGLMSVGEDKPESVYDSLKNIGYIGDTPASYKENEIDAHFE
LHIEQGPILEDENKAIGIVTGVQAYNWQKVTVHGVGAHAGTTPWRLRKDALLMSSKMIVAASEIAQRHNGLFTCGII
DAKPYSVNIIPGEVSFTLDFRHPSDDVLATMLKEAAAEFDRLIKINDGGALSYESETLQVSPAVNFHEVCIECVSRSA
FAQFKKDQVRQIWSGAGHDSCQTAPHVPTSMIFIPSKDGLSHNYYEYSSPEEIENGFKVLLQAIINYDNYRVIRGHKL
*

>5I4M_A4JQA0
MDAVSETAKRAALDTSIKVDGRRLWDSLMEVAKIGATPKGGVCRLALTDLDKAARDLIVGWAKAAGCTVTVDTM
GNVFMRRAGRVADAAPVVTGSHADSQPTGGRFDGIYGVLGGLEVIRSLNDHGIETEHPVEVVIWTNEEGSRFAPAM
VASGVFAGVFPLEYGLSRKDVDGKTIGEELARIGYAGDAPCGGRKLHAAFELHIEQGPILEAECKTIGVVTDAQGQR
WYEITFTGQEAHAGPTPMPRRRDALLGASRVVDLVNRIGLDHAPYGCATVGMMQVHPNSRNVIPGRVFFTVDFRH
PDDAVLAKMDAALRDGVARIAADIGLDTALEQIFYYAPIAFDSACVAAVRAAADRFGYSHRDIVSGAGHDACYLA
QVAPTSMVFVPCIDGISHNEIEDATPAWIEAGANVLLHAMLSRACEPVS*

>3N5F_Q53389.1
IQGERLWQRLMELGEVGKQPSGGVTRLSFTAEERRAKDLVASYMREAGLFVYEDAAGNLIGRKEGTNPDATVVLV
GSHLDSVYNGGCFDGPLGVLAGVEVVQTMNEHGVVTHHPIEVVAFTDEEGARFRFGMIGSRAMAGTLPPEALECR
DAEGISLAEAMKQAGLDPDRLPQAARKPGTVKAYVELHIEQGRVLEETGLPVGIVTGIAGLIWVKFTIEGKAEHAGA
TPMSLRRDPMAAAAQIIIVIEEEARRTGTTVGTVGQLHVYPGGINVIPERVEFVLDLRDLKAEVRDQVWKAIAVRAE
TIAKERNVRVTTERLQEMPPVLCSDEVKRAAEAACQKLGYPSFWLPSGAAHDSVQLAPICPIGMIFVRSQDGVSHSP
AEWSTKEDCAAGAEVLYHTVWQLAQG*

>1Z2L_P77425
ITHFRQAIEETLPWLSSFGADPAGGMTRLLYSPEWLETQQQFKKRMAASGLETRFDEVGNLYGRLNGTEYPQEVVL
SGSHIDTVVNGGNLDGQFGALAAWLAIDWLKTQYGAPLRTVEVVAMAEEEGSRFPYVFWGSKNIFGLANPDDVRN
ICDAKGNSFVDAMKACGFTLPNAPLTPRQDIKAFVELHIEQGCVLESNGQSIGVVNAIVGQRRYTVTLNGESNHAGT
TPMGYRRDTVYAFSRICHQSVEKAKRMGDPLVLTFGKVEPRPNTVNVVPGKTTFTIDCRHTDAAVLRDFTQQLEND
MRAICDEMDIGIDIDLWMDEEPVPMNKELVATLTELCEREKLNYRVMHSGAGHDAQIFAPRVPTCMIFIPSINGISHN
PAERTNITDLAEGVKTLALMLYQLAWQK*

>1FO6_Q44185
TRQMILAVGQQQGPIARAETREQVVGRLLDMLTNAASRGVNFIVFPELALTTFFPRWHFTDEAELDSFYETEMPGPVV
RPLFETAAELGIGFNLGYAELVVEGGVKRRFNTSILVDKSGKIVGKYRKIHLPGHKEYEAYRPFQHLEKRYFEPGDL
GFPVYDVDAAKMGMFICNDRRWPETWRVMGLKGAEIICGGYNTPTHNPPVPQHDHLTSFHHLLSMQAGSYQNGA
WSAAAGKVGMEEGCMLLGHSCIVAPTGEIVALTTTLEDEVITAALDLDRCRELREHIFNFKAHRQPQHYGLI
AEF*

8.6 Plasmid maps

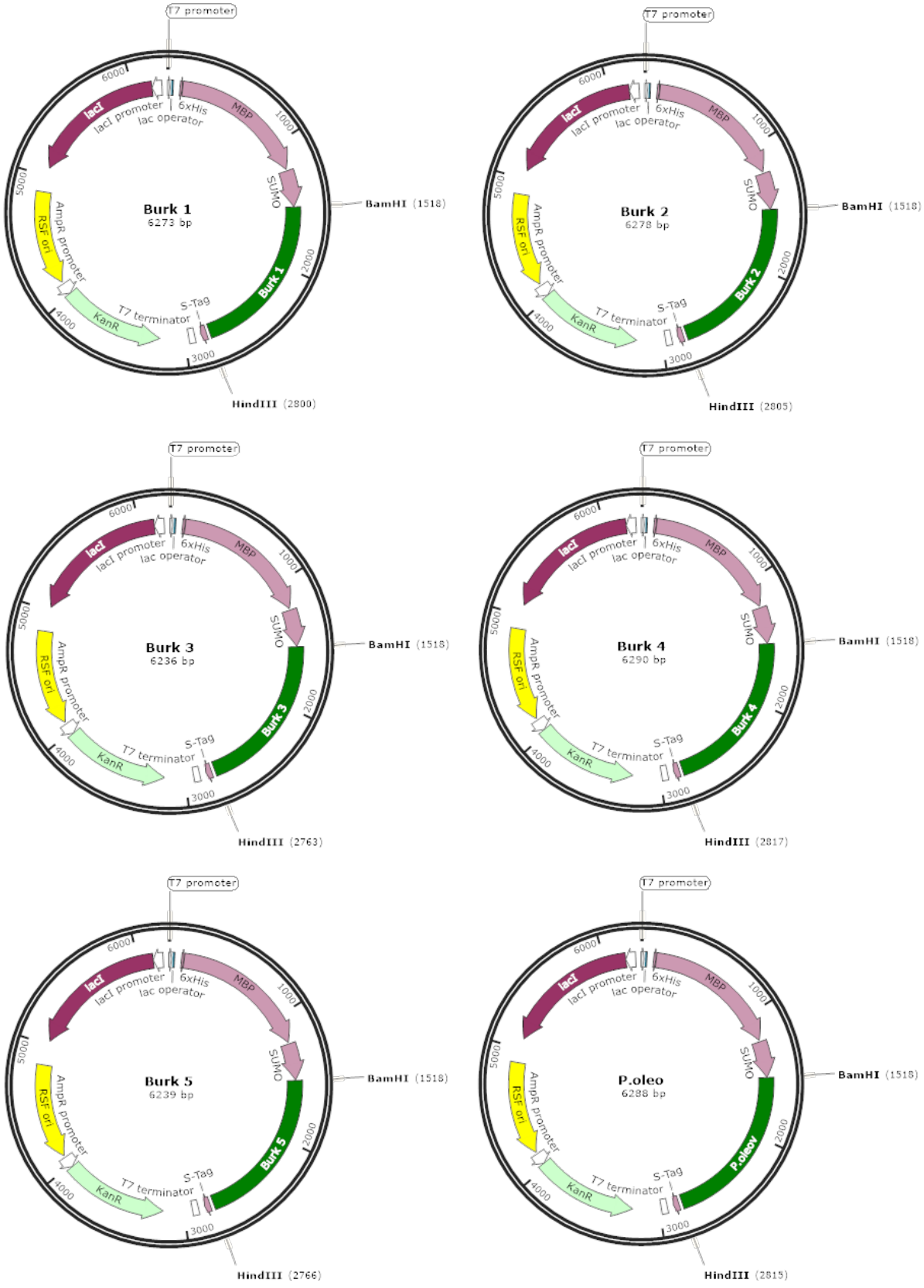

Figure 63: Plasmid maps of Burk1-5 and P.oleo
All genes are cloned into pLJSRSF7 vector.

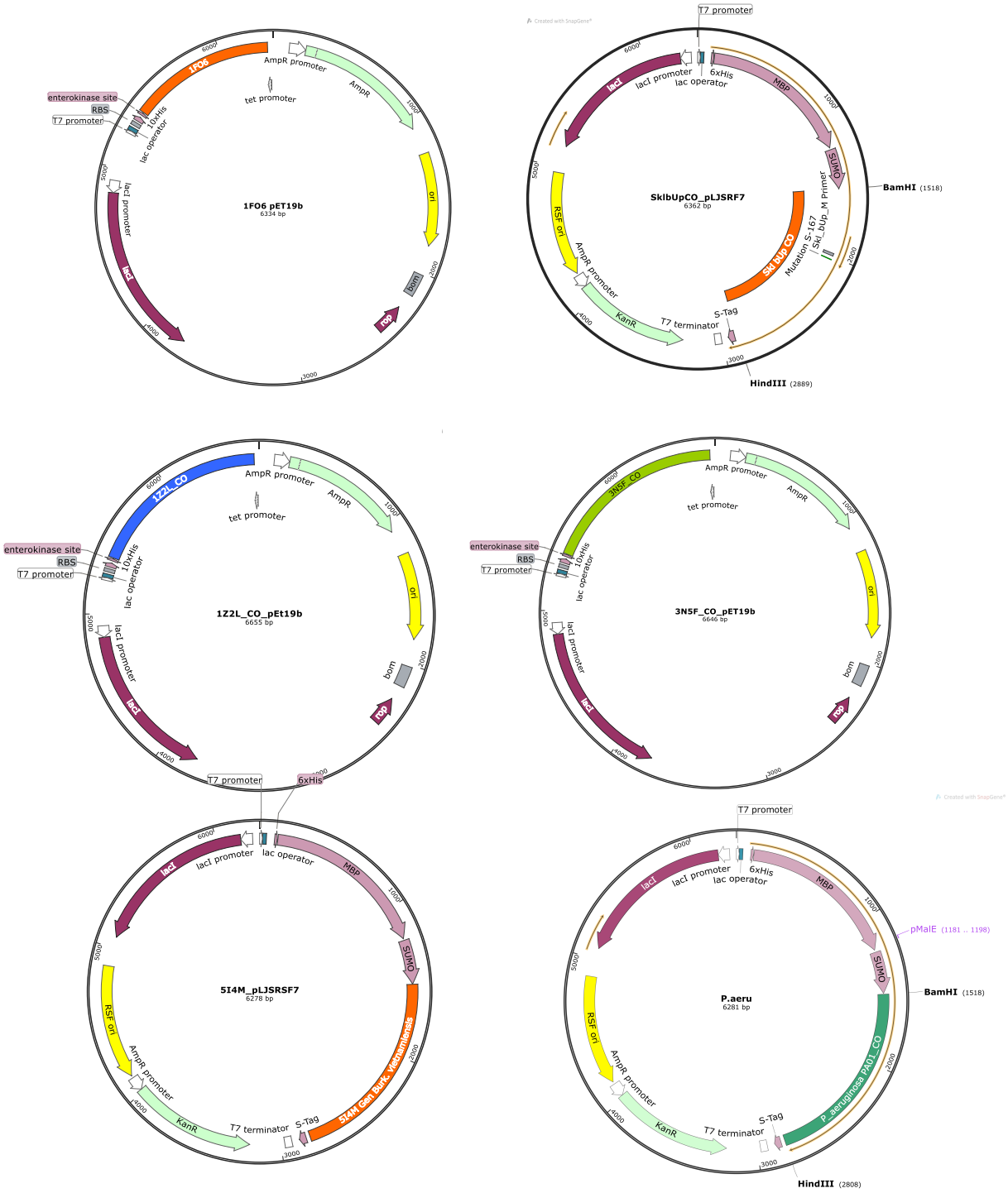

Figure 64: Plasmid maps of 1FO6, SklbUp (2V8H), 1Z2L, 3N5F, 5I4M and P.aeru.
P.aeru and 2V8H are cloned in pLJSRSF7 vector. All other genes are cloned into pET19.

8.7 NMR-spectra

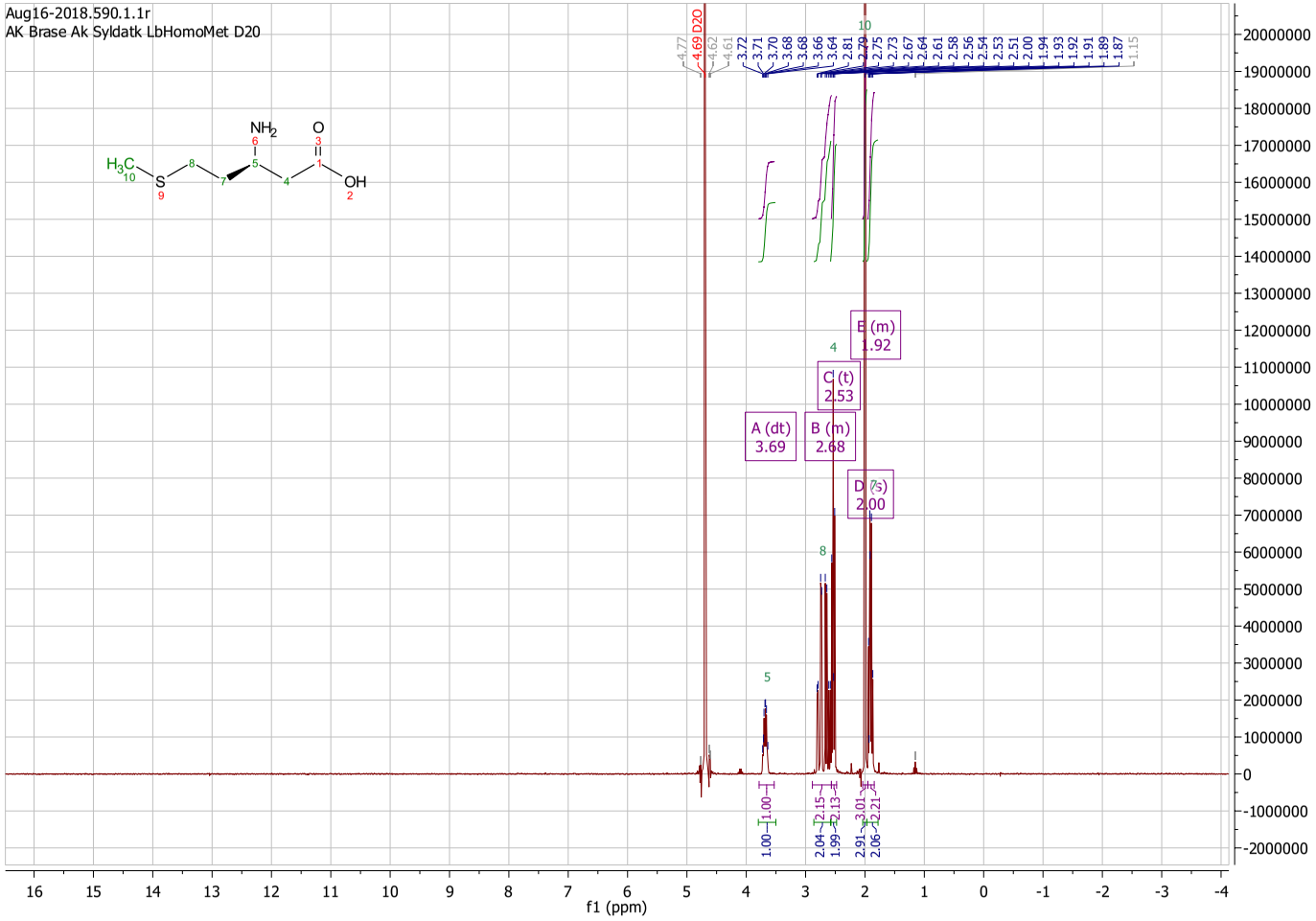

Figure 65: NMR spectrum of Lβ-homo-methionine.

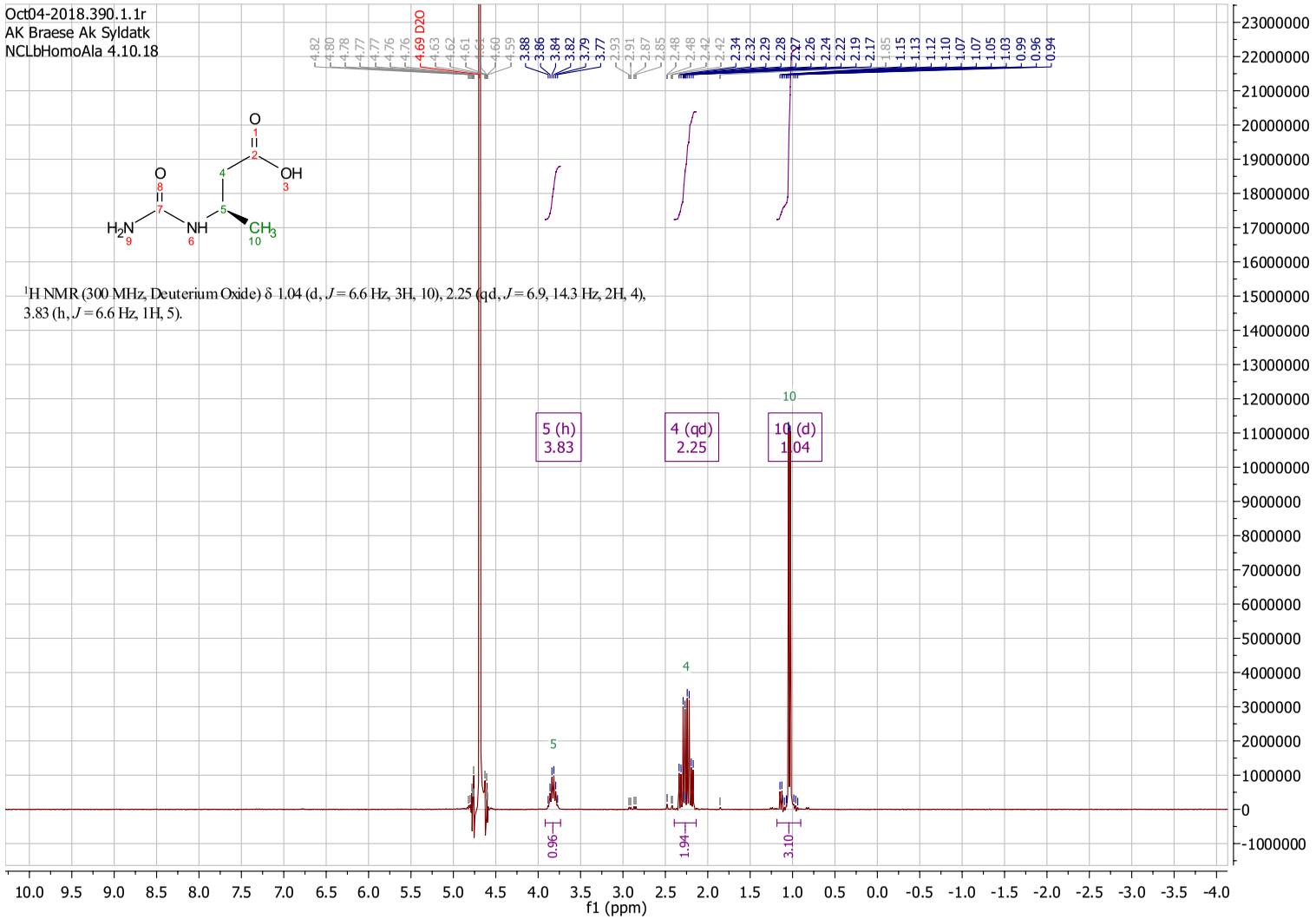

Figure 66: NMR spectrum of *N*-carbamoyl-L-β-homo-alanine.

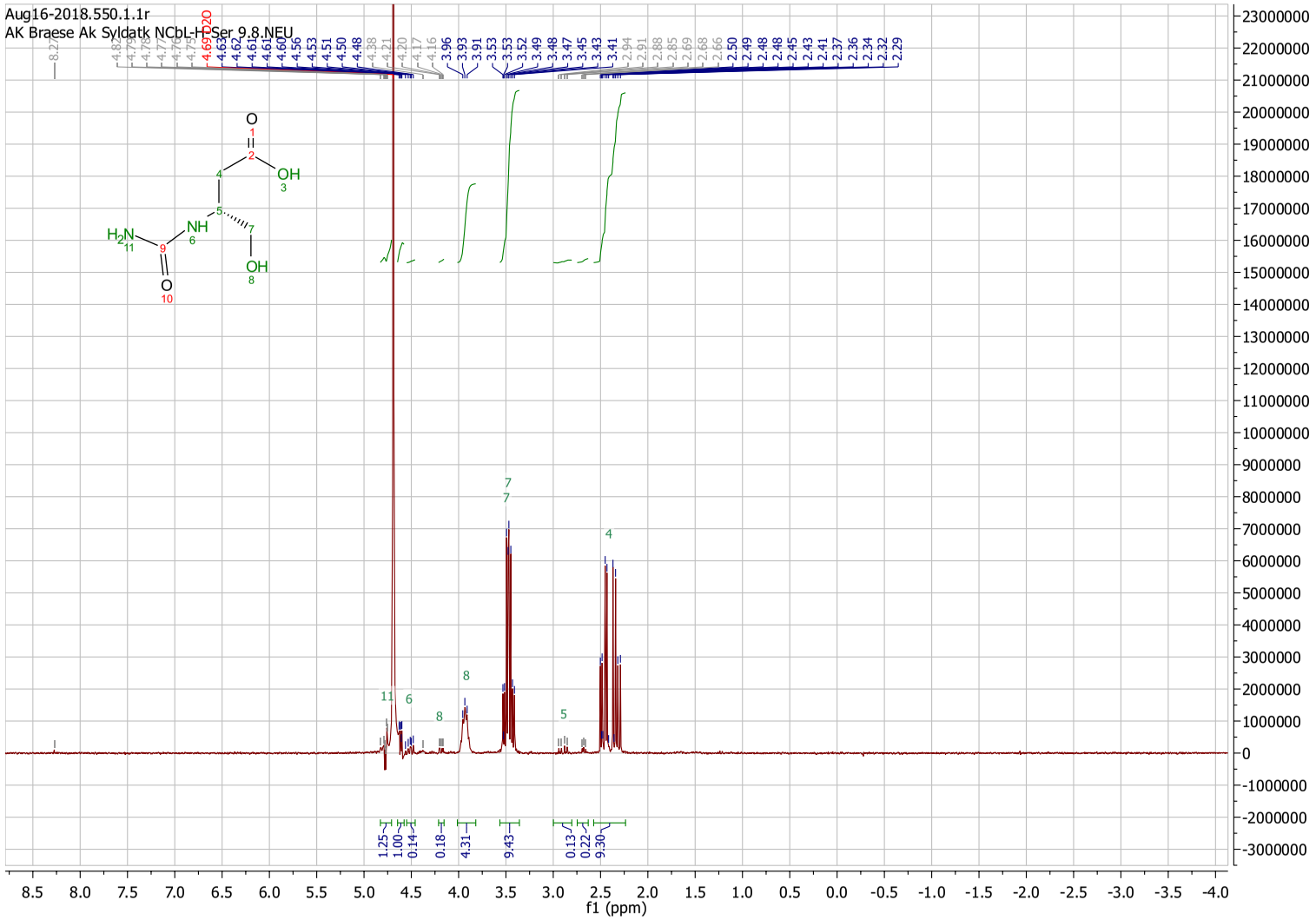

Figure 67: NMR spectrum of *N*-carbamoyl-L-β-homo-serine.

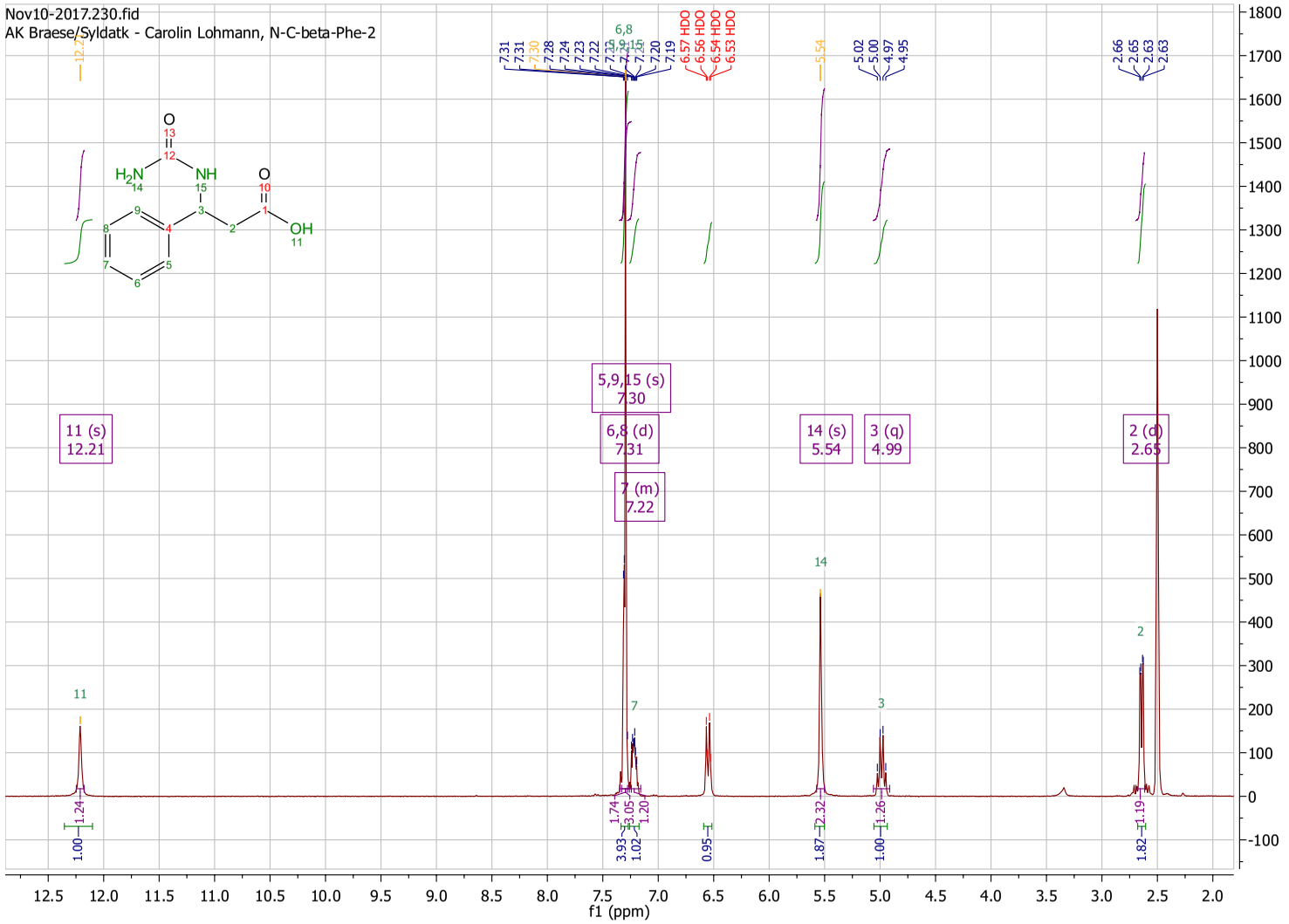

Figure 68: NMR spectrum of *N*-carbamoyl-D/L-β-phenylalanine

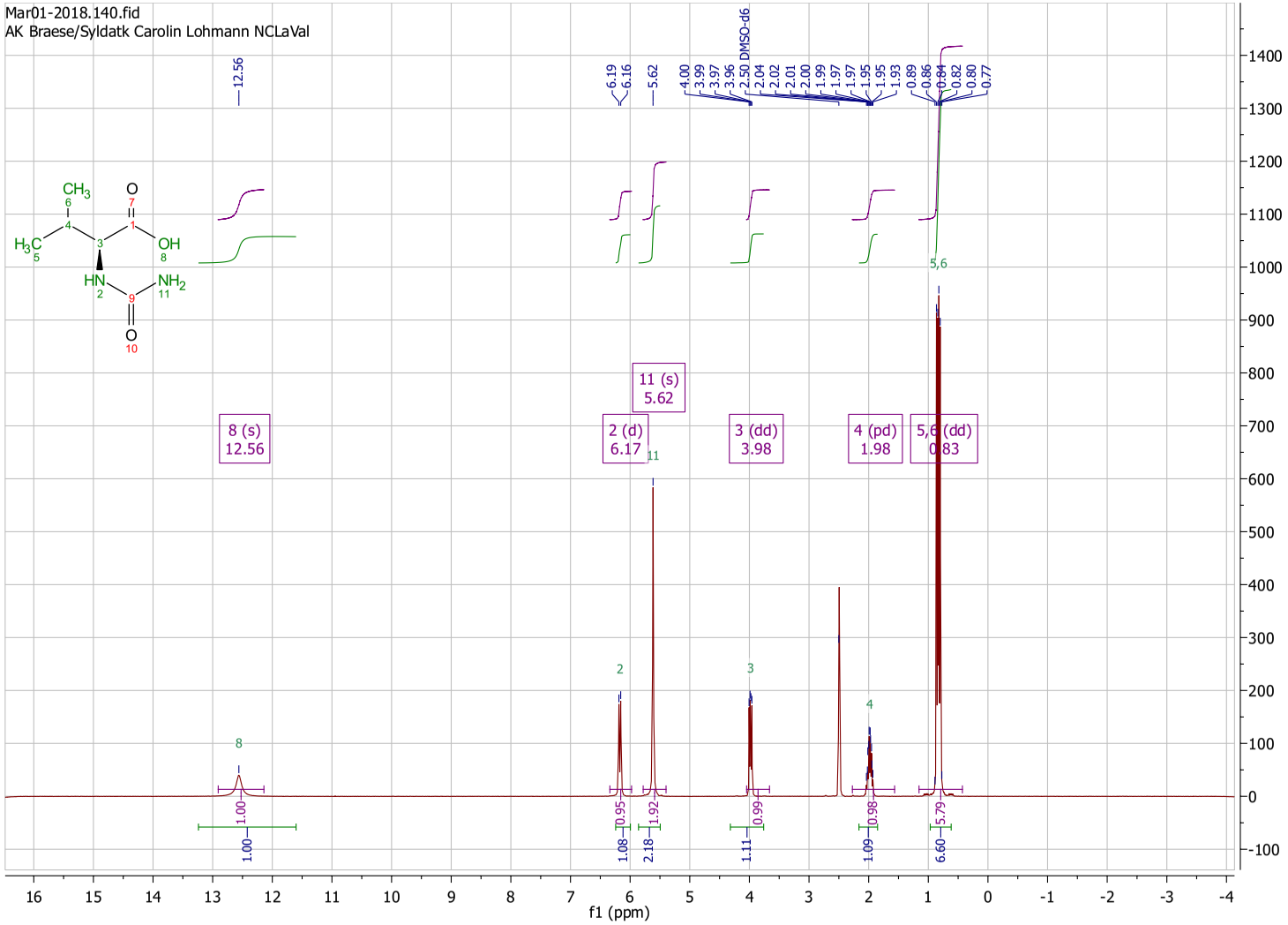

Figure 69: NMR spectrum of *N*-carbamoyl-L-valine.

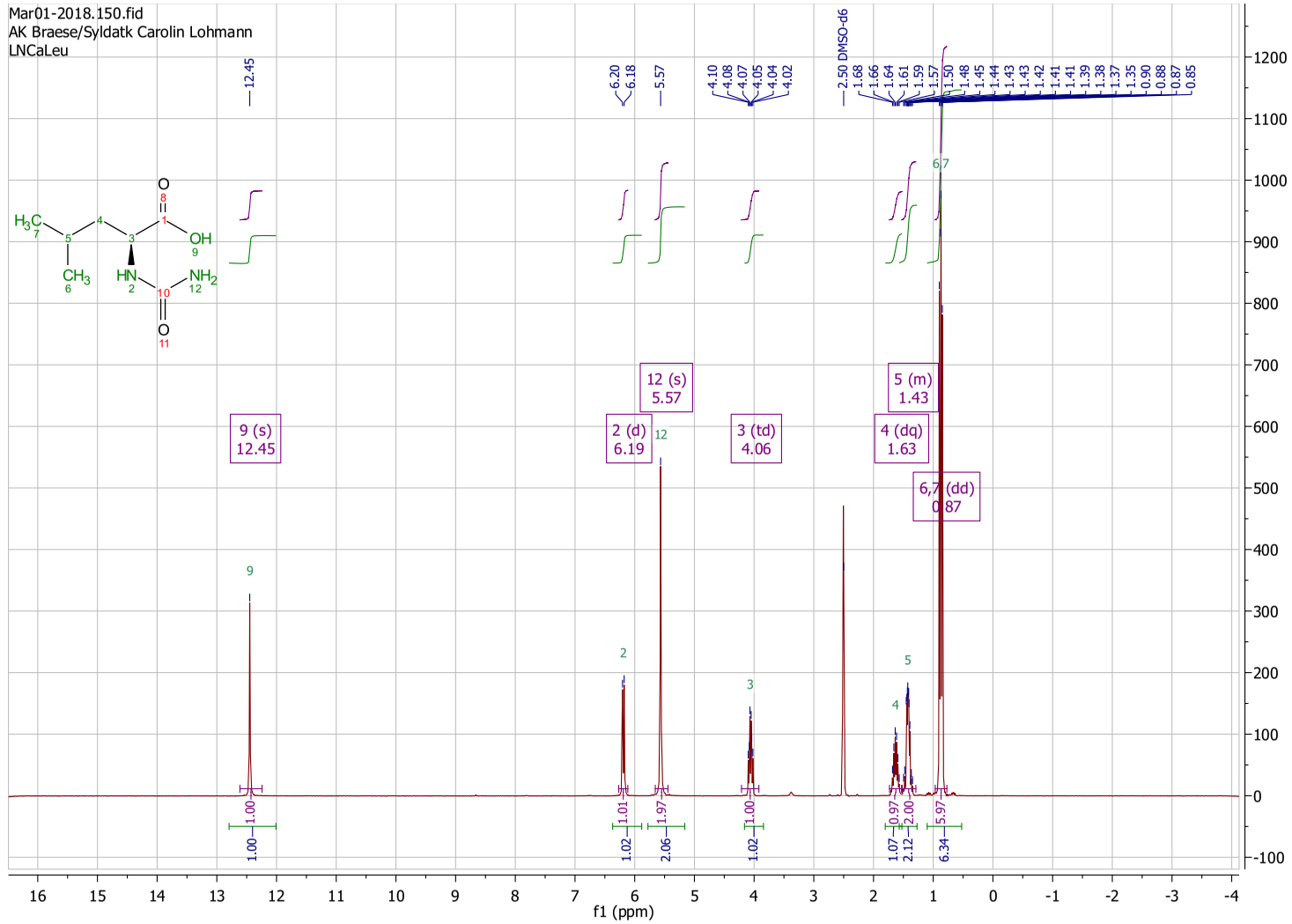

Figure 70: NMR spectrum of *N*-carbamoyl-L-leucine.

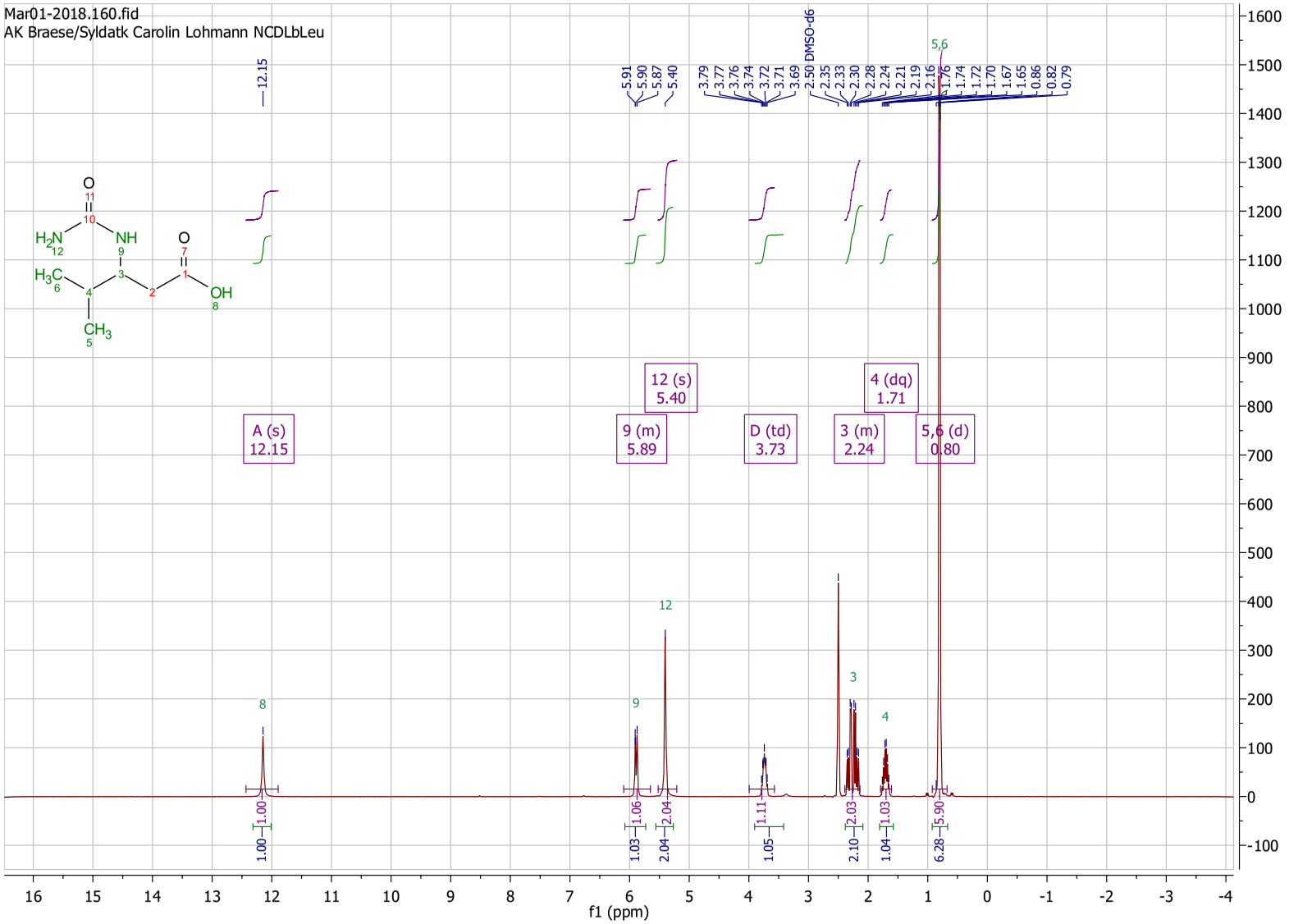

Figure 71: NMR spectrum of *N*-carbamoyl-D/L-β-leucine

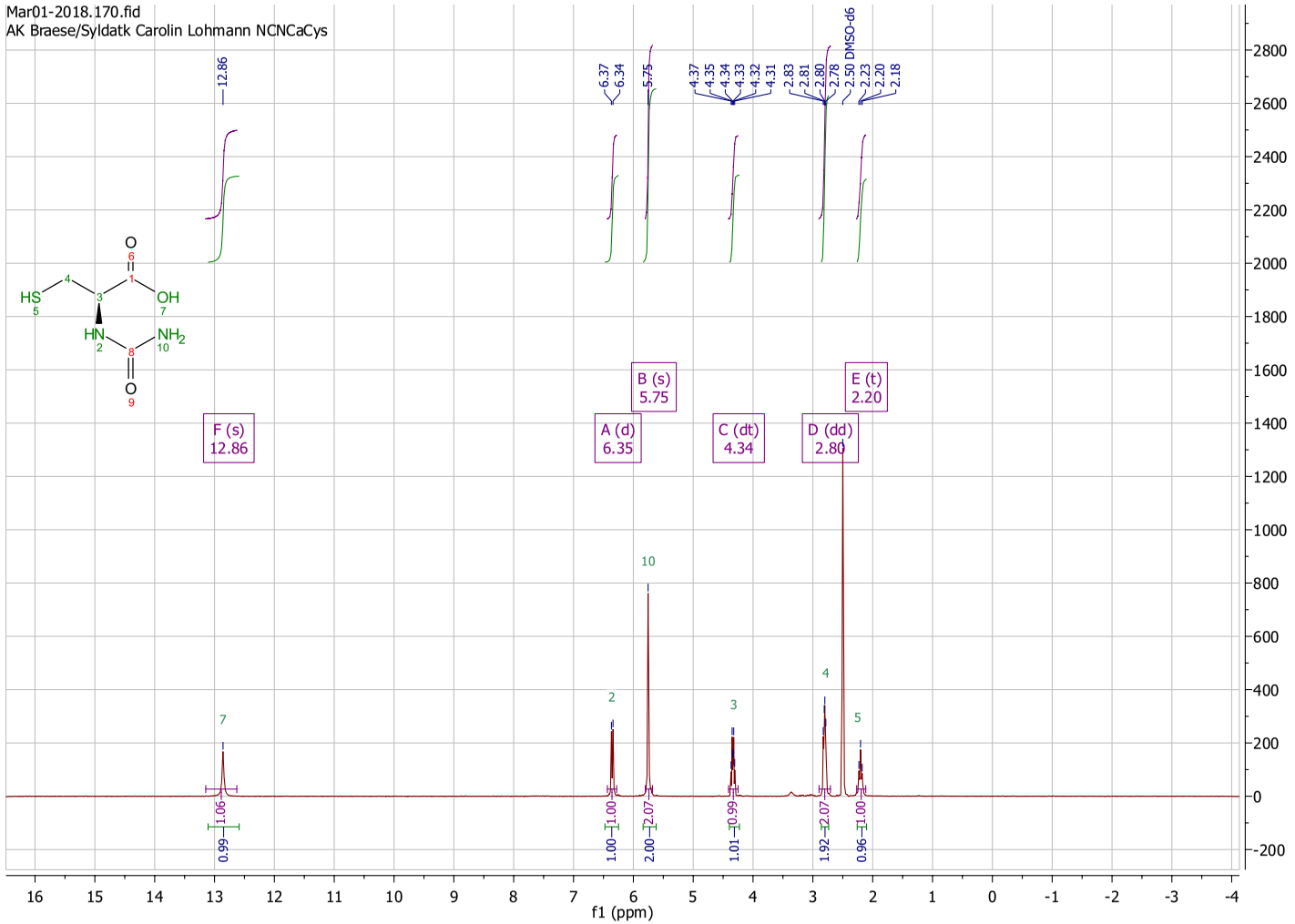

Figure 72: NMR spectrum of *N*-carbamoyl-L-cysteine.

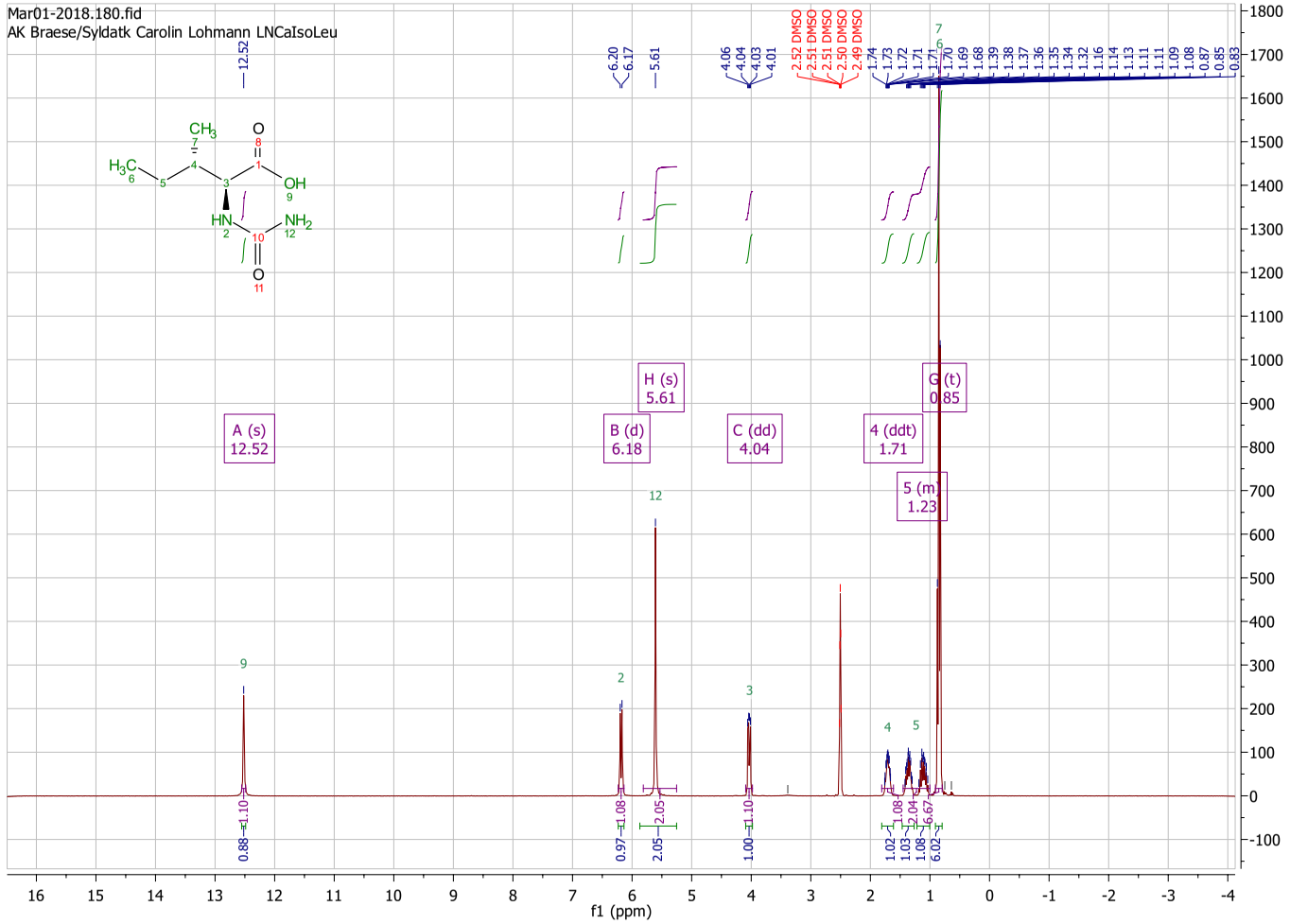

Figure 73: NMR spectrum of *N*-carbamoyl-L-isoleucine

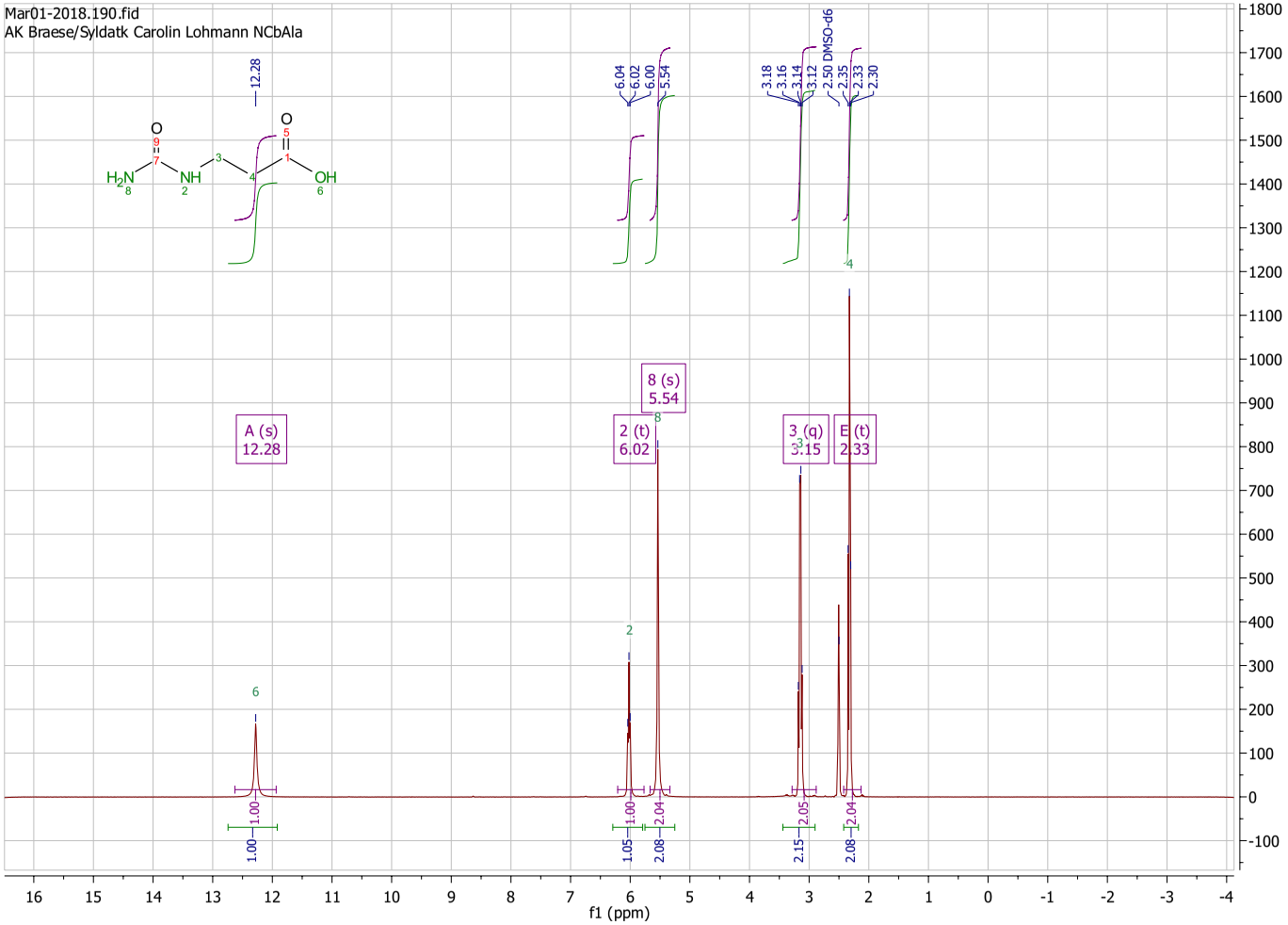

Figure 74: NMR spectrum of *N*-carbamoyl-β-alanine.

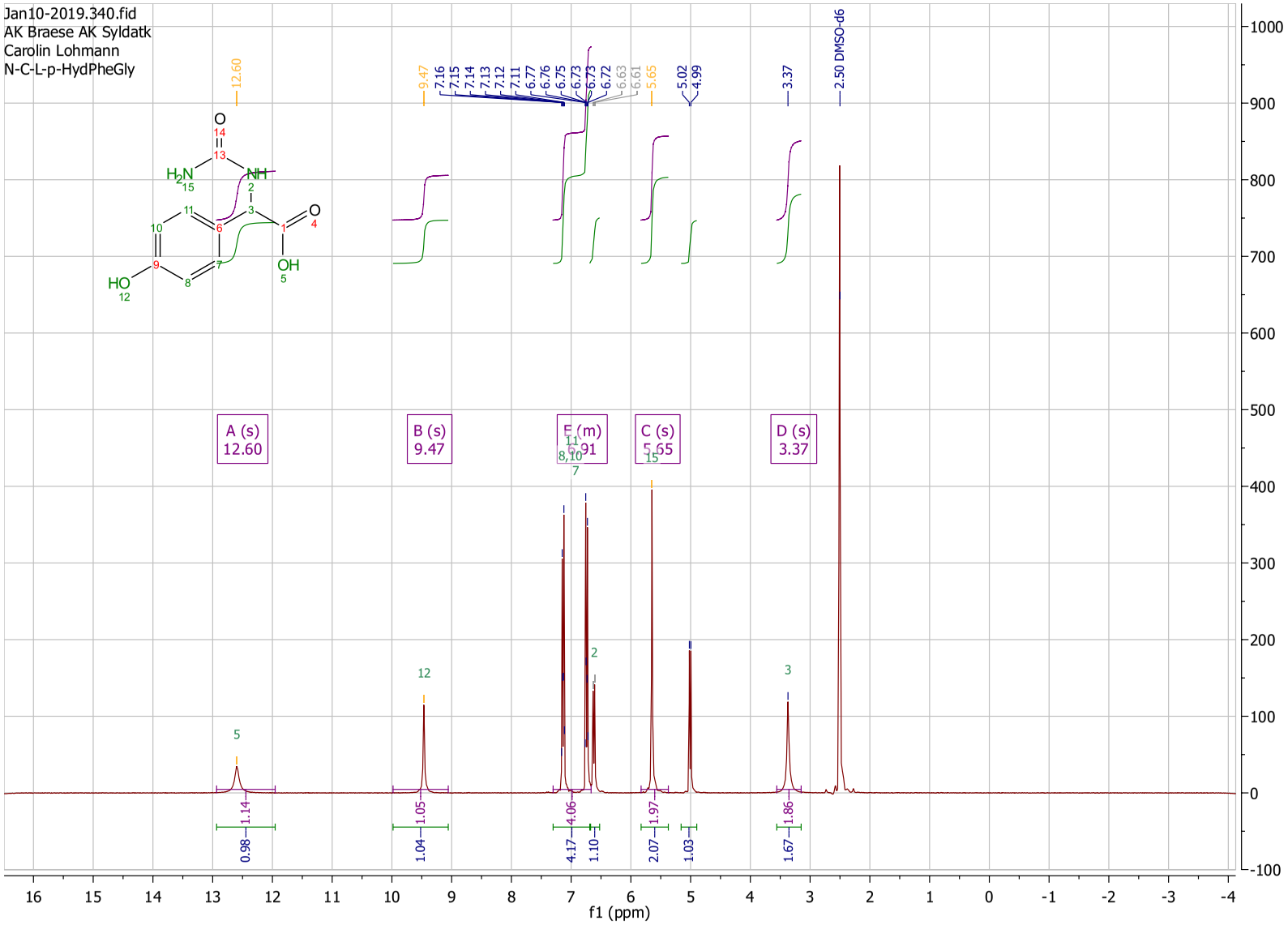

Figure 75: NMR spectrum of *N*-carbamoyl-L-para-hydroxy-phenylglycine.

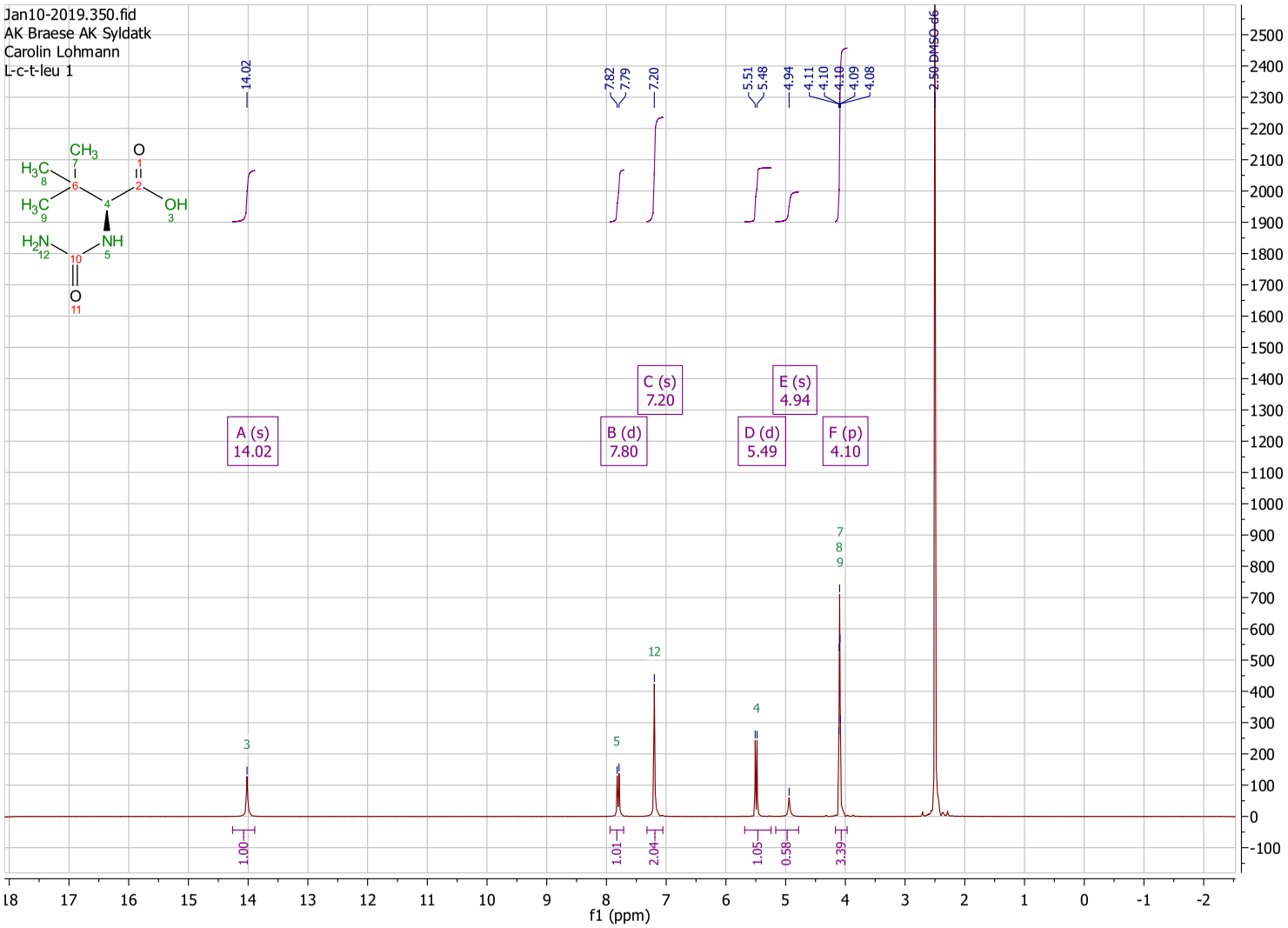

Figure 76: NMR spectrum of *N*-carbamoyl-L-tertiary-leucine.

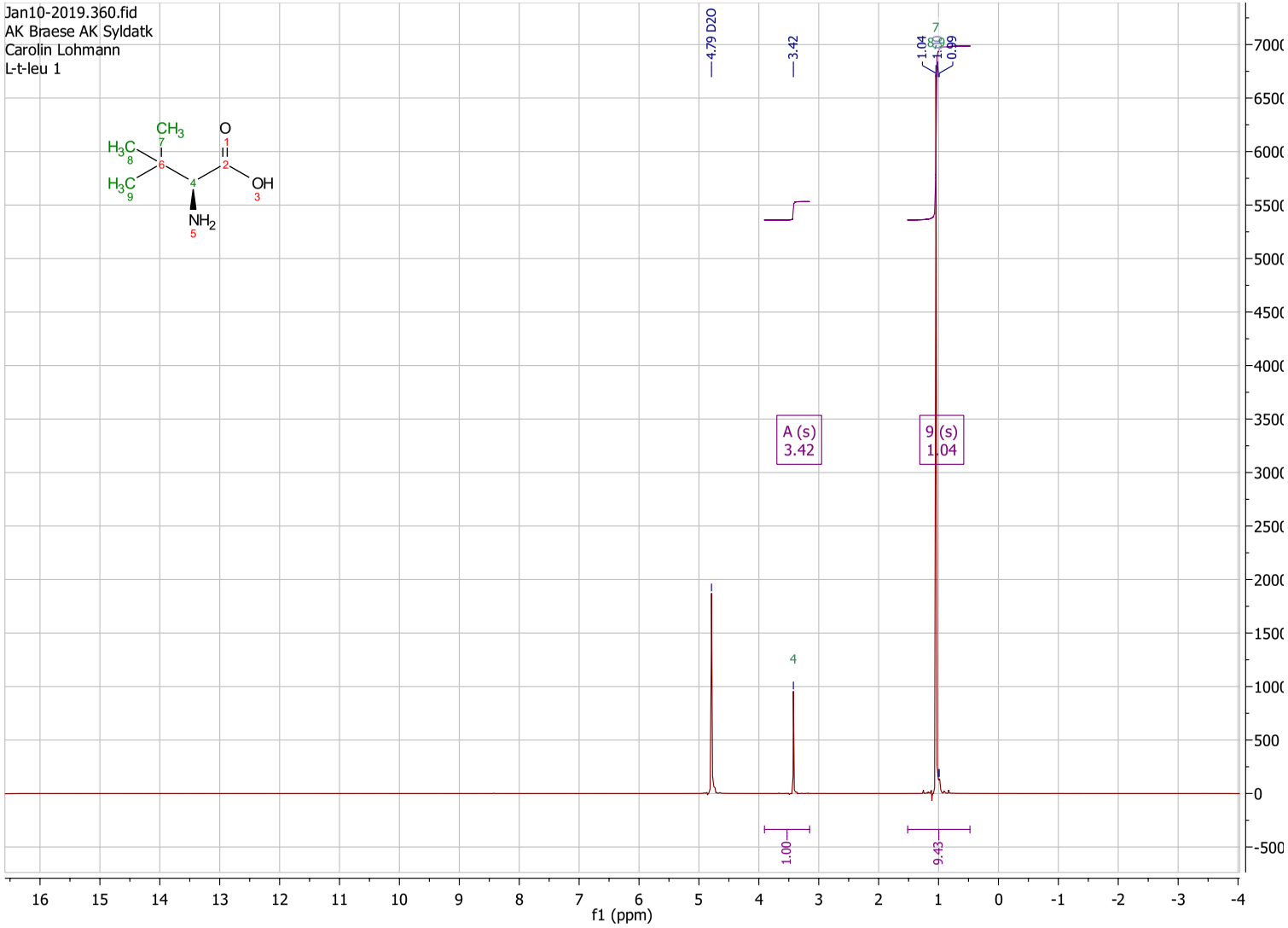

Figure 77: NMR spectrum of L-tertiary leucine.

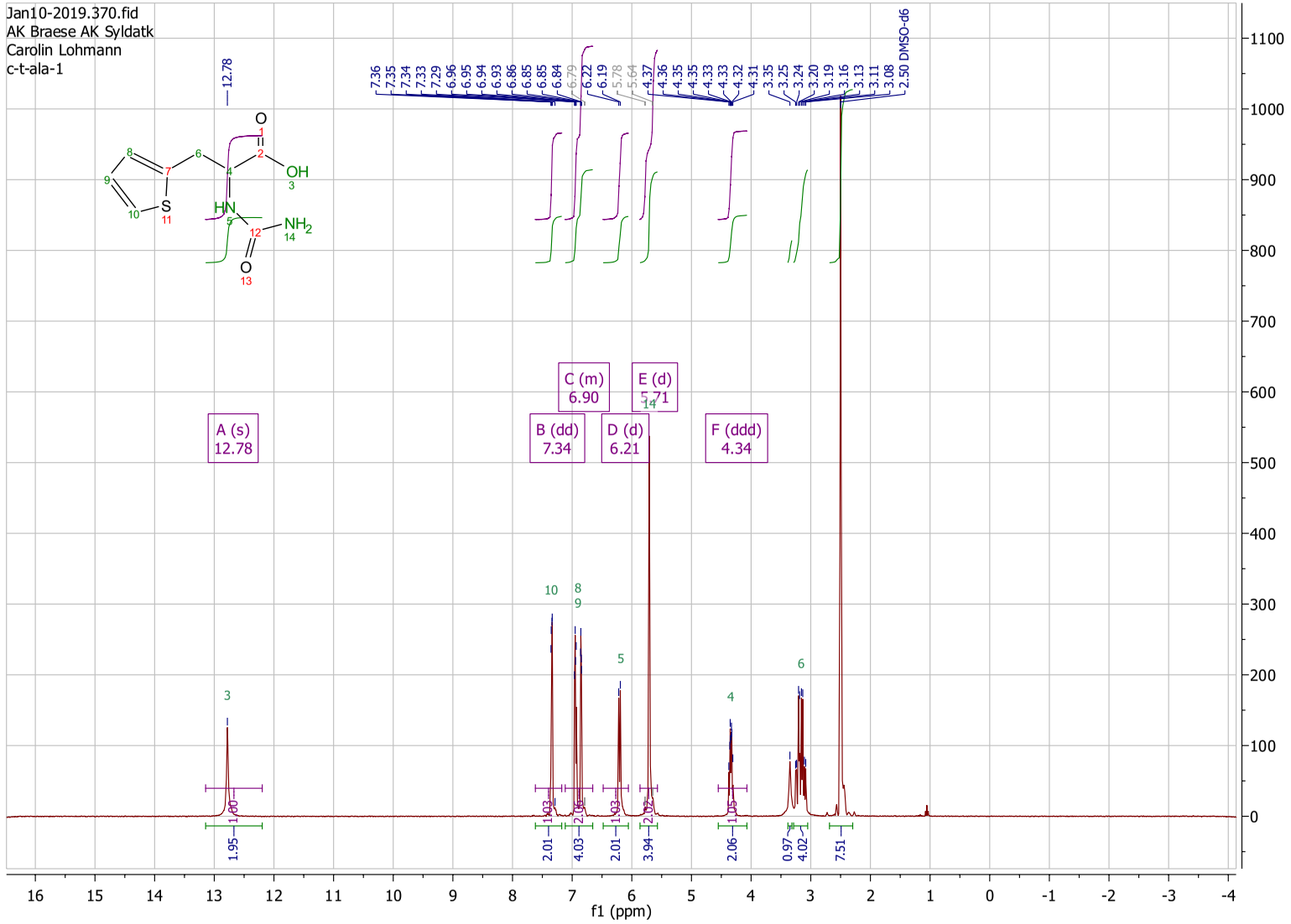

Figure 78: NMR spectrum of *N*-carbamoyl-L-β-2-thienylalanine.

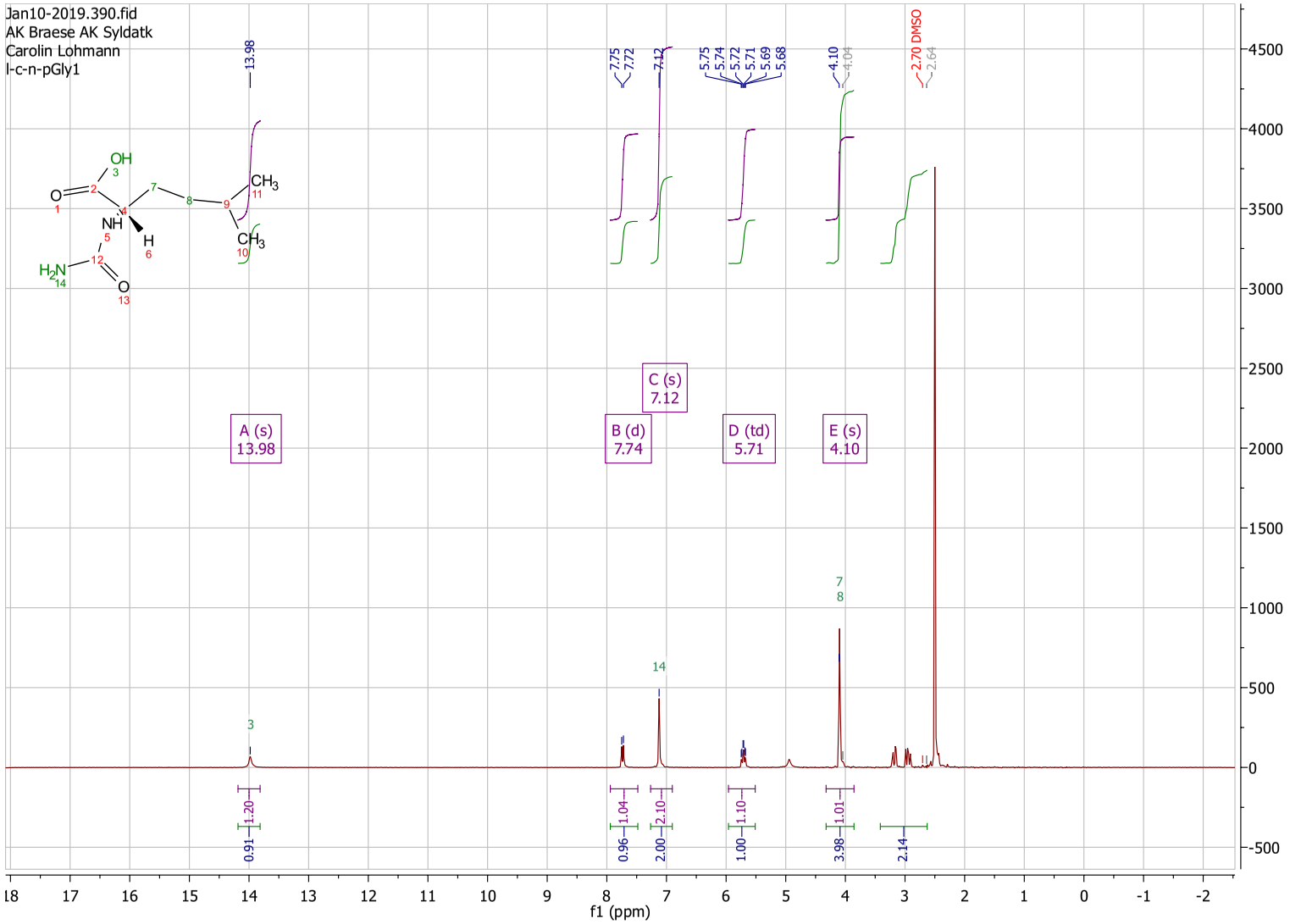

Figure 79: NMR spectrum of *N*-carbamoyl-L-neopentylglycine.

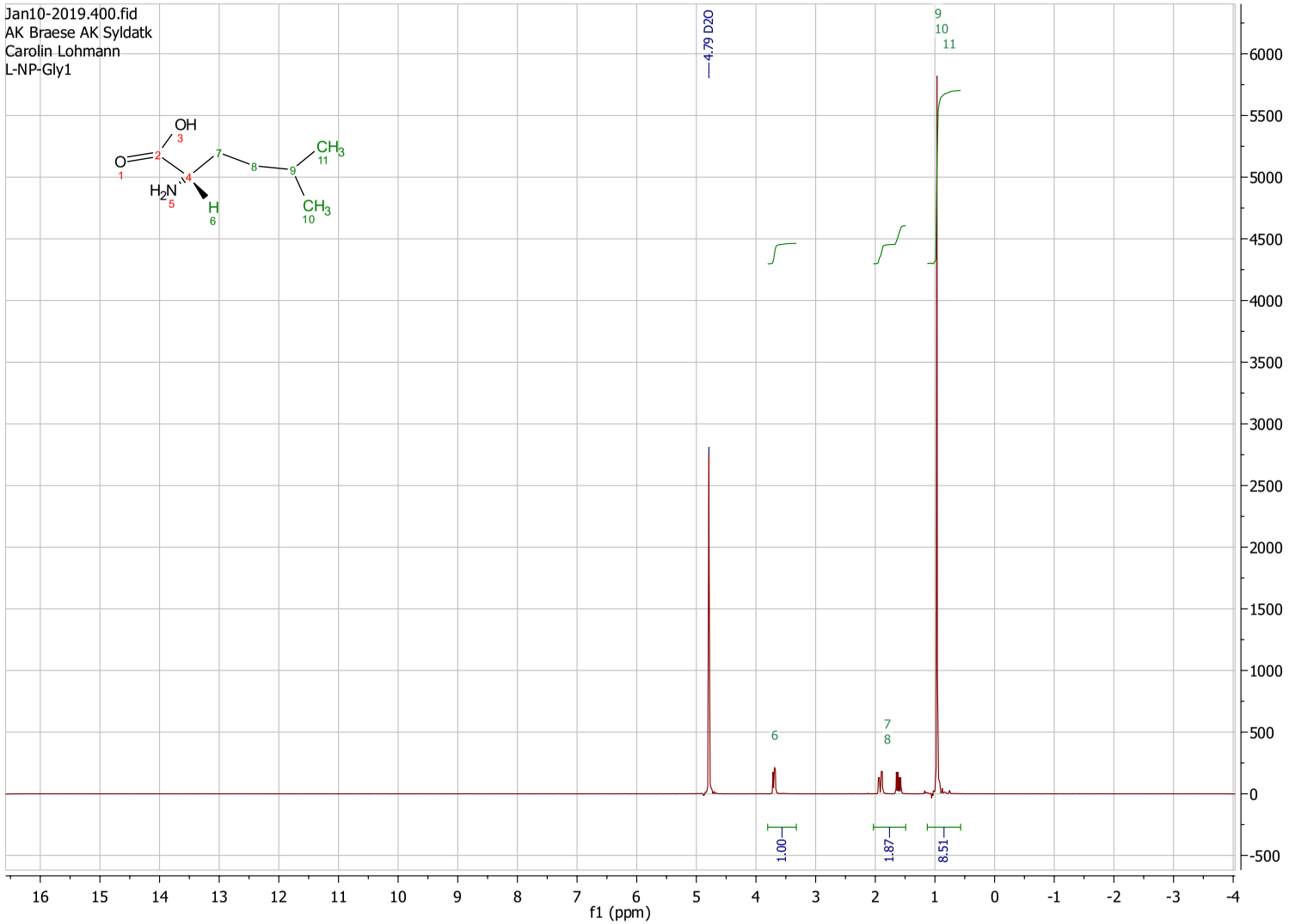

Figure 80: NMR spectrum of L-neopentylglycine.

8.8 Mass spectra

N-carbamoyl-L- α-tert-Leu

M = 174,1 g/mol; ESI [M+ H^+]

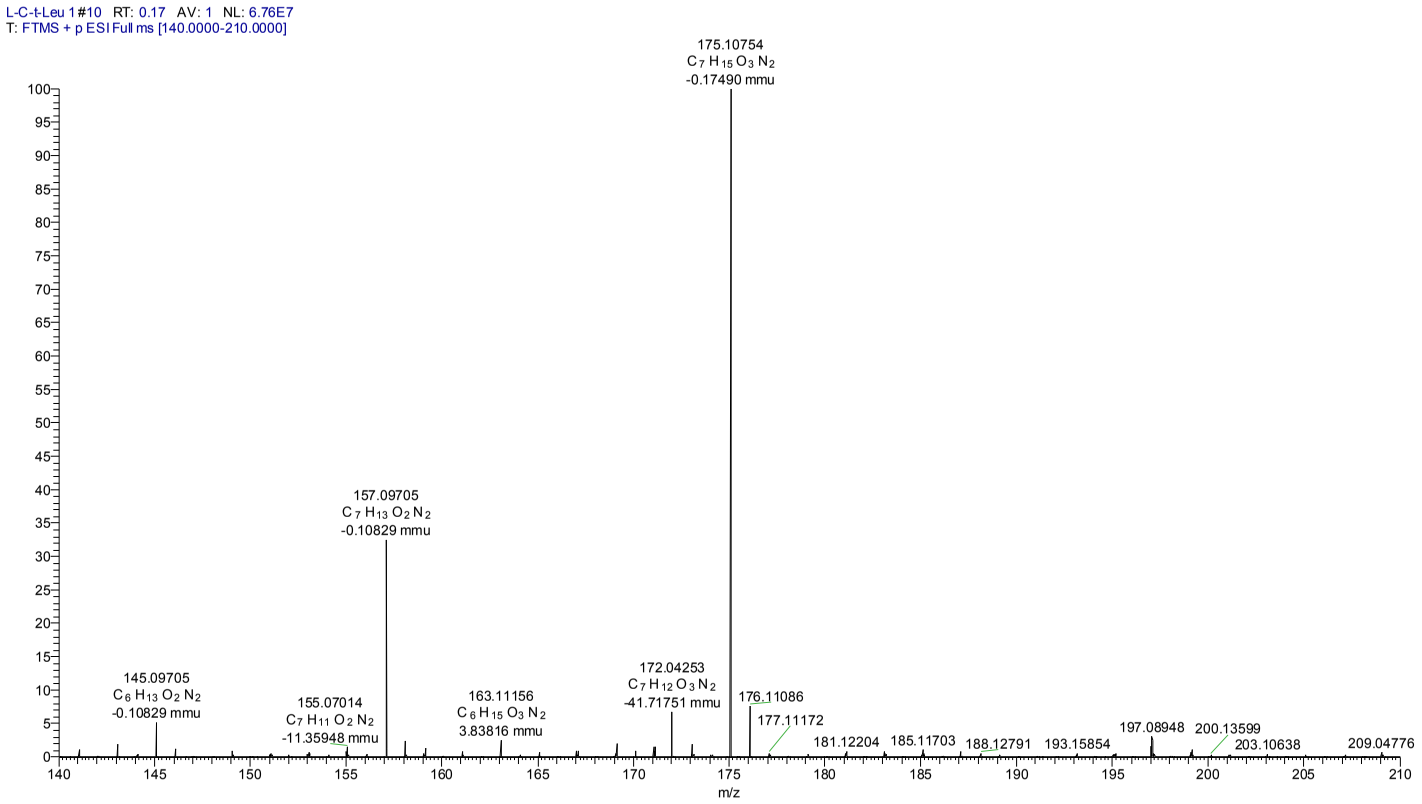

Figure 81: Mass spectrometry chromatogram of *N*-carbamoyl-L- α-tert-Leu.

M = 131,09 g/mol; ESI [M+H$^+$]

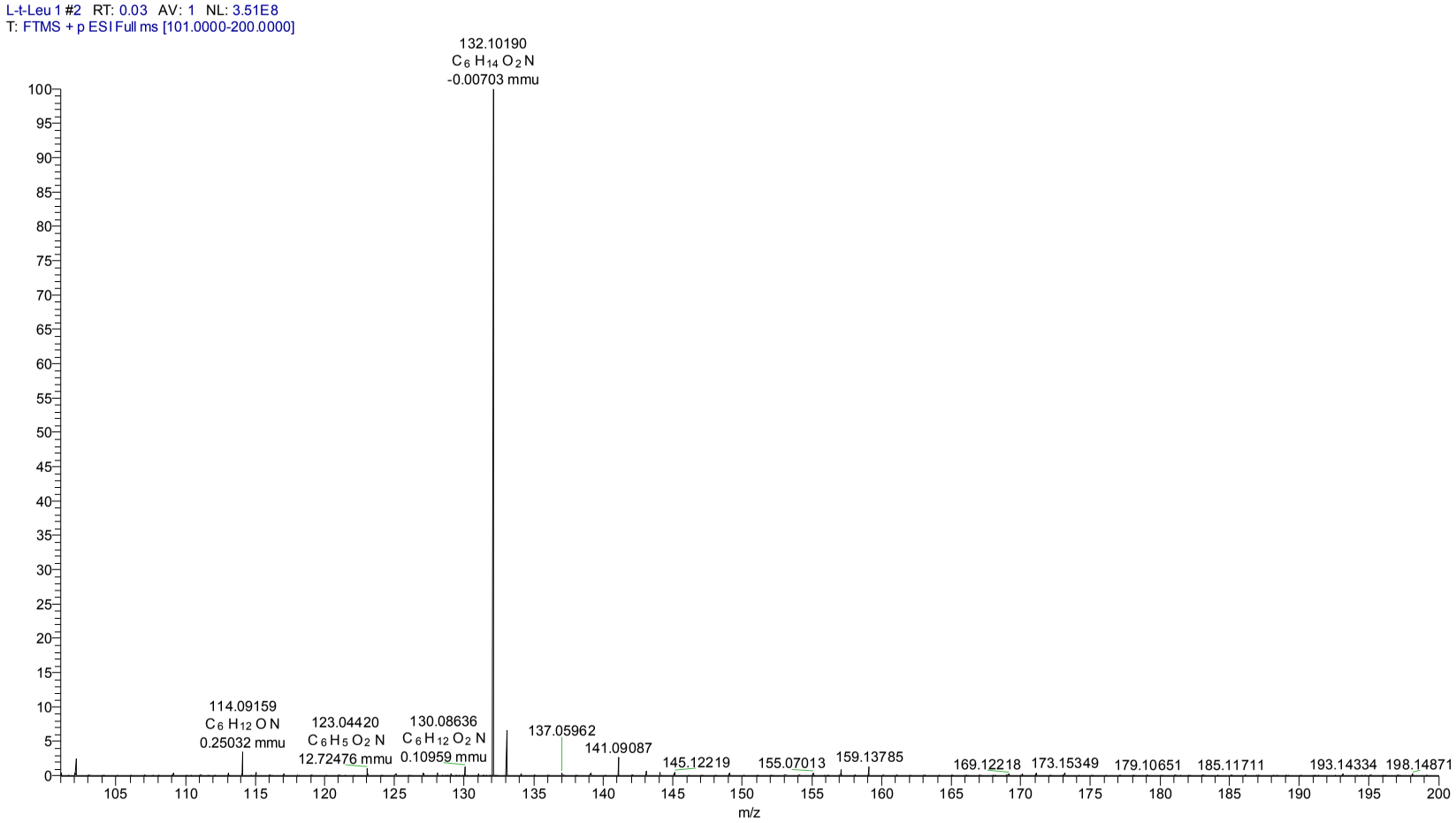

Figure 82: Mass spectrometry chromatogram of L- α-tert-Leu.

N-carbamoyl-L-β-thienylalanine

M = 214,04; [ESI $M+H^+$]

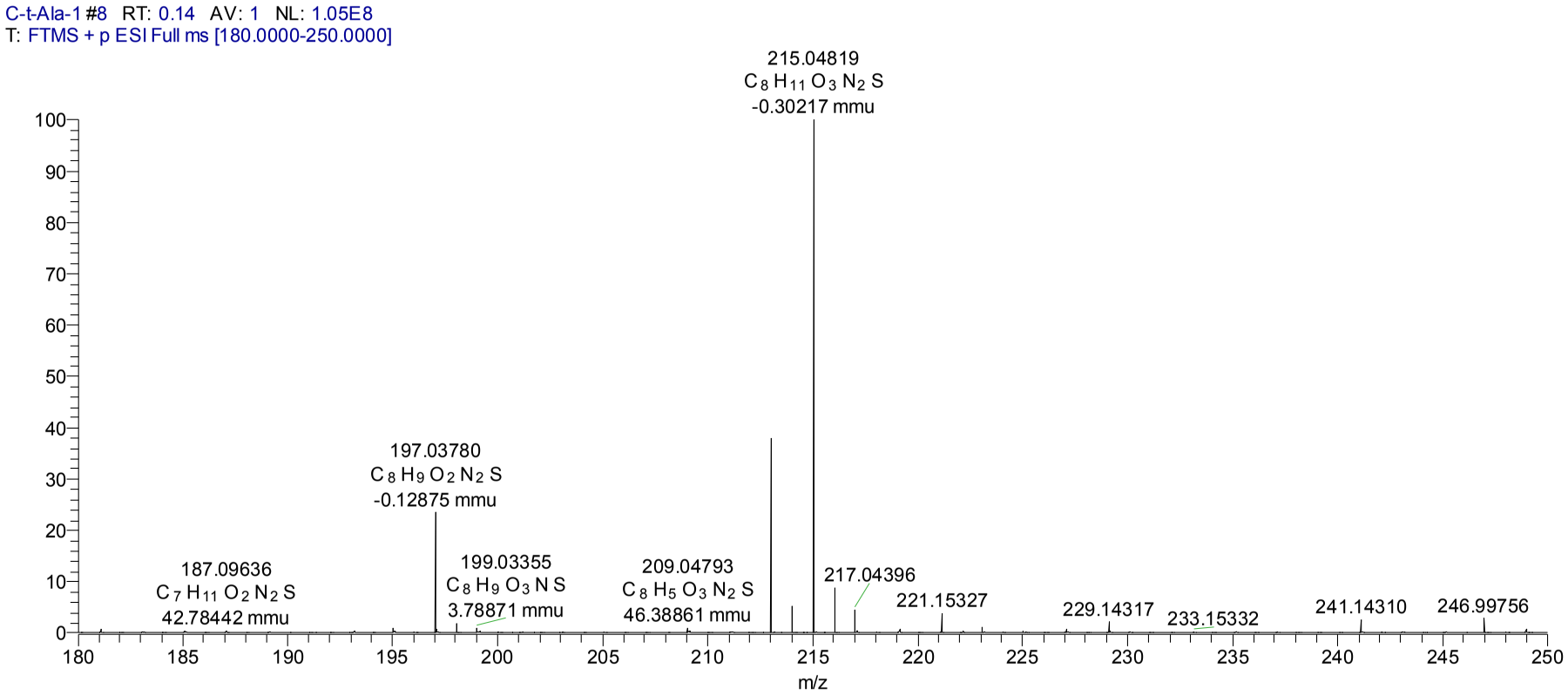

Figure 83: Mass spectrometry chromatogram of *N*-carbamoyl-L- β-thienylalanine.

β-2-thienyl-alanine

M = 171,21; ESI [M+H$^+$]

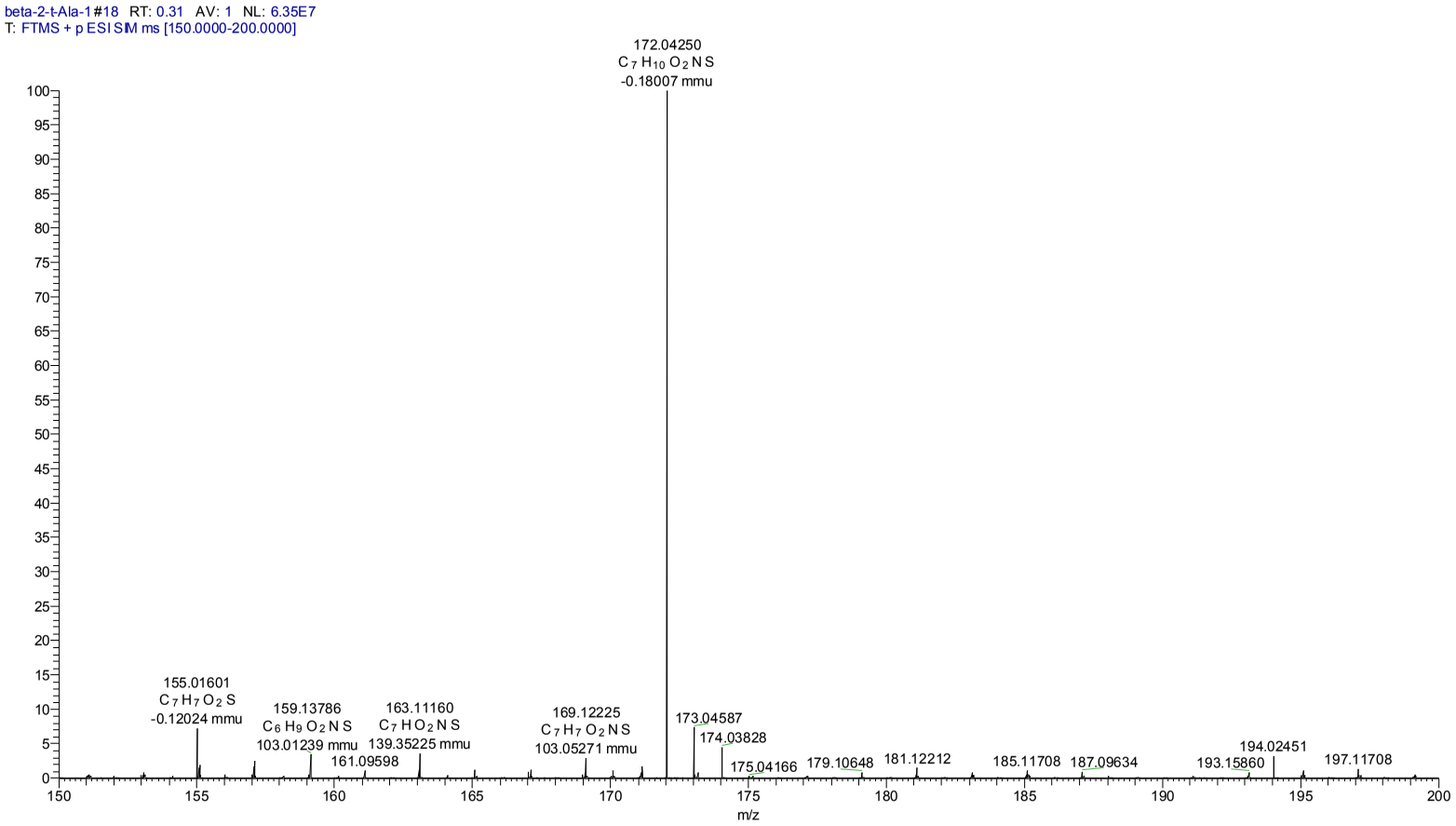

Figure 84: Mass spectrometry chromatogram of L- β-thienylalanine.

N-carbamoyl-L-α-neopentylglycine

M = 188,12; ESI [M+H$^+$]

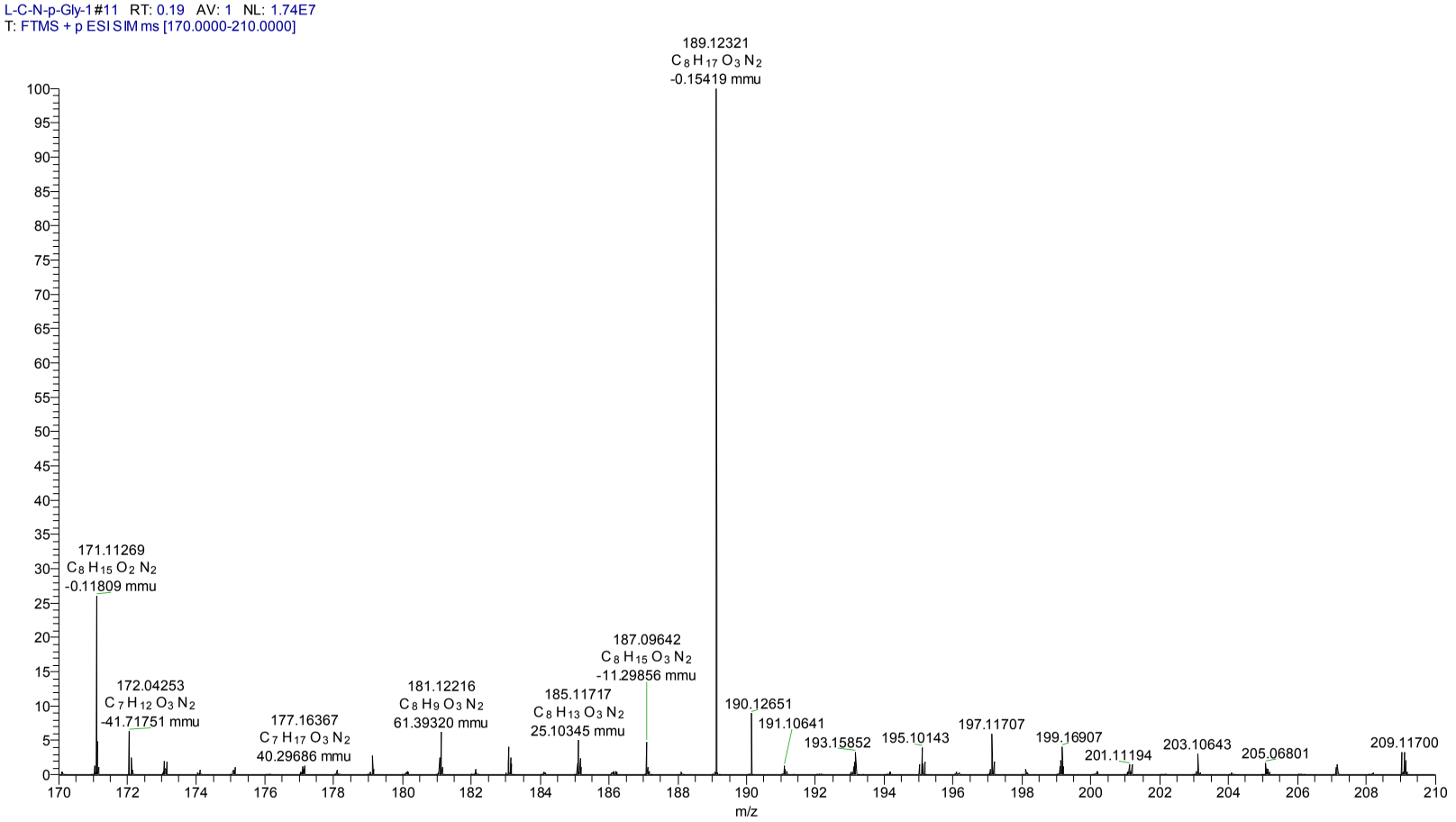

Figure 85: Mass spectrometry chromatogram of *N*-carbamoyl-L- α-neopentylglycine.

L-α-neopentylglycine

M = 145,11; ESI [$M+H^+$]

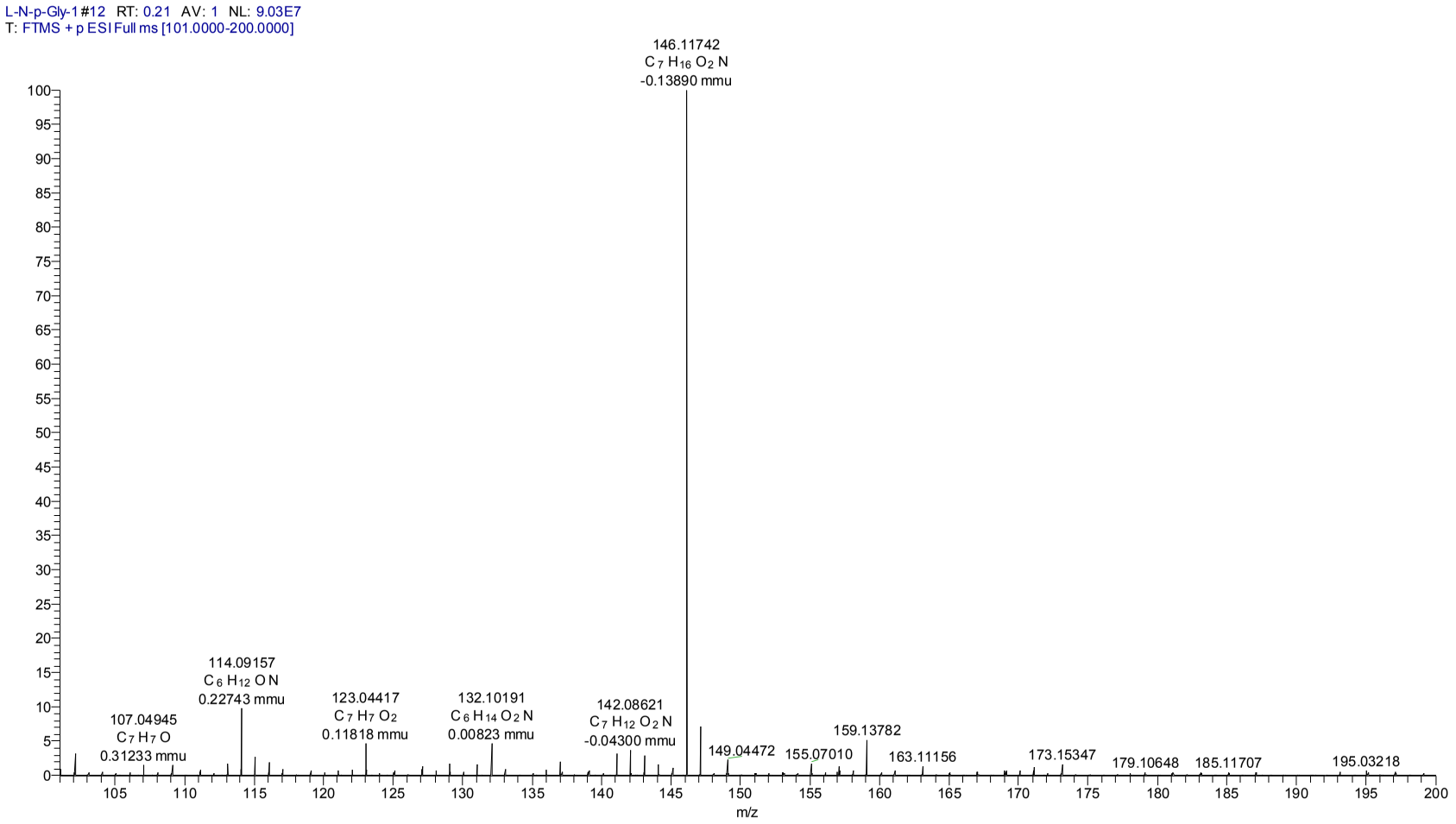

Figure 86: Mass spectrometry chromatogram of L- α-neopentylglycine.

N-carbamoyl-L-α-para-hydroxy-phenylglycine

M = 210,19 g/mol, ESI [$M+H^+$]

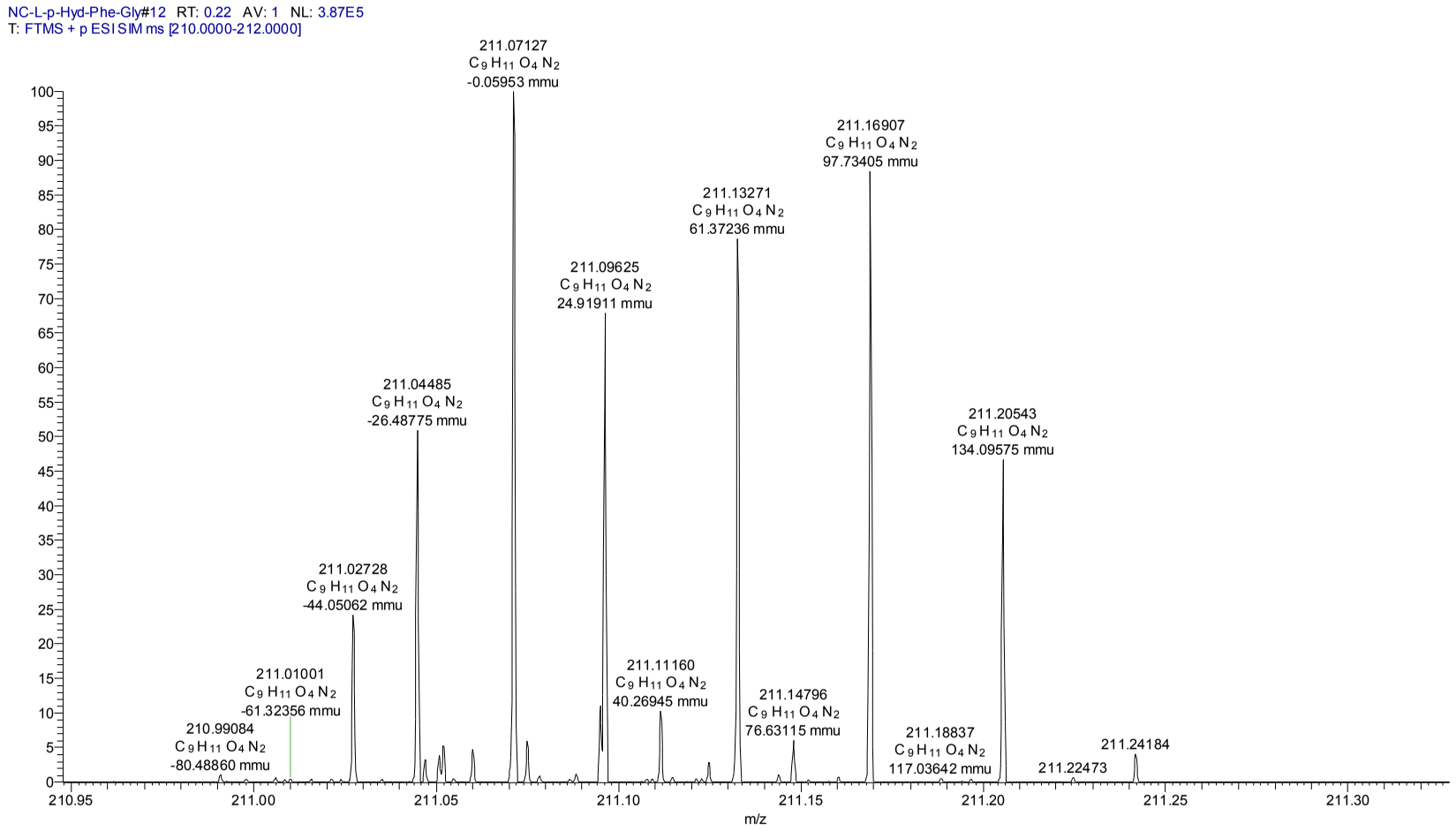

L-α-para-hydroxy-phenylglycine

M = 167,06; ESI [$M+H^+$]

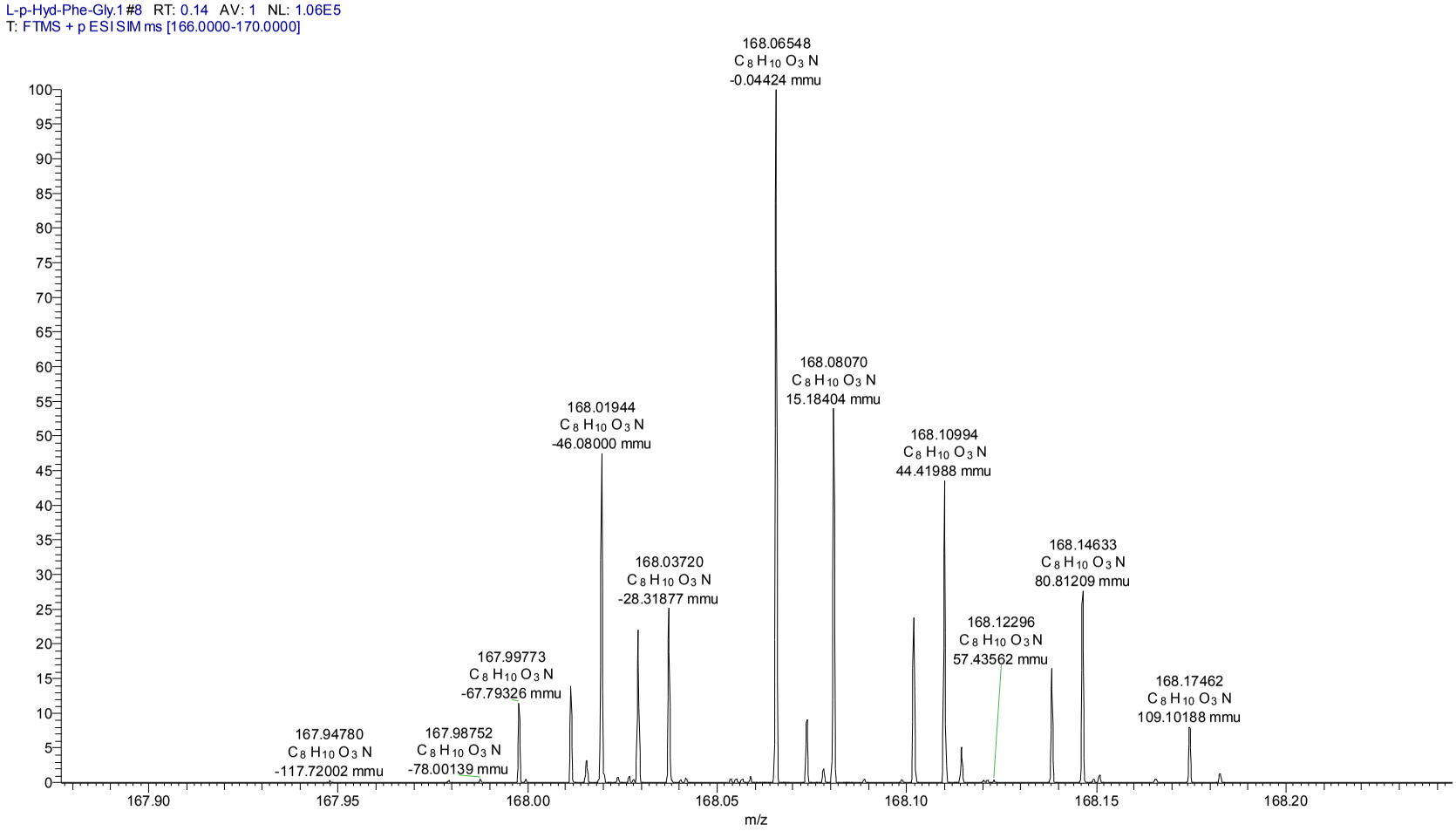

Figure 87: Mass spectrometry chromatogram of L- α-para-hydroxy-phenylglycine.

L-α-phenylglycine

M = 151,06; ESI [$M+H^+$]

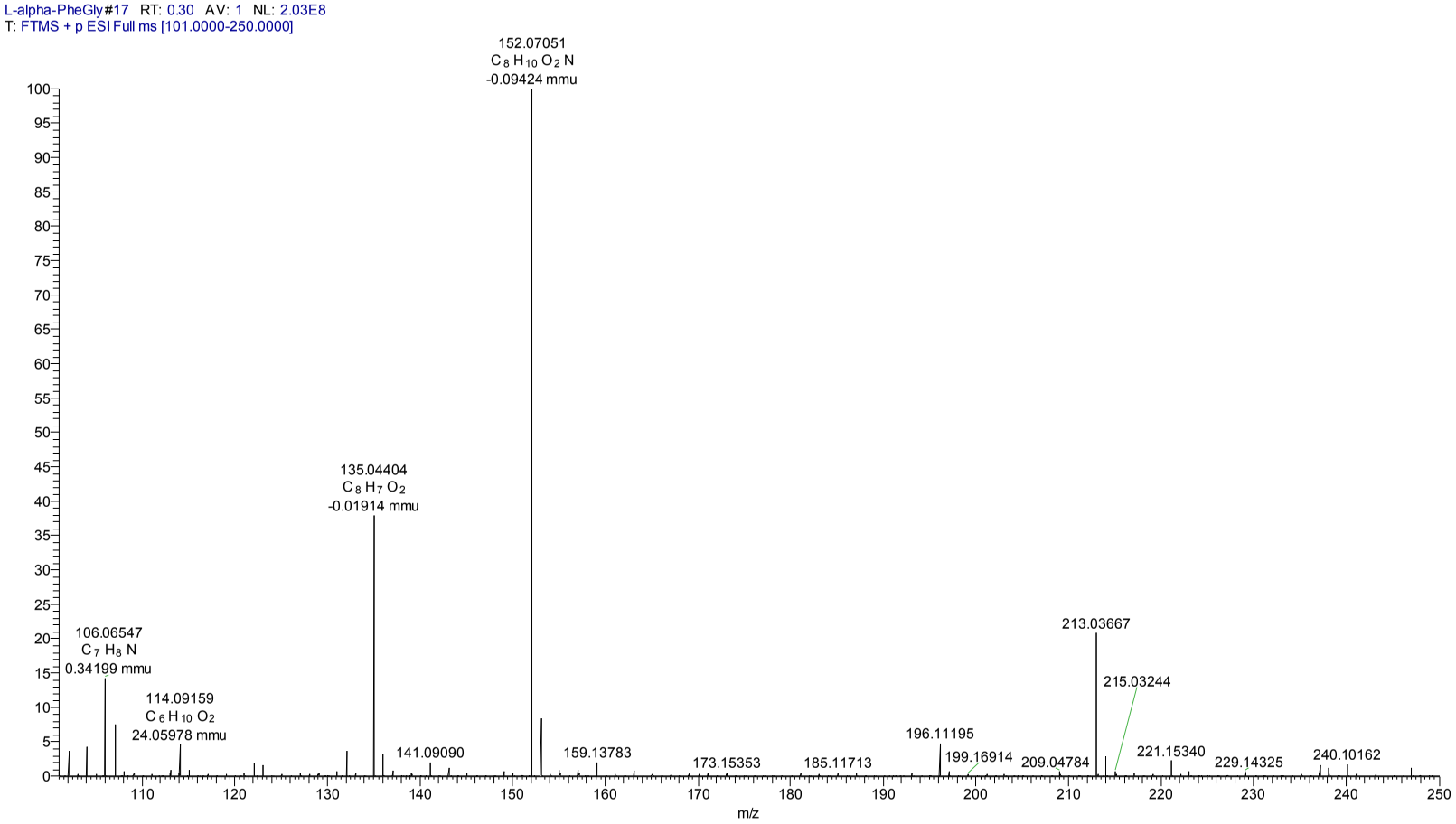

Figure 88: Mass spectrometry chromatogram of L-α-phenylglycine.

N-carbamoyl-L-β-homo-alanine

M = 146,18; ESI [$M+H^+$]

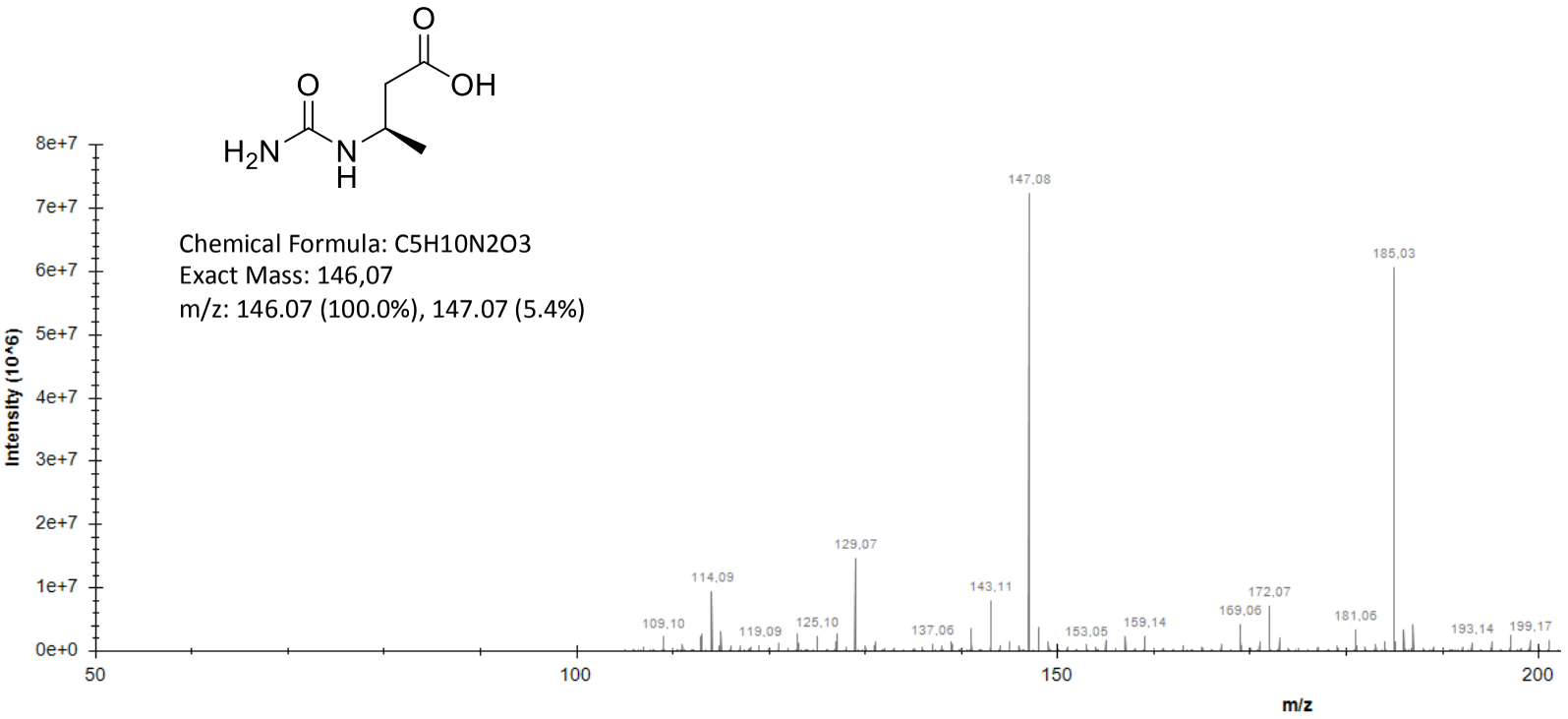

Figure 89: Mass spectrometry chromatogram of *N*-carbamoyl-L-β-homo-alanine.

N-carbamoyl-L-β-homo-serine

M = 162,18, ESI [$M+H^+$]

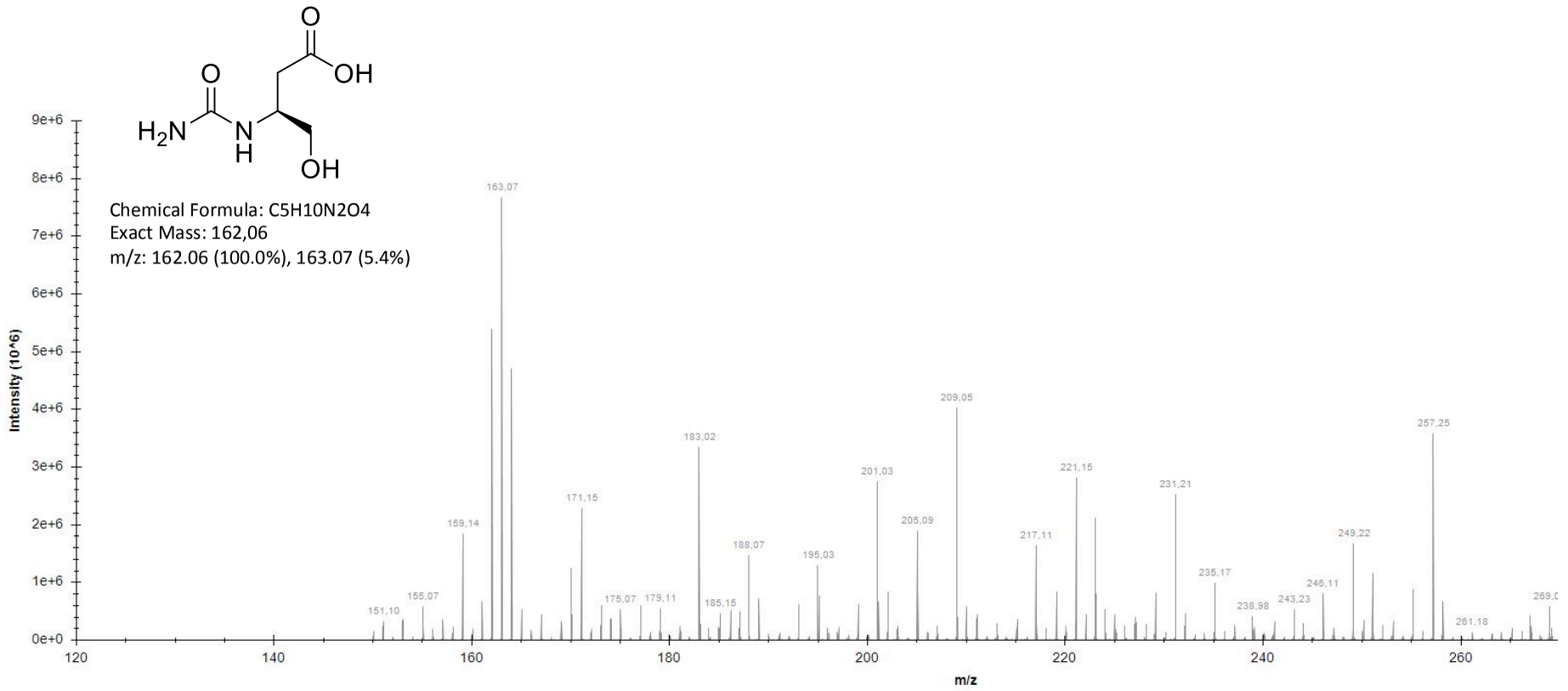

Figure 90: Mass spectrometry chromatogram of *N*-carbamoyl-L-β-homo-serine.

N-carbamoyl-L-β-homo-methionine

M= 206,3 FAB^+ [$M\text{-}NH_3^+$]

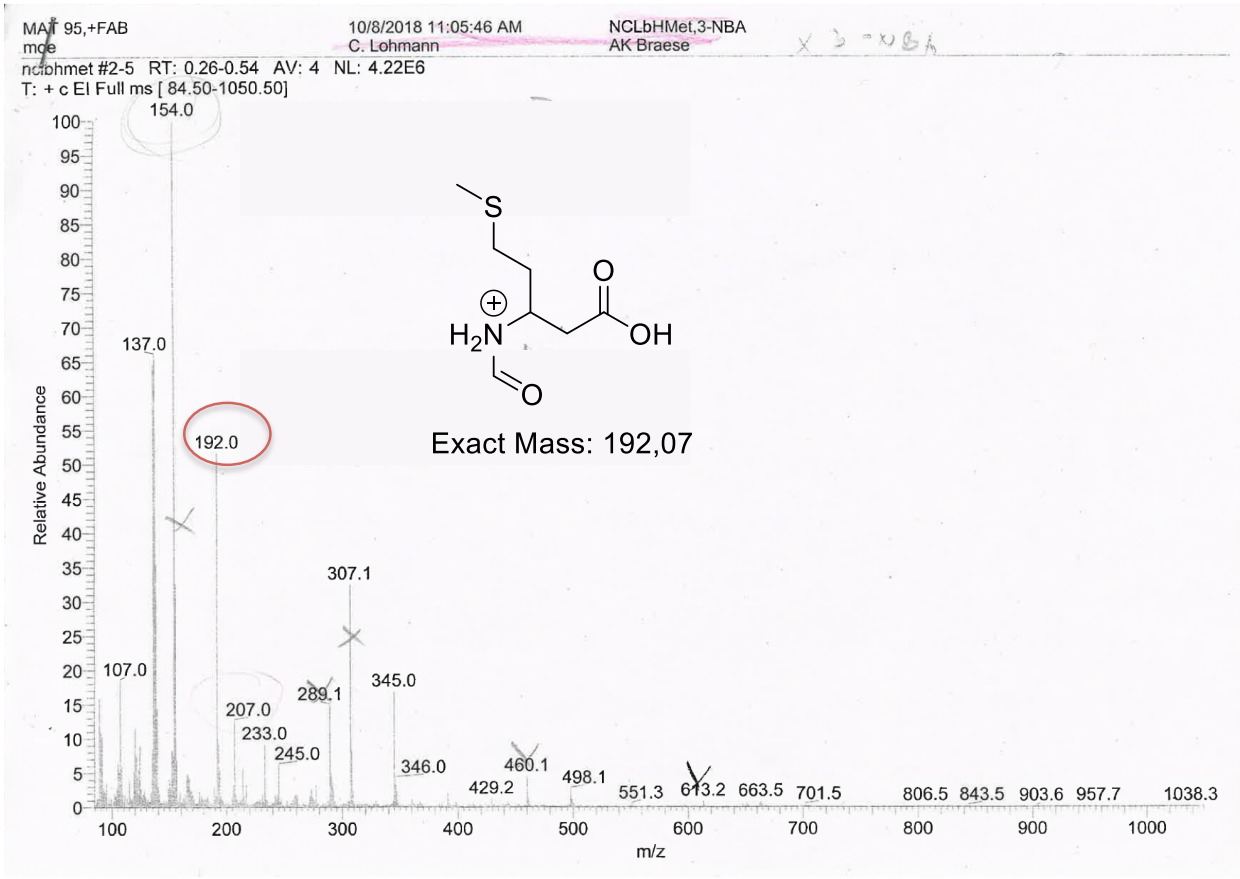

Figure 91: Mass spectrometry chromatogram of *N*-carbamoyl-L-β-homo-methionine.

Allantoic acid

M = 176,13, FAB^+ [M-CH_3NO^+]

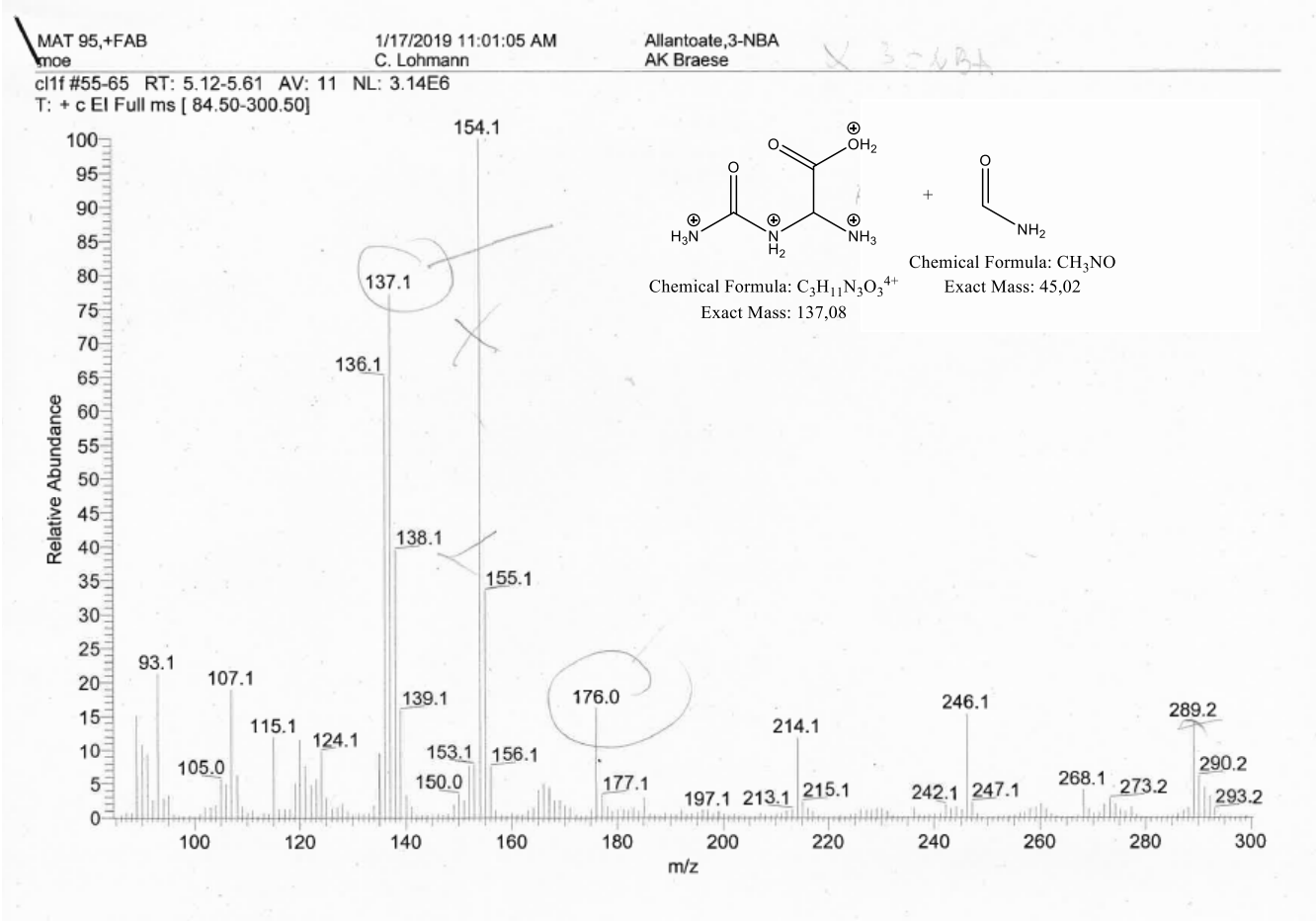

Figure 92: Mass spectrometry chromatogram of allantoic acid.

8.9 FPLC purifications

2V8H

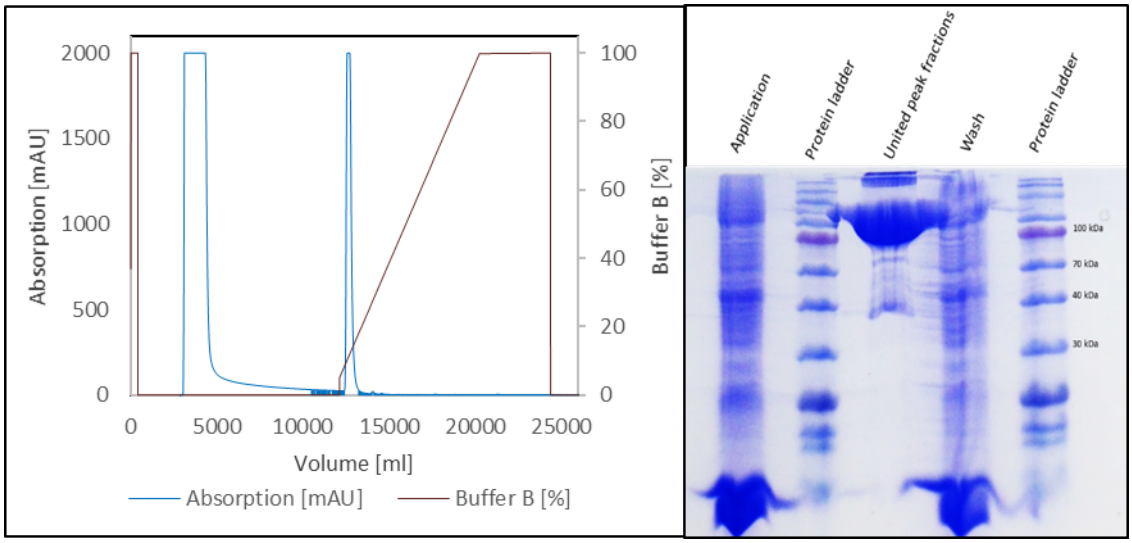

Figure 93: FPLC chromatogram and SDS-Gel of 2V8H purification.
Figure was made in the master thesis of Camilla Werle [272]. PageRuler™ Prestained Protein Ladder (Thermo Fisher).

2V8H-S-167 Mutant

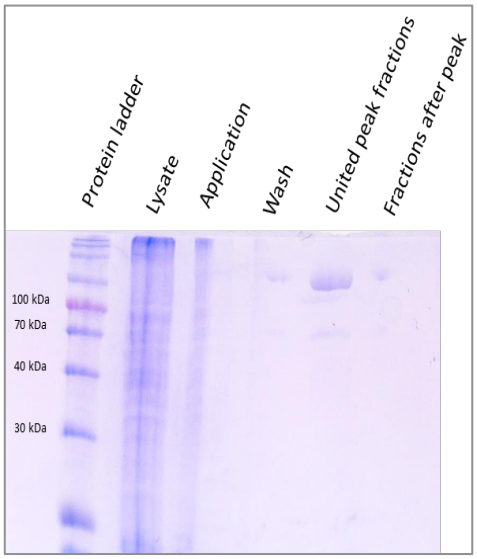

Figure 94: SDS-Gel of 2V8H-mutant S-167 after FPLC purification.
Figure was made in the master thesis of Camilla Werle [272]. PageRuler™ Prestained Protein Ladder (Thermo Fisher).

5I4M

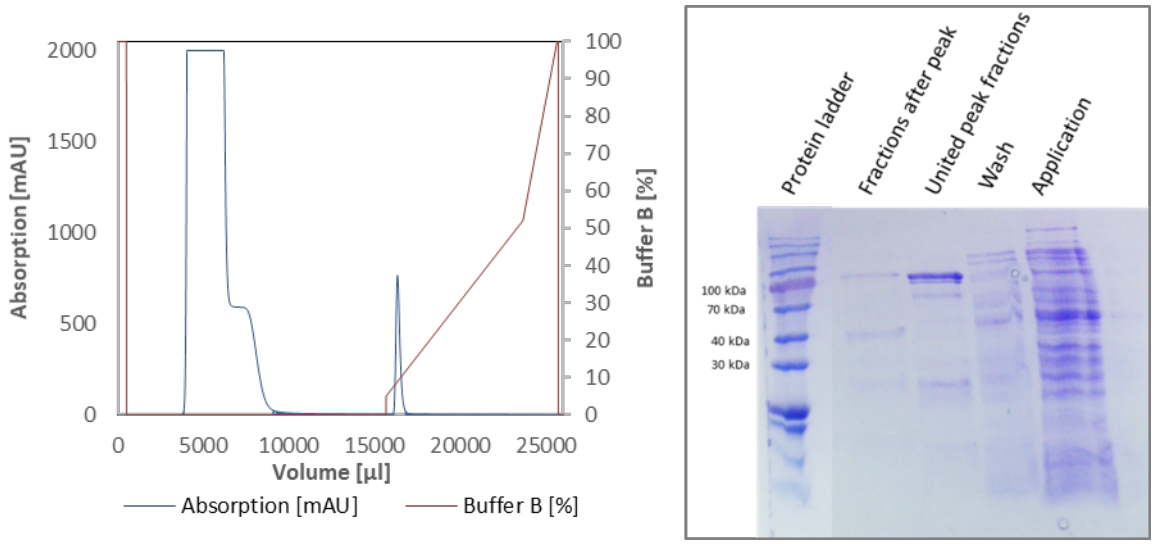

Figure 95: FPLC chromatogram and SDS-Gel of 5I4M purification.
Figure was made in the master thesis of Camilla Werle [272]. PageRuler™ Prestained Protein Ladder (Thermo Fisher).

3N5F

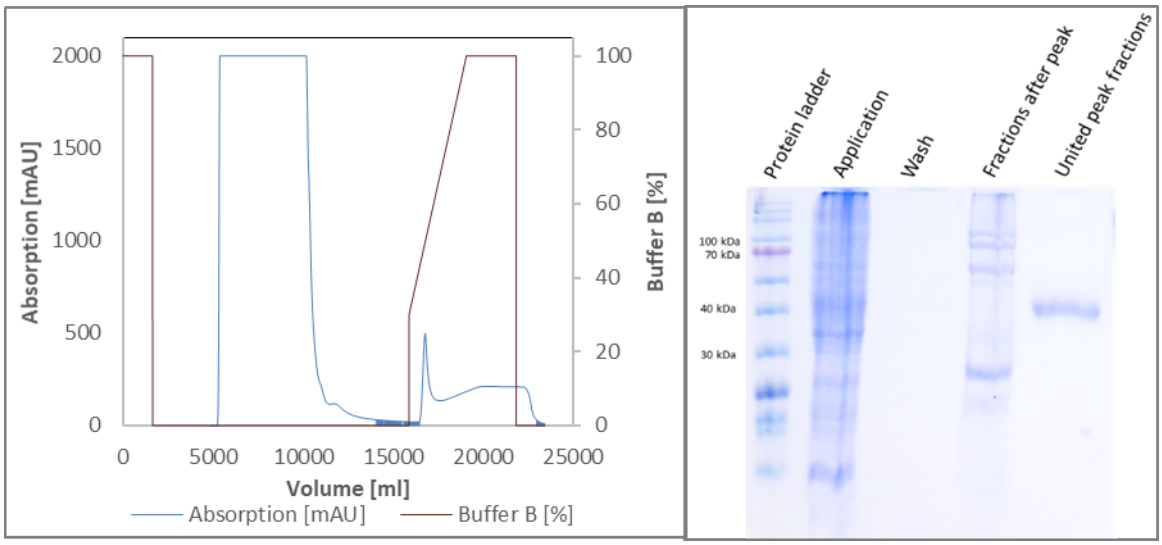

Figure 96: FPLC chromatogramm and SDS-Gel of 3N5F purification.
Figure was made in the master thesis of Camilla Werle [272]. PageRuler™ Prestained Protein Ladder (Thermo Fisher).

1Z2L

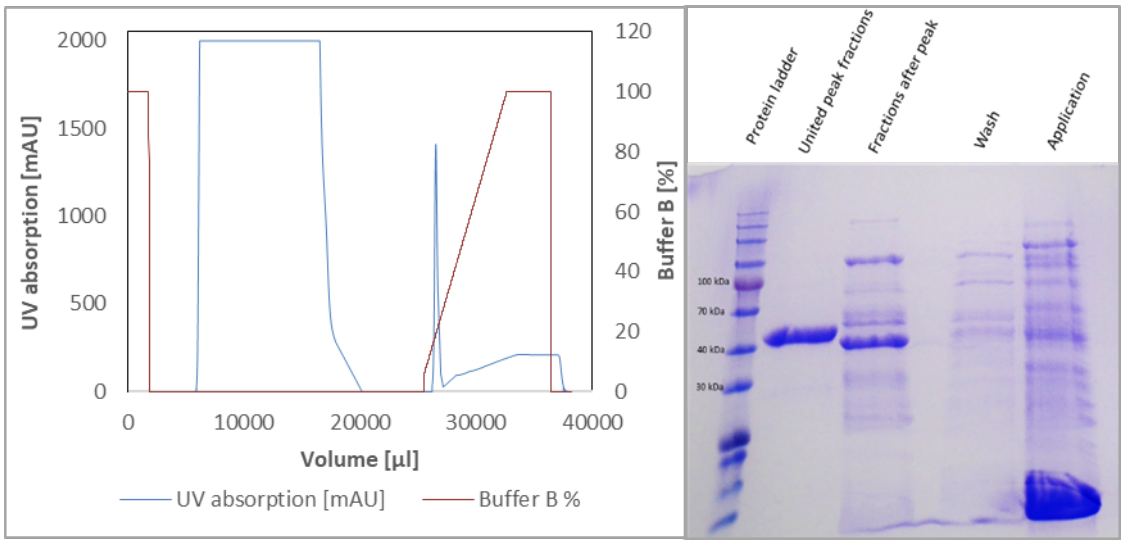

Figure 97: FPLC chromatogram and SDS-Gel of 1Z2L purification.
Figure was made in the master thesis of Camilla Werle [272]. PageRuler™ Prestained Protein Ladder (Thermo Fisher).

1FO6

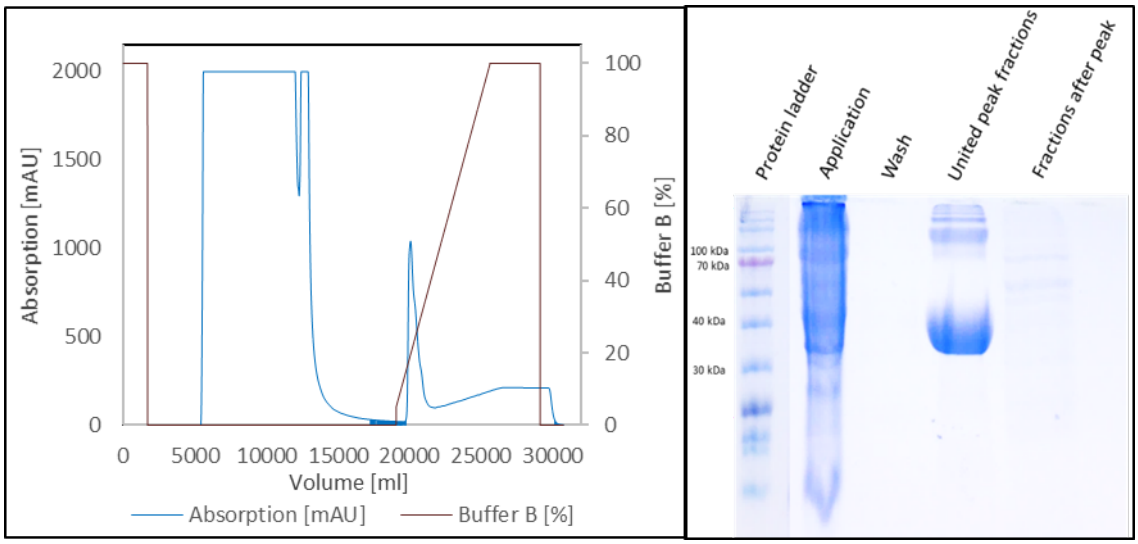

Figure 98: FPLC chromatogram and SDS-Gel of 1FO6 purification.
Figure was made in the master thesis of Camilla Werle [272]. Protein Ladder: PageRuler™ Prestained Protein Ladder (Thermo Fisher).